

ON RUPTURE ZONES AND GEODYNAMIC PROCESSES OF GREAT EARTHQUAKES ALONG THE HIMALAYAN CONVERGENT PLATE MARGIN

A THESIS

*submitted in fulfilment of the
requirements for the award of the degree*

of

DOCTOR OF PHILOSOPHY

in

EARTH SCIENCES



By
VINEET KUMAR GAHALAUT



DEPARTMENT OF EARTH SCIENCES
UNIVERSITY OF ROORKEE
ROORKEE - 247 667, INDIA

OCTOBER, 1994

Gratis

CANDIDATE'S DECLARATION

I hereby certify that the work which is being presented in the thesis entitled **ON RUPTURE ZONES AND GEODYNAMIC PROCESSES OF GREAT EARTHQUAKES ALONG THE HIMALAYAN CONVERGENT PLATE MARGIN** in fulfillment of the requirements for the award of the Degree of **Doctor of Philosophy**, submitted in the **Department of Earth Sciences, University of Roorkee**, is an authentic record of my own work carried out during the period from January, 1990 to October, 1994 under the supervision of Dr.R.Chander and Dr.P.K.Gupta.


The matter embodied in this thesis has not been submitted by me for the award of any other degree.

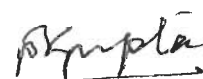


(VINEET KUMAR GAHALAUT)

This is to certify that the above statement made by the candidate is correct to the best of our knowledge.

Date :


October 10, 1994
(Dr R Chander)
Professor
Department of Earth Sciences
University of Roorkee
Roorkee 247 667


(Dr P K Gupta)
Lecturer
Department of Earth Sciences
University of Roorkee
Roorkee 247 667

The Ph.D. Viva-Voce examination of Mr **Vineet Kumar Gahalaut**, Research Scholar, has been held on 20 March 1995.


Roorkee Chander
20.3.1995
Signature of Supervisor(s)


Signature of External Examiner

ACKNOWLEDGEMENTS

I acknowledge with gratitude the immeasurable help and guidance provided by my supervisors Dr.R.Chander and Dr.P.K.Gupta.

I would like to take this opportunity to express my indebtedness to Dr.R.Chander, who aroused my interest in seismology, presented the problems of great Indian earthquakes and provided both academic and personal advice throughout the period of research. I am under obligations of Dr.P.K.Gupta, who offered help in understanding the world of mathematical modelling.

I am thankful to Prof. (late) R.K.Goel and Prof. A.K.Jain for their ready cooperation as Heads of the department.

I am thankful to Profs. V.K.Gaur, V.I.Keilis-Borok, Drs. I.V.Kuznetsov, A.M.Gabrielov, V.G. Kossobokov, I.M. Rotwain, G.F.Panza and Prof. V.Raiverman for their help and stimulating discussions. The help provided by IEM (Trieste, Italy) staff, during my stay in Italy is acknowledged.

Profs. A.K.Jain, H.Sinvhal, V.N.Singh, S.N.Pandey, Drs. M.S.Pandian R.G.S.Sastry, provided motivation through enquiries and prodding to complete the thesis.

The completion of this thesis has depended largely on the the tremendous cooperation, understanding, help and moral support from my wife Kalpna. I wish to acknowledge the cooperation and patient help provided by my family members.

Verma, Semwal, Peeku, Dharmu, Bharati, Kiran Bhatt and Navneet, my greatest friends through the years, have always been ready to help and source of inspiration through the years.

I thank Sandeep Singh, Saral Jain, Anupma, V.Bhadra and R.C.Patel, who were very much helpful throughout the research period.

Manoj Sharama, Sanjeev, Triparna, Manju, Vivek, V.Sriram, A.Manglik and Arvind were always ready to spare their valuable time for help and encouragement.

I would like to acknowledge the cooperation rendered by Sanjeev Juyal, Mr.Sarvesh, Shashank, Mr.Nair and Mr.Sitaram.

I am thankful to Kali Prasad, Baburam for their help.

Finally, I thank University Grants Commission for granting financial assistance.



(VINEET K GAHALAUT)

ABSTRACT

This thesis is a compilation of six distinct yet complementary studies of great and moderate earthquakes along the Himalayan convergent plate margin. In the first study the extant largely qualitative evidence for ground level changes during the 1897 earthquake is reinterpreted to suggest that a mid-crustal detachment was ruptured over an area of 170x100 km² by thrust faulting. The rupture was located under the western Shillong Plateau and the Brahmaputra valley and does not extend upto the Himalaya several tens of kilometres further to the north. Geodetic observations of coseismic ground elevation changes during the Kangra earthquake of 1905 suggest, in a second study, that the causative rupture had an area of 280x80 km² in the low angle thrust fault type detachment under the Outer and Lesser Himalaya. The same data set was analysed by trial and error and more rigorous minimum norm inversion methods. The lower bound of maximum slip on the detachment was 5-7 m. Interseismic levelling observations along a line in the Himalaya of central Nepal were analysed in the third study. It is concluded that aseismic permanent deformation and recoverable earthquake generating strains are accumulating in the region simultaneously. The latter will be released either fully or partially in the next great earthquake of central Nepal Himalaya. The fourth study is similar but based upon much more limited observations in the Dehradun region. It is concluded that preparations for a great earthquake are in progress in this region also though its date of occurrence cannot be predicted. The fifth study pertains to modelling of stresses for the occurrence of great and moderate earthquakes along the detachment under Himalaya. Within the framework of classical rock mechanics, we are forced to conclude that either very high pore pressures or very low frictional coefficients or both should occur along the detachment. Finally a statistical study of seismicity of the Himalaya was carried out to see if the Uttarkashi earthquake of 1991 in the Garhwal Himalaya could be retrodicted from the available seismicity data for the Himalaya and southern Tibet. The K function of CN algorithm proposed by Keilis-Borok and group to depict the spatio-temporal variation of seismicity was found to be a sensitive parameter for this purpose.

Regarding seismic hazards along the Himalayan convergent plate margin, we argue in several of above studies as follows. Firstly, the length of the Himalaya which has released strain through the four great earthquakes of the last 100 years is probably much less than considered by recent investigators. Secondly, the geodetic evidence reveals that earthquake generating strains are accumulating at least along two segments and probably throughout the Himalaya. Thirdly, the detachment lying at depths between 5 to 17 km beneath the Outer and Lesser Himalaya is probably the nearest active fault for most dam sites in the region.

Two cumulative impressions from these studies are as follows. Firstly, the data analysed here are consistent with plate tectonics hypothesis as applied to the Himalayan convergent plate margin. Secondly, seismic hazards in the Himalaya and the adjoining Indo-Gangetic plains are much more severe than is being acknowledged by most Indian seismologists and civil engineers.

CONTENTS

ACKNOWLEDGEMENTS	(i)
ABSTRACT	(iii)
CHAPTER I Introduction and review	
1.1 Introduction	1
1.1.1 General	1
1.1.2 Need for studying great earthquakes of the Himalaya	3
1.1.3 Difficulties in studying great earthquakes of the Himalaya	3
1.1.4 The niche of the present thesis in the heirarchy of Himalayan earthquake studies	5
1.2 A review of plate tectonics related studies in the Himalaya	5
1.2.1 Terminology	6
1.2.3 Origin of the Himalaya	9
1.2.4 Spatial and depth distribution of earthquakes in the Himalaya	12
1.2.4.1 Moderate earthquakes	12
1.2.4.2 Great earthquakes	14
1.2.4.3 Small earthquakes	15
1.2.5 Focal mechanism of Himalayan earthquakes	18
1.2.6 Studies of seismic gaps in the Himalaya	21
1.2.7 Other studies supporting the plate tectonics view of underthrusting in the Himalaya region	24
1.2.7.1 Gravity anomalies in the Himalaya	24
1.2.7.2 Studies of P_n and S_n wave propogation beneath the Himalaya	25
1.2.7.3 Deep seismic sounding studies in the Himalaya and southern Tibet	26
1.3 Summary of the review	26
1.4 Repetition in text	27
CHAPTER II Theoretical considerations	
2.1 Introduction	28
2.2 Elastic dislocation theory	29
2.2.1 Theoretical developments	29
2.2.2 Applications for inversion	29
2.3 Formulas for ground displacements due to finite ruptures in faults	30
2.4 Methods employed to solve the inverse problems	33
2.4.1 General remarks	33
2.4.2 Inversions using the trial and error method	34
2.4.3 Direct inversion for fault slip using the minimum norm inversion method	34

CHAPTER III A rupture model for the great Assam earthquake of 1897, northeast India

3.1 Introduction	37
3.2 Terminology	39
3.3 Method of analysis	39
3.4 Source model	40
3.5 Critique of the source model	42
3.5.1 Northern limit of the rupture zone	42
3.5.2 Eastern limit of the rupture zone	43
3.5.3 Western limit of the rupture zone	44
3.5.4 Southern limit of the rupture zone	45
3.5.5 Inferred rupture zone and observations of lineaments	45
3.5.6 Depth of rupture	45
3.5.7 Direction of slip	48
3.5.7.1 Fault plane solutions evidence	48
3.5.7.2 Geological consideration	48
3.5.8 On the assumption of uniformity of slip across rupture in a single fault	49
3.6 Implications of the rupture model for the geodynamics of the region	50
3.7 Implications of the proposed rupture model for seismic risk in parts of NE India	52
3.7.1 Seismicity of the HCPM and Himalaya	53
3.7.2 Seismic gap in Central and Eastern Himalaya	54
3.8 Summary	55

CHAPTER IV A rupture model for the great Kangra earthquake of 1905, NW Himalaya, based on geodetic levelling observations

4.1 Introduction	57
4.2 Previous analyses of Kangra earthquake data	58
4.3 Motivation for and aim of the present work	59
4.4 Observations of elevation changes in the Dehradun region	60
4.4.1 History of observations	60
4.4.2 Errors in observations	61
4.4.2.1 Errors of observation	61
4.4.2.2 Errors due to possible pre-seismic level changes	64
4.4.3 Overall Quantity and quality of observations	64
4.5 Estimation of the cross-sectional shape of the fault, extent of rupture and amount of fault slip using the trial and error procedure	64
4.5.1 Preliminary assumptions about fault models	65
4.5.2 Results	65
4.5.3 Major implications of the analysis	66
4.6 Estimating the fault slip using the minimum norm inversion	68
4.6.1 Enunciation of the problem	68
4.6.2 Method	69

4.6.3 Other considerations	69
4.6.3.1 Trade off	69
4.6.3.2 Relative position of rectangular rupture vis-a-vis the levelling line	70
4.6.4 Resulting model of slip variation	71
4.6.5 Quality of inversion	72
4.6.5.1 R matrix	73
4.6.5.2 S matrix	74
4.7 Discussion	74
4.7.1 Kangra earthquake rupture model and plate tectonics	74
4.7.2 Depth of the Kangra earthquake source	75
4.7.3 Magnitude of slip	76
4.7.4 Current tectonic status of the MCT, MBT and MFT	77
4.7.4.1 MCT	77
4.7.4.2 MBT	77
4.7.4.3 MFT	78
4.7.5 Hazard assessment	79
4.8 Summary	81

CHAPTER V Evidence for accumulation of earthquake generating strains in the Himalaya of central Nepal from short term interseismic levelling observations

5.1 Introduction	83
5.2 Data	84
5.2.1 Errors in the levelling observations	84
5.2.2 Data used	89
5.3 Basic analysis	89
5.3.1 Possibility of bias in observations	89
5.3.2 Preferred model	89
5.4 Interpretation of the estimated annual slip rate on the detachment	90
5.5 Discussion	92
5.5.1 On the interpretation of ground elevation change data	92
5.5.2 Causes of elevation changes	93
5.5.3 Elastic Strain accumulation for a great earthquake	94
5.5.4 Return period of great Himalayan earthquake	94
5.5.5 Stage of strain accumulation	95
5.5.6 Current tectonic status of the MFT	95
5.6 Summary	96
5.7 Note	96

CHAPTER VI Interpretation of post Kangra earthquake levelling observations in the Dehradun region

6.1 Introduction	97
6.2 Observational data	97
6.2.1 Possible extent of random errors in elevation changes	100
6.2.2 Stability of benchmarks in the 1926-28 to 1974-75 data	100
6.2.3 The elevation changes during 1905-07 and 1926-28 as the post-seismic changes	102
6.3 Method of analysis	103
6.4 Resulting model of slip variation	103
6.4.1 Quality of inversion	108
6.4.1.1 1905-07 to 1926-28 data	108
6.4.1.2 1926-28 to 1974-75 data	109
6.5 Interpretation of the estimated annual slip rate	109
6.5.1 Major similarities in uplift rate data of Dehradun and central Nepal regions	110
6.6 Discussion	112
6.6.1 Sensitivity of the slip estimates	112
6.6.2 Possible influence of microseismicity on the elevation changes	112
6.6.3 Current tectonic status of MFT	112
6.6.4 Possibility of a locked zone on the detachment under the Dehradun region	115
6.7 Summary	115

CHAPTER VII A simulation of stresses for nucleation of great and moderate earthquakes on the Himalayan detachment

7.1 Introduction	117
7.2 Review of the literature about the stress field in the Himalaya	118
7.3 Present simulation of stress field in the Himalaya	121
7.3.1 Notation	122
7.3.2 Model	123
7.3.2.1 Topographic load	123
7.3.2.2 Simulation of buoyancy forces	125
7.3.3 Results	126
7.3.3.1 First look at combined stresses due to topography and buoyancy	126
7.3.3.2 Consideration of additional stress from other sources : dry rock calculations	127
7.4 Discussion	130
7.4.1 Applicability of rock mechanics considerations for modelling earthquake nucleation	130
7.4.2 Pore pressure versus low friction coefficient	131
7.4.2.1 Friction coefficient	131
7.4.2.2 Considerations of pore pressure	132
7.4.2.3 Principal stresses of plate tectonic origin oriented obliquely	134
7.4.3 Nature of detachment	135

7.4.4 Triggering of earthquakes on the detachment by rupture initiation on high angle reverse faults normal to it	135
7.4.5 Triggering of moderate and great Himalayan earthquakes during episodes of uplift of the Higher Himalaya relative to the Lesser Himalaya	137
7.5 Summary	137

CHAPTER VIII Retrodiction of the 1991 Uttarkashi earthquake

8.1 General	139
8.1.1 Long term prediction	139
8.1.2 Short term prediction	140
8.1.3 Intermediate term prediction	141
8.2 Review of studies related to the prediction of earthquakes in the Himalaya and adjoining regions	141
8.3 Present study	144
8.3.1 Motivation of the study	144
8.3.2 Data	144
8.4 Temporal variation of seismicity	145
8.5 Results	146
8.5.1 Regionalisation	146
8.5.2 Behaviour of K function in the selected region	148
8.6 Discussion	150
8.6.1 Further tests	150
8.6.2 Behaviour of function K	151
8.6.3 A clarification	151
8.7 Summary	152

CHAPTER IX General discussion

9.1 General	153
9.2 Applicability of plate tectonics to the Himalaya	153
9.3 Association of great Himalayan earthquakes with the detachment	154
9.4 About slip on the detachment under the Himalaya	155
9.5 Stresses for the nucleation of great and moderate Himalayan earthquakes along the detachment	156
9.6 A statistical search for a pattern in seismicity to predict moderate and great Himalayan earthquakes	156
9.7 On the seismic hazards in the Himalaya	157
9.7.1 On the extent of seismic gap in the northeastern Himalaya	157
9.7.2 Implications for the Tehri dam	158
9.8 Evidence of preparation for great earthquakes in the Himalaya	159
9.9 Summary	159

CHAPTER X Conclusions	160
References	164
Papers published on the basis of studies in the thesis	189

CHAPTER I

Introduction and review

1.1 Introduction

1.1.1 General

In his efforts to live and thrive on the planet earth, man's progress has been closely related to his increasing ability to understand and master the forces of nature. The forces unleashed during large earthquakes are truly awesome. Since the dawn of history, mankind has been reminded frequently of the ruinous potential of earthquakes. Thus the need to predict earthquakes has been felt by man for a long time. But scientific efforts to identify phenomena precursory to large destructive earthquakes have begun only recently.

The Himalayan mountain chain is associated with one of the relatively more active seismic belts of the world (Fig.1.1). A vast majority of earthquakes of the Indian subcontinent occur along this belt. They span the whole range of magnitudes from the very largest to those which can be detected only with sensitive seismographs. The observational database and our understanding of the Himalayan earthquakes is as yet very limited. Two steps need to be undertaken urgently. Firstly, the database should be broadened. Secondly, efforts should be made to interpret and reinterpret the existing observations in light of worldwide developments in earthquake studies.

The present thesis is an effort of the second kind. Here a motivated reinterpretation of extant macroseismic and relevant geodetic observations has been undertaken with a view to quantify several processes and features related to the occurrence of great earthquakes along the Himalaya.

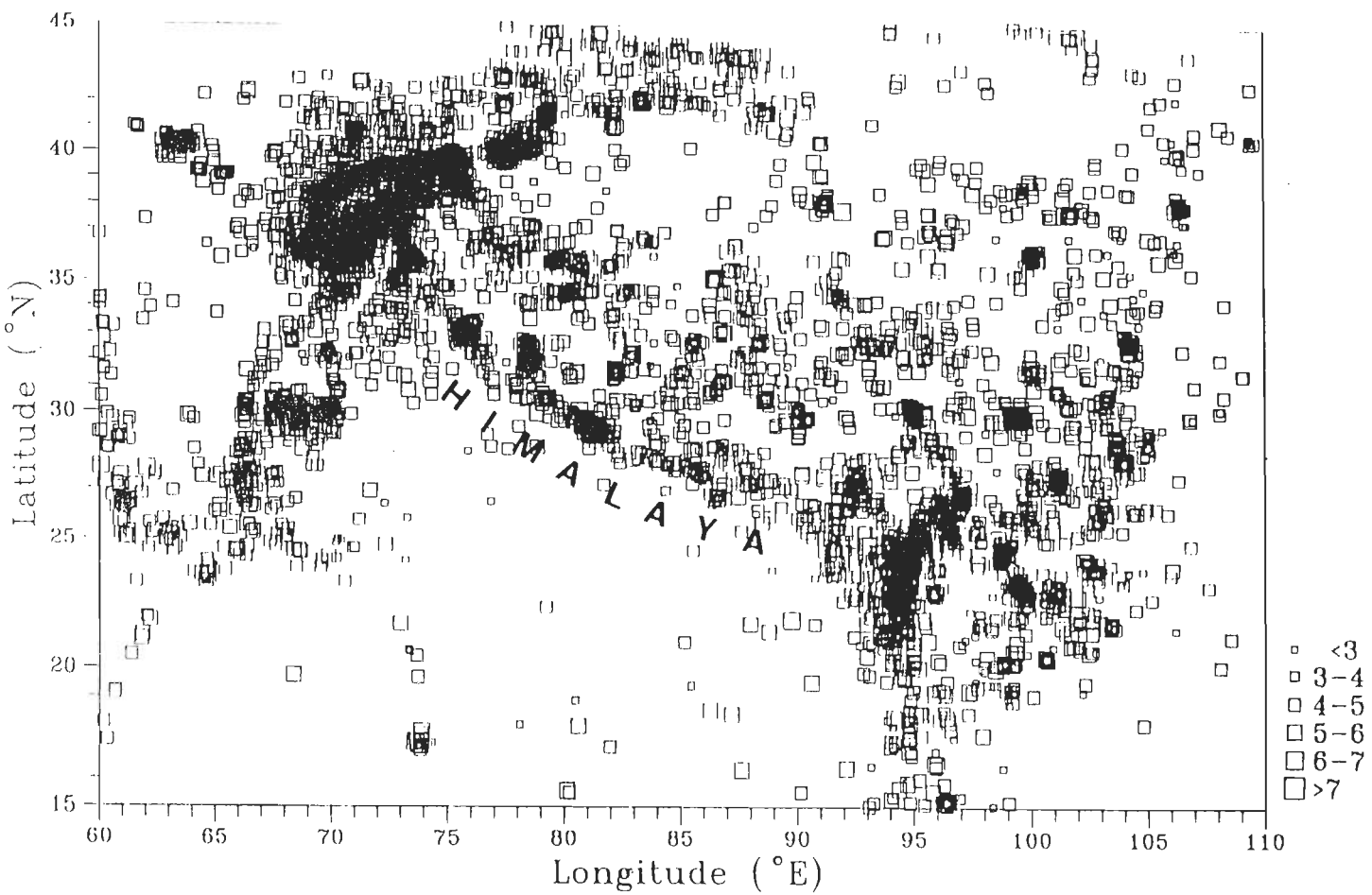


Fig.1.1 Epical map of the Himalayan and adjoining regions showing USGS-NEIC locations for earthquakes occurring between 1970-1991.

1.1.2 Need for studying great earthquakes of the Himalaya

During the twentieth century a census of population has been taken in India at the beginning of every decade. These enumerations have charted a meteoric rise in the population. Although the growth has been witnessed in all parts of India but in the Indo-Gangetic plains it has been extraordinary. Also an important fact to emerge from the studies of the four great earthquakes along the Himalayan convergent plate margin during the last 100 years is that in each case parts of the Indo-Gangetic Plains and the Brahmaputra valley contiguous to the epicentral tract have experienced heavy destruction and great loss of life.

Forty four years have elapsed now since a great earthquake has occurred along the Himalyan seismic belt. While the date and time of the next such earthquake cannot be predicted scientifically at present, yet it is certain that due to the growth in population the loss of life will be horrendous regardless of the time of day or night when the impending earthquake occurs. During this period of waiting we can only turn to the available information about the past earthquakes to seek patterns in the nature and extent of damage and thus to evolve strategies for reducing the losses during the next great earthquake.

1.1.3 Difficulties in studying great earthquakes of the Himalaya

A serious drawback in this agenda is that even the most recent of these great earthquakes occurred in 1950, before the modern era in instrumental seismology began with deployment of the Press-Ewing and Benioff seismograph in a worldwide network and before most of the present seismograph stations of Indian national network had been set up. Thus much of the available information about past great earthquakes of the Himalaya is of qualitative nature.

A second problem with the study of great earthquakes of the Himalaya is that historical records of such earthquakes are largely lacking. Although India claims a civilization as old as the Chinese, yet whereas the Chinese court records chronicle great and destructive earthquakes over a period of more than 2500 years, in India it is difficult to be sure about Himalayan

earthquakes which seem to have occurred at the beginning of the 19th century. To some extent this lack of historical record can be overcome by paleoseismicity studies. The first step in this direction has been the convening of a meeting in 1993 under the sponsorship of the Department of Science and Technology, Government of India. Results of any investigations under this programme can only be expected a few years from now.

Although this thesis is devoted primarily to the study of great Himalayan earthquakes, it is not out of place to make a few remarks about observations of moderate, small and micro-earthquakes in the Himalaya. Much of the seismicity information, on which the definition of the Himalayan seismic belt rests, has come after the publication of Gutenberg and Richter's "Seismicity of the Earth" from teleseismic determinations of hypocentral data regarding moderate magnitude Himalayan earthquakes. Although currently USGS preliminary determinations of epicentres for Himalayan earthquakes indicate rms errors in epicentral latitude and longitude of the order of 1-2 km, yet in a recent study of a moderate magnitude earthquake recorded teleseismically and with a local network installed for microearthquakes studies (Khattri et al., 1989), it was demonstrated that the USGS epicentre was located 23 km away from that estimated from the local network data. The situation regarding focal depth estimates of moderate magnitude earthquakes is even worse. While ISC and USGS have reported focal depth of such earthquakes in the range of 0-98 km, revised focal depth estimates are consistently in the range of 10-18 km. On the basis of investigations and arguments by a number of recent investigators (Molnar, 1990), it appears now plausible to assume that the rupture zones of great Himalayan earthquakes may also lie in the depth range of 10-18 km and may be spatially linked with the zone of hypocentres of moderate magnitude earthquakes in the upper brittle crust.

About 30 years ago it was suggested that observations of micro-earthquakes with networks of sensitive, portable seismographs may shed light on larger magnitude earthquakes that occur less frequently. So far reliable results from investigations of small magnitude and micro-earthquakes have been obtained only for a small lengthwise segment of the Himalaya.

But no significant information regarding larger earthquakes of the region has been deduced from these data.

1.1.4 The niche of the present thesis in the hierarchy of Himalayan earthquake studies

In the present thesis an effort has been made to enhance our understanding regarding the occurrence of great earthquakes in the Himalaya from analysis of available observations. To this end we have assembled six distinct studies each of which has a bearing upon this topic. The unifying theme of all the investigations is the view that Himalayan earthquakes are related to the ongoing convergence and collision between the Indian and Eurasian plates. In four of the studies we adopt the view that observations and interpretations of interseismic and coseismic ground elevation changes could shed light on the processes of strain accumulation and release associated with great earthquakes of this convergent plate margin. In the fifth study the focus is on the simulation of limiting upper crustal stresses necessary for the occurrence of such earthquakes. The final study is a more abstract statistical pattern recognition exercise which addresses the question whether the occurrence of great Himalayan earthquakes could be influenced by the occurrence of earthquakes in the adjoining regions, notably southern Tibet.

1.2 A review of plate tectonics related studies in the Himalaya

A substantial increase in our knowledge about the Himalaya has occurred at about the same time as the concept of plate tectonics has been taking root as the latest paradigm in earth sciences. The current views about the occurrence of great Himalayan earthquakes that we also subscribe to, can be exposed through a review of several plate tectonics related geophysical studies in the Himalaya. In the following subsections we undertake a thematic rather than a chronological review of these studies. In the first two subsections general information about the Himalaya and their origin has been provided. The later subsections are devoted to the brief

review of important geophysical studies in the Himalaya.

1.2.1 Terminology

In the present thesis we shall frequently use some terms related specially to the Himalaya. We introduce them here briefly along with some general information about the Himalaya.

The Himalaya, an important segment of the tertiary mountain chain which runs from the Atlas mountain of northwest Africa through the Alps in Europe and Burmese mountains in south east asia, are the world's highest mountain chain. They are convex to the SSW and extend over nearly 2500 km from Indus river gorge near Nanga Parbat in the northwest to the Brahmaputra gorge near Namch Barwa in the east. On their northern side they are separated from the trans Himalayan zone by the valleys of the Indus and Tsangpo. Toward the south they are fringed by the Indo- Gangetic Plains. Between these limits the width of the Himalaya varies from 200 to 250 km. The Himalaya may be divided longitudinally into four lithotectonic as well as physiographic units that run over much of their length. Proceeding northwards these units are called the Outer, Lesser, Higher and Tethys Himalaya (Fig.1.2). Southern limits of the three southern most division are demarcated by the north dipping thrust zones and topographic breaks.

The Outer (or Sub) Himalaya consist of the folded and faulted Siwalik molasse sediments of Miocene to Pleistocene age. They form the low hills of elevations upto 1300 m. They are separated from the alluvium of Indo-Gangetic Plains by a thrust plane called the Main Frontal Thrust (MFT) (Fig.1.2). However at places the surface trace of this thrust is not very well marked and is probably buried (Lillie et al., 1987; Baker et al., 1988; Penock et al., 1989; Nakata, et al. 1990; Yeats and Lillie, 1991).

The Precambrian to Palaeozoic sedimentary rocks of the Lesser Himalaya (Fig.1.2) are intruded by granites and have experienced low grade metamorphism. The maximum elevation is upto about 4500 m. Lesser Himalaya are separated in the south from the Outer Himalaya

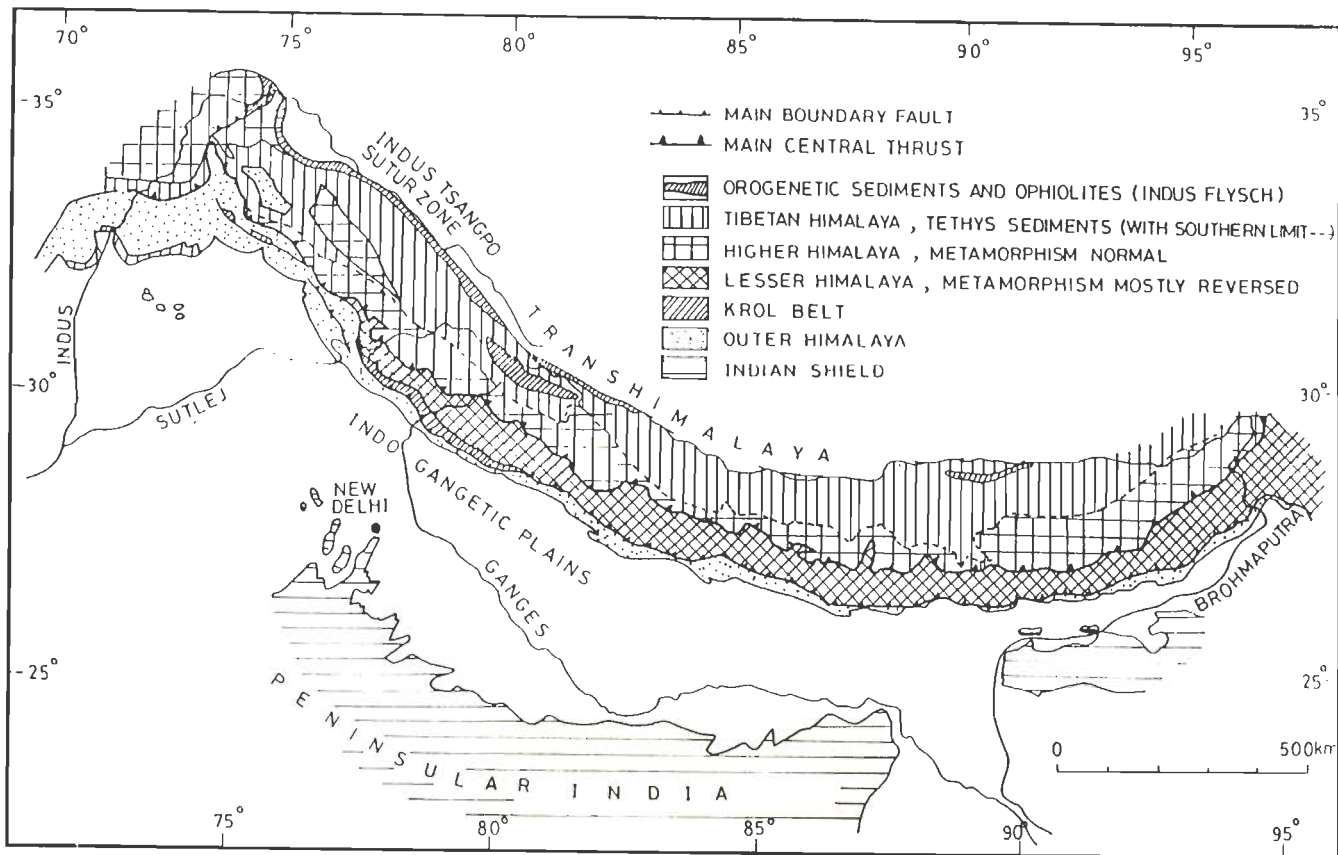


Fig.1.2 General geological map of the Himalaya (after Gansser, 1964).

by the Main Boundary Thrust (MBT) (e.g. Gansser, 1964; 1977; 1993; Fuchs, 1975; Wadia, 1966), which is a series of steep thrust planes (usually 60° - 90° , Stocklin, 1980) that appear to flatten at depth (Valdiya, 1980).

The Higher Himalaya are made up of high grade metamorphic rocks. The mountains have elevation in excess of 7300 m, the maximum being 8848 m for Sagar Matha. The Higher Himalayan rocks are separated from the rocks of Lesser Himalaya by the Main Central Thrust (MCT) (Fig.1.2). At the surface, MCT appears to dip at an angle of about 30 - 45° (e.g. Gansser, 1964) in the north direction. The thrust is characterized by a zone of intense shearing (e.g. Valdiya, 1980; Sinha-Roy, 1982). An abrupt change in the style of structures, especially folding and in the grade of metamorphism is the main manifestation of the presence of the MCT.

The Tethys Himalaya are comprised of fossiliferous sediments of Paleozoic to Mesozoic age. They are bordered on their north by an ophiolite and melange suite associated with the Indus Tsangpo Suture Zone (ITSZ), (e.g. Gansser, 1964, 1980, Lefort, 1975; Stocklin, 1980). Beyond the suture zone lie the Trans-Himalayan geological units (Fig.1.2).

The current activity of the MFT, MBT and MCT is the topic of debate but there is unanimity that the ITSZ is inactive. ITSZ developed during subduction following the late Cretaceous-early Tertiary closure of the Tethys sea. The MCT which appears to have developed since mid-Tertiary time, shows some geological indications of minor recent movements (e.g. Stocklin, 1980; Valdiya, 1980). On the other hand Seeber and Armbruster (1984) inferred that the rivers in the Himalaya are characterized by steep gradients through Higher Himalaya and by low gradients downstream in the Lesser and Outer Himalaya. They concluded that the steep river gradients (knickpoints) are associated with a deep seated fault called the basement thrust front (BTF) and not with the surface trace of MCT. According to Seeber and Armbruster (1984) BTF demarcates the transition between seismic and aseismic thrust movement and it coincides with the belt of moderate magnitude earthquakes in the

Himalaya. Regarding the activity on the MBT, which has developed since Pliocene time, Mathur and Evans (1964), Lefort (1975), Valdiya (1980) opined that it is less active than MCT. Valdiya (1986) argued that the Outer Himalaya are rising relative to the Lesser Himalaya as is evident from the higher gradients (15-20°) of beds of streams in the Outer Himalaya as compared to gentler gradients (about 5°) in the Lesser Himalaya. But poorly delineated MFT seems seismically inactive (Valdiya, 1980). On the contrary, Nakata et al. (1990) and Yeats and Lillie (1991) argued that MFT is active and it forms the present boundary between the Indian and Eurasian plates.

1.2.3 Origin of the Himalaya

In the first half of the 19th century the research on mountain building processes was characterized by the view point that they are the result of vertical uplift. It was not until the late 19th and early 20th century that the role of horizontal movements in tectonics was recognized. The concept of underthrusting of the lithosphere of one continent beneath that of another continent as the cause of mountain building and plateau uplift was first proposed by Argand (1924). The concept of plate tectonics was fully developed during the 1960's. Numerous models for the evolution of the Himalaya have been proposed within this concept. Dewey and Bird (1970) suggested that the Himalaya were formed solely by the collision of an Atlantic type continental margin with the Asian continent bordered by a marginal trench. Powell and Conaghan (1973, 1975) and Powell (1979) proposed an evolutionary model in which the subduction along ITSZ took place in Mesozoic-early Tertiary period when India collided with Eurasia. The intercontinental fractures developed within the Indian continent during the middle Tertiary and underthrusting has occurred along these fractures from Miocene time to the present.

In last two decades, with an increasing amount of data on the Himalaya and Tibet, mainly four types of plate tectonics models have been proposed for the evolution of the Himalaya.

Among these models, following points are common (i) convergence between Indian and Eurasian plates along the ITSZ ended in the Cretaceous -Eocene time and (ii) subsequent to the closure of Neotethys, the Himalaya were built up due to further convergence between India and Eurasia. The estimated total amount of this convergence ranges from 2000 to 3000 km (Molnar et al. 1977). About 350 km of convergence could be accounted along the Himalayan mountain belt (Lyon-Caen and Molnar, 1983 and 1985). To explain this shortening various further models have been suggested (Beghoul et al. 1993).

(i) **The escape model** (e.g. Molnar and Tapponier, 1975; Tapponier et al., 1982; Peltzer and Tapponier, 1988, Armijo et al. 1989, Tapponier et al., 1990 and Avouc and Tapponier, 1993): It is proposed in this model that, in response to the above shortening, eastward extension of the Tibetan Plateau occurs with horizontal motion on the Altyn-Tagh and Kunlun strike slip faults.

(ii) **The hydraulic pump model** (e.g. Zhao and Morgan, 1985; 1987; Zhao and Yuen, 1987): It is suggested that the underthrusting Indian plate acts like the piston of a hydraulic pump. The weak lower crust of Tibet acts as the fluid in this pump and it causes uniform uplift of Tibet.

(iii) **The accordian model** (e.g. Dewey and Burke, 1973; England and Houseman, 1986; Jordan et al., 1989; Gonjian et al., 1990): It is suggested that the shortening is absorbed by diffuse thickening of the Tibetan plateau lithosphere. As the amount of shortening is very large, it could lead to a thinning of much of the thickened mantle lid (Houseman et al., 1981).

(iv) **The underthrusting model** (e.g. Lefort, 1975; Seeber and Armbruster, 1981; Barazangi and Ni, 1982; Molnar and Lyon-Caen, 1983; 1985; Ni and Barazangi, 1984; Barazangi, 1989; Molnar, 1992): It is proposed that underthrusting of the Indian plate beneath the Moho of Tibetan plateau leads to crustal thickening. A shield like mantle lid beneath the plateau is inferred. We discuss this model in further details in the following paragraphs.

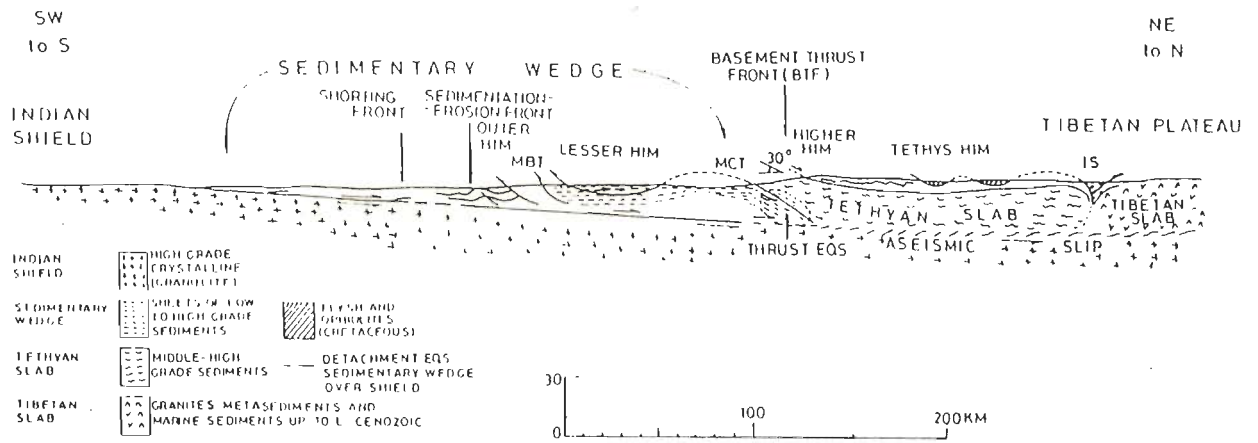


Fig.1.3 Steady state underthrusting model of Seeber and Armbruster (1981).

Seeber and Armbruster (1981) proposed a steady state underthrusting model (Fig.1.3) for the evolution of the Himalaya. This model requires that the MBT and MCT should be contemporaneous features. An important feature of Seeber and Armbruster's (1981) model is that a detachment (decollement) surface underlies the Outer and Lesser Himalaya. Seeber and Armbruster (1981) also postulated the presence of a Basement Thrust Front (BTF) where the northerly dipping MCT merges with the shallow dipping detachment. They interpreted the available seismological data to indicate that most of the moderate thrust type earthquakes occur along the BTF. However, the great Himalayan earthquakes occur along the detachment surface beneath the Outer and Lesser Himalaya (Seeber and Armbruster, 1984, Molnar, 1990, Khattri and Tyagi, 1983a, Chander, 1988, 1989a). The deformation further north occurs aseismically on the downdip side of the detachment (Seeber and Armbruster, 1981).

Another point which may be discussed here is regarding the rate of crustal shortening or convergence which is accommodated at least under the Himalaya through underthrusting of Indian plate beneath Eurasian plate.

DeMets et al. (1990) reviewed and analysed the available data regarding the spreading rates

at mid oceanic ridges, transform fault azimuths and earthquake slip vectors and presented a model of current plate motion. They estimated a convergence rate of 50 mm/year between Indian and Eurasian plates. The geomorphic evidence for the active faulting in the Himalaya and Tibet suggests a similar magnitude (53 ± 13 mm/year) of the crustal shortening (Molnar et al., 1987). From the analyses of age of sediments deposited in the Gangetic plains and the age and height of the highest terraces in the Kali Gandaki valley, Lyon-Caen and Molnar (1985) and Molnar (1987a) estimated that 18 ± 7 mm/year out of the total of 50 mm/year convergence is accommodated at the Himalaya. A similar estimate is suggested by Avouc and Tapponier (1993) on the basis of kinematic model of active deformation of Himalaya and Tibet.

1.2.4 Spatial and depth distribution of earthquakes in the Himalaya

1.2.4.1 Moderate earthquakes

The Himalaya are the relatively more seismically active regions in the world. Earthquake detection and location capabilities for Himalaya had been extremely poor until about 1960 and have improved during the last three decades following the installation of WWSSN and local seismic networks. In general, the earthquakes are more frequent in the Hindukush Pamir region and at the syntaxes at Assam and Kashmir. In Tibet the distribution of earthquakes is irregular and no definite trends are identified while in the Himalaya epicentres of moderate sized earthquakes are located between MCT and MBT (Molnar, et al., 1973; Chandra, 1978; 1981; Seeber et al., 1981; Ni and Barazangi, 1984). This belt is about 50 km in width and the majority of earthquakes are located just south of MCT (Ni and Barazangi, 1984) (Fig.1.4).

Focal depths reported by the ISC for Himalayan earthquakes are generally unreliable because of the trade off between depth and origin time in routine earthquake location procedures. However, the focal depths of about twenty moderate magnitude earthquakes have

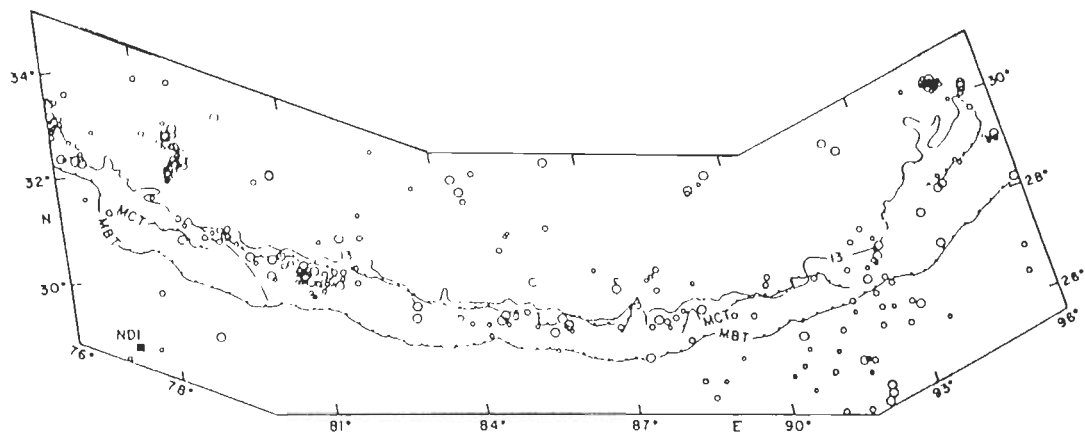


Fig.1.4 A selected map (Lambert conic conformal projection) of the Himalayan region showing International Seismological Centre locations for earthquakes occurring between 1961 and 1981. Large, medium and small open circles represent very good, good and fair quality of epicentres. The MCT and many of the Himalayan earthquakes lie south of the 13,000 ft (=4 km) contour (after Ni and Barazangi, 1984).

been estimated using waveform modelling method and in some cases depth phases have been used as well (Molnar, 1990). The results of these exercises show that the moderate earthquakes occur at depths between 10-18 km (Seeber et al., 1981; Baranowski, 1984; Ni and Barazangi, 1984) (Fig.1.5). Thus the focal depths of these earthquakes are assumed to coincide with the depth of detachment (Ni and Barazangi, 1984) and hence it is suggested that these earthquakes occur in response to the underthrusting of Indian shield rocks beneath the Himalaya.

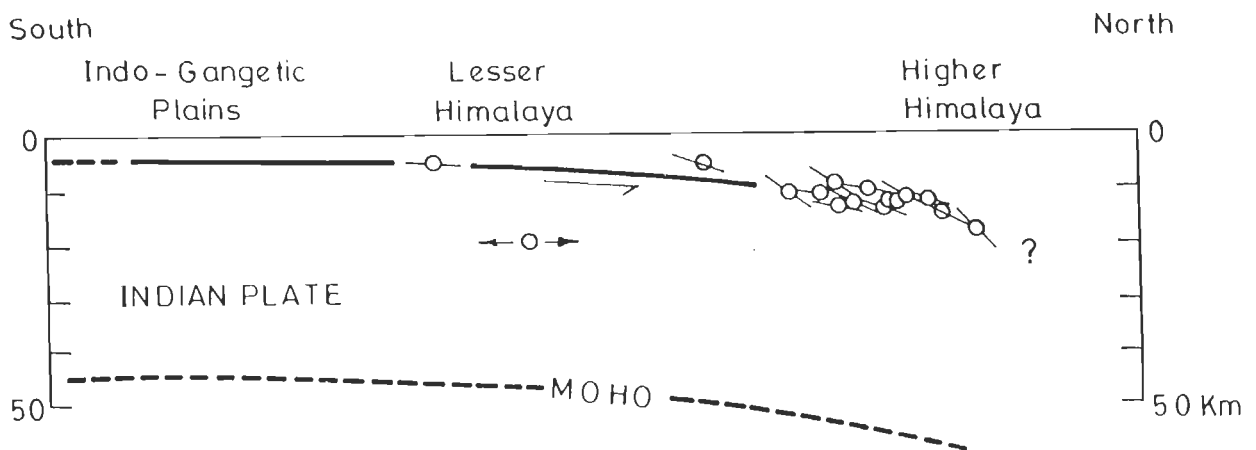


Fig.1.5 Projections of hypocentres and nodal planes onto a profile across the Himalaya (modified after Ni and Barazangi, 1984).

1.2.4.2 Great earthquakes

The surface effects of the four great Indian earthquakes (Fig.1.6) of past 100 years have been reported and studied in detail (Oldham, 1899; Middlemiss, 1910; Dunn et al., 1939; Ramchandra Rao, 1953). Deformation associated with the 1897 earthquake occurred over most of the Shillong plateau, but no primary surface faulting was observed. Molnar et al. (1977) and Molnar (1987b) suggested that faulting beneath the Shillong plateau rather than the Himalaya is associated with this great earthquake. Similarly for the other three great earthquakes, no surface faulting was observed but their ruptures are assumed to lie on shallow gently dipping thrust faults under the Lesser and Outer Himalaya (Seeber and Armbruster, 1981; Molnar and

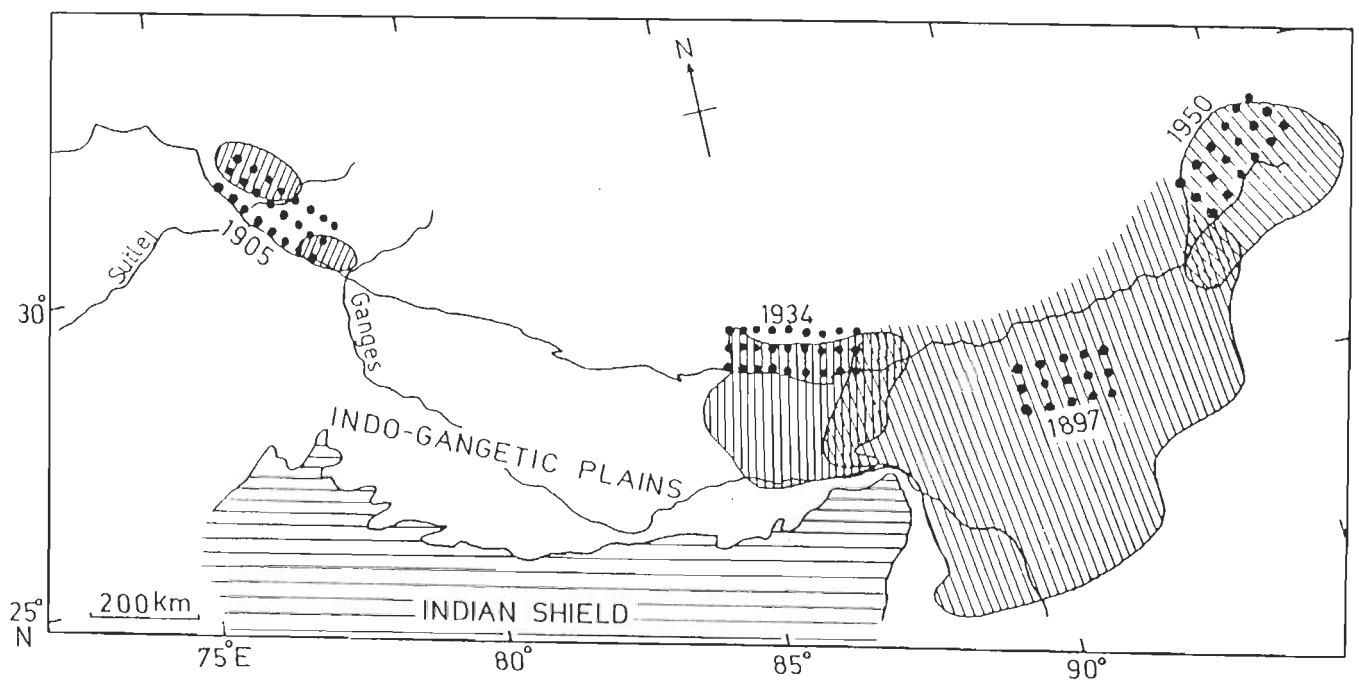


Fig.1.6 A composite map of the region of perceptible damage during the great earthquakes of 1897, 1905, 1934 and 1950 are shown by hatching. The areas identified by solid dots indicate estimated rupture zones of these earthquakes. The ruptures of 1905 and 1897 earthquakes are identified in the Chapters III and IV of the present thesis. The rupture of 1934 is after Chander (1989a) and that of 1950 after Molnar and Pandey (1989) (modified after Seeber and Armbruster, 1981; Molnar and Pandey, 1989; Chander, 1989a).

Pandey, 1989; Molnar 1987b and 1987c). Seeber and Armbruster (1981) assumed that they lie on the detachment (Fig. 1.3). In case of 1934 earthquake Seeber and Armbruster (1981) assumed that the rupture extended southward beneath the Indo-Gangetic Plains also. However, Chen and Molnar (1977) and Chander (1989a) concluded that the rupture was located in a buried thrust fault under the Lesser and Outer Himalaya in a manner similar to that deduced for the 1905 Kangra earthquake (Molnar, 1987c; Chander, 1988; 1989b; Molnar and Pandey, 1989). The rupture zone of 1950 earthquake was inferred on the basis of aftershocks which were dispersed over a broad area extending both westward and south-southwestward from the epicentre of the mainshock. A reassessment of the location of these aftershocks indicates (Molnar and Chen, 1977; Molnar and Deng, 1984; Molnar and Pandey, 1989) that virtually all of them occurred beneath the Himalaya and not southwest of mainshock. Thus the rupture of 1950 earthquake also lies under the Lesser and Outer Himalaya.

In short the ruptures of great Himalayan earthquakes of 1905, 1934 and 1950 are assumed to lie on the detachment under the Outer and Lesser Himalaya. Their northern limit is assumed to coincide with the seismic belt of moderate magnitude earthquakes (Seeber and Armbruster, 1981; Chander, 1988; 1989a; Molnar, 1990).

1.2.4.3 Small earthquakes

Despite the fact that the errors in hypocentral locations are less in case of locally recorded earthquakes, as compared to those recorded teleseismically, the data from local seismic networks in the Himalaya are very limited. Here we discuss the well reported results of microearthquake studies from two regions in the Himalaya, (1) the Garhwal Kumaun Himalayan region of Uttar Pradesh, India, (Gaur, et al. 1985; Khattri et al., 1989) (Fig. 1.7) and (2) Hazara arc region of northern Pakistan (Armbruster et al., 1978; Seeber et al., 1980) (Fig. 1.8). The micro-earthquakes in Garhwal Himalaya occur along a fairly narrow belt which crosses the surface trace of MCT several times. It coincides with the trend of epicentres of moderate

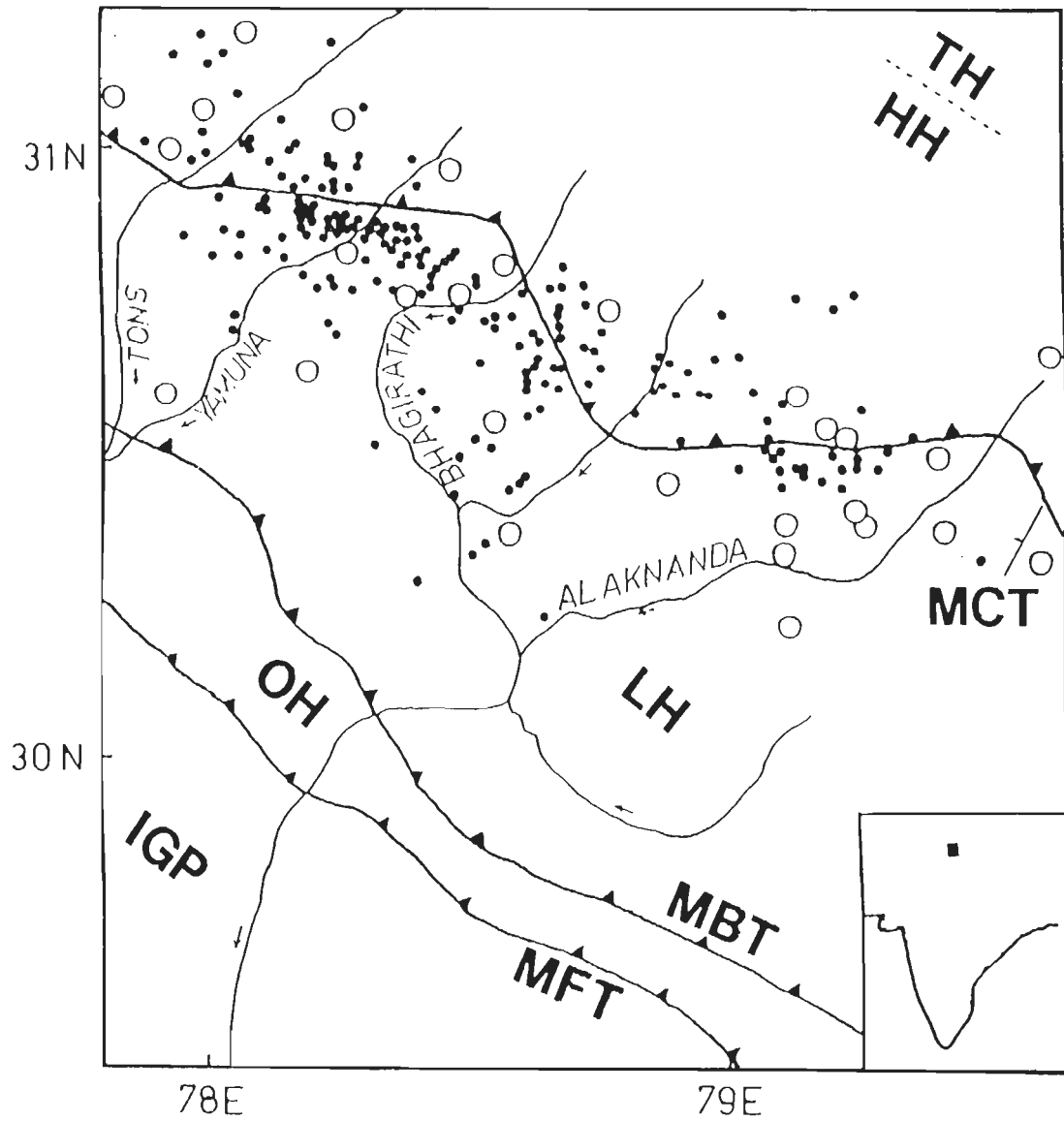


Fig.1.7 Microearthquakes in the Garhwal Himalaya are shown with the dots (modified after Khattri et al., 1989). Open circles denote the epicentres of moderate earthquakes.

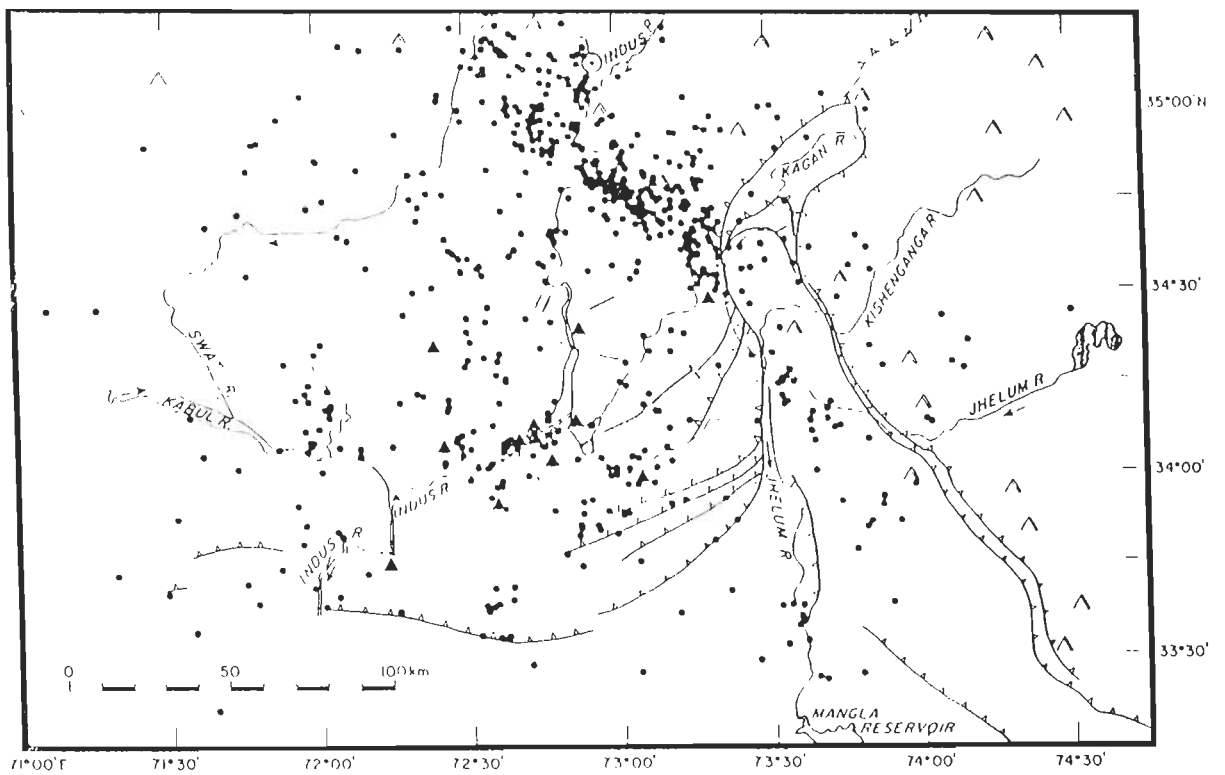


Fig.1.8 Microearthquakes, shown by dots, recorded by the Tarbela seismic network, recording stations shown by the solid triangles, from August 15, 1973 to July 12, 1974. A topographic front, as indicated by the >3000 m high mountain peak, is also shown (after Armbruster et al., 1978).

magnitude earthquakes in the region. The majority of micro-earthquakes have focal depths less than 13 km and hence it appears that they occur due to the internal deformation of the overthrusting Himalayan wedge above the detachment.

The micro-earthquakes in Hazara arc, however, occur along the detachment which outcrops at the Salt range (Fig.1.9). In Hazara arc region, the Indus Kohistan Seismic Zone (IKSZ), a major blind thrust zone associated with a topographic front, is interpreted as the extension of BTF of the Himalaya (Seeber and Armbruster, 1981). In this region the focal depths of the micro-earthquakes have a sharp upper bound at a depth of about 10 km and do not reach the surface. This substantial sharp boundary to the intense seismicity on the IKSZ is interpreted as a detachment, which can be traced from the seismicity data far to the south of IKSZ and which appears to outcrop at the Salt range in northern Pakistan (Armbruster et al., 1978; Seeber et al., 1980).

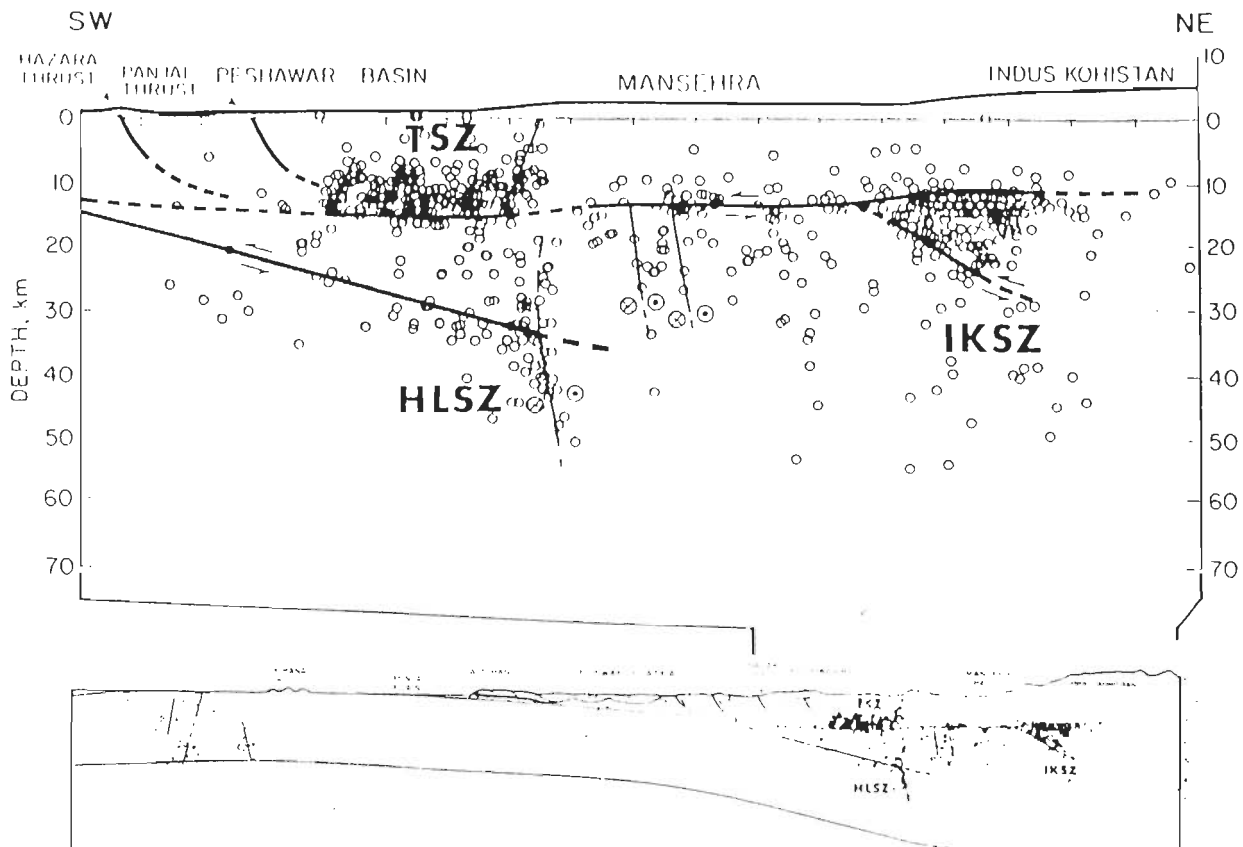


Fig.1.9 Earthquake hypocenters from a local network in Hazara projected onto a NE section. TSZ- Tarbela Seismic Zone, HLSZ- Hazara Lower Seismic Zone, IKSZ- Indus Kohistan Seismic Zone (after Seeber and Armbruster, 1983).

1.2.5 Focal mechanism of Himalayan earthquakes

Focal mechanisms along with the depth distribution of earthquakes have provided evidence for plate tectonics hypothesis. Fitch (1970) presented the first focal mechanism solutions, based on teleseismic and regional data for thirteen earthquakes in the Himalaya and adjoining region. Epicentres of four of these earthquakes are located in the Himalayan region. The sense of slip on the preferred nodal plane for the thrust type focal mechanisms of these four earthquakes is consistent with the underthrusting of Indian plate beneath the Himalaya (Fitch, 1970).

At the moment, fault plane solutions based on waveform synthesis are available for about twenty earthquakes of the Himalayan seismic belt (Fig.1.10) (Baranowski et al., 1984; Ni and

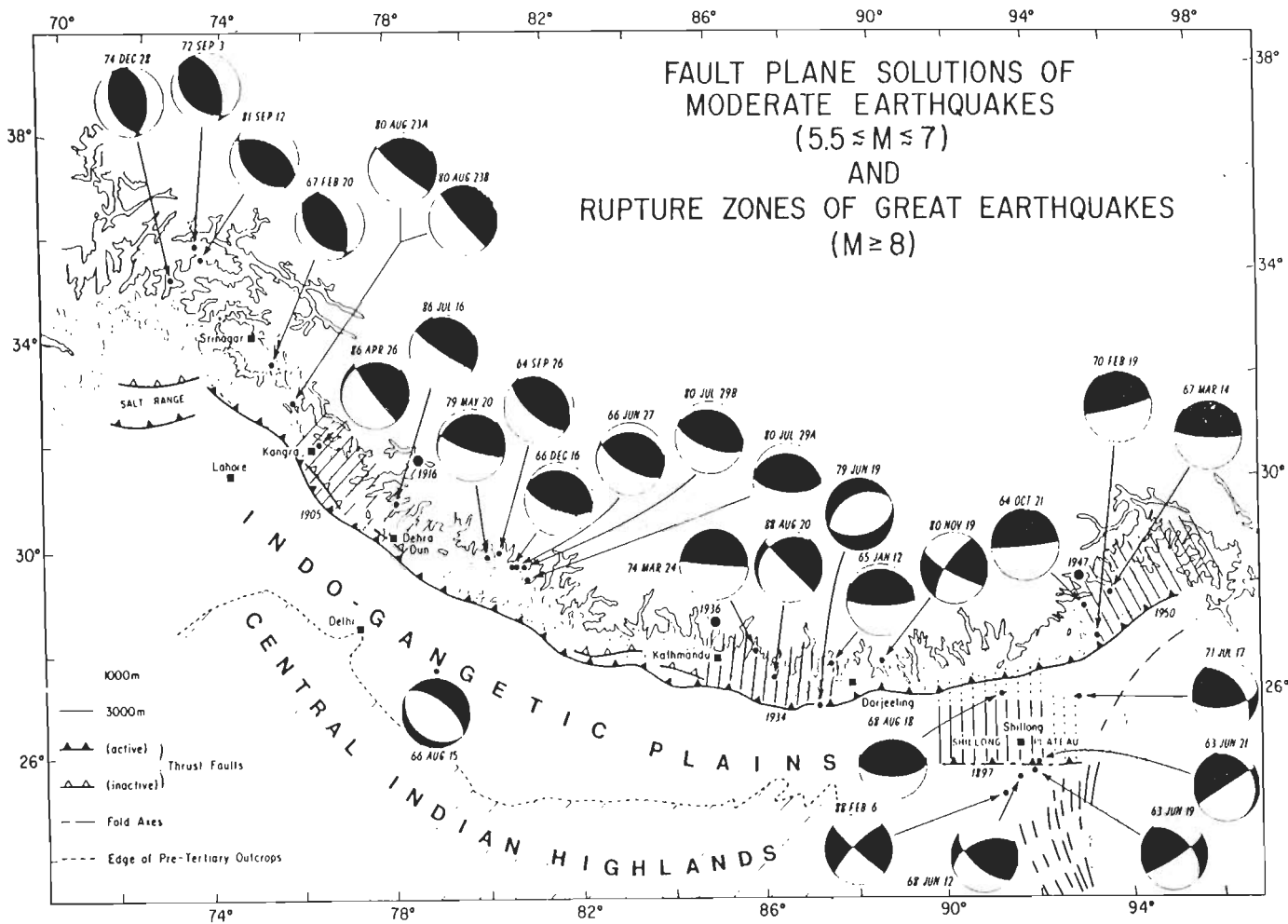


Fig.1.10 Map showing epicentres and fault plane solutions of moderate earthquakes since 1963, epicentres of major earthquakes ($M \geq 7$) since 1900 and rupture zones of great earthquakes since 1897. In lower hemisphere projections of focal spheres, blackened quadrants include compressional first motions and T axes (after Molnar, 1990).

Barazangi, 1984; Ekstrom, 1987; Dziewonski et al., 1989; Molnar and Lyon-Caen, 1989). They indicate thrust faulting with the one nodal plane dipping gently northward or northeastward and with the other plane dipping steeply southward or southwestward. It is generally accepted that the shallow north dipping nodal planes are the fault planes (Molnar, 1990). Thus these fault plane solutions are consistent with the view that underthrusting of Indian plate occurs beneath the Outer and Lesser Himalaya. One strike slip fault plane solution has also been observed. This has been found to be associated with transverse tectonic structures in the Himalaya (e.g. Valdiya, 1976; Khattri and Tyagi, 1983b; Ni and Barazangi, 1984; Verma and Krishna Kumar, 1987). The earthquakes occurring under the Tibetan plateau show normal and strike slip faulting (Molnar, 1992). This agrees with the east-west crustal extension of the high plateau. The two events beneath the Indo-Gangetic Plains and Outer Himalaya also show normal faulting with tension axis approximately perpendicular to the strike of the Himalayan arc. These events are most probably due to flexing of the Indian plate as it bends and underthrusts the Himalaya (Molnar et al., 1977; Molnar and Chen, 1982; Ni and Barazangi, 1984).

The fault plane solutions of the great Himalayan earthquakes of 1897, 1905 and 1934 are not available but they are assumed to have occurred due to the thrust type motion on the detachment under the Outer and Lesser Himalaya (Seeber and Armbruster, 1981; Molnar and Deng, 1984; Khattri, 1987; Molnar, 1987c; Chander, 1988; 1989a; Molnar and Pandey, 1989). Although the epicentre of the 1897 earthquake was assumed to lie under the Shillong plateau which is to the south of the Himalaya, the motion on the causative fault was deduced to be of thrust type (Oldham, 1899; Molnar, 1987b). For the 1950 earthquake the fault plane solution is not well constrained. Initially Tandon (1955) inferred slip on either a steeply or a gently dipping east trending normal fault, whereas Ben-Menahem et al. (1974) inferred pure right lateral strike slip motion on a plane dipping 55° to the east and striking northwest southeast. Chen and Molnar (1977) found the data to be equally consistent with a thrust fault dipping

gently (12°) to the north, which is similar to the solutions of other earthquakes in the Himalaya. Although the distribution of aftershocks suggests a mixture of thrust and strike slip faulting, yet Molnar and Pandey (1989) concluded that the reexamination of relocated aftershocks suggests that the rupture occurred primarily on a gently north-northwest dipping thrust fault.

Thus the above review suggests a broad consensus among several investigators that the moderate and great earthquakes in Himalaya involve thrust motion on a shallow gently dipping plane which is assumed to coincide with the surface of detachment.

1.2.6 Studies of seismic gaps in the Himalaya

Within the framework of plate tectonics, the seismic gap hypothesis has been applied at the convergent plate boundaries where oceanic crust is involved. The hypothesis states that great earthquakes are likely to occur along sections of the detachment of convergent plate margins which have ruptured in past but have not experienced great earthquakes at least in the past few decades. The probability of occurrence of great earthquakes increases proportionally with the time elapsed since the last great earthquake because strain accumulates as a consequence of plate movements over decades or centuries. One of the important prerequisites of the hypothesis is the good understanding of the tectonics. In case of continental plate boundaries which are more diffused and complex and hence in general poorly understood, the gap concept becomes more difficult to apply.

Seeber and Armbruster (1981) estimated the rupture extents of four great Himalayan earthquakes on the basis of their intensity contours and other macroscopic effects. They suggested a rupture length of about 300 km for the 1905, 1934 and 1950 earthquakes, whereas for the 1897 earthquake, a rupture length of about 500 km is suggested. West of 1905 Kangra earthquake rupture, they identified a segment of detachment unruptured since 1800. This segment, located in Kashmir region, lies between ruptures of 1885 and 1905 earthquakes

(Fig.1.11). However, as the tectonics of this region is poorly understood they were not sure whether the detachment can generate great earthquake. Further Seeber and Armbruster (1981) concluded that a seismic gap exists between the ruptures of 1905 and 1934 provided the ruptures of 1803 and 1833 are not as large as the great Himalayan earthquakes (Fig.1.11). They inferred that the ruptures of 1934 and 1897 and those of 1897 and 1950 abut, thus leaving no seismic gap in between these ruptures (Fig.1.11). They have suggested the repeat time of a great Himalayan earthquake to be about 200 - 270 years.

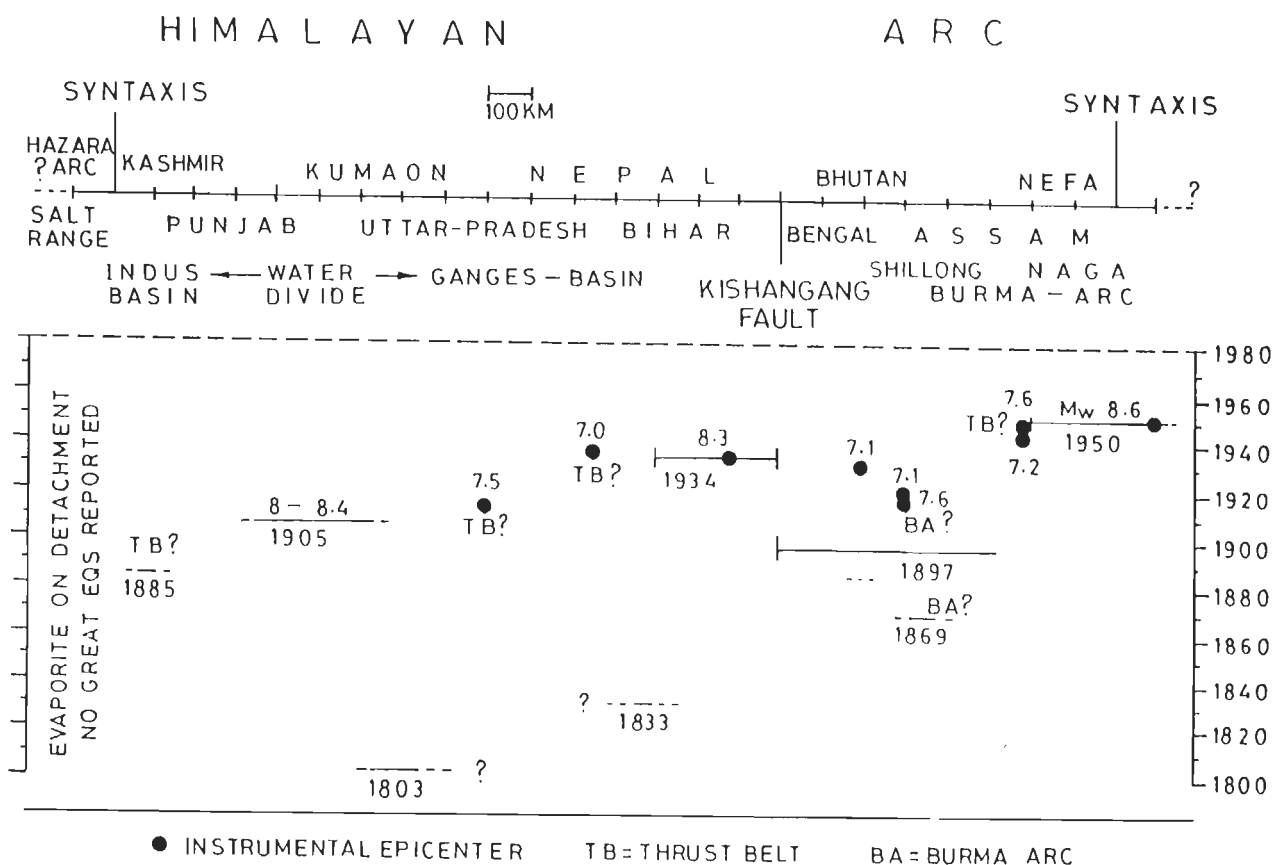


Fig.1.11 Space time diagram of detachment ruptures along the Himalaya after 1800 (after Seeber and Armbruster, 1981).

Khattri and Tyagi (1983a) and Khattri (1987) studied the space time distribution of earthquakes along the Himalayan convergent plate margin and showed that all great earthquakes were preceded by seismically quiescent periods of at least 19 years. They identified three seismic gaps (Fig. 1.12) along the plate margin (i) Kashmir gap: the unruptured area lying west to the 1905 rupture (ii) Central gap : between 1905 and 1934 earthquake ruptures and (iii) Assam gap : situated between the ruptures of 1897 and 1950 earthquakes. Further they reported a decrease in seismicity following the year 1970 in the Central gap, just east of the 1905 earthquake rupture, and in the Assam gap. Thus according to Khattri (1987) these two gaps are the regions of high seismic potential from the point of view of future great earthquakes.

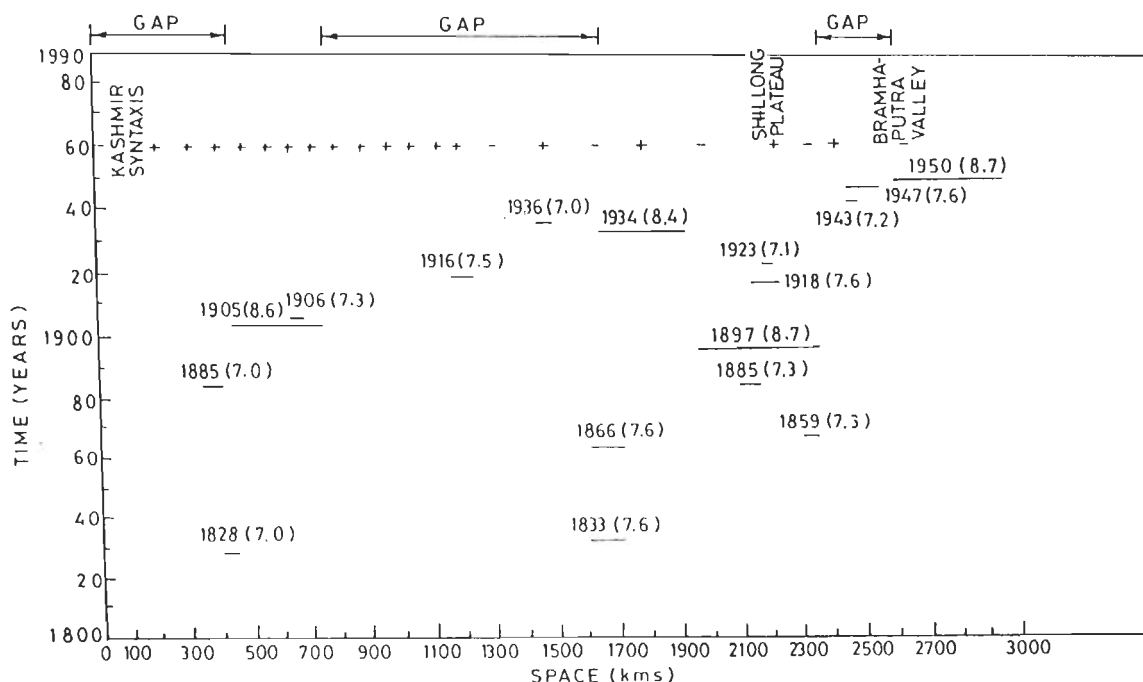


Fig.1.12 Rupture zones of major earthquakes ($M \geq 7$) in the Himalaya and adjacent regions. The three seismic gaps namely, Kashmir, Central and Assam gaps are also identified in the figure (after Khattri, 1987).

Molnar (1987b and 1987c), Molnar and Pandey (1989) and Molnar (1992) identified the rupture lengths of great Himalayan earthquakes of 1905, 1934, 1897 and 1950 to be about 280

km, 200 ± 40 km, 200 ± 100 km and 250 km respectively. Thus according to them only 30 - 35% of the plate margin has ruptured in the last 100 years. In accord with the views of Khattri and Tyagi (1983a) they inferred that the areas most likely to rupture next are those that did not rupture in these great earthquakes. Further, they proposed that the recurrence intervals of such earthquakes are likely to be between 200 and 500 years with a likely value of 300 years.

Chander (1988) interpreted the observed ground level changes due to the 1905 Kangra earthquake and concluded that the rupture of this earthquake had a length of about 280 km. He proposed that the rupture of this earthquake lies on the detachment under the Outer and Lesser Himalaya. For the 1934 Bihar-Nepal earthquake Chander (1989a) argued that the rupture of this earthquake was similar to that of 1905 and that it did not extend under the Indo-Gangetic Plains as deduced by Seeber and Armbruster (1981). He identified that the seismic gap of nearly 700 km between the rupture zones of 1934 and 1905 earthquakes is now vulnerable.

1.2.7 Other studies supporting the plate tectonics view of underthrusting in the Himalayan region

1.2.7.1 Gravity anomalies in the Himalaya

Gravity anomalies in the Himalaya are used to place constraints on the deep structure and the dynamics of mountain building (Warsi and Molnar, 1977; Qureshy and Warsi, 1980; Karner and Watts, 1983; Lyon-Caen and Molnar, 1983; 1985; Verma and Prasad, 1987). Large Bouguer anomalies in the Himalaya become increasingly negative as the elevation increases. The large negative isostatic anomalies over the Gangetic plains and large positive anomalies in the Higher Himalaya indicate deviation from local isostatic compensation (e.g. Warsi and Molnar, 1977; Lyon-Caen and Molnar, 1983). The former can be explained by the several kilometre thick low density upper Cenozoic sediments, whereas the latter could be a result of thickening of a basaltic layer in the lower crust (Qureshy and Warsi, 1980).

The undercompensation of the Himalaya and overcompensation of the Gangetic plains can be understood if we assume that the Indian plate is flexed down by the load of the Himalaya and its strength supports part of the mass of the Himalaya (Karner and Watts, 1983; Lyon-Caen and Molnar, 1983). However, Lyon-Caen and Molnar (1983) found the load of the Higher Himalaya to be too large to be supported solely by the strength of the Indian plate without additional forces applied to it. They found that the Higher Himalaya can be supported by the Indian plate if an external force or a moment is applied to end of the plate and suggested that the source of this external force could be gravity acting on the cold mantle part of the Indian lithosphere detached from the crust (Lyon-Caen and Molnar, 1983).

The analyses and interpretation of gravity anomalies over Indo-Gangetic Plains and the Himalaya (Lyon-Caen and Molnar, 1983 and 1985) suggest a very gentle dip (2° - 3°) of Moho beneath the Lesser Himalaya and steeper dip (10° - 15°) under the Higher Himalaya. This is consistent with the Indian plate extending intact northward beneath the Himalaya and being flexed down as an effectively elastic plate (Molnar, 1990).

1.2.7.2 Studies of P_n and S_n wave propagation beneath the Himalaya

The P_n and S_n travel times from the Himalayan earthquakes to the Worldwide Standard Seismograph Network (WWSSN) stations in northern Afghanistan, India and to the local network stations in northern Pakistan have been used to resolve the uppermost mantle P and S wave velocities (Menke and Jacob, 1976; Ni and Barazangi, 1983). The high P_n and S_n velocities of about 8.5 and 4.7 km/sec (Ni and Barazangi, 1983) indicate that the uppermost mantle structure beneath the Himalaya is not significantly different from that of India and southern Tibet and is consistent with the underthrusting of Indian plate beneath the Himalaya and southern Tibet.

1.2.7.3 Deep seismic sounding studies in the Himalaya and southern Tibet

Deep seismic sounding studies in the Himalaya and Tibet have provided significant information about their velocity structures (Kaila et al., 1978; Belousov et al., 1980; Hirn and Sapin, 1984; Hirn et al., 1984a and 1984b; Hirn, 1988; Zhao et al., 1993). The unreversed profile in the western Himalaya indicates a moderate 15° - 20° northwesterly dip of Moho (Kaila et al., 1978). Hirn and his colleagues collected the wide angle reflection data in the Tethys and Higher Himalaya. Seismograms from Arun and Kathmandu valleys showed two clear phases. The later phases were interpreted as reflections from Moho at a depth of 75 km (Lepine et al., 1984). The earlier phases were attributed to reflection from the top surface of underthrusting Indian plate (Hirn and Sapin, 1984). The seismograms from stations located north of Higher Himalaya (Hirn et al., 1984a) show a southward dipping reflector from 45-50 km depth. Hirn et al. (1984a) interpreted it as the southward dipping Moho whereas Molnar (1988) argued that it can be associated with reflections from an interface within the crust. In his view reflections are consistent with a Moho depths increasing smoothly from 50-55 km depth under the Higher Himalaya to about 70 km beneath the southern Tethys Himalaya.

Recently Zhao et al. (1993) reported results of a deep seismic reflection study along a 100 km long profile located in the Tethys Himalaya. The profile shows midcrustal reflections that probably mark the active detachment thrust fault along which the Indian plate is underthrusting beneath Himalaya and southern Tibet (Zhao et al., 1993). At the southern end of the profile the reflections are at about 28 km depth and at the northern end at about 40 km depth, suggesting a northward dip of about $9 \pm 2^{\circ}$ for the detachment (Zhao et al., 1993). The profile also shows Moho reflections at a depth of about 75-80 km. It thus supports the view of crustal thickening beneath the southern Tibet.

1.3 Summary of the review

The data available to us being limited and mostly qualitative, we are not in a position to

spin out new quantitative models for the Himalayan earthquakes. Our best option is to test available hypotheses and views in light of the data at hand. The two features important to us that emerge from the review are as follows. Firstly, the rocks of the Outer and Lesser Himalaya are separated from those of the Indian shield along a gently dipping thrust fault type surface of detachment. Secondly, the seismicity and active tectonics of the Himalaya are linked with plate-tectonics slip on the detachment.

1.4 Repetition in text

A new problem is taken up and discussed at length in each of Chapters III to VIII. This has involved certain amount of repetition in text for the sake of completeness in local context. Still we have made every effort to keep such repetitions to a minimum.

CHAPTER II

Theoretical considerations

2.1 Introduction

We solve an inverse problem every time we analyze or interpret a set of geophysical observations. In such problems we know the effects (observations) and simulate their causes within the earth. The inverse problems solved in the next four chapters have a common feature in that observations of ground elevation changes are explained on the assumption that they arise only due to the slips on subsurface faults. We provide the relevant theoretical formulations in this chapter.

Solution of an inverse problem is dependent on the availability of the solution to the corresponding direct problem, i.e., the problem in which we know the causes within the earth and have to predict their effects. The direct problem for us is to predict the surface elevation changes when the model of slip on a buried fault or a set of faults is given. This problem has been solved in the literature using the elastic dislocation theory, which is reviewed in Section 2.2 below.

The present inverse problem is non-linear for most parameters related to subsurface faults. But it is linear for amount of slip on the faults if other fault parameters are fixed. We have tackled both classes of problems in the following chapters. The non-linear inverse problems have been solved by the interactive trial and error method. The linear inverse problems of estimating slips on set of faults of prescribed orientations and locations have been solved using the regularized minimum norm inversion method.

2.2 Elastic dislocation theory

2.2.1 Theoretical developments

V. Volterra appears to have been the first to consider the elastic theory of dislocations during the first decade of this century (see Love, 1944, p.221). Steketee (1958) used Volterra's formulation and calculated the static displacement field due to slip on a vertical strike-slip fault by treating it as a point source buried in an elastic half space. Corresponding expressions for vertical strike-slip faults of finite extent were derived by Chinnery (1961, 1963). Further expressions for ground displacement due to buried vertical strike-slip and vertical dip slip faults were derived by Maruyama (1964), Press (1965) and Savage and Hastie (1966). The case of a rectangular fault of arbitrary orientation and oblique slip has also been solved (Mansinha and Smylie, 1971; Sato and Matsu'ura 1974, Yamazaki 1975, Matsu'ura 1977, Iwasaki and Sato, 1979, Matsu'ura and Tanimoto, 1980, Davis 1983 and Okada, 1985).

The effects on displacement fields of earth's curvature (McGinly, 1969; Ben-Menahem et al., 1969; 1970; Smylie and Mansinha, 1971), surface topography (Ishii and Takagi, 1967a; Takemoto, 1981; Segall and McTigue, 1984), horizontally uniform crustal layers (Ishii and Takagi, 1967b; McGilney, 1969; Ben-Menahem and Gillon, 1970; Singh, 1970, Sato, 1971; Rybicki, 1971; Chinnery and Jovanovich, 1972; Sato and Matsu'ura, 1973; Jovanovich et al, 1974 a and b; Matsu'ura and Sato, 1975; Singh and Garg, 1985; Ma and Kusznir, 1993), horizontally non-uniform crustal layers (Sato, 1974; Sato and Yamashita, 1975) and of lateral material inhomogeneities (Rybicki, 1971; 1978; Rybicki and Kasahara, 1977; McHugh and Johnston, 1977; Niewiadomski and Rybicki, 1984) have been considered.

2.2.2 Applications for inversion

The first practical geophysical application of the dislocation theory was by Rochester (1956). He studied the displacement field due to slip on the San Andreas fault during the San Francisco earthquake of 1906. Savage and Hastie (1969) used this theory to interpret the 1964

Alaska earthquake data. The theory has now become popular for inversion of geodetic observations of crustal movements to infer the slip distribution on subsurface causative faults and also to estimate approximately the rate of aseismic slip at plate margins. Such work on the Loma-Prieta earthquake is especially notable.

The analyses of ground elevation change observations have been carried out so far by assuming an isotropic, homogeneous elastic half space and simple rupture geometries (Stein and Lisowski, 1983; Barrientos, 1988; Chander, 1988; Lin and Stein, 1989; Ward and Valendise, 1989; Barrientos and Ward, 1990) largely because this provides convenient but useful results consistent, to a first approximation, with the quality of crustal movement data available (see also Okada, 1985).

We have used the mathematical expressions of Mansinha and Smylie (1971) for our analyses of Chapters III to VI where we interpret respectively the coseismic data pertaining to the 1897 Assam and 1905 Kangra earthquakes and the interseismic data from the central Nepal and Dehradun regions.

2.3 Formulas for ground displacements due to finite ruptures in faults

Let us assume a homogeneous, isotropic and perfectly elastic solid half space. Let the origin O of an $Ox_1x_2x_3$ coordinate system lie in the free surface of the half space (Fig.2.1). Let the x_3 axis be normal to the free surface pointing downward and x_1 axis be along the strike of the fault which lies along the intersection between the fault plane and free surface. Let θ be the dip of a fault relative to the assumed horizontal free surface of the half space. Let ξ be the dip parallel distance of a general point in the fault plane from the x_1 axis. Thus a point with coordinates (ξ_1, ξ) in the fault plane has coordinates $(\xi_1, \xi \cos\theta, \xi \sin\theta)$ in the $Ox_1x_2x_3$ coordinate system of Fig.2.1. Let the rectangular rupture in the fault plane be delineated by $-L \leq \xi_1 \leq L$ and $d \leq \xi \leq D$.

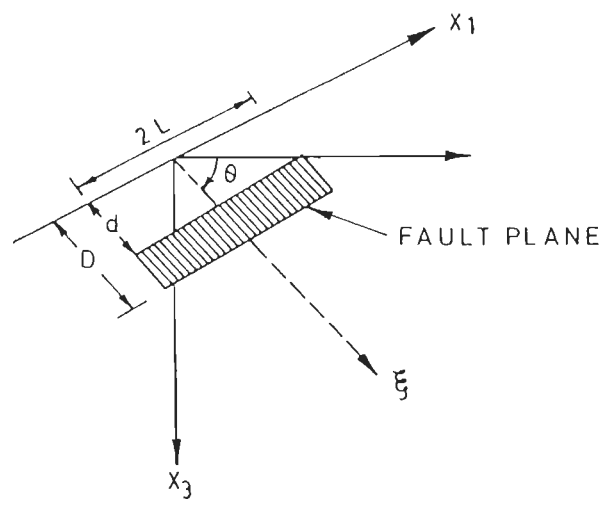


Fig.2.1 Fault geometry and coordinate system.

Thus the rupture in the fault has a length $2L$ along strike and width $b (=D-d)$ along dip of the fault. Let U_d and U_s respectively be the uniform slips in the dip and strike directions across the ruptured section of the fault. As a result of this slip, the particles of the medium will oscillate but will settle down eventually in positions which are in general different from their pre-slip positions. Let u_1 , u_2 and u_3 be the x_1 , x_2 and x_3 components of such permanent displacement. Mansinha and Smylie (1971) give the following general formula applicable to all components of displacement at a point in the free surface of the half space.

$$u_i(x_1, x_2, 0) = f_i(L,D) - f_i(L,d) - f_i(-L,D) + f_i(-L,d), \quad (i=1,2,3) \quad \dots(2.1)$$

The detailed mathematical expressions for the f_i 's for dip component U_d of fault slip are as follows.

$$\begin{aligned} f_1(\xi_1, \xi) = & U_d/12\pi[(x_2-\xi_2)\sin\theta\{(6/R)-(3/(R+\xi_3))\} \\ & -\cos\theta\{3\ln(R+\xi_3)-6\xi_3/R\} \\ & +3/\cos\theta\{\ln(R+\xi_3)-\sin\theta \ln(R-r_3+\xi)\}] \end{aligned} \quad \dots(2.3a)$$

$$\begin{aligned} f_2(\xi_1, \xi) = & U_d/12\pi[\sin\theta\{3(x_1-\xi_1)/(R+\xi_3)+6(x_2-\xi_2)^2/R(R+x_1-\xi_1)\} \\ & -\cos\theta\{-6(x_2-\xi_2)\xi_3/R(R+x_1-\xi_1) \\ & +6\tan^{-1}((x_1-\xi_1)(x_2-\xi_2)/(h+\xi_3)(R+h)) \\ & -6\tan^{-1}((x_1-\xi_1)(r_3-\xi)/r_2R)\} \\ & +6\{(1/\cos\theta)\tan^{-1}((k-r_2\cos\theta)(R-k)+(-r_3+\xi)k\sin\theta/ \\ & (x_1-\xi_1)(-r_3+\xi)\cos\theta)\}] \end{aligned} \quad \dots(2.3b)$$

$$\begin{aligned} f_3(\xi_1, \xi) = & U_d/12\pi[\sin\theta\{(x_2-\xi_2)\{-6\xi_3/R(R+x_1-\xi_1) \\ & -6\tan^{-1}((x_1-\xi_1)(x_2-\xi_2)/(h+\xi_3)(R+h)) \\ & -9\tan^{-1}((x_1-\xi_1)(r_3-\xi)/r_2R)\} \\ & -6\cos\theta\{\xi_3^2/R(R+x_1-\xi_1)\}] \end{aligned} \quad \dots(2.3c)$$

where

$$R^2 = (x_1 - \xi_1)^2 + (x_2 - \xi_2)^2 + \xi_3^2$$

$$r_2 = x_2 \sin \theta$$

$$r_3 = x_2 \cos \theta$$

$$h^2 = r_2^2 + (-r_3 + \xi)^2$$

$$k^2 = (x_1 - \xi_1)^2 + r_2^2$$

Similarly the detailed mathematical expressions for the f_1 's for strike component U_s of fault slip are as follows.

$$\begin{aligned} f_1(\xi_1, \xi) = & U_s / 12\pi [(x_1 - \xi_1) \{ 2x_2 \sin \theta / R (R + x_2 \cos \theta - \xi) - \\ & 4x_2 \sin \theta / R (R - x_2 \cos \theta + \xi) - 3 \tan \theta / R \} \\ & 6 \tan^2 \theta \tan^{-1} \{ (k - x_2 \sin \theta \cos \theta) (R - k) + (-x_2 \cos \theta + \xi) k \sin \theta \} / \\ & (x_1 - \xi_1) (-x_2 \cos \theta + \xi) \cos \theta \} \\ & \tan^{-1} \{ (x_1 - \xi_1) (x_2 \cos \theta - \xi) / x_2 \sin \theta R \}] \end{aligned} \quad \dots (2.2a)$$

$$\begin{aligned} f_2(\xi_1, \xi) = & U_s / 12\pi [\cos \theta \ln (R + x_2 \cos \theta - \xi) + \\ & (1 + 3 \tan^2 \theta) \ln (R - x_2 \cos \theta + \xi) - 3 \tan \theta \sec \theta \ln (R + \xi_3) \\ & 6x_2 \sin^2 \theta / R - 2x_2 \sin \theta / R (R + x_2 \cos \theta - \xi) \\ & + 4x_2 \sin \theta / R (R - x_2 \cos \theta + \xi)] \end{aligned} \quad \dots (2.2b)$$

$$\begin{aligned} f_3(\xi_1, \xi) = & U_s / 12\pi [\cos \theta \{ \ln (R + r_3 - \xi) + (1 + 3 \tan^2 \theta) \ln (R - r_3 + \xi) - \\ & 3 \tan \theta \sec \theta \ln (R + \xi_3) \} \\ & + 6r_2 \sin \theta / R - 2r_2^2 \cos \theta / R (R + r_3 - \xi) \\ & + 4r_2 r_3 \sin \theta / R (R + r_3 + \xi)] \end{aligned} \quad \dots (2.2c)$$

2.4 Methods employed to solve the inverse problems

2.4.1 General remarks

Since the observations to be interpreted in following four chapters pertain to ground elevation changes we mould rest of the discussion of this chapter in that light. Also, since we invert most of the observations in terms of pure dip slip relative motion across ruptured sections of causative faults, we describe here the procedure using expressions of Eqns. 2.1 and 2.2c only. Similar procedure applies for the strike slip component of fault slip as well as for the inversions based on Eqn.2.4.

Let $y_1 \dots y_m$ be the ground elevation changes observed at m benchmarks. We shall equate the y 's with the u_3 displacement components at surface points of the elastic half space considered in the preceding section. Let $(x_{1i}, x_{2i}, 0; i=1,2,..m)$ be the coordinates of the m benchmarks when simulated on the surface of the half space of Fig.2.1. Then

$$u_{3i}(x_{1i}, x_{2i}, 0) = F(L, d, D, U_d, \Theta, x_{1i}, x_{2i}), \quad i=1 \dots m \quad \dots(2.4)$$

where,

$$F = U_d a(\mathbf{p}, x_{1i}, x_{2i}) \quad \dots(2.5)$$

Explicit forms of F and a are obtainable from Eqns. 2.1 and 2.2c. \mathbf{p} denotes a vector of all the fault parameters except U_d . Thus the elements of \mathbf{p} include fault length ($2L$), locations d and D of the shallower and deeper fault edges parallel to fault strike and the fault dip (Θ). Also involved in u_{3i} is the position $(x_{1i}, x_{2i}, 0)$ of the i th benchmark.

In Eqn.2.5 the function a is nonlinear for all its arguments. Consequently the function F is also nonlinear for these fault parameters, however it is linear in fault slip U_d as it appears in it as a multiplicative factor.

We consider in Chapters III to VI ground elevation changes due to slips on sets of rectangular ruptures either in the same fault or different faults. Let there be n faults with parameter vectors $\mathbf{p}_1, \mathbf{p}_2 \dots \mathbf{p}_n$ and slip amounts $U_{d1}, U_{d2} \dots U_{dn}$ respectively. Then

$$\begin{aligned}
u_{3i} &= \sum_{j=1}^n F(\mathbf{p}_j, U_{dj}, x_{1i}, x_{2i}) \\
&= \sum_{j=1}^n U_{dj} a_{ij} \quad (i=1 \dots m) \quad \dots(2.6)
\end{aligned}$$

where a_{ij} is the $a(\mathbf{p}_j, x_{1i}, x_{2i})$ of Eqn.2.5.

2.4.2 Inversions using the trial and error method

In many of the inversions, we attempt to minimize the total squared error $\sum (y_i - u_{3i})^2$ using the trial and error procedure. However, if the number of unknown parameters is very large, as happens for multiple fault models considered in present studies, it would be difficult to arrive at objective estimates of these parameters by this procedure alone. All we can do in such cases is to formulate hypotheses about the subsurface faults, thereby prescribing values to most of the fault parameters. The values of remaining fault parameters and slips are altered by the trial and error method until a minimum in the total squared error $\sum (y_i - u_{3i})^2$ is achieved. The assumed values of fault parameters along with the values of remaining parameters obtained in this way yield the model which explains the observed coseismic or interseismic elevation changes in the least squared error sense.

2.4.3. Direct inversion for fault slip using the minimum norm inversion method

If the parameter vectors $\mathbf{p}_1 \dots \mathbf{p}_n$, for a given set of n faults are completely specified, then the relation between each of the surface displacements $u_{31} \dots u_{3m}$ and fault slips $U_{d1} \dots U_{dn}$ is linear and certain rigorous inversion methods may be applied directly on the observations of ground elevation changes $y_1 \dots y_m$ to estimate the causative fault slips. We discuss here one such method, namely, the minimum norm inversion method. Thus, we replace u_{3i} 's by y_i 's in Eqn.2.6 and rewrite it in matrix form as follows.

$$\mathbf{y} = \mathbf{A}\mathbf{U}_d \quad \dots(2.7)$$

Here \mathbf{U}_d and \mathbf{y} are the column vectors of the unknown slips on different faults and the observed elevation changes respectively. \mathbf{A} is a matrix with elements a_{ij} as defined above just after Eqn.2.6.

The linear problems that can be represented by Eqn.2.7 are among the simplest and the best understood inverse problems. When \mathbf{A} is a square, non-singular matrix, the solution of Eqn.2.7 is

$$\mathbf{U}_d = \mathbf{A}^{-1}\mathbf{y}. \quad \dots(2.8)$$

When \mathbf{A} is a rectangular matrix, the methods of solving such linear equations are based on a norm of column vector \mathbf{U}_d and/or on the vector of misfits $(\mathbf{y}-\mathbf{u}_3)$ between the results predicted by solving the forward problem and observations. If the number (n) of unknown fault slips is less than the number (m) of observations but greater than the rank (k) of matrix \mathbf{A} , then the least square inverse is used, and the misfit between the calculated and observed values is minimized in least squared sense. However, for the case when $n > m = k$, the minimum norm inverse may be adopted. Here we seek an n dimensional column vector of fault slips \mathbf{U}_d whose L_2 norm is minimum.

Such minimum norm solution of Eqn.2.7 is given as follows (Menke, 1984).

$$\mathbf{U}_d = \mathbf{A}^T(\mathbf{A}\mathbf{A}^T)^{-1}\mathbf{y}. \quad \dots(2.9)$$

However, a case may arise when this solution is not stable. This may happen when (i) $\mathbf{A}\mathbf{A}^T$ is singular, (ii) some of its eigen values are very small, or (iii) there are errors in observational data. In such cases the suggested solution (Menke, 1984) is

$$\mathbf{U}_d = \mathbf{A}^T(\mathbf{A}\mathbf{A}^T + \lambda^2\mathbf{I})^{-1}\mathbf{y}, \quad \dots(2.10)$$

where λ^2 is the regularizing parameter and its magnitude depends upon the signal to noise ratio in the observations and on the magnitude of the smallest non-zero eigen value of matrix \mathbf{A} .

Certain measures, such as the parameter resolution matrix (\mathbf{R}) and the data information density matrix (\mathbf{S}), have been proposed to assess the quality of inverted results. The closeness

of the \mathbf{R} and \mathbf{S} matrices to the corresponding identity matrices serves as a pointer to the resolution quality of the inverted (1984) parameters and to the extent of contribution made by each observation to solution. The \mathbf{R} and \mathbf{S} matrices are defined as follows (e.g. see Menke, 1984).

$$\mathbf{R} = \mathbf{A}^T(\mathbf{A}\mathbf{A}^T + \lambda\mathbf{I})^{-1}\mathbf{A}, \quad \dots(2.11)$$

and

$$\mathbf{S} = \mathbf{A}\mathbf{A}^T(\mathbf{A}\mathbf{A}^T + \lambda\mathbf{I})^{-1}. \quad \dots(2.12)$$

We now turn to use these theoretical considerations for interpreting data on coseismic and interseismic ground elevation changes.

Chapter III

A rupture model for the great Assam earthquake of 1897, northeast India

3.1 Introduction

On June 12, 1897, a great earthquake ($M=8.7$, Richter, 1958) occurred under the western Shillong plateau in northeastern India. It is the largest well documented earthquake in India and probably one of the largest in the world (Seeber and Armbruster, 1981). Richter (1958) regards Oldham's (1899) report on the effects of this earthquake as one of the most valuable source books in seismology. His inferences about the causes of this earthquake are remarkably consistent with the modern plate tectonics view about the seismicity of India, in general, and source processes of great Indian earthquakes in particular (Chander, 1992). Using the observations of surface faulting, fissures, slumps, tilts, changes in water level along the Brahmaputra and other rivers of the region, landslides, intensity of shaking, projection of partly buried boulders, reports of aftershocks etc., Oldham (1899) inferred a bell shaped epicentral tract spanning the western Shillong Plateau and regions to the north and having maximum extent of about 300 km and 150 km in the east-west and north-south directions (Fig.3.1). The earthquake was felt by human observers upto a distance of about 1500 km from the middle of the epicentral tract.

Seeber and Armbruster (1981) went over the evidence compiled by Oldham (1899) and argued that the extent of rupture zone was about 550 km x 300 km upto the limit of soil liquefaction in the north, west and south of the Shillong Plateau (Fig.3.1). More recently, on the other hand, Molnar (1987b) and Molnar and Pandey (1989) concluded from the same observation set that the east-west extent of the rupture zone was 200 ± 40 km. They put the southern limit of the rupture zone along the southern edge of the Shillong plateau. But they

were not certain whether the northern limit of the rupture extended upto the Himalaya.

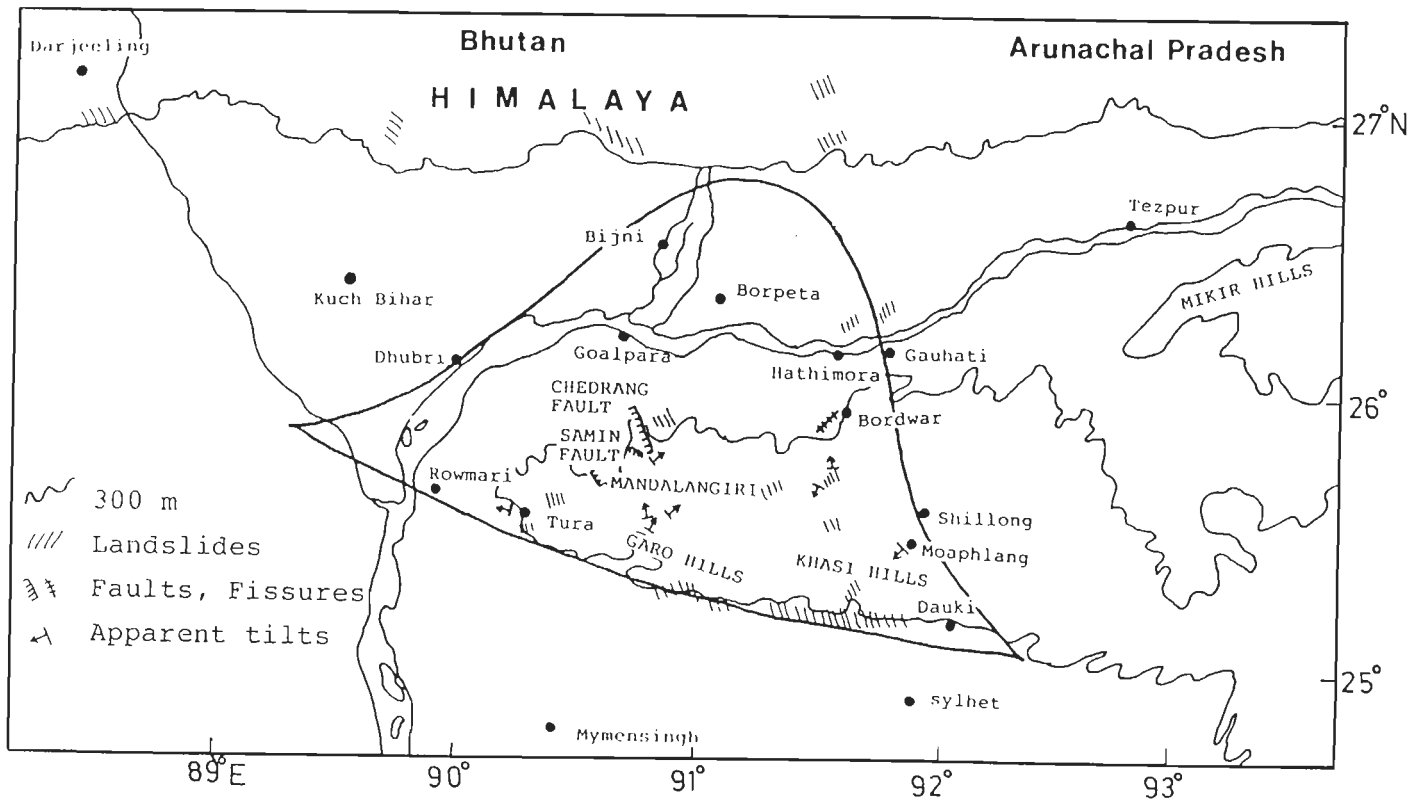


Fig.3.1 Map of the Shillong plateau showing surface effects of the great Assam earthquake. The bell shaped region is the epicentral tract of the 1897 earthquake as demarcated by Oldham (1899). Many permanent changes of the ground were observed in this region and destruction was most severe here.

Oldham (1899, p.175) estimated that the 1897 earthquake occurred on a gently dipping thrust fault at a depth of about 15 km (9.3 miles) but subsequently (see Richter, 1958, p.55) he revised the estimate of depth to 320 km (200 miles). Richter (1958) argued from an examination of the available seismograms (Oldham, 1899, plate.41) that the 1897 earthquake had a normal focal depth.

We attempt in this study to constrain the extent and location of the rupture zone and the depth of causative fault of the 1897 earthquake by considering those observations of Oldham

(1899) that deal with permanent vertical movements of the ground in the epicentral tract.

3.2 Terminology

For the sake of explicitness we define here a few terms which, although well known, require that the meaning we attach to them should be clearly stated.

Causative fault : Fault surface which is the seat of the earthquake.

Fault rupture : Segment of the causative fault where slip occurs during the earthquake.

Oldham (1899) was the first to draw attention to the fact that an earthquake may occur due to slip on a limited section of an extended fault. In other words, the entire fault need not take part during the occurrence of an earthquake.

Rupture zone : Area of the earth surface immediately above the buried fault rupture. The concept of rupture zone is especially relevant to thrust fault type earthquakes.

3.3 Method of analysis

We used the theory of Mansinha and Smylie (1971), discussed in Chapter II (Eqns.2.1 and 2.2c), to predict permanent ground level changes due to a rectangular rupture in a planar fault buried in an elastic half space. Using the basic model of rectangular rupture in a low angle predominantly thrust fault dipping north, computations were carried out for a large number of cases generated by varying (i) the extent and location of rupture zone, (ii) the depth of ruptured section of the fault and (iii) the amount and direction of slip across the rupture. The general nature of predicted ground elevation changes was similar in all these cases, namely maximum ground uplift around the southern long edge and maximum ground subsidence around the northern long edge of the rupture zone. The contours of ground elevation changes were skewed relative to the rupture zone when the slip was oblique on the fault.

3.4 Source model

We display in Fig.3.2 our preferred model of the rupture zone for the 1897 earthquake. It is definitely non-unique, but the ground level changes predicted for it can explain reasonably

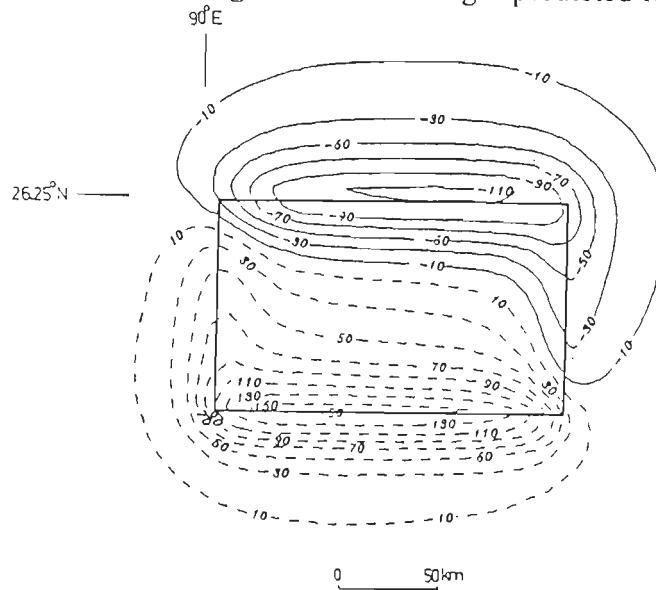


Fig.3.2 Contours of elevation changes due to the $170 \times 100 \text{ km}^2$ buried rupture. Contour values are in cm. Contours of ground elevation and subsidence are shown with dashes and continuous lines respectively. Asymmetry of the contours is due to oblique slip. Approximate latitude of the northern edge and longitude of the western edge of the rupture zone are shown to place it in the context of Fig.3.1.

many of the available, mostly qualitative observations from the epicentral tract of the earthquake. Thus we suggest that northern long edge of the rupture zone lay at the latitude (26.25°N) of Brahmaputra River between its Kholbandha to Hathimora reach (Fig.3.3). The western short edge passed just east of Rowmari (90°E longitude). The southern long edge coincided with the southern limit of the Shillong plateau and eastern short edge was near the line joining Gauhati and Shillong, slightly west of 92°E longitude. This rupture zone has dimensions of about 170 km and 100 km in the east-west and north-south directions respectively. The fault containing the rupture is estimated to have had a dip of 5° due north. The estimated slip of the hanging wall was 4.0 m southerly in the updip direction and 1.0 m westerly in the strike direction. The southern edge of the buried rupture was constrained to

have a depth of 15 km and consequently the depth of the northern edge came out to be 23 km for the assumed dip of the fault. The details of evidence and arguments in support of these estimates are set out in the following paragraphs.

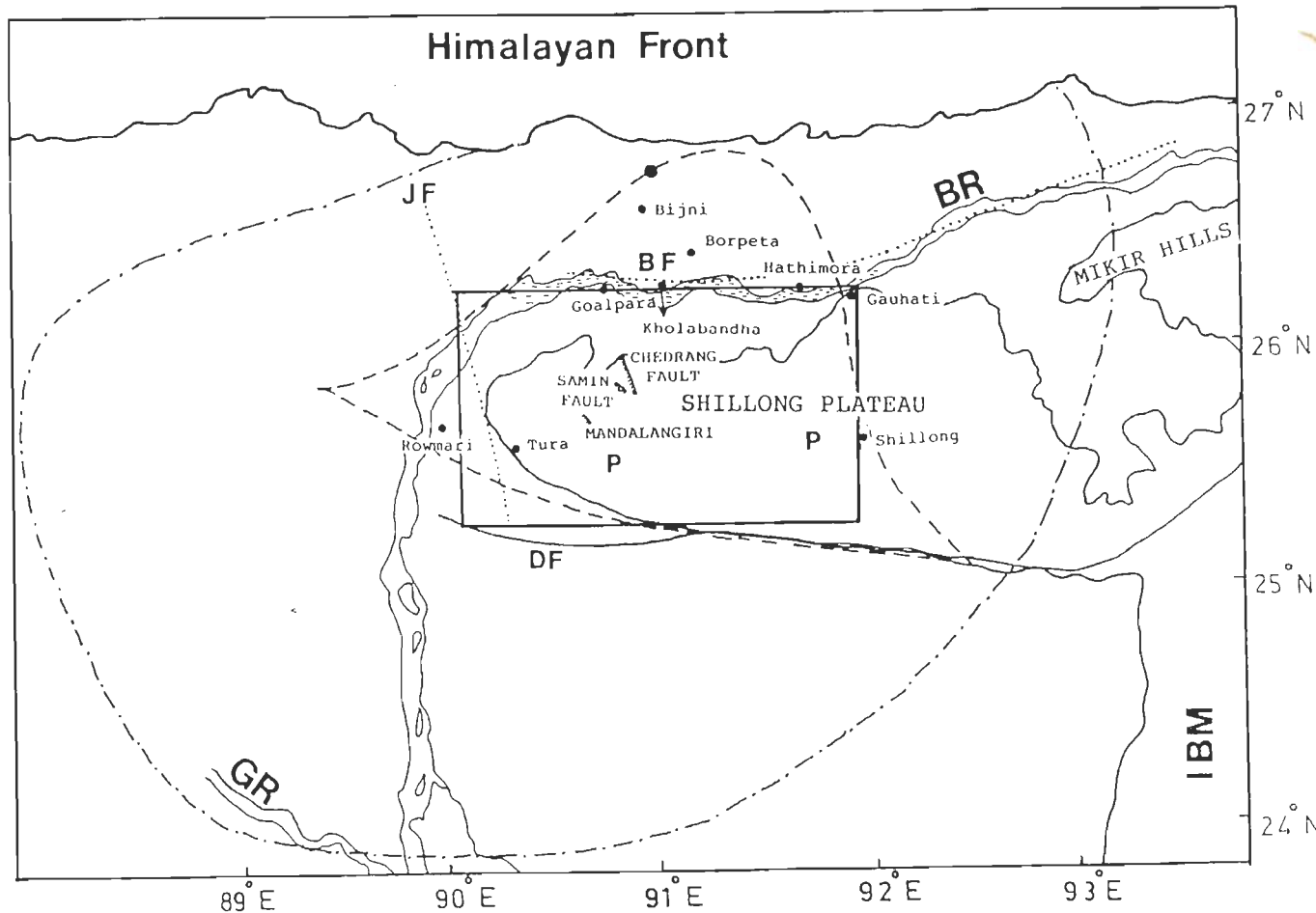


Fig.3.3 The bell shaped region is the epicentral tract of the 1897 earthquake demarcated by Oldham (1899). The dash-dot line indicates the rupture zone of the earthquake as inferred by Seeber and Armbruster (1981). The solid rectangle indicates the rupture zone according to us. P- Localities where ponding of rivers occurred, DF- Dauki. The dotted lines indicate lineaments identified by Nandi and Dasgupta (1986) from landsat imageries: BF- Brahmaputra Fault, JF- Jamuna Fault, where applicable downthrow sides of the faults are shown by short dashes. Other notations are as follows : BR- Brahmaputra River, GR- Ganges River, IBM- Indo-Burmese mountains. The solid circle is the focus of the 1968 earthquake studied by Chen and Molnar (1990).

3.5 Critique of the source model

3.5.1 Northern limit of the rupture zone

On the basis of changes of level along the course of Brahmaputra River and the fact that a large number of aftershocks were felt at Borpeta and Bijni, Oldham (1899, p.169) suggested that the northern limit of 1897 rupture zone extended upto north of Borpeta (Fig.3.3). Molnar (1987b) agreed with this conclusion and inferred that high acceleration, high intensities and frequent aftershocks as far north as Gauhati and Goalpara indicated that the rupture zone extended upto north of Goalpara and Borpeta but " ... whether it extended upto the Himalaya (as suggested by Seeber and Armbruster, 1981) was not clear" (Molnar, 1987b) (Fig.3.3).

Oldham (1899, p.105-108; 161-163) divided evidence on flooding along the Brahmaputra river into two categories. First, he referred to the floods which occurred immediately after the earthquake but passed off in the course of the next day or two. Oldham (1899, p.107) attributed these floods to large volume of water poured out from the sand vents. The second category of floods occurred along the Brahmaputra River during the ensuing wet season. Not only were these floods more severe than usual, but they lasted well into the dry season. Oldham (1899, p.161) attributed these floods to a combination of (i) ground subsidence " ... due to deep seated causes ..." and (ii) shaking down of loose material on the banks of river and consequent filling up of the river bed. The most clearcut evidence of ground subsidence according to Oldham was in the Kholbandha district "... where the floods were unusually deep and extensive" (Oldham, 1899, p.163) (see our Fig.3.1 and 3.3). He further added that "There is here every appearance of a depression having been formed, which has not yet been completely filled up by the river".

Evidence of flooding along the Brahmaputra river was also prominent at Hathimora upstream and to the east of Kholbandha district at about same latitude (Fig.3.3). Oldham (1899, p.161) considered two causes again, namely, (i) subsidence of the rocky floor beneath the Brahmaputra River and (ii) formation of a barrier across the river slightly downstream of

Hathimora. Molnar (1987b) in his reevaluation of Oldham's interpretation has preferred the second cause. But our modelling of ground level changes makes Oldham's first suggestion more attractive.

Since maximum subsidence at the ground surface due to rectangular rupture on a buried thrust fault coincides with the down-dip edge of the rupture, we infer that the northern limit of the 1897 rupture zone had an east-west trend and lay at latitude (26.25°N) of the Brahmaputra River in its Hathimora- Kholbandha reach (Fig.3.3).

As argued by Chinnery (1966) and Fitch and Scholz (1971) the strain is not released fully at the edges of the rupture of a large earthquake. Hence secondary faulting and aftershock activity may be observed there. Due to lack of instrumental recording, Oldham (1899, p.124, 359) only listed the places, where numerous aftershocks of the 1897 earthquake had been felt without being able to determine the epicentral locations of specific events. Oldham (1899, p.124, 359) reported that numerous aftershocks were felt in the north near Borpeta, Gauhati, Goalpara, etc. (Fig.3.3). The northern limit of the rupture zone suggested by us is thus consistent with Oldham's reports seen in light of Chinnery's (1966) and Fitch and Scholz's (1971) arguments. As noted above, Molnar (1987b) also used these arguments, although his estimate of northern limit of rupture zone is vague and, at the very least, slightly to the north of our estimate.

3.5.2 Eastern limit of the rupture zone

Oldham (1899, p.171) suggested a NW-SE trending eastern limit through Gauhati "... tailing off in the direction of Jaintiapur further south of Gauhati" (see Fig.3.1). Molnar (1987b) inferred the eastern limit of rupture zone east of 92°E longitude on the basis of lower level of destruction and shaking at locations east of Shillong. On the basis of observations of intense liquefaction, Seeber and Armbruster (1981) put this limit at about 93°E longitude (Fig.3.3).

We rely upon the evidence of flooding in Brahmaputra river once again to locate the eastern

edge of the rectangular rupture zone. Oldham (1899, p.162) inferred tentatively from river level data that the ground subsided by one third of a metre at Gauhati. We suggest on the basis of modelling of ground level changes that the subsidence was small at Gauhati because it lay at the eastern end of the region of maximum subsidence and consequently near the northeastern corner of the rupture zone (Fig.3.3). This consideration is supported by the fact that Oldham (1899) did not report any unusual flooding in the Brahmaputra River upstream of Gauhati.

3.5.3 Western limit of the rupture zone

Oldham (1899, p.171) placed the western limit of the rupture zone in the alluvial plains west of the Shillong plateau on the basis of his observations of the destruction due to the earthquake and aftershock activity. Molnar (1987b) agreed with the above conclusion. But Seeber and Armbruster (1981), on the basis of observations of liquefaction, fissures and vents, suggested that the rupture zone extended upto 88°E abutting with the rupture zone of the 1934 Bihar-Nepal earthquake (Fig.3.3).

Oldham (1899, p.159) reported that a heliograph had been in operation between Tura on the Shillong plateau near its western edge and Rowmari in the Brahmaputra plains west of the plateau. Before the 1897 earthquake the operation of the heliograph was barely possible with a grazing ray over the crest of an intervening hill. But after the earthquake a broad stretch of the plains east of Brahmaputra became visible from Tura.

On the basis of our modelling above, if the rupture zone were to have extended west of Rowmari, then the relative change in the elevations of Tura and Rowmari would have been so small that it would be difficult to explain Oldham's report. The computed tilt of the ground turns out to be significant if the western edge of the rupture zone is assumed to lie between Rowmari and western edge of the Shillong plateau (Fig.3.3). We suggest that this is a good constraint on the western limit of the rupture zone.

3.5.4 Southern limit of the rupture zone

Oldham (1899, p.170) on the basis of his observations of permanent changes of the ground suggested that the southern limit of rupture zone coincided with the southern limit of the plateau. Seeber and Armbruster (1981) put the southern limit of rupture zone at about 24°N latitude, more than 100 km south of the Shillong plateau on the basis of liquefaction observations. Molnar (1987b), however agreed with Oldham. We adopt Oldham (1899) and Molnar's (1987b) estimate (Fig.3.3).

3.5.5 Inferred rupture zone and observations of lineaments

Nandi and Dasgupta (1986) identified a number of N-S, NNW- SSE and E-W trending lineaments that are traceable for more than 100 km across the Shillong plateau. They suggested that some of the lineaments may be active, but could not determine their ages and senses of motion. Brahmaputra and Dauki faults, reported by Nandi and Dasgupta (1986), are important from our standpoint because they respectively lie close to the northern and southern limits of the inferred rupture zone (Fig.3.3). Similarly Jamuna fault inferred from satellite imageries lies close to our estimate of the western limit of the rupture zone although its strike shows divergence of about 10°.

3.5.6 Depth of rupture

Northeastern India is a region of widespread seismicity. However, estimates of earthquake focal depths suffer from lack of control due to absence of sufficient seismograph stations in the region. To date the most reliable focal depths have been reported by Chen and Molnar (1990) for six earthquakes of NE India on the basis of P waveform modelling. Only the earthquake of Aug.18, 1968, is pertinent here because its epicentre lay in the Brahmaputra valley, north of the Shillong plateau. A focal depth of 29 ± 3 km was estimated.

The available data on the ground level changes did not provide the requisite constraints on

the depth of 1897 rupture. We adopted a depth of 15 km for the southern edge and 23 km for the northern edge of the rupture for the following reasons (Fig.3.4). First, this would place the rupture in an anomalous heterogeneous zone in the middle crust (depth range of 12-25 km) inferred by Mukhopadhyay (1990) by analysing local earthquake data for a velocity model of the crust under the western Shillong plateau. Second, Mukhopadhyay (1990) observed a marked decrease in the frequency of small earthquakes per unit depth interval below about 12 km. Third, if the rupture zone had the above estimated size (170x100 km²) but the rupture depth was greater, then the zone of permanent changes in the ground should have been wider and

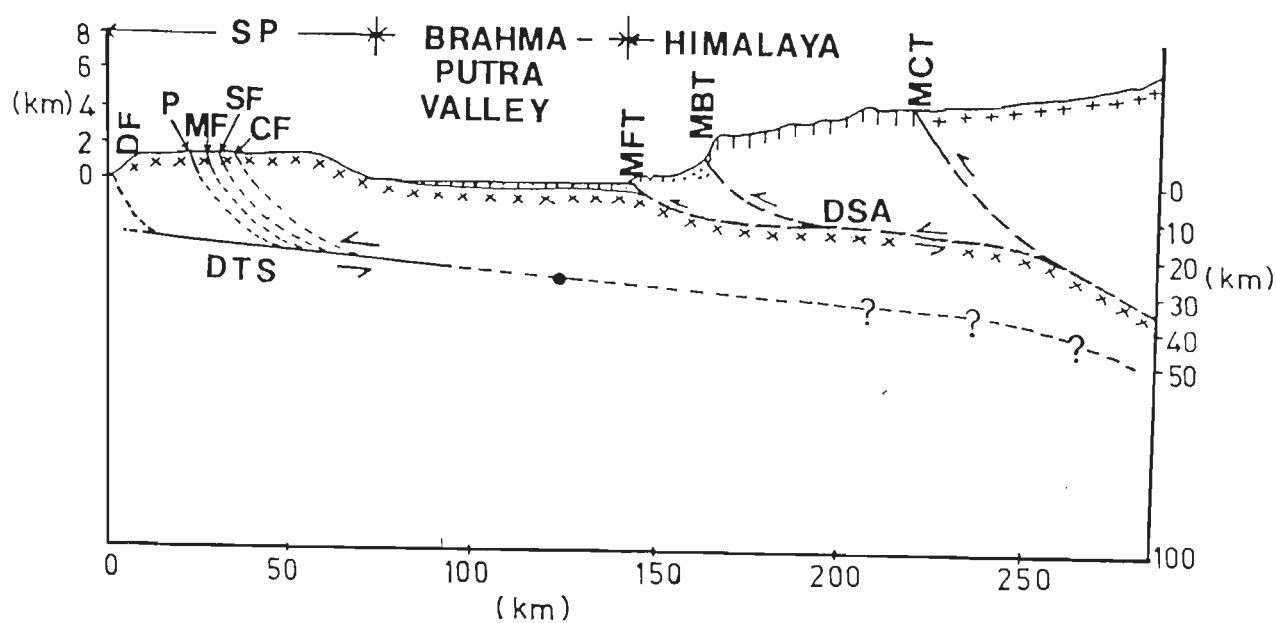


Fig.3.4 A schematic north-south cross-section through the region of the western Shillong plateau. DSA- Detachment according to Seeber and Armbruster (1981) across which relative slip between Indian shield rocks and Himalayan rocks occurs. It is the seat of the 1905, 1934 and 1950 ruptures. DTS- Detachment within the shield crust proposed in this study as the seat of the 1897 rupture. CF (Chedrang fault), MF (Mandalangiri fault), SF (Samin Fault). Splay faults associated with P (Pounding), CF, MF and SF are speculative as explained in the text. The solid circle is the focus of the 1968 earthquake studied by Chen and Molnar (1990). The topography above sea level is schematic. Crosses indicate Indian shield basement, pluses indicate gneisses and schist of Higher Himalaya, vertical dashes indicate metasediment of Paleozoic and older age and dots indicate Tertiary and Recent sedimentary rocks and sediments. Other abbreviations are the same as in Fig.3.3.

the severity of effects less pronounced. Fourth, the focus of the above mentioned earthquake of Aug. 18, 1968, investigated by Chen and Molnar (1990) could lie on the northward extension of the buried fault inferred to be responsible for the 1897 earthquake (Fig.3.4).

Indirect evidence on the depth of 1897 rupture comes from a reinterpretation of the cause of a belt of positive Bouguer anomalies along the southern margin of the Shillong plateau. Verma and Mukhopadhyaya (1977) interpreted these gravity observations and suggested that the crust underlying the Shillong plateau is probably denser as well as thicker than normal for its elevation. Chen and Molnar (1990) interpreted the same data to suggest that the Indian plate had been underthrust beneath the plateau which is completely uncompensated. They ruled out the possibility of a thickened crust under the Shillong plateau.

We suggest that the cause of this anomaly should be primarily above or below the fault in which the 1897 rupture occurred because if the origin of this anomaly were due to a feature which spanned the entire crust vertically then it would have been offset by repeated slip during earlier large earthquakes along the same fault. Our analysis of the anomaly profile using the ribbon model (Grant and West, 1965, p.273) indicates that it can be explained with a 5 km thick dyke like structure dipping at 30° to the north and extending upto a depth of 15 km only (Fig.3.5).

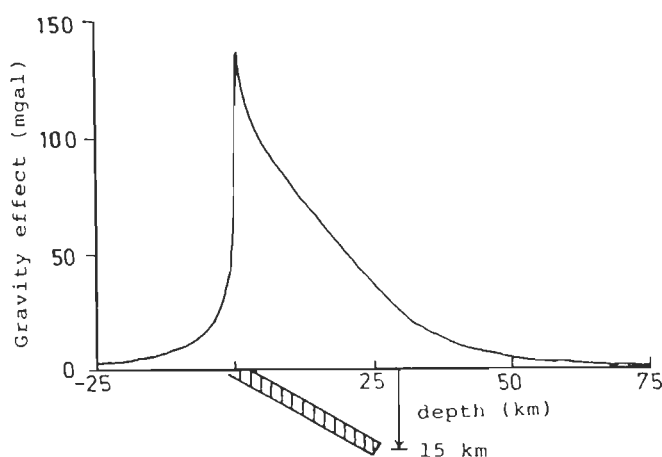


Fig.3.5 North-south gravity profile across the Shillong plateau (Verma and Mukhopadhyay, 1977). The density contrast of the interpreted dyke (shaded vertically) and host rock is 500 kg/m^3 .

3.5.7 Direction of slip

We now turn to an assessment of the inferred (SSW) direction of slip of the hanging wall.

3.5.7.1 Fault plane solutions evidence

A number of authors (e.g. Fitch, 1970; Chandra, 1975,1978; Verma et al.,1976; Baranowski et al., 1984; Le Dain, et al. 1984; Ni and Barazangi, 1984; Verma and Krishna Kumar, 1987; Khattri et al., 1988; Chen and Molnar, 1990 etc.) have discussed fault plane solutions for moderate earthquakes of northeastern India, the eastern segment of the Himalaya and the northern segment of the Indo-Burmese mountains. However, there is only one fault plane solution pertaining specifically to the region of interest here. Chen and Molnar (1990) used waveform modelling to infer the fault plane solution and focal depth for the earthquake of Aug.18, 1968. The solution was not well constrained (Chen and Molnar, 1990) but the northward dipping nodal plane with the pure thrusting motion was selected as the fault plane (Fig.1.10). Since we are postulating a predominantly thrust motion on the rupture, our result is in general conformity with the preferred solution reported by Chen and Molnar (1990).

3.5.7.2 Geological consideration

Evans (1964) concluded on the basis of similarities in rock types of the Rajmahal Hills and Shillong plateau that during Mio- Pliocene times the latter moved 250 km eastward along the right- lateral strike-slip Dauki fault at the southern edge of the plateau (Fig.3.6). Auden (1972) partially contradicted this view by pointing out that Eocene and even older Gondwana sediments were present in the region between Rajmahal Hills (Fig.3.6) and the Shillong plateau. Chen and Molnar (1990) also found no evidence of right lateral slip along the Dauki fault.

We suggest on the basis of our analysis that even if the Dauki fault was a right-lateral strike slip fault in Mio-Pliocene times, it may be under reactivation with a predominantly reverse and

partly left lateral slip motion at the present time.

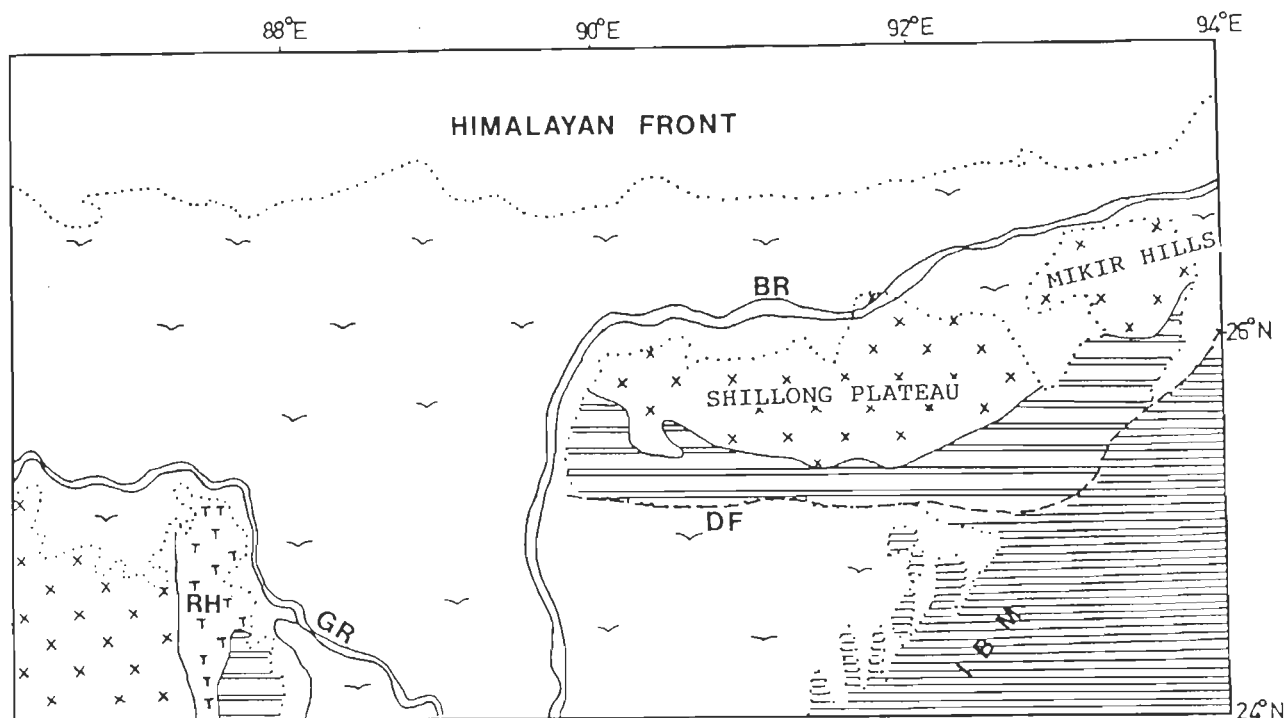


Fig.3.6 Geology of NE India according to Evans (1964). Shading by crosses indicate basement shield rocks, double horizontal lines indicate Tertiary shelf sediments, close horizontal lines indicate geosynclinal sediments of Indo-Burmese mountains, T's indicate trap rocks of Rajmahal Hills (RH), swallows indicate recent alluvium. Rest of terminology as in Fig.3.3.

3.5.8 On the assumption of uniformity of slip across rupture in a single fault

Oldham (1899) delineated an extended epicentral tract for the 1897 earthquake (Fig.3.1). But he documented only three instances of surface faulting in a relatively small area near the northern edge of the Shillong plateau. The most important of these faults was the Chedrang fault (Fig.3.1) which was traced by Oldham (1899, p.146) over a distance of 20 km with an upthrow of 9.5 m for the eastern block. The Samin fault with a nearly east-west trend was traced for a distance of 4 km and there was an upthrow of 4 m for the northern block. A west-north-west trending fault was traced for a fraction of a km near Mandalangiri and there

was a throw of 0.6 m with the north side moving up. From surface evidence Oldham (1899) concluded that these faults were near vertical and there was no strike-slip component. We agree with Oldham (1899) and Molnar (1987b) that these limited faults are not the primary faults responsible for 1897 earthquake. The small area over which these faults were observed, suggests to us two possibilities. First, a small area of the buried major rupture in the geographic vicinity of these surface faults was a pocket of high slip which led to surface breaks on the Chedrang, Samin and Mandalangiri faults. Second, as suggested by Oldham (1899, p.179) the buried thrust fault may have many splays extending towards the surface. The Chedrang, Samin and Mandalangiri faults may be associated with one or more of such splays.

Oldham (1899, p.152) also cited instances where lakes or pools were formed due to interruptions of gradients of south flowing streams in the southern half of the Shillong plateau (Fig.3.1). Oldham (1899) attributed these to upwarping of the river beds. Although the region of these earthquake-created lakes or pools coincided broadly with the region of uplift predicted by the above numerical modelling, the formation of multiple pools on the same stream suggests that locally there were areas of relatively higher ground uplift either due to other local pockets of nonuniform slip on the ruptured section of the subsurface thrust or due to reactivation of splays from the buried thrust or a combination of these causes.

In short, while the model of a uniform slip on rupture in a single thrust fault is useful to delineate the broad areal extent of the buried source, the possibility of local pockets of nonuniform slip on the inferred rupture or the possibility that the slip may have occurred on the main fault as well as on other associated faults of limited extent, cannot be ruled out.

3.6 Implications of the rupture model for the geodynamics of the region

Having proposed a model for the 1897 rupture, it is necessary to ascertain the relationship of the fault associated with it with the detachment under the Outer and Lesser Himalaya on

which the great 1905, 1934 and 1950 earthquakes occurred. South of the Himalayan mountain front the surface of the detachment should continue updip as the boundary between Indian shield rocks and overlying sedimentary rocks and sediments of Indo-Gangetic basin along the northwestern and central segments of the Himalayan convergent plate margin (HCPM) and between the sediments of the Brahmaputra valley and the Indian shield rocks along the eastern segment of the HCPM (Fig.3.4).

We have argued above that the causative rupture of the 1897 earthquake had depths of about 15 km and 23 km beneath the southern and northern margins of the rupture zone respectively. Thus this fault could not lie on the southward extension of the surface of the above mentioned detachment in eastern Himalaya, because that surface should outcrop north of the Shillong plateau (Fig.3.4). We shall term the intracrustal low angle thrust fault responsible for the 1897 earthquake as an intracrustal detachment.

We suggest the following hypothesis for the origin of this intracrustal detachment. The continental crust of the Shillong plateau and Mikir Hills could not subduct under the continental crust of the Eurasian plate along the northern Indo-Burmese mountains during the period when the motion of the Indian plate had a large eastward component. That eastward motion ceased 1 Ma (Le Dain et al. 1984; Chen and Molnar, 1990). Now the intracrustal detachment is under reactivation because of the NNE motion of the Indian plate relative to the eastern Himalaya and the northern Indo-Burmese mountains.

Regarding the geographic extent of the intracrustal detachment, we suggest that, at the very least, it lies under the Shillong plateau and Mikir Hills. Its northward and eastward extensions could be ascertained by relocation of hypocentres and fault plane solutions of earthquakes occurring along the eastern Himalaya and the northern part of the Indo-Burmese mountains. The western and southern limits of this detachment may tentatively be taken along the 90°E longitude, just west of the Shillong plateau, and along the Dauki fault respectively.

If it turns out from the observations and analysis just suggested that the intracrustal

detachment extends much under the eastern Himalaya, then it also may participate actively in accommodating the convergence of Indian and Eurasian plates in this sector of HCPM. This would be consistent with Molnar's (1987b) explanation for the observation that the eastern Himalaya have a relatively lower height as compared to the central and northwestern Himalaya because the plate convergence is accommodated here on two surfaces (Fig.3.4).

The above cited evidence (Chen and Molnar, 1990 and Mukhopadhyay, 1990) on earthquake focal depths in NE India suggests that, under the region, parts of the crust both above and below the intracrustal detachment are seismogenic.

Also, support for the possibility that the crust above this intracrustal detachment is broken up into blocks comes from the fact that, as noted above, the inferred limits of the 1897 rupture zone coincide approximately with lineaments deduced from satellite imageries on at least the north, west and southern sides. In other words, it is possible that in response to continued convergence of Indian and Eurasian plates, a block of the upper crust, south of the Himalayan front in the eastern segment of the HCPM, slipped south-south-westward by several meters on this intracrustal detachment during the 1897 earthquake.

3.7 Implications of the proposed rupture model for seismic risk in parts of NE India

The theory of seismic gaps is now an accepted tool for the assessment of seismic risk along plate margins. A widely held view is that small, moderate and great earthquakes occur in a seismic belt associated with the Himalaya, the so called Himalayan seismic belt (HSB). However it is only recently, with the accumulation of data for small (Khattari et al., 1989) and moderate (Ni and Barazangi, 1984) earthquakes, and re-analysis of the observations for the great Indian earthquakes (Seeber and Armbruster, 1981; Molnar, 1987b; 1987c; Chander, 1988; 1989b and Molnar and Pandey, 1989) that a detailed view of the seismicity associated with the HCPM has begun to emerge within the framework of plate tectonics hypothesis, and a

demarcation of seismic gaps along the HCPM can be attempted. We suggest that it has become necessary to distinguish between the terms "seismicity of the Himalaya" and "seismicity associated with the HCPM". A small or moderate earthquake of HCPM may now be considered to belong to the HSB only if its epicentre falls geographically within the limits of Himalayan mountain ranges. Similarly a large earthquake of HCPM may be considered to belong to the HSB only if its rupture zone lies predominantly in the Himalayan ranges.

3.7.1 Seismicity of the HCPM and Himalaya

It has been noted earlier that the small and moderate earthquakes occur along a fairly narrow belt in the Himalaya. These earthquakes, along with the great earthquakes of 1905, 1934 and 1950 belong to the HSB. A few earthquakes have been located under the Indo-Gangetic plains along the NW and central Himalaya. They are relatively more frequent in the region around New Delhi (Chandra, 1978). In 1965 an earthquake epicentre was also located in the Indo-Gangetic plains, approximately 200 km east of New Delhi (Chandra, 1978). These earthquakes may be regarded either as a part of the overall minor intraplate seismicity within the Indian shield or as a part of seismicity associated with the HCPM but they should not be clubbed with earthquakes of the HSB.

Also, as already noted, along the eastern segment of the HCPM, small and moderate earthquakes regularly occur south of Himalayan mountain front. Their occurrence may be ascribed to a complex system of stresses arising from the interaction of Indian shield blocks of the Shillong plateau and Mikir Hills simultaneously with the Himalayan and Indo-Burmese mountain arcs. Thus these earthquakes along with the 1897 earthquake may be taken to belong to the HCPM but not to the HSB.

3.7.2 Seismic gap in Central and Eastern Himalaya

Seeber and Armbruster (1981) suggested that no seismic gap existed between the 1934 and 1897 earthquake ruptures. They proposed that even if a small gap of 100 km existed between the 1897 and 1950 ruptures, it may have been filled by the two earthquakes in 1943 (M-7.2) and 1947 (M-7.6). Thus according to them this small gap is a possible but not a likely site for the next great earthquake in the region.

Khattari and Wyss (1978) proposed that a gap, approximately between 92°E and 95°E longitude (about 350 km in length), existed between the eastern and western termination of 1897 and 1950 rupture zones. Khattari et al. (1983) reestimated the length of gap to be 240 km. They suggested that the earthquake of 1943 ruptured only 40 to 50 km length of this gap and that the rupture zone of 1947 earthquake was located in the Himalaya, 200 km north of the gap and therefore could not have filled this gap. Hence according to Khattari et al. (1983) a gap of about 240 km still exists.

Molnar (1987b) suggested that seismic gaps existed between the segment of Himalaya, lying just north of the Shillong plateau and the segments that ruptured in 1934 to the west and in 1947 and 1950 to the east. Although he put the northern limit of the 1897 rupture zone south of the Himalaya yet he noted that, "... even if it extended upto Himalaya, it is not safe to assume that this part of the Himalaya will be spared a great earthquake" (Molnar, 1987b)

According to our analysis also, the 1897 rupture zone did not extend upto the Himalaya, and we have suggested above that this earthquake belonged to the HCPM but not to the HSB. Therefore adopting a conservative strategy in which it is better to overestimate rather than underestimate seismic risk, we suggest that a seismic gap should be assumed to exist along an approximately 700 km length of the HSB, between the eastern limit of the 1934 rupture zone at about longitude 88°E and the western limit of the 1950 rupture zone at about longitude 95°E (Fig.3.7).

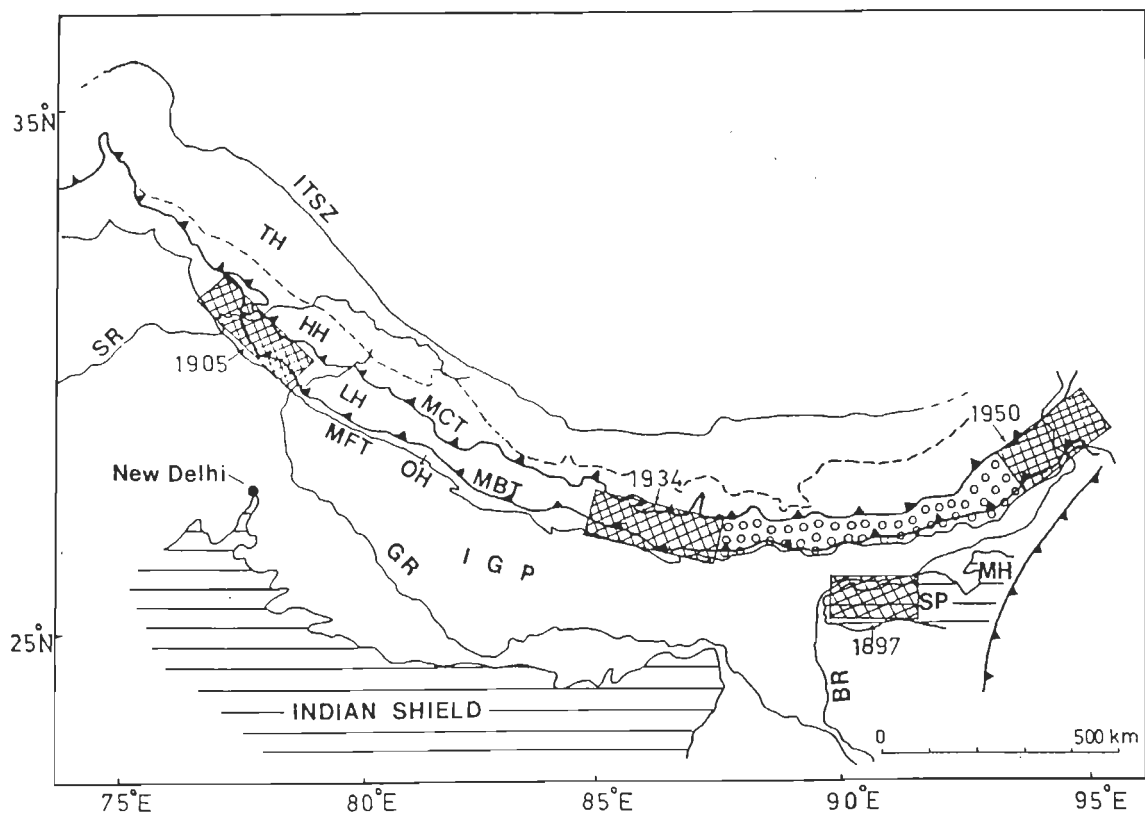


Fig.3.7 Seimotectonics of the Himalayan Convergent Plate Margin. The Main Frontal Thrust (MFT) MBT and MCT represent the Main Boundary and Main Central Thrusts which divide the Himalaya longitudinally into Outer (OH), Lesser (LH) and Higher Himalaya (HH). Tethys Hiamalaya (TH), lying north of the Higher Himalaya are bounded on their north by the Indus Tsangpo Suture zone (ITSZ). The cross hatched areas represent rupture zones of the four great earthquakes; the 1905 rupture zone is according to Chander (1988) and Molnar (1987c), 1934 rupture zone according to Chander (1989) and Molnar and Pandey (1989), 1897 rupture zone according to our study and 1950 rupture zone after Molnar and Pandey (1989). The section of the Himalaya shown shaded with small circles is identified in this study as a seismic gap for the first time. SR- Satluj River, IGP- Indo-Gangetic Plains, rest of terminology as in Fig.1. Background geology after Gansser (1964).

3.8 Summary

1. Ascribing the heavy flooding along part of the Brahmaputra River in the wet season of 1897 to earthquake induced ground subsidence, the northern limit of the 1897 rupture zone is constrained to the Brahmaputra River area north of the western Shillong plateau but well south of the Himalayan mountain front.

2. Modelling of changes in the line of sight between Tura and Rowmari suggests that the western limit of the rupture zone was along the western margin of the plateau.
3. A $170 \times 100 \text{ km}^2$ rupture is estimated to have occurred in a predominantly thrust fault dipping north at about 5° and having a depth of about 15 km below the southern margin of the plateau.
4. It is hypothesized that such a seismogenic fault should be of the nature of a midcrustal detachment. It may extend under the Himalaya, but it is suggested that it is spatially different from the shallower detachment in which the ruptures of 1905, 1934 and 1950 great earthquakes are assumed to have occurred.
5. The development of this intracrustal detachment is attributed to the fact that continental crust of the Shillong plateau and Mikir Hills could not subduct easily under the continental sections of the Eurasian plate to the east and north across Indo-Burmese mountains and the eastern Himalaya respectively.
6. Differentiating between earthquakes of the Himalayan seismic belt and the Himalayan convergent plate margin, it is concluded that 1897 earthquake did not belong to the former. It is suggested that while the 1897 earthquake rupture zone may have filled a gap in the HCPM, conservatively, a 700 km gap still exists along the Himalaya between about 88°E and 95°E longitudes.

CHAPTER IV

A rupture model for the great Kangra earthquake of 1905, NW Himalaya, based on geodetic levelling observations

4.1 Introduction

The Kangra earthquake of April 4, 1905 was assigned a magnitude of 8.6 by Richter (1958). A report on the effects of this earthquake was coordinated and compiled by Middlemiss (1910). He identified two areas of intensity RF (short for Rossi Forel) VIII or greater within an elongated RF VII isoseismal (Fig.4.1). The northwestern and southeastern high intensity zones surrounded the towns of Kangra and Dehradun respectively (Fig.4.1). Great damage occurred around the town of Kangra. Hence isoseismals of intensities RF X and IX were also

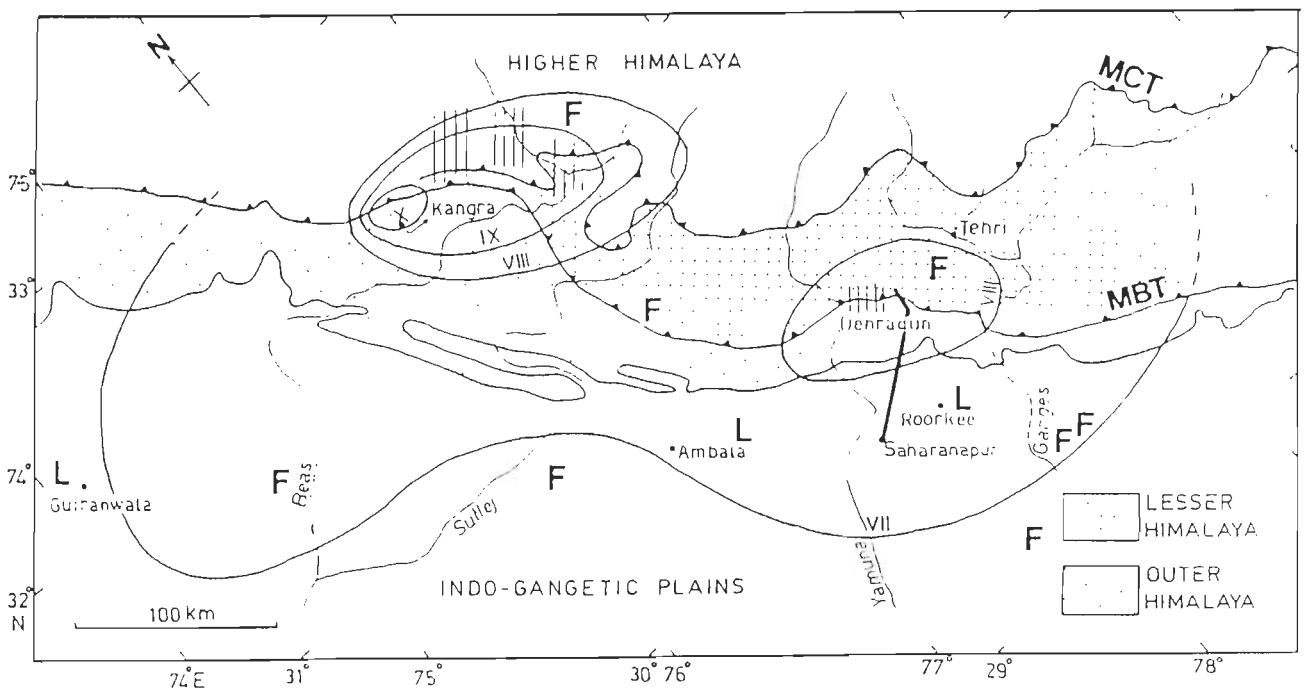


Fig.4.1 Rossi-Forel intensity contours and some surface effects of the 1905 Kangra earthquake (Middlemiss, 1910). F and L represent the regions where foreshocks were felt and the regions where phenomena of soil liquefaction was observed respectively. The vertical hatching denotes the regions where landslides were observed. Levelling line from Saharanpur to Mussoorie via Dehradun is also shown. MBT-Main Boundary Thrust and MCT-Main Central Thrust.

drawn enclosing Kangra. Both the Kangra and Dehradun high intensity areas straddled the Main Boundary Thrust (MBT). Middlemiss (1910) also reported the occurrence of landslides in the Himalaya and soil liquefaction at a few places in the Indo-Gangetic Plains due to this earthquake (Fig.4.1). A few foreshocks of this earthquake were also felt (Middlemiss, 1910, p.355). Finally, Middlemiss included in his report levelling observations along a line in the Dehradun region (Fig.4.1) which documented earthquake induced ground elevation changes in the region.

4.2 Previous analyses of Kangra earthquake data

Although the above facts about the Kangra earthquake have been quoted repeatedly, after Middlemiss (1910), the first significant new analysis within the framework of a cohesive theory, in the present case the plate tectonics theory, was by Seeber and Armbruster (1981). They used all these observations qualitatively to argue that the 1905 rupture zone extended for about 300 km from Kangra to Dehradun and the rupture occurred in the detachment. Molnar (1987c) again reexamined the available intensity data and suggested three possibilities for the length of the rupture zone along the strike of the Himalaya, namely, (i) the rupture zone could be about 280 km long from northwest of Kangra to southeast of Dehradun, (ii) there could have been two separate ruptures, one extending from northwest of Kangra to southeast of Mandi (Fig.4.1) and the other near Dehradun, and (iii) the rupture had a linear extent of about 100 km only, from northwest of Kangra to Mandi.

Chander (1988) used the observations of ground elevation changes along the levelling line in the Dehradun region to estimate the general size and geographic location of the rupture responsible for the Kangra earthquake. He concluded that a buried $280 \times 80 \text{ km}^2$ rupture extended lengthwise between the vicinities of Kangra and Dehradun and widthwise northeastward from the vicinity of Dehradun. He estimated that the dip of the causative thrust fault in which this rupture occurred was about 5° to the northeast. Since the depths of 10 and

17 km along the SW and NE long edges of the rupture were obtained, Chander (1988) agreed with Seeber and Armbruster (1981) that the Kangra earthquake rupture lay in the detachment.

Recently Yeats and Lillie (1991) have proposed on geological grounds that the 1905 Kangra earthquake occurred on a blind thrust since no evidence of primary surface faulting was observed. Further, they argued that since the coseismic elevation changes in the Dehradun region (Middlemiss, 1910) showed growth of the Dehradun valley and Mohand anticline in the Outer Himalaya with respect to the Lesser Himalaya immediately to the northeast, "...this earthquake was expressed at the surface as a fold." Yeats and Lillie (1991) regarded this event as the largest fold related earthquake recorded in a continental area.

4.3 Motivation for and aim of the present work

We also adopt the view that the Kangra earthquake rupture occurred on the detachment, and that the rupture zone extended lengthwise between Kangra and Dehradun. However, whereas Chander (1988) considered that the rupture extended southwestward only upto the vicinity of Dehradun, Yeats and Lillie (1991) argued that it extended upto the southwestern limit of the Outer Himalaya. Also, while Yeats and Lillie (1991) postulated that the Kangra earthquake occurred on a blind thrust, it is widely regarded that its southwestern limit coincides with the geologically mapped and tectonically active Main Frontal Thrust (MFT). Lastly while Chander (1988) simulated the coseismic elevation changes using rupture models with uniform slip, there are several reasons to consider the possibility of non planar causative faults as well as variable slip within rupture in this fault.

Therefore we reanalyze the available observations of coseismic elevation changes (Middlemiss, 1910 and Rajal et al., 1986) along the levelling line in the Dehradun region to examine the following points: (i) the southwestern limit of the Kangra earthquake rupture (ii) depth of rupture at this end, (iii) cross-sectional shape of the causative fault and rupture and (iv) the distribution of slip in the ruptured segment of the causative fault. Our modelling sheds light

also on the current tectonic status of the MBT and the MFT as also, to some extent, on the seismic hazards due to great earthquakes of the Himalayan region.

4.4 Observations of elevation changes in the Dehradun region

4.4.1 History of observations

The history of geodetic observations in the Indian subcontinent goes back approximately to two hundred years (Phillimore, 1945). Repeat geodetic observations for measurement of coseismic crustal deformation were suggested for the first time in India by Oldham (1899) following the great earthquake of 1897. However, the repeat triangulation carried out in epicentral zone of the earthquake was not extensive enough to be useful (Oldham, 1899). The first use of repeat levelling observations to detect coseismic ground elevation changes was carried out following the great Kangra earthquake of 1905 (Middlemiss, 1910).

The levelling benchmarks along the Saharanpur- Dehradun- Mussoorie highway were first surveyed from Saharanpur to Dehradun in 1862 and from Dehradun to Mussoorie in 1904 (Fig.4.2). The complete line from Saharanpur to Mussoorie was relevelled after the 1905

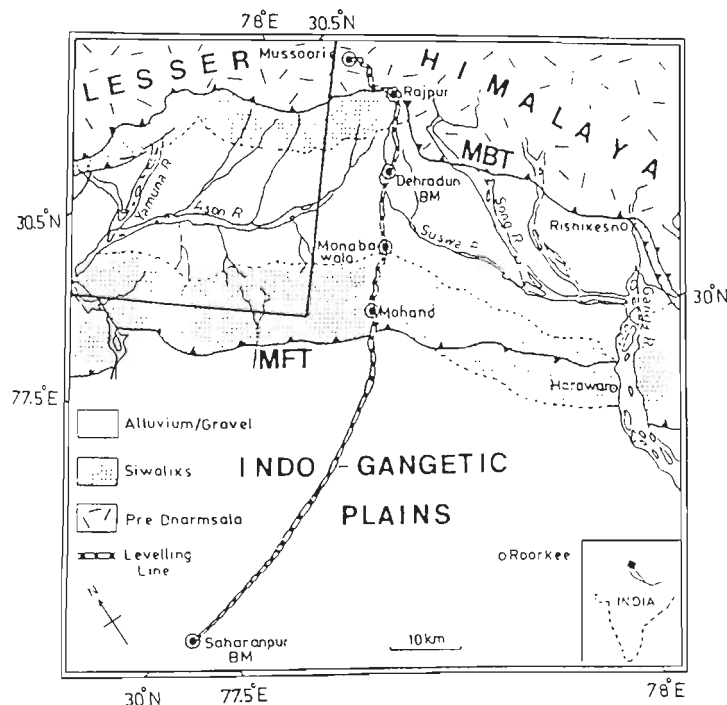


Fig.4.2 The levelling line from Sharanpur to Mussorie. Some of the important benchmarks along the line are also identified. The inferred location of the southwestern and southeastern edges of the 1905 Kangra earthquake rupture is also shown. Geology and tectonic features adopted from Raiverman et al. (1983). The abbreviations used are MBT- Main Boundary Thrust, MFT- Main Frontal Thrust.

Kangra earthquake in 1906-07. The differences in the heights of benchmarks (Fig.4.3 and Table 4.1) between the pre- and post-earthquake surveys are reported by Middlemiss (1910) and Rajal et al. (1986). The differences were estimated on the assumption that the benchmark at Saharanpur had not been affected by the Kangra earthquake. The maximum measured uplift was about 14 cm at a benchmark in Dehradun. These differences were attributed to the coseismic elevation changes during the 1905 Kangra earthquake by Middlemiss (1910), Rajal et al. (1986) and Chander, (1988).

4.4.2 Errors in observations

4.4.2.1 Errors of observation

Middlemiss, (1910) did not provide estimates of possible random and systematic errors of observations in these levelling data. However, he mentioned that "...the greatest care was taken in levelling over such a long and mountainous tract, the reliability of the staves and the comparison of them with a standard steel unit kept at Dehradun being duly attended to" (Middlemiss, 1910, p.348).

We may adopt the standard formula of geodesy (see Bomford, 1978),

$$e = \alpha\sqrt{L}. \quad \dots(4.1)$$

for a general estimate of the accumulated random error (e), expressed in mm, with increase in distance along the levelling line. Here α is a constant depending upon the standard of the survey and L is the distance in kilometre along the levelling line. We adopt the value of 1.1 for α as has been done recently for levelling in the mountainous terrain of Nepal Himalaya (Jackson et al., 1992). Eqn.4.1 indicates that the cumulative random error could be about ± 1 cm at the end of the 80 km long levelling line in the Dehradun region. All the reported elevation changes are

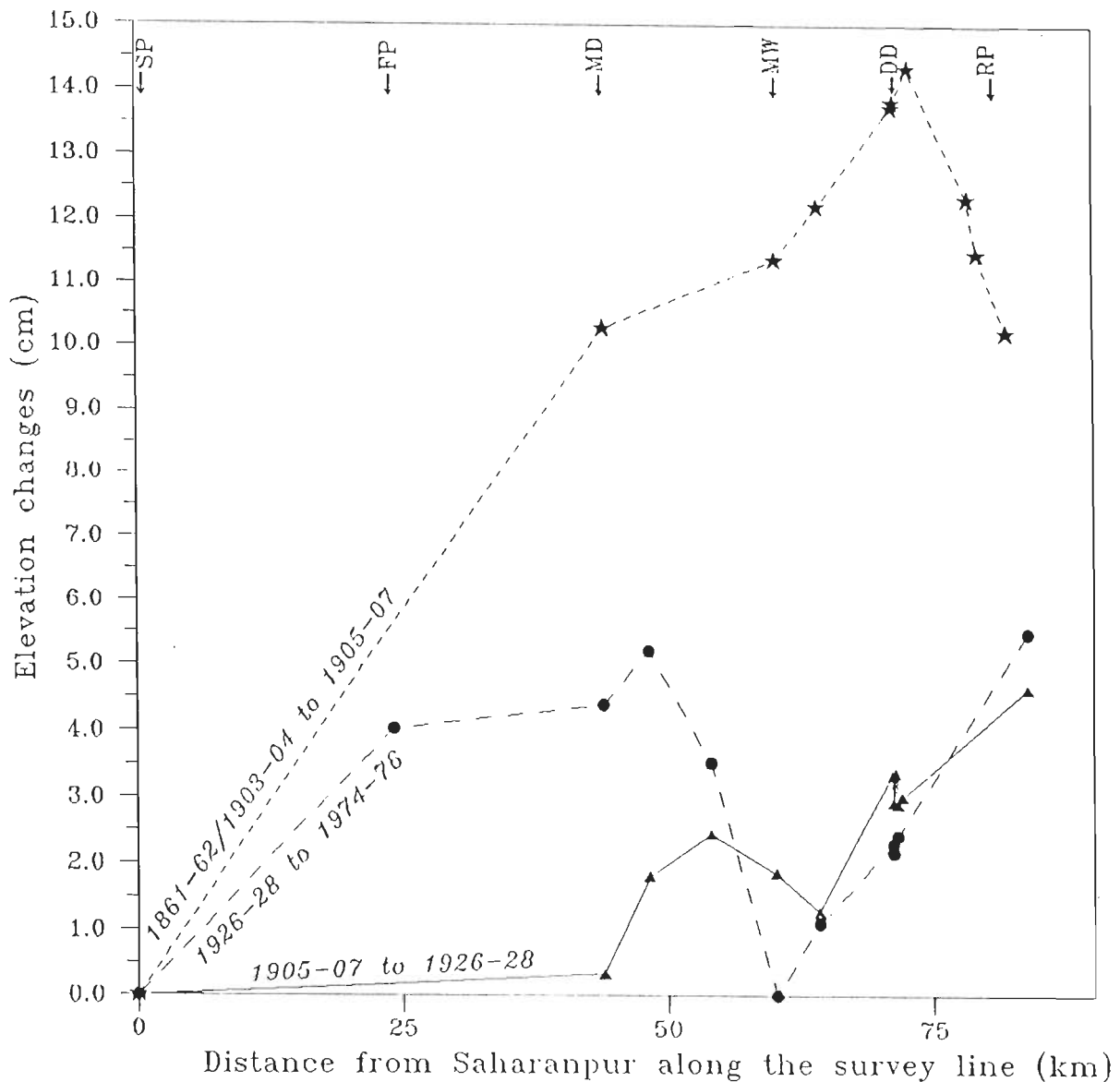


Fig.4.3 The elevation changes of the benchmarks along the levelling line in Fig.4.2 (Rajal et al., 1986) are plotted with distance from the Saharanpur benchmark. The elevation changes denoted by stars are due to coseismic uplift during the 1905 Kangra earthquake and are used in this chapter. The triangles and circles denote the interseismic uplift during the two periods indicated in the figure. The abbreviations used are SP- Saharanpur, FP- Fatehpur, MD- Mohand, MW- Mohabawala, DD- Dehradun and RP- Rajpur.

Table 4.1 Observed coseismic elevation changes.

Description of the benchmark	Distance from Saharanpur (km)	Observed Elevaation changes (cm)
G.T.S.Saharanpur	0.00	0.00
Mohand	44.05	10.27
Mohabawala	60.17	11.37
Colonel Everest's upper mark Dehradun	64.20	12.19
GTS iron plug, GB office, Dehradun	71.26	13.74
Cut on stone on Rajpur road	72.81	14.33
Cut on stone on Rajpur road	78.33	12.32
Cut on stone at Rajpur	79.19	11.46
Rajpur Bajar	81.87	10.21

much above twice this value. We have to double the estimate because we are comparing the results of pre- and post-earthquake levelling observations.

Nothing can be done today regarding estimates of systematic errors in the surveys. Thus we interpret the level changes as reported.

4.4.2.2 Errors due to possible pre-seismic level changes

Another source of error in these data could be due to the fact that the pre-earthquake levelling for five benchmarks between Saharanpur and Dehradun was carried out about 43 years before the earthquake. The inferred elevation changes for these benchmarks may have contributions from pre-seismic strains in the crust also. The possible errors arising from this cause have been ignored mainly because their magnitudes and sign are unknown due to lack of observations.

4.4.3 Overall Quantity and quality of observations

Finally the location of levelling line and the number of benchmarks considered leave much to be desired. Observations of elevation changes are available only at nine benchmarks along a line at the southeastern end of the Kangra earthquake meizoseismal area.

4.5 Estimation of the cross-sectional shape of the fault, extent of rupture and amount of fault slip using the trial and error procedure

As discussed earlier in Chapter 2, the problem of inverting simultaneously for fault slip, rupture dimensions and location of rupture zone with respect to the levelling line is non-linear. We used for the purpose the trial and error procedure discussed in Section 2.4.2.

4.5.1 Preliminary assumptions about fault models

Chander (1988) assumed that the causative fault of the earthquake was planar. However, we permit the fault to be non-planar and simulate it as a composite with three or five planar segments joined edge to edge in dip section. Each fault segment may have a rectangular rupture. Following Richter (1958), we consider only the case where all the individual ruptures are joined so as to form a single simply connected extended rupture running across different fault segments. The number of unknown parameters increases dramatically with each rectangular rupture segment added to the model. As mentioned in Section 2.4.2, we make assumptions to reduce the number of unknowns to be inverted. We thus assume that each planar fault segment had a NW-SE strike and the corresponding rupture segment had lengths of 280 km, which is approximately the distance between Dehradun and Kangra. The buried northeastern edge of the connected rupture was constrained to lie in the deepest fault segment beneath the surface trace of the Main Central Thrust (MCT) near Uttarkashi. We also assumed for all the fault models considered by us that, in map view, the composite fault rupture extends southwestward in the shallowest fault segment upto the SW limit of the Outer Himalaya.

Through modelling we tried to estimate the dips and widths of the planar fault segments, strikewise distances of the southeastern edges of ruptures in these segments from the levelling line, as also the amounts of slips on individual rupture segments.

A large number of variants were considered for each of the three and five segment fault models. In each category the parameters mentioned in the preceding paragraph were chosen by trial and error so that the root mean square error (see Section 2.4.2) was as small as possible.

4.5.2 Results

A very large number of models were considered in this analysis. But for the sake of brevity we present here only the three most pertinent fault and rupture models. Since we have adopted the view that the Kangra earthquake occurred in the detachment, the fault models presented here

simulate the detachment and its possible splays under the Outer and Lesser Himalaya.

Model 1 The detachment was conceived in this case as a listric thrust fault with an outcrop at the SW limit of the Outer Himalaya (Fig.4.4a). However, for computational purposes, the curved cross section of the fault was simulated through three planar segments joined edge to edge such that the deepest fault had the smallest dip and vice-versa. The contributions to the ground elevation changes at different benchmarks due to slips across ruptures in these fault segments were calculated separately using Eqns. 2.1 and 2.2c and the results were summed as in Eqn.2.6. Thus, to some extent, the spurious variations in the computed curve (Fig.4.4a) are the result of representing a continuous listric fault by three planar faults. Similar remarks apply to the variations in the computed curves of Fig.4.4 b and c. The possibility, however, remains that if the benchmarks had been more closely spaced, such variations of ground elevation changes might have been observed also and that would have provided better constraints on the fault rupture model.

Model 2 The composite fault of Model 2 consists again of three segments (Fig.4.4 b). However, the shallowest fault segment does not outcrop along the SW limit of the Outer Himalaya. Thus this model is a simulation of Yeats and Lillie's (1991) conception of buried detachment near the SW limit of the Outer Himalaya. The curve of computed elevation changes is the smoothest and oscillations are the most muted in this case.

Model 3 The composite fault in this case has five segments (Fig.4.4c). The steep ramp located farthest to the NE in this model is assumed to lie beneath the surface trace of the MBT approximately.

4.5.3 Major implications of the analysis

The total number of unknowns for a multiple segmented fault rupture model being incommensurately large as compared to the nine coseismic observations of elevation changes, the possibility of a very high degree of non-uniqueness in interpretation is self-evident. We

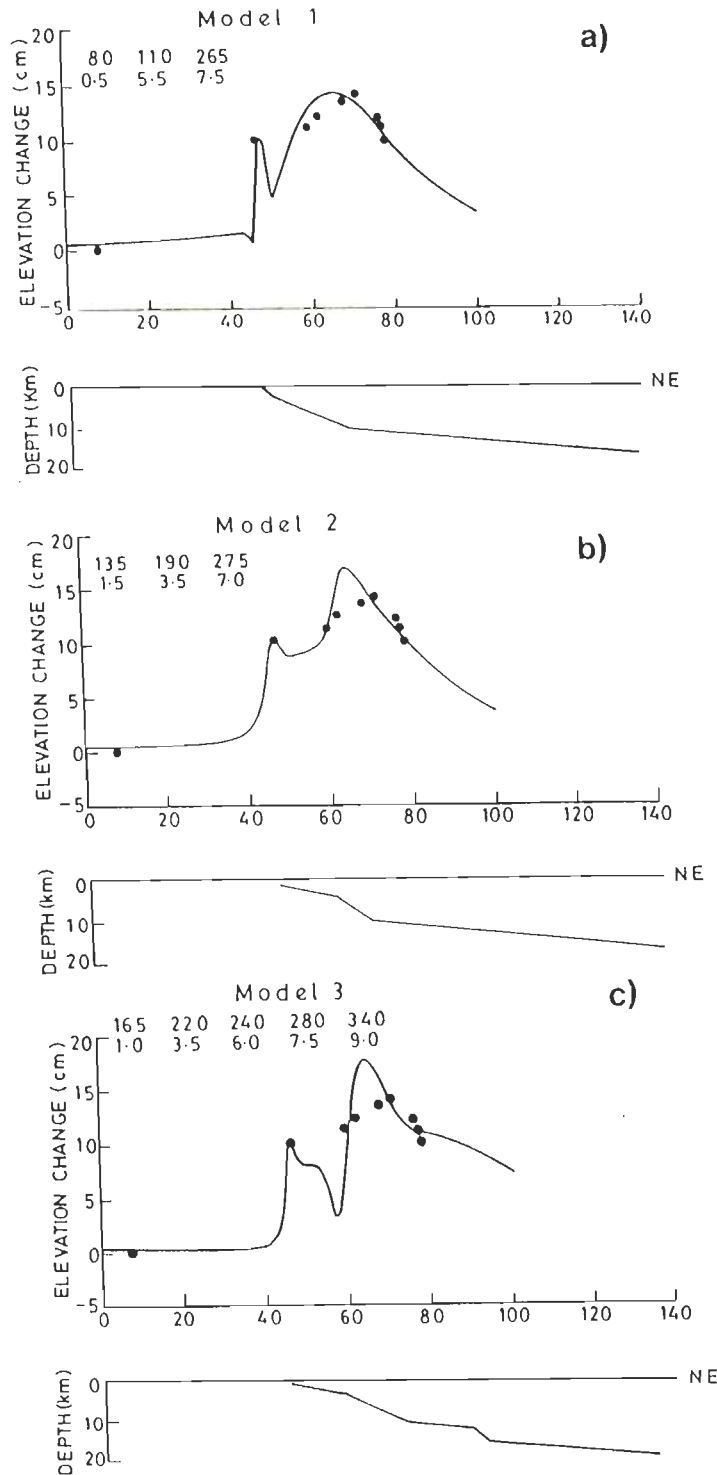


Fig.4.4 Three models of the cross-sectional shape of the Kangra earthquake rupture are shown in the lower parts of the figure a, b and c. The comparisons of observed (solid circles) and theoretical (continuous curves) estimates of ground elevation changes are shown in upper parts. The units of the horizontal scale are in km. The horizontal axis represents distances_χ^(km) from 29°55'N and 77°30'E in the NE direction. In Fig.3a the numbers at the top left are to be read as follows. 80 cm is the estimated slip on the left most rupture shown in lower part of the figure. 0.5 km is the distance of the southeastern limit of this rupture to the northwest of the levelling line. Similar meaning is to be attached to 110 cm and 5.5 km for the middle rupture in Fig.3a and so on.

are constrained to draw only qualitative conclusions from the preceding calculations. Thus firstly, the available observations and above three models permit us to conclude that the southwestern limit of the Kangra earthquake rupture could have extended upto the southwestern limit of the Outer Himalaya. Secondly, we have to conclude from models 1 and 2, that the available observations cannot resolve the question as to whether the Kangra earthquake rupture outcropped near the southwestern limit of the Outer Himalaya or it was buried, as contended by Yeats and Lillie (1991). The absence of geologic evidence for formation of fresh fault scarps during the earthquake leads us to prefer the latter view. Thirdly, the available observations do not constrain the cross-sectional shape of the causative fault in any significant way. Fourthly, on the basis of the above models, the observations permit the possibility that, as discussed further below, the slip could vary atleast along the dip direction of the multi-segment causative fault.

4.6 Estimating the fault slip using the minimum norm inversion

Although the calculations reported above have led to purely qualitative conclusions because of the quality and quantity of data, we discuss now a case in which we endeavoured to pose a hypothesis about the Kangra earthquake source for which some quantitative interpretational results could be obtained along with quantitative measures of their quality. Thus taking the cue from the features of minimum norm inversion discussed in Chapter 2, we considered the possibility of variable slip on a planar fault rupture model of the Kangra earthquake source.

4.6.1 Enunciation of the problem

Let the detachment under Kangra-Dehradun segment of the NW Himalaya be planar with a dip of 5° to the northeast. Let the 1905 Kangra earthquake be caused by slip on a 280×80 km² rectangular shaped rupture in this fault which extended upto the southern limit of the Outer Himalaya and remained buried at a depth of 5 km at this end. Let this rectangle be

subdivided into 16 smaller rectangles, each of area $280 \times 5 \text{ km}^2$ with the long sides of the main and small rectangles being parallel to the strike of the fault and the magnitude of slip on each small rectangle being uniform. However, the slip varies from one small rectangle to another. Let the direction of slip in each segment be such that pure dip-slip type thrust motion occurs. Then, with reference to Eqn.2.7, it is required to determine the vector \mathbf{U}_d of slips on the sixteen fault segments.

4.6.2 Method

We have nine observations of elevation changes at the benchmarks along the levelling line whereas there are 16 slip parameters to be determined. The problem is an underdetermined one and its solution is given schematically by Eqn.2.9. The matrix \mathbf{A} for this equation is constructed for the above geometry by using Eqns.2.1 and 2.2c.

4.6.3 Other considerations

4.6.3.1 Trade off

A trade off exists between the closeness of fit of observed and computed estimates of elevation changes on the one hand and the smoothness of variation of slip along the dip section of the fault on the other. This is an important consideration because the choice of discrete jumps of slip along the fault, although convenient for mathematical computations related to superposition, implies violation of the concept of conservation of matter in a strict theoretical sense. The severity of this problem increases with the increase in magnitude of jump in slip across the boundary between adjoining fault segments. Commensurate with the quality and quantity of observations available we have opted for a subjective assessment of the acceptable compromise in this trade off.

4.6.3.2 Relative position of rectangular rupture vis-a-vis the levelling line

The inverted slip estimates are found to be sensitive to the relative location of the southeastern edge of the rupture in the fault with respect to the levelling line on the earth's surface. While Chander (1988) assumed that the horizontal distance between levelling line and southeastern edge of the rectangular rupture zone was about 15 km, in the trial and error method, discussed in section 4.5, it was observed to vary between 1 to 9 km. It is desirable to consider this separation as an unknown parameter to be estimated along with the slips on the rupture segments. But this was not done because this parameter enters elements of matrix A of Eqn.2.7 in a non-linear fashion and a non-linear inversion scheme has to be formulated. In view of the quality and quantity of the data we devised a grid search procedure. We carried out the minimum norm inversion for different possible separations between rupture zone and levelling line and calculated the rms error between the observed and predicted elevation changes. We found that the rms error is minimum (Fig.4.5) for a separation of 10 km (Fig.4.2). Thus this objective estimate is adopted here.

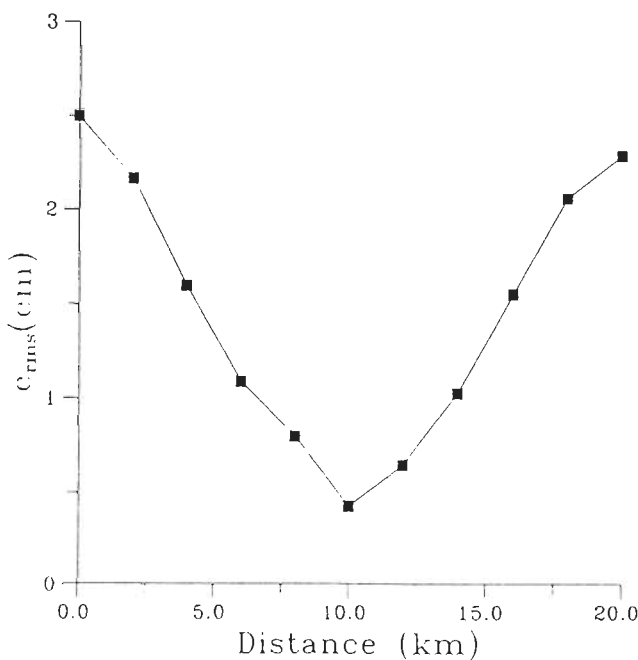


Fig.4.5 The graph displays the variation of rms errors with the distance between the levelling line and the southeastern edge of the rupture.

4.6.4 Resulting model of slip variation

Fig.4.6a and Table 4.2 are the comparisons of observed elevation changes with the theoretical values computed using the inferred set of slip values shown in Fig.4.6b. The root mean square error (e_{rms}) is ± 0.43 cm. The magnitude of regularizing parameter which yielded best results is 2.5×10^{-6} which is of the order elements of matrix **A**.

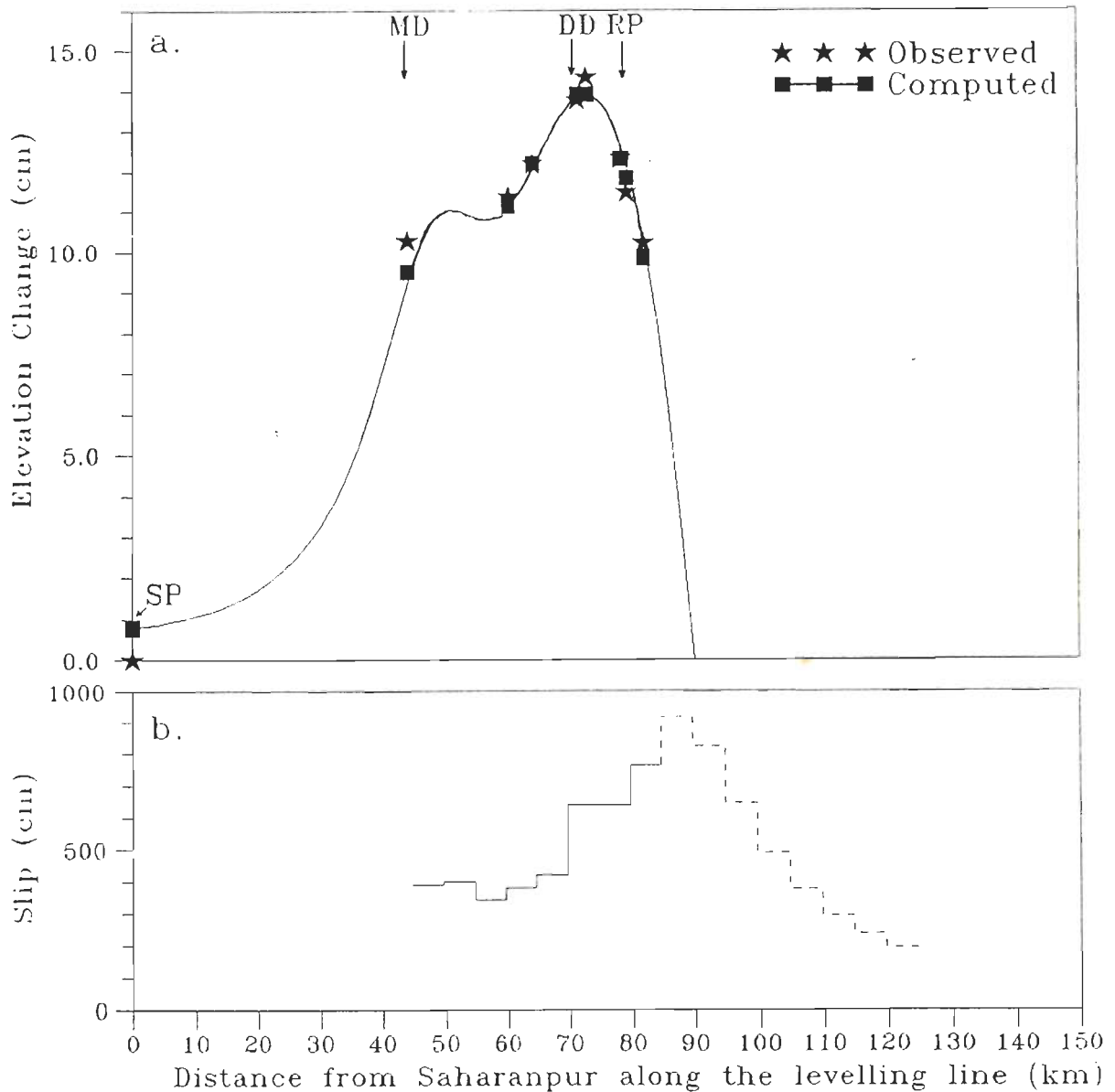


Fig.4.6 Comparison between observed and computed elevation changes during the 1905 Kangra earthquake along the levelling line are shown in the upper part. Positions of benchmarks at Saharanpur (SP), Mohand (MD), Dehradun (DD) and Rajpur (RP) are also indicated. The estimated distribution of slip in the dip section of the planar fault is shown in lower part (b). The slip estimates shown by solid lines are well resolved by the data and those with the dashed lines are poorly resolved.

Table 4.2 Comparison of the observed and computed elevation changes.

Description of the benchmark	Distance from Saharanpur (km)	Elevation changes (cm)	
		Observed	Computed
G.T.S.Saharanpur	0.00	0.00	0.78
Mohand	44.05	10.27	9.52
Mohabawala	60.17	11.37	11.15
Colonel Everest's upper mark Dehradun	64.20	12.19	12.21
GTS iron plug, GB office, Dehradun	71.26	13.74	13.92
Cut on stone on Rajpur road	72.81	14.33	13.92
Cut on stone on Rajpur road	78.33	12.32	12.32
Cut on stone at Rajpur	79.19	11.46	11.83
Rajpur Bajar	81.87	10.21	9.85

4.6.5 Quality of inversion

In order to assess the quality of inversion, we constructed the parameter resolution (**R**) and data information density (**S**) matrices (see Eqns.2.11 and 2.12).

4.6.5.1 R matrix

$$\mathbf{R} = \begin{pmatrix}
 .46 & .43 & .04 & -.11 & .04 & .01 & -.02 & .00 & .00 & .00 & .00 & .00 & .00 & .00 & .00 \\
 .43 & .47 & .22 & -.02 & -.04 & .01 & .00 & -.01 & -.01 & -.01 & .00 & .00 & .00 & .00 & .00 \\
 .04 & .22 & .51 & .31 & -.12 & -.03 & .03 & -.02 & -.03 & -.02 & -.01 & .00 & .00 & .00 & .00 \\
 -.11 & -.02 & .31 & .58 & .30 & -.07 & -.05 & .04 & .01 & -.01 & -.01 & -.01 & .00 & .00 & .00 \\
 .04 & -.04 & -.12 & .30 & .64 & .23 & -.07 & -.04 & .00 & .01 & .01 & .01 & .01 & .01 & .01 \\
 .01 & .01 & -.03 & -.07 & .23 & .64 & .29 & -.09 & -.07 & -.01 & .01 & .02 & .02 & .02 & .01 \\
 -.02 & .00 & .03 & -.05 & -.07 & .29 & .56 & .33 & .03 & -.07 & -.07 & -.05 & -.03 & -.02 & -.01 \\
 .00 & -.01 & -.02 & .04 & -.04 & -.09 & .33 & .47 & .22 & .07 & .02 & .02 & .02 & .02 & .02 \\
 .00 & -.01 & -.03 & .01 & .00 & -.07 & .03 & .22 & .29 & .25 & .19 & .14 & .11 & .08 & .06 \\
 .00 & -.01 & -.02 & -.01 & .01 & -.01 & -.07 & .07 & .25 & .27 & .22 & .16 & .12 & .09 & .07 \\
 .00 & .00 & -.01 & -.01 & .01 & .01 & -.07 & .02 & .19 & .22 & .18 & .13 & .10 & .08 & .06 \\
 .00 & .00 & .00 & -.01 & .01 & .02 & -.05 & .02 & .14 & .16 & .13 & .10 & .08 & .06 & .05 \\
 .00 & .00 & .00 & .00 & .01 & .02 & -.03 & .02 & .11 & .12 & .10 & .08 & .06 & .04 & .03 \\
 .00 & .00 & .00 & .00 & .01 & .02 & -.02 & .02 & .08 & .09 & .08 & .06 & .04 & .03 & .03 \\
 .00 & .00 & .00 & .00 & .01 & .01 & -.01 & .02 & .06 & .07 & .06 & .05 & .03 & .03 & .02 \\
 .00 & .00 & .00 & .00 & .01 & .01 & -.01 & .02 & .05 & .06 & .05 & .04 & .03 & .02 & .02
 \end{pmatrix}$$

It is seen from the \mathbf{R} matrix that the magnitude of the diagonal element in each of the first eight columns is greater than the magnitudes of the immediate off-diagonal elements in the corresponding row or column. Also, the magnitude of the diagonal elements falls off rapidly after the eighth column. Hence the matrix \mathbf{R} suggests that the first eight slip parameters are better resolved by the observational data. Thus the maximum value of estimated slip is 9.2 m (Fig.4.6b) for the ninth diagonal element of matrix \mathbf{R} . But it is poorly resolved with the available data. The highest value of estimated slip that is well resolved by the data is 7.6 m and it corresponds to the eighth diagonal element of \mathbf{R} matrix. This value refers to slips of points on the fault at distances of 40-45 km from the southwestern edge of the rupture zone (Fig.4.6b).

4.6.5.2 S matrix

$$\mathbf{S} = \begin{bmatrix}
 .01 & .05 & .01 & .00 & .00 & .00 & -.01 & -.01 & .01 \\
 .05 & .94 & .01 & -.02 & .00 & .00 & .00 & .00 & -.01 \\
 .01 & .01 & .88 & .14 & -.07 & -.01 & .04 & .02 & -.03 \\
 .00 & -.02 & .14 & .79 & .15 & -.01 & -.07 & -.03 & .05 \\
 .00 & .00 & -.07 & .15 & .51 & .43 & .00 & -.03 & -.01 \\
 .00 & .00 & -.01 & -.01 & .43 & .46 & .14 & .07 & -.09 \\
 -.01 & .00 & .04 & -.07 & .00 & .14 & .46 & .40 & .04 \\
 -.01 & .00 & .02 & -.03 & -.03 & .07 & .40 & .39 & .18 \\
 .01 & -.01 & -.03 & .05 & -.01 & -.09 & .04 & .18 & .84
 \end{bmatrix}$$

On the other hand, the diagonally dominant nature of matrix \mathbf{S} confirms that the elevation changes for all benchmarks except the Saharanpur benchmark have significant contributions from all the sixteen elements of the vector \mathbf{U}_d (Eqn.2.10) of fault slips.

4.7 Discussion

4.7.1 Kangra earthquake rupture model and plate tectonics

Chander (1988) presented four planar fault models for the 1905 Kangra earthquake. Yeats and Lillie (1991) have also presented a model based upon the levelling observations. In the preceding paragraphs, four more models have been presented and they are typical of a much larger number considered by us. Thus the non-uniqueness in the interpretation of coseismic elevation change data is made apparent. Nevertheless it is possible to look at all these models in a broad way in which the differences in the shapes proposed for the causative fault becomes secondary and all are simulation of the detachment. Thus our analysis also reiterates the conclusion by Chander (1988) and Yeats and Lillie (1991) that the plate tectonics model for great Himalayan earthquakes proposed by Seeber and Armbruster (1981) is consistent with the levelling observations related to the Kangra earthquake. In other words the earthquake occurred on a broadly low angle thrust fault which can be equated with the detachment. It would be

surprising if it was a mathematically planar surface. However, the precise nature of departures from planarity cannot be constrained adequately by the observations.

4.7.2 Depth of the Kangra earthquake source

As discussed in Section 4.1, there are not enough instrumental observations to constrain the focal depths of the four great Indian earthquake of the past hundred years. Regarding the Kangra earthquake specifically, Middlemiss (1910) estimated the focal depth to be about 30 km mainly from a consideration of the observed intensities. Subsequently Krishnaswamy et al. (1970) estimated again that the earthquake occurred at a depth of about 25-30 km. Chander (1988) estimated from the analysis of coseismic elevation changes that the earthquake occurred in the detachment in the depth range of 10 to 17 km. In our models the rupture zone of the earthquake is assumed to extend further southwestward, than was assumed by Chander (1988). The detachment should become shallower in this direction. Our models 1 to 3 based on nonlinear analysis and the model based on the minimum norm inversion rest on the assumption that the causative fault at the southwestern limit of the causative rupture, was located between the ground surface and a depth of about 5 km. These depth estimates are in accord with the analyses of Seeber and Armbruster, (1981); Ni and Barazangi, (1984); Lyon-Caen and Molnar, (1983); Molnar, (1987c) and (1990) regarding the depth of the detachment under the Outer and Lesser Himalaya.

However, we have to distinguish clearly between the hypocentral depth of the earthquake and depths of the causative fault and rupture. Of course, the hypocentre has to be within the ruptured portion of the causative fault. The above analyses of elevation changes between pre- and post-earthquake positions of ground particles give no indication about the location of the hypocentre within the rupture. Still we may adopt the view expressed by Kelleher (1972) that great earthquakes along convergent plate margin nucleate near the deeper edge of the causative rupture. Hence, according to us, the hypocentral depth of the Kangra earthquake could have

been upto 17 km.

4.7.3 Magnitude of slip

The isoseismal map drawn by Middlemiss (1910) makes it very plausible that the amount of slip on the causative rupture of the Kangra earthquake may not have been uniform. However, because of the limitations of the theoretical formulae used, the analysis of Chander (1988) assumed uniform slip throughout an extended planar rupture, while our analyses discussed in Sections 4.5 and 4.6 are on the assumption that there was uniformity of slip along the rupture strike direction while possibility of variation of slip in dip direction was admitted.

The maximum amount of slip estimated by Chander (1988) was of the order of 5 m. In our minimum norm inversion the maximum slip estimated with reliability is 7.5 m with indication that it might have been even higher in the downdip direction.

Ward and Barrientos (1986) were the first to attempt modelling of variable slip on the causative fault for the 1983, Borah Peak, Idaho earthquake. The method was later applied to the 1985 Central Chile (Barrientos, 1988) and the 1915 Avezzano, Italy, (Ward and Valensise, 1989) earthquakes. Recently Barrientos and Ward (1990) used the surface deformation data of the 1960 Chile earthquake to invert for the fault geometry as well as variable slip on it. Thus Barrientos and Ward (1990) inferred a uniform slip of 17 m for the great 1960 Chile earthquake ($M_S=8.3$), whereas in their variable slip model the fault slip was as high as 40 m. Thus we suggest that the estimated maximum slip of 7.5 m using the variable slip model is only nominally greater than Chander's (1988) estimate of 5 m based on the uniform slip model.

We argue that this slip estimate is still a lower bound estimate, mainly because of three reasons. Firstly, the method of inversion adopted here gives the vector of slips whose norm is minimum. Secondly, since this estimate corresponds to the slip in the Dehradun region where damage was less as compared to the Kangra region, we propose that the fault slip was even higher in the Kangra region. Finally, relatively higher estimates of slips are inferred for great

earthquakes of the world, e.g., about 20 m for both the Chile earthquake (Barrientos and Ward, 1990) and the great Alaska earthquake (Plafker, 1972).

4.7.4 Current tectonic status of the MCT, MBT and MFT

As is evident from the review of plate tectonics literature on the Himalaya (Chapter 1), there is considerable speculation about the configuration at depth, time of formation and current tectonic status of three major thrust faults, namely, MCT, MBT and MFT, mapped geologically in the Himalaya. We consider here the implications of the coseismic elevation changes observed for the Kangra earthquake.

4.7.4.1 MCT

In all the models considered by us the surface trace of MCT in the Garhwal Himalaya is the northeastern limit of the rupture zone. Since the levelling line did not extend upto this point, not much can be said about the precise involvement of MCT in the occurrence of this earthquake. However, it is our conjecture that MCT was not involved.

4.7.4.2 MBT

Fig.4.7, based on computations using Eqns. 2.1 and 2.2c, shows ground uplift and subsidence due to thrusting motion along the MBT. Specifically, here ground subsidence is predicted at Dehradun whereas ground uplift of upto 14 cm was observed. Hence, it is unlikely that slip occurred on the MBT during the Kangra earthquake.

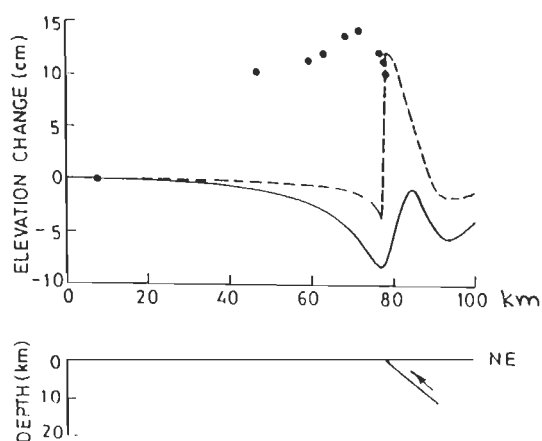


Fig.4.7 Estimated ground subsidence near Dehradun, if the earthquake had occurred on MBT. The two different curves correspond to two different locations of the levelling line related to buried rupture (see e.g., Kasahara, 1981, p.77, Figs.4-15).

Here an important point of terminology has to be raised. Molnar (1990) has consistently remarked that great Himalayan earthquakes occur on the downdip extension of the MBT. Since both Seeber and Armbruster (1981) and Molnar (1990) agree that great Himalayan earthquakes occur on a shallow dipping thrust fault under the Himalaya, it is, to some extent, a matter of terminology as to whether the earthquake occurred on the MBT or the detachment. However, to some extent the use of these terms by these investigators reflects their specific tectonic model about the Himalaya. The levelling observations cannot differentiate between these models. Thus when we say that the MBT was not involved in the occurrence of the Kangra earthquake, we specifically imply that near surface segment of the geologically mapped MBT was not involved. This point has to be emphasized because many Indian earth-scientists still cling to the notion that the Kangra earthquake occurred on the MBT and they have in mind the geologically mapped thrust fault.

4.7.4.3 MFT

There is considerable debate in the Indian geological literature also regarding the meaning of the phrase MFT (Nakata et al., 1990; Valdiya, 1986 and Yeats and Lillie, 1991). In earlier literature, e.g., Wadia (1976), the phrase MFT does not occur although existence of many thrusts along the southwestern limit of the Himalaya is noted. More recently a thrust contact between the Siwalik rocks of the Outer Himalaya Indo-Gangetic alluvium has been emphasized and the phrase MFT used relatively frequently (e.g. Nakata et al., 1990; Valdiya, 1986 and Yeats and Lillie, 1991).

Several investigators, notably Nakata et al. (1990) and Valdiya (1986), have remarked upon the neotectonic activity around the southwestern limit of the Outer Himalaya. Yeats and Lillie (1991) while propogating their views about fold earthquakes, have suggested that the causative fault of the Kangra earthquake extended southwestward upto the limit of the Outer Himalaya, but it did not outcrop. Our analysis with models 1 and 2 above, indicates that the available coseismic elevation change data cannot resolve the question, whether MFT was or was not

involved in the occurrence of the Kangra earthquake. But the above analysis suggests strongly that the neotectonic activity along the SW limit of the Outer Himalaya has not subsided and manifests itself at present partly through great earthquakes. This point is raised again in the following two chapters.

4.7.5 Hazard assessment

An important motivation for the present thesis was our desire to reinvestigate the extant observations about great Himalayan earthquakes from the stand point of seismic hazards along the Himalayan mountains. Unfortunately, while the desire of earthquake engineers and earthquake seismologists regarding seismic hazards is to inquire about dynamic parameters such as peak ground acceleration, the geodetically measured elevation change observations can shed light only about the amount of permanent ground displacements.

We estimated the permanent horizontal and vertical displacements of the ground particles over a surface area of about $400 \times 200 \text{ km}^2$ lying vertically above and around the estimated $280 \times 80 \text{ km}^2$ rupture in the buried fault with the slip values as shown in Fig.4.6b. We note that while the estimated maximum horizontal and vertical displacements are 0.66 m and 0.14 m respectively along the survey line, they are about 4 m and 1.4 m respectively a few kilometers to the northwest of the levelling line (Figs.4.8 and 4.9), i.e., just above the buried rupture. Unfortunately, there are no geodetic observations to verify these calculations. But two reasons can be advanced to suggest that these are lower bound estimates. Firstly, we have used the minimum norm technique for inversion which, in our case, gives an estimate of a slip vector \mathbf{U}_d (Eqn.2.10) of minimum norm. Secondly, according to Middlemiss (1910) the damage during the 1905 Kangra earthquake was less in the Dehradun region than that in the Kangra region. If more geodetic data with better geographic spread were available and inversion were to be carried out for slip varying along both strike and dip of the fault, then we surmise that even higher magnitudes of slip in the Kangra region would have been indicated.

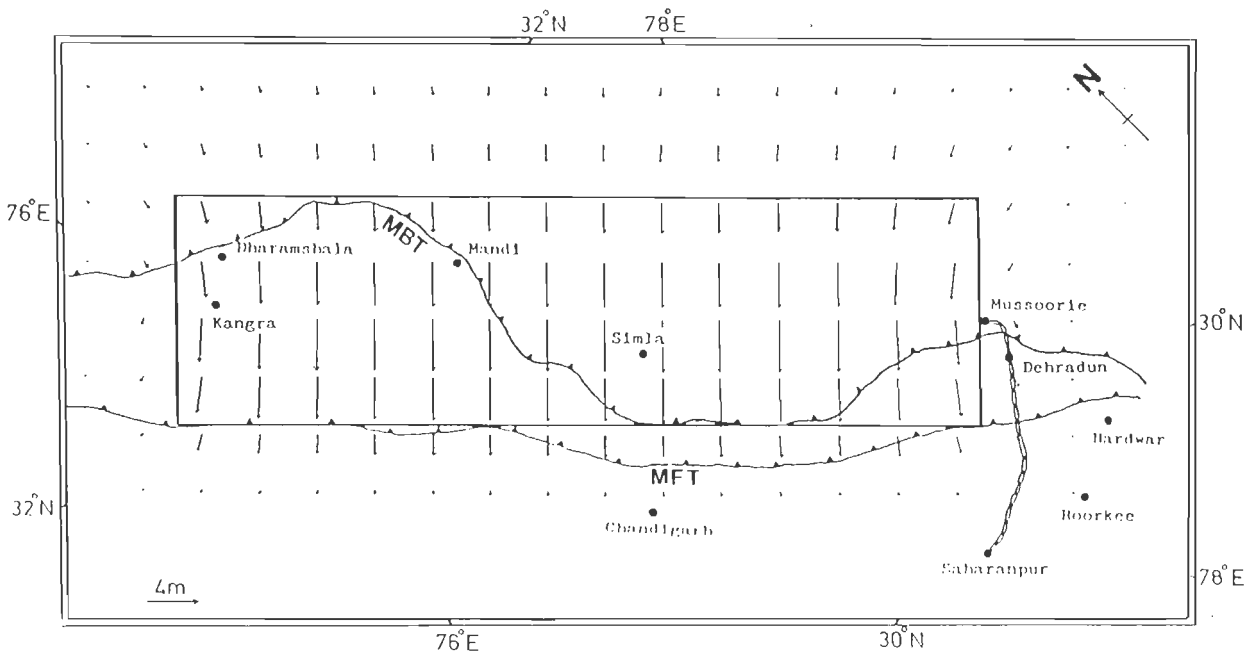


Fig.4.8 The predicted horizontal displacements on the ground surface due to slip distribution of Fig.4.6 on the planar fault. The tail of an arrow indicates the geographic location of the point for which the arrow signifies the direction of horizontal movements. Important localities of the region are also shown for completeness. Tectonic information adopted from Raiverman et al. (1983). Abbreviations are same as in Fig.4.1 and 4.2.

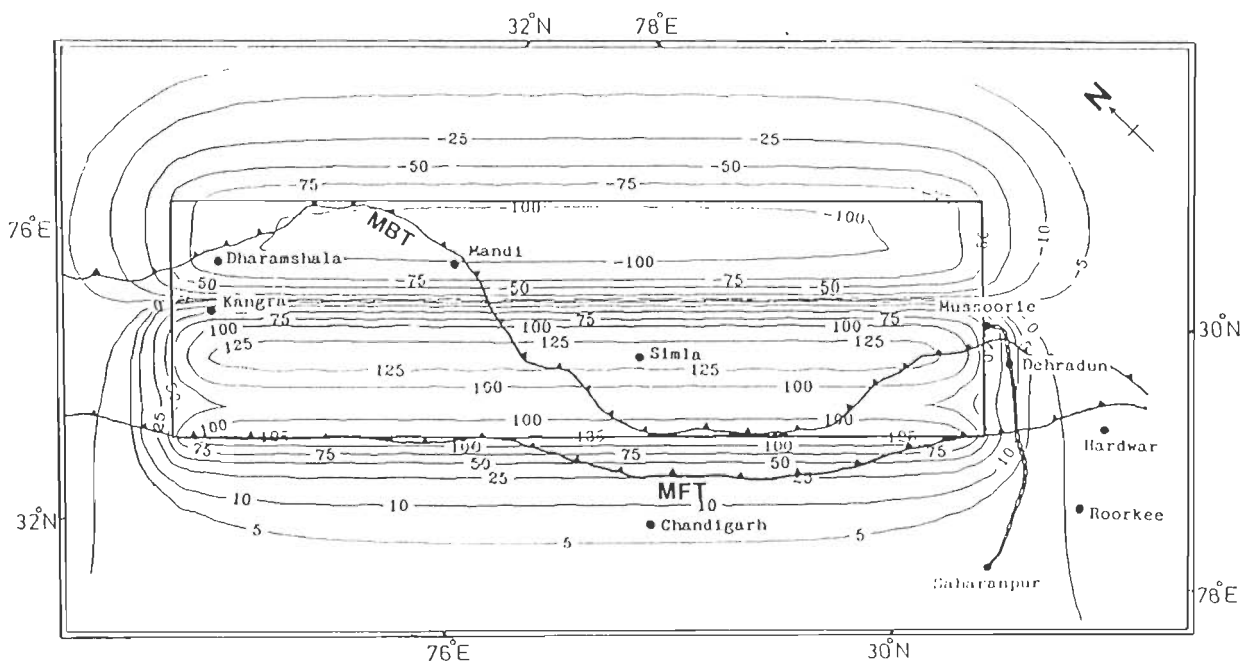


Fig.4.9 Analogous to Fig.4.8, but showing contours of predicted vertical displacements on the ground surface.

An implication of suspected higher slips on the fault under the Kangra region for hazard assessment is that the 1905 earthquake probably did not relieve as much strain in the Dehradun region as it did in Kangra region. It may be that the strain in the Dehradun region had been released already by an earlier smaller magnitude earthquake which did not affect the Kangra region (Molnar, 1987c). Alternatively, relative probability of occurrence of the next great earthquake is more for the Dehradun region than for the Kangra region. But this probability is less than that for the region east of Dehradun lying in the central seismic gap (Khattri, 1987).

We note in passing that the transient displacements of ground particles during an earthquake should exceed their permanent displacements as measured from respective initial equilibrium positions (see synthetic seismograms computed, for example, by Benmanahem and Singh, 1981).

4.8 Summary

The results of the inversion of elevation change data due to 1905 Kangra earthquake along the Saharanpur - Dehradun - Mussoorie levelling line may be summarized as follows.

1. The rupture involved in Kangra earthquake lay in the detachment under the Outer and Lesser Himalaya. It had a width of about 80 km extending in the NE direction from Mohand (SW limit of the Outer Himalaya) and a length of about 280 km in the NW direction from Dehradun.
2. The southeastern limit of Kangra earthquake rupture was about 10 km northwest of Saharanpur-Dehradun-Mussoorie levelling line.
3. The estimated depth of rupture was between 0 to 5 km below the southeastern limit of the Outer Himalaya and about 10 km below Dehradun.
4. The MBT was not involved in the occurrence of Kangra earthquake. But involvement of the MFT cannot be ruled out.

5. A reasonable lower bound estimate of maximum slip on the causative fault of the Kangra earthquake is 7.5 m.
6. Correspondingly the lower bound estimates of the permanent maximum horizontal and vertical ground displacements induced by the 1905 Kangra earthquake, are of the order of 4.0 m and 1.5 m respectively.

CHAPTER V

Evidence for accumulation of earthquake generating strains in the Himalaya of central Nepal from short term interseismic levelling observations

5.1 Introduction

Recurrence of great earthquakes along different segments of the convergent plate margins around the globe, implies that recoverable elastic strains accumulate in upper crustal rocks of each segment more or less regularly during the respective interseismic periods. Geodetic observations have been used for detecting and measuring the accumulation of strain from the ongoing tectonic processes in many regions in the world (Shimazaki, 1974; Scholz and Kato, 1978; Savage et al. 1979; Thatcher, 1979; 1983; 1984; Savage, 1983; Savage and Gu, 1985; Weldon and Sieh, 1985; Prescott and Yu, 1986; Scholz, 1992; and Dragert et al., 1994). However, sufficiently detailed systematic studies in this regard have been and are being conducted mainly along the San-Andreas fault in California and along the southern coast of Japan. Geodetic triangulation networks were established in 1880's in California and subsequently resurveyed at infrequent intervals. Also data have been obtained from geodimeter networks regularly since about 1970 (Scholz, 1992). In the last ten years, measurements using the very long baseline interferometry (VLBI) and other space based techniques have been made. Geodetic measurements in Japan started in 1890's and are being repeated at regular intervals since then. These data sets from both triangulation and levelling constitute the largest body of data on the crustal deformation (Scholz, 1992).

A brief review of repeat geodetic observations for detecting coseismic changes in the ground has been given in the previous chapter. Repeat triangulation and levelling observations have been carried out also in recent years for measurement of aseismic crustal deformations

at a few sites in the Himalaya (e.g., Arur and Hasija, 1986; Arur and Singh, 1986; Omura et al., 1986 and Rajal et al. 1986). But again, due to the limited spatial extents of these surveys, and also the poor quality and quantity of observations, modelling of aseismic slips on causative faults has not been attempted so far. The only exception to this is in the case of post Kangra earthquake levelling observations along the Saharanpur-Mussoorie highway. Their interpretation is the subject of the following chapter.

Recently, Jackson et al. (1992) reported elevation changes over a 7 to 13 year period along a 350 km long levelling line between the southern and northern borders of Central Nepal. In this chapter we interpret a part of these data in terms of plate-tectonics related slips on the detachment and find that elastic strain is building up for a great earthquake in Central Nepal Himalaya.

5.2 Data

Jackson et al. (1992) provide details about the sequence and method for acquisition of levelling data in central Nepal. The line connects the levelling networks of India and Tibet (Jackson et al., 1992). It passes through the southern plains, Outer and Lesser Himalaya and parts of Higher Himalaya in Central Nepal (Fig.5.1). The data interpreted in this chapter are picked from the graphical display of ground elevation changes given in Fig.2 of Jackson et al. (1992). The time elapsed for repeat levelling was 13 years for most sections of the line and 7 years for the remaining sections (Jackson et al., 1992) (Fig.5.2). In order to have uniformity in this regard, we calculated the annual uplift rates.

5.2.1 Errors in the levelling observations

Cumulative random error (e) in levelling is estimated using the Eqn.4.1, where α has a value of 1.1 (Jackson et al. 1992). Thus at the beginning of the levelling line at its southern end in the Indo-Gangetic plains, this error is zero and it increases upto ± 2 cm at the northern end

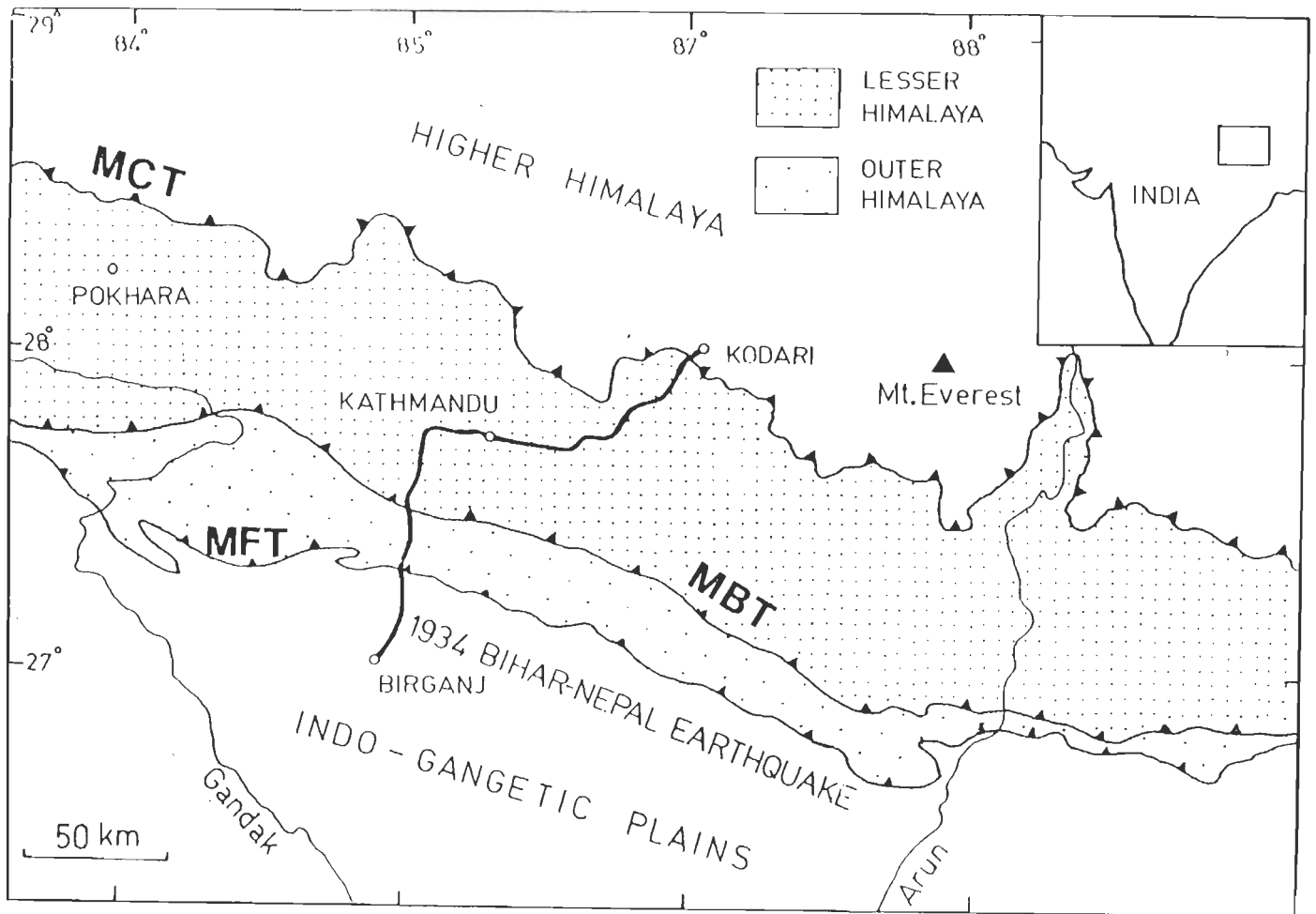


Fig.5.1 Simplified geologic map of the Central Nepal Himalaya. The thick line shows the route along which repeat levelling was carried out in Central Nepal. The segment of the Himalaya affected by the great 1934 Bihar-Nepal earthquake is indicated. MFT- Main Frontal Thrust, MBT- Main Boundary Thrust and MCT- Main Central Thrust.

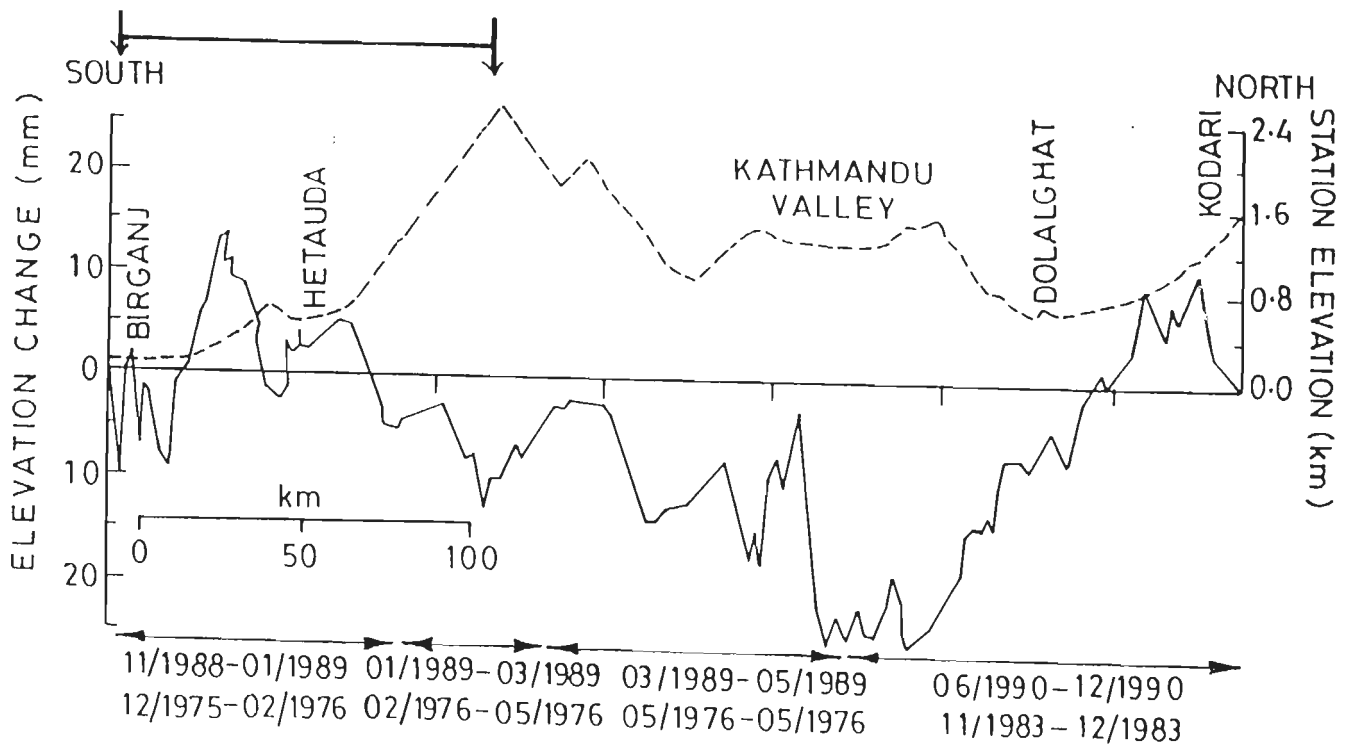


Fig.5.2 Height changes (solid lines) and the elevations (dotted lines) of benchmarks in central Nepal (after Jackson et al., 1992). The part of the line between the two thick arrows is used in our study. Measurement intervals are used to compute rate of uplift of Fig.5.3a.

of the levelling line on the Nepal-Tibet border (Fig.5.2). The observed elevation changes fall within the error bars over a significant part of the line.

5.2.2 Data used

The published data (Jackson et al., 1992) are unique and deserve an effort at interpretation. Our main concern in this thesis is for seismic hazards due to great earthquakes in the Himalaya. Our modelling shows that the elevation change signal of most interest, in this regard, is the prominent signal at about 25 km in projected distance from the southern end of the levelling line. It may be emphasized here that for our study we have not used the complete data set of Jackson et al. (1992) rather we have used only a part of it as shown in Fig.5.3a after projection onto a line perpendicular to the local trend of the Himalaya. This part of the line is approximately along the direction of convergence between Indian and Eurasian plates (DeMets et al., 1990 and Nakata et al., 1990). The estimated random error at the northern end of this part of the line is of the order of ± 0.7 cm and this signal is certainly well above the noise level.

The reason for not using the remaining part of levelling line are as follows. Firstly, over much of this segment the signals are within the error bars. Secondly, the segment of the levelling line, lying immediately to the north of that analysed here has a significant east-west component (Fig.5.1). The level change signal in this segment could have contributions conceivably due to processes subparallel to the strike of the Himalaya. Thirdly, the northernmost part of the levelling line lies in the northern Lesser and Higher Himalaya and the level change signal there may reflect geodynamics of the Higher Himalaya. This, in itself, is of considerable interest but we thought it prudent to await acquisition of data over longer time spans so that the signals are strong and above the random errors of the observations.

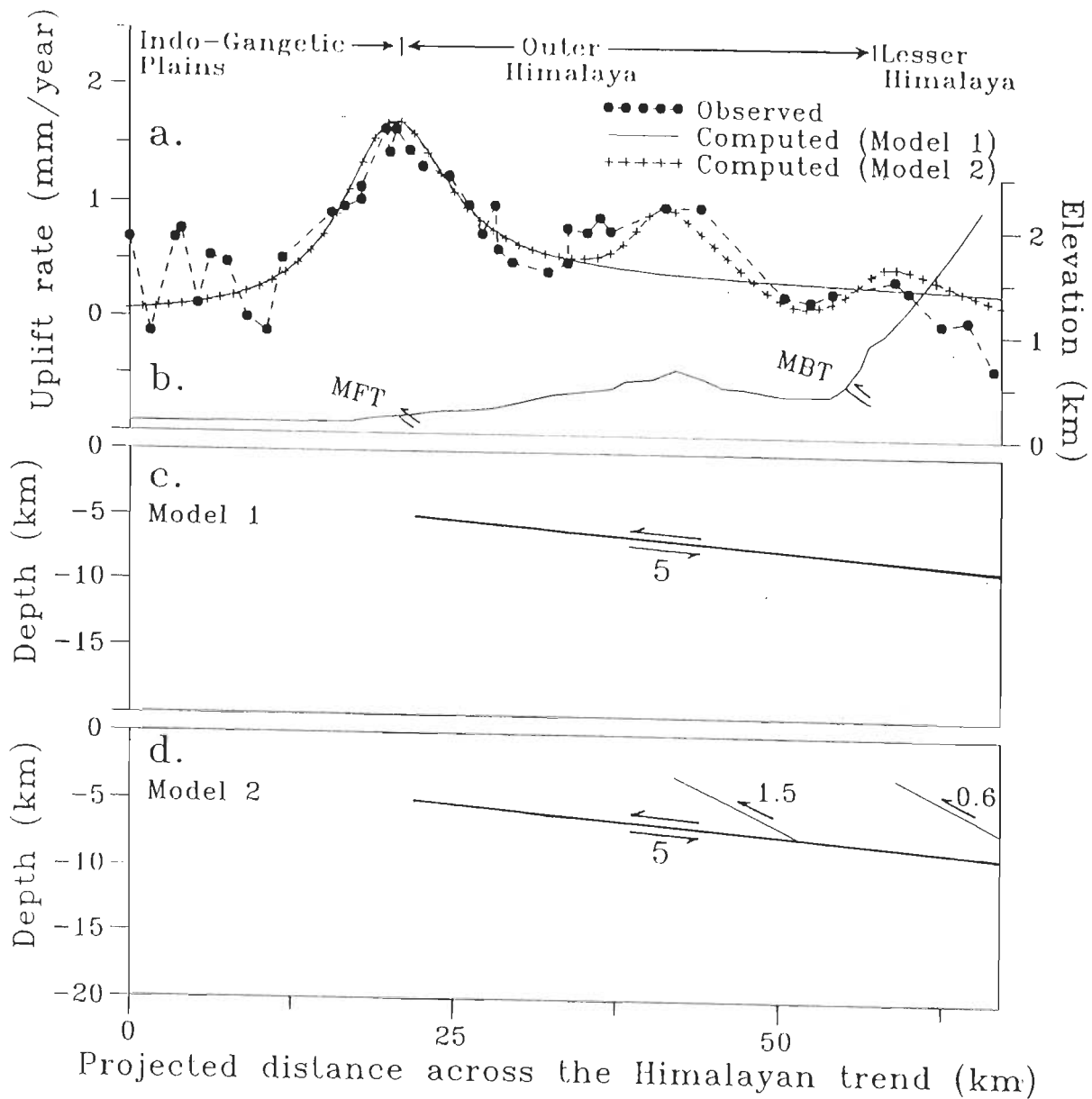


Fig.5.3 (a) is a comparison of the observed and calculated uplift rates along the part of the levelling line considered in this study. (b) shows the topography along the levelling line. The calculated uplift rates in (a) are the result of slip in mm/year on the faults of the models shown in (c) and (d). The single fault in (c) and the main fault in (d) corresponds to the detachment on which the slip of 5 mm/year is indicated.

5.3 Basic analysis

We invert the selected data for the causative slip on the subsurface faults using the theory of Mansinha and Smylie (1971) and the method of trial and error discussed in Chapter 2.

5.3.1 Possibility of bias in observations

A large number of fault models were considered. Thrust fault models received maximum attention within the framework of plate tectonics. But it was found necessary to assume for every successful thrust fault type model that the benchmark of the levelling network which was the starting point of the Nepalese levelling line and which was considered stationary during the period between the first and second surveys has itself subsided by approximately 8 mm in 13 years. In support of this hypothesis we point out that the observed ground elevation change curve of Fig.5.2 shows several oscillations with peak to peak variations of 8-12 mm near the southern end of the line in the plains of Central Nepal. Jackson et al. (1992) ascribed this scatter in observations to instabilities of benchmarks located in alluvium. The southernmost of these benchmarks was located in alluvium also. It too could be subject to such instabilities and could have experienced the estimated subsidence of about 8 mm during the 13 year period. For these reasons the rest of the discussion is based on the assumption that a uniform bias of 8 mm has crept into the observations.

5.3.2 Preferred model

All the data of Fig.5.3a cannot be explained with a single fault model. Thus predicted results for surface uplift rates due to slips on multiple faults are superposed as necessary for the interpretation. The main long wavelength features in the observations can be explained with a relatively simple three - fault model (Fig.5.3c). The agreement between observations and computed results can be improved with the introduction of additional small faults with minimal slip rates (Fig.5.3d). The small reverse faults of the model may simulate imbrication under the

Outer and Lesser Himalaya.

The main result of these analyses is that a single major fault is most active under the Outer and most of the Lesser Himalaya. We equate this fault with the thrust fault type detachment surface (Seeber and Armbruster, 1981). The depth of this fault at its southern end is 5 km and its dip is 5° . These numerical values are in close accord with those estimated for the detachment by several investigators (e.g. Lyon-Caen and Molnar, 1983; 1985; Ni and Barazangi, 1984; Chander, 1988 and Schelling, 1992).

Further, the annual slip rate on the detachment estimated from the Nepalese data is 5 mm/year. It is controlled primarily by the magnitude of maximum uplift rate and width of the region of high uplift rates in the Outer and southern Lesser Himalaya. It may be alluded here that in this part of Himalaya the estimated maximum random error in the uplift rate is of the order of ± 0.6 mm/year (7.7mm/13 years) as compared to the observed uplift signal of 2 mm/year. Thus the resulting error in the estimated slip rate will be even less than ± 0.5 mm, as compared to the estimated slip rate of 5 mm/year.

5.4. Interpretation of the estimated annual slip rate on the detachment

We now propose a possible explanation for the fact that the observed ground elevation changes can be explained with a slip rate of about 5 mm/year on the detachment whereas Lyon-Caen and Molnar (1983) opined that out of the estimated 50 mm/year (DeMets et al., 1990) of convergence between the Indian and Eurasian plates, 18 ± 7 mm/year is accommodated at the Himalaya.

We have to postulate as follows. Firstly, we assume that the observed ground elevation changes are the result of two competing deformations of the upper crust, namely, the permanent aseismic deformations and the recoverable earthquake generating strains. The possibility of aseismic slip on buried faults in the Higher Himalaya has been mooted in the literature (e.g.,

Seeber and Armbruster, 1981). Although specific observational evidence has to be collected, yet we entertain the possibility that even in the Lesser and Outer Himalaya, some of the ongoing, plate tectonics driven slip on the detachment and associated faults may not be giving rise to earthquakes, but producing permanent aseismic deformations in the upper crust.

Secondly, both types of deformations occur simultaneously due to slips on buried upper crustal faults in response to the continuing convergence of the Indian and Eurasian plates. Of course, the detachment is the most important of these faults.

Thirdly, we assume for simplicity of analysis that the partitioning of fault slip for producing permanent and recoverable deformations is the same on all upper crustal faults of the region.

Fourthly, we assume that the ground elevation changes due to both of these deformations can be estimated (e.g. see also King et al., 1988; Chander, 1989; Lin and Stein, 1989) using the above mentioned elastic theory of Mansinha and Smylie (1971). In particular we note that Linde and Silver (1989) used the formulae given by Okada (1985), which are entirely equivalent to those of Mansinha and Smylie (1971), to estimate deformation due to aseismic creep on the causative fault.

Fifthly, we make use of the fact that the ground elevation changes due to pre-seismic accumulation of earthquake generating strains should have signs opposite to those for the coseismic ground elevation changes due to the release of stored strain.

Finally, repeat levelling observations along the Saharanpur - Dehradun - Mussoorie line (Middlemiss, 1910 and Rajal et al., 1986) indicate that in the Outer Himalaya of that region the coseismic elevation changes due to the great Kangra earthquake of 1905 (Fig.4.3) as well as the interseismic changes (Rajal et al., 1986) both produce increases in heights of benchmarks. Since increases of ground elevations are observed also in the Outer Himalayan section of Nepalese levelling line (Jackson et al., 1992), we have to conclude in view of the fifth postulate that the ground elevation changes due to aseismic deformation are larger in magnitude than those for the concurrent accumulation of earthquake generating strains in the region. We assume

that this holds for the magnitudes of both the deformations over the entire levelling line.

These assumptions allow us to partition the convergence rate of 18 ± 7 mm/year (Lyon-Caen and Molnar, 1985) accommodated at Himalaya, into components responsible for aseismic deformations and storage of recoverable earthquake generating strains in the Nepal region. Let U_a and U_c represent the necessary annual slip rates on the detachment for simulating the two deformations respectively.

Then

$$U_a + U_c = 18 \pm 7 \text{ mm/year} \quad \dots(5.1)$$

$$U_a - U_c = 5 \text{ mm/year} \quad \dots(5.2)$$

Hence U_a and U_c should be 11.5 ± 3.5 mm/year and 6.5 ± 3.5 mm/year. In view of the various uncertainties attached to these estimates we round off and adopt the rates of 12 ± 4 mm/year and 7 ± 4 mm/year respectively. Using the relations given by Kasahara (1981), the annual slip rate on the detachment required for smaller magnitude earthquakes of the Himalayan seismic belt was estimated to be about 1 mm/year and hence ignored in these calculations.

Much more important than the estimated magnitudes of the partitioned slip rates is the fact emerging from this analysis that a significant part of the total estimated convergence rate of 18 ± 7 mm/year (Molnar, 1990) is currently causing accumulation of recoverable elastic strains in the upper crust and they will lead to a great earthquake (see Discussion) in the Central Nepal region in due course of time.

5.5 Discussion

5.5.1 On the interpretation of ground elevation change data

Jackson et al. (1992) did not interpret these ground elevation change data in terms of slips on buried faults because "...in the absence of microearthquake activity in the region, or a moderate to large historic earthquake from which a subsurface fault plane may be deduced,

there exists a range of possible models to explain the observed deformation. Moreover, it is possible to explain the deformation in terms of active folding without discrete displacement on a rupture surface". We have proceeded on the assumption that within the plate tectonics paradigm, as applied to the Himalaya, an active thrust type surface of detachment exists all along this convergent plate margin (Seeber and Armbruster, 1981; Khattri, 1987; Chander, 1988). Also, there is a body of opinion supported by observations and arguments (Seeber and Armbruster, 1981; Ni and Barazangi, 1984; Khattri, 1987; Chander, 1989a; Yeats and Lillie, 1991) that great Himalayan earthquakes occur by extended rupture in this surface. Specifically, the great Bihar-Nepal earthquake of 1934 is assumed to have occurred on the detachment (Chander, 1988 and Seeber and Armbruster, 1981). The meizoseismal area of this earthquake extended as far west as Kathmandu in Central Nepal.

5.5.2 Causes of elevation changes

A fundamental assumption of this analysis is that the ground elevation changes are ascribed to slips on the detachment. We acknowledge that there are differing views about the manner in which crustal deformations occur in the Himalaya occur. One extreme view is that the current uplift of the Himalaya could be driven by erosion alone (Burbank, 1992). Burbank (1992) analysed the drainage systems of the Indus and the Ganges rivers in the foreland basins and suggested that the importance of transverse drainage relative to longitudinal drainage can be interpreted in terms of erosion driven rather than thrust driven uplift. The other extreme view is that a part of the observed ground elevation changes in Central Nepal may arise from active folding and/or crustal thickening under parts of the levelling line.

However, we follow the view that this uplift is driven by thrusting due to plate convergence (Seeber and Armbruster, 1981 and Molnar, 1990). The possibility that these processes may operate simultaneously is also there. At the very least, analyses of ground elevation changes, based upon the thrust model should yield worthwhile end-member estimates for great Himalayan

earthquakes. Moreover, we consider here only the end member fault slip model for elevation changes because a set of mathematical formulae are available to calculate the effects to a first order approximation.

5.5.3 Elastic Strain accumulation for a great earthquake

The belt of small and moderate magnitude earthquakes lies in the Lesser Himalaya close to the Main Central Thrust (MCT) (Ni and Barazangi, 1984 and Khattri et al., 1989). However, the rupture zones of great Himalayan earthquakes lying in the detachment extend widthwise from this seismic belt southward under southern Lesser Himalaya and even under the Outer Himalaya (Seeber and Armbruster, 1981; Molnar and Pandey, 1989; Molnar, 1990; Chander, 1988; 1989a and Chapter 4 of the present thesis). Since the main elevation change signal of the Nepalese levelling data (Fig.5.3a) lies in the Outer and southern Lesser Himalaya, therefore, in view of the above analysis, this signal should imply strain accumulation for a great earthquake in the Central Nepal region.

5.5.4 Return period of great Himalayan earthquake

The estimated slip rate (7 ± 4 mm/year) for accumulation of recoverable crustal strain bears upon the return periods of great Himalayan earthquakes. The observed coseismic ground elevation changes during the 1905 Kangra earthquake (Middlemiss, 1910) (Fig.4.3) could be explained by assuming a slip of about 5 m on the detachment (Chander, 1988). This could be typical for great Himalayan earthquakes generally (Molnar, 1990 and Chander, 1989). Thus we estimate the return periods for great earthquakes in Central Nepal to be 700 years (i.e. $5 \text{ m} / 7 \pm 4 \text{ mm/year}$) with a range of 450 to 1700 years.

Alternatively, we may adopt for the sake of argument 10^{-4} as the limiting value of earthquake generating upper crustal strains. Then the annual slip rate of 7 ± 4 mm/year in conjunction with an estimate of 17 km for the depth of the detachment in the Main Central

Thrust (MCT) region where the great Himalayan earthquakes nucleate (Ni and Barazangi, 1984; Molnar and Pandey, 1989 and Molnar, 1990), yields a rate of shear strain accumulation of $0.35 \pm 0.2 \times 10^{-6}$ per year and return periods of 245 years with a possible range of 165 to 475 years. The depth of 17 km for nucleation of great Himalayan earthquakes in the detachment is adopted here because it corresponds to the maximum depth reported by Ni and Barazangi (1984) for revised estimates of focal depth for moderate Himalayan earthquakes. This would be the depth of brittle - ductile transition under the outcrop of the MCT generally (Fig.5.1).

Return periods have been estimated to be 180 to 240 years by Seeber and Armbruster (1981) and 100 to 1000 years by Molnar (1990).

5.5.5 Stage of strain accumulation

There is no indication from the levelling data as to the current stage of strain accumulation in the recurrence cycle of great earthquakes in Central Nepal. Hence the time of occurrence of the next great earthquake cannot be predicted. The difficulty is compounded by lack of sufficiently long historical record for past great earthquakes of the region. As noted earlier eastern half of Nepal has experienced the great earthquake of 1934 while the western half probably experienced a comparable earthquake in 1833 (Seeber and Armbruster, 1981).

5.5.6 Current tectonic status of the MFT

Since the data interpreted here are derived from the graphical display of Fig.5.2 of Jackson et al. (1992), the exact locations of the tectonic features such as the MFT and MBT with respect to the plotted section (Fig.5.3a) are not known to us. The locations shown in Fig.5.3a are our best estimates. However, the continuing interseismic uplift of the Outer and southern Lesser Himalaya is clearly evident in the elevation change profile.

The most prominent uplift signal in the Outer Himalaya coincides approximately with the surface trace of the MFT. It is simulated in our model mainly by slip on the buried detachment.

But models comprising subsurface faults with varying slip and including a fault outcropping near the surface trace of MFT may be made consistent with the data also.

Thus the situation is analogous to that encountered while interpreting the coseismic data in the previous chapter. The interseismic geodetic data are also not conclusive about the current activity of the MFT. The period involved here is too short to seek such evidence using geological observations.

5.6 Summary

In short the recent levelling observations in Central Nepal indicate that the slip of 7 ± 4 mm/year on the detachment, i.e., about 40% of the total of 18 ± 7 mm/year plate convergence accommodated at the Himalaya, is causing build up of recoverable earthquake generating strains which will be released either partially or completely in the next great earthquake of the region. But due to lack of suitable other constraints, the data do not permit us to predict the date and time of the earthquake.

5.7 Note

Since the article by Jackson et al. (1992) did not contain a comprehensive interpretation of the data, the analysis reported in this chapter was undertaken during the summer of 1993. Our results were communicated to Tectonophysics in the form of an article in fall 1993. Subsequently in early 1994 from the communication in connection with the review of our manuscript by Dr. Bilham, it emerged that Drs. Jackson and Bilham have undertaken an interpretation of this data set after incorporating certain corrections. While the two methods of analysis differ, the main result from our standpoint, that the detachment under the Outer and Lesser Himalaya is required to slip by about 5 mm/year only during the interseismic period of interest here, is exactly identical in the two studies although we have used the data published in 1992 and Drs. Jackson and Bilham used the subsequently revised and corrected data.

CHAPTER VI

Interpretation of post Kangra earthquake levelling observations in the Dehradun region

6.1 Introduction

In last chapter we discussed and interpreted the interseismic elevation changes along a part of the 350 km long levelling line in the central Nepal Himalaya. The only other observations of interseismic elevation changes along a moderately long levelling line in India are from the Dehradun region of Garhwal Himalaya. Although the line is just 80 km long yet the similarity in the observations of elevation changes with those in the central Nepal, permits us to interpret these data. Rajal et al. (1986) used these observations to infer an uplift rate of about 1 mm/year for the Outer Himalaya. Yeats and Lillie (1991) analyzed these data qualitatively to support their hypothesis of the existence of a blind active thrust under the Outer and Lesser Himalaya.

We interpret these data as a result of slips on the subsurface detachment under the Outer and Lesser Himalaya. Taking the cue from the analysis of Chapter V, we find evidence of strain accumulation for a great earthquake in the Dehradun region also.

6.2 Observational data

Rajal et al. (1986) reported three sets of elevation change data along a levelling line from Saharanpur to Mussoorie via Dehradun. The levelling line passes through the Indo-Gangetic plains and Outer Himalaya (Fig.6.1 and 6.2). A few benchmarks are also located further north in the southern Lesser Himalaya. However, this part of the levelling line follows an almost east-west trend and hence the observations of elevation changes from these benchmarks are of little use in an analysis that deals with tectonic processes normal to the local (NW-SE) strike of the

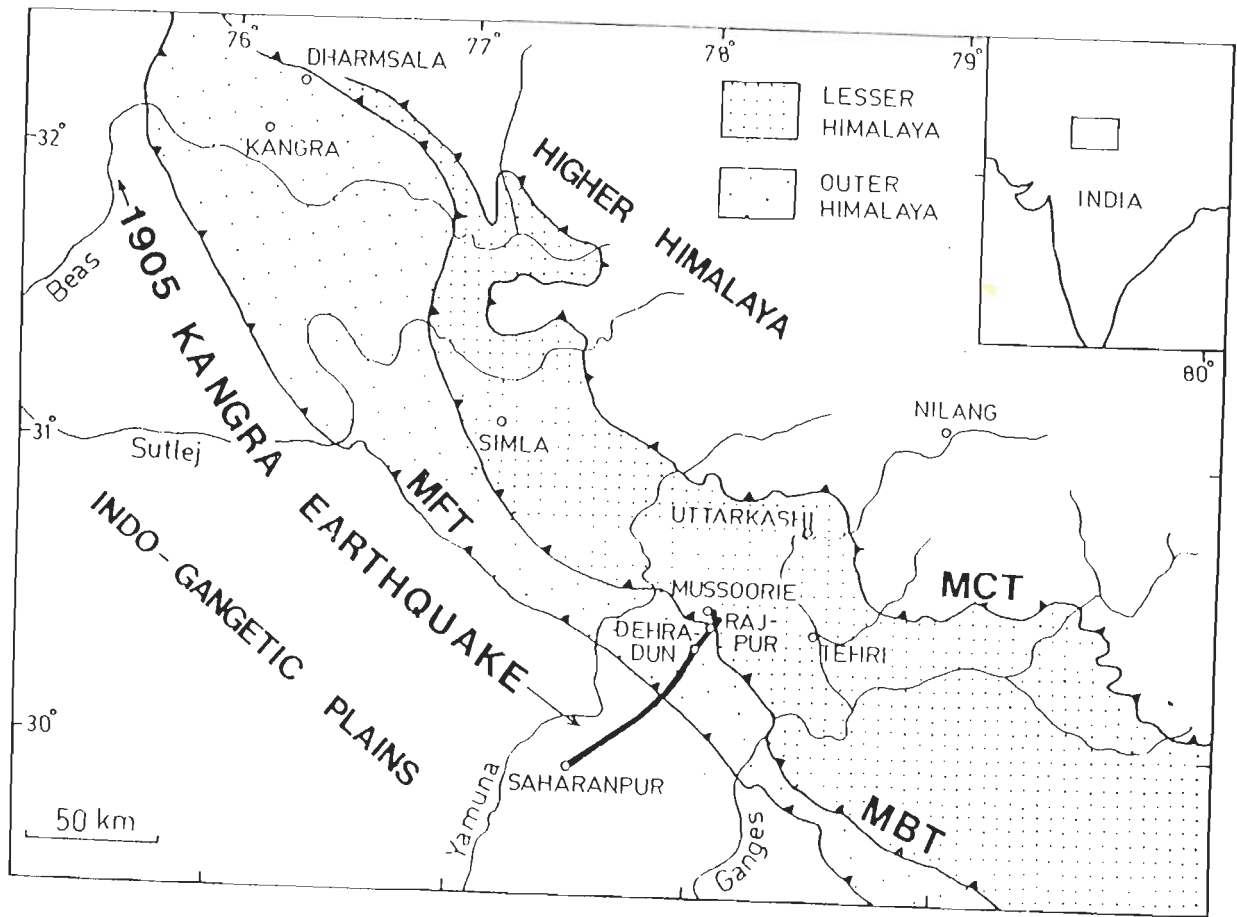


Fig.6.1 General geology of Garhwal and Himalachal Himalaya. Region affected by 1905 Kangra earthquake is also shown. The levelling line between Saharanpur and Mussorie is denoted with a thick line. MBT-Main Boundary Thrust and MCT- Main Central Thrust.

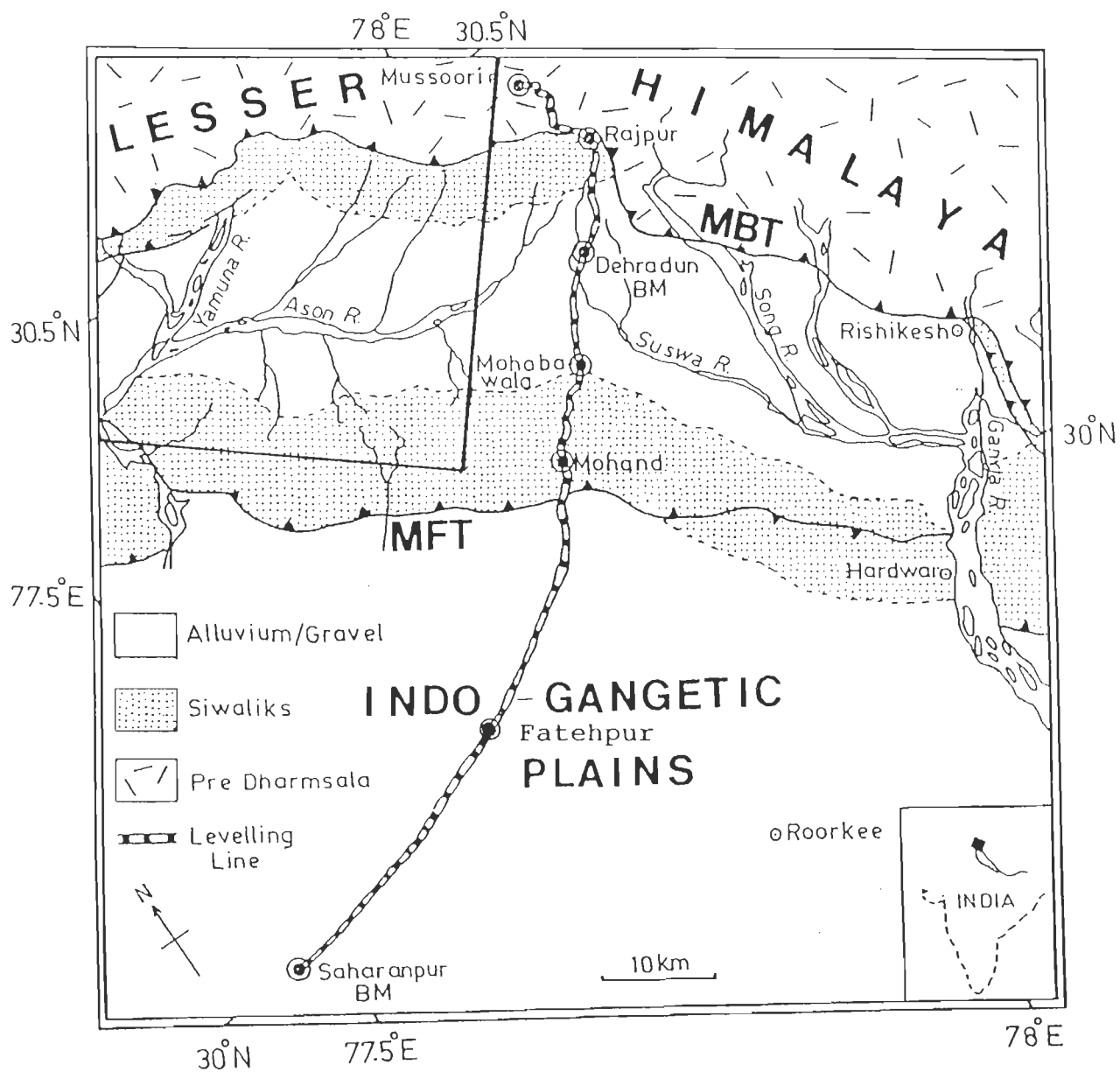


Fig.6.2 The levelling line from Sharanpur to Mussorie. Some of the important benchmarks along the line are also identified. The inferred location of the southwestern and southeastern edges of the 1905 Kangra earthquake rupture is also shown. Geology and tectonic features adopted from Raiverman et al. (1983). The abbreviations used are MBT- Main Boundary Thrust, MFT- Main Frontal Thrust.

Himalaya. The first set of data for the period from 1861-62 to 1905-07 pertains to the coseismic elevation changes induced by the Kangra earthquake. These data were analyzed by us in Chapter IV. The elevation change data for the period 1905-07 to 1926-28 and 1926-28 to 1974-75 (Fig.6.3) are the subject of analysis in this chapter. For the sake of brevity we call them as 21 and 47 year data. Since no great or even major earthquake has occurred in the Dehradun region during the period of these observations, we regard these two sets of elevation changes as a manifestation of aseismic slip on the detachment and of the associated deformation of the overlying rocks during a period between two great earthquakes of the region.

6.2.1 Possible extent of random errors in elevation changes

Rajal et al. (1986) did not report any estimates about the magnitudes of random errors. Still to get an idea about the errors in the elevation changes we use Eqn.4.1 again. Since these observations are taken along the same line along which the observations of coseismic elevation changes due to 1905 Kangra earthquake were taken, the estimates of the accumulated random errors are the same for all three periods (see Section 4.4.2.1). Thus at the end of about 80 km long line the estimated maximum possible random error in a level change observation is of the order of about ± 2 cm.

6.2.2 Stability of benchmarks in the 1926-28 to 1974-75 data

A comparison of the estimated elevation changes for the 21 and 47 year periods raises the question of stability of many benchmarks. The benchmarks referred here are especially those located in the Indo-Gangetic alluvium south of Mohand and in alluvium and gravel covered areas between Mohabawala and Rajpur in Dehradun valley (Fig.6.2). Three sets of remarks appear necessary. Firstly, the isolated benchmark at Fatehpur shows a marked increase in elevation during the 47 year period (Fig.6.3). But the data on the elevation of this benchmark in the preceding 21 year period are not available (Rajal et al., 1986). In our opinion a few

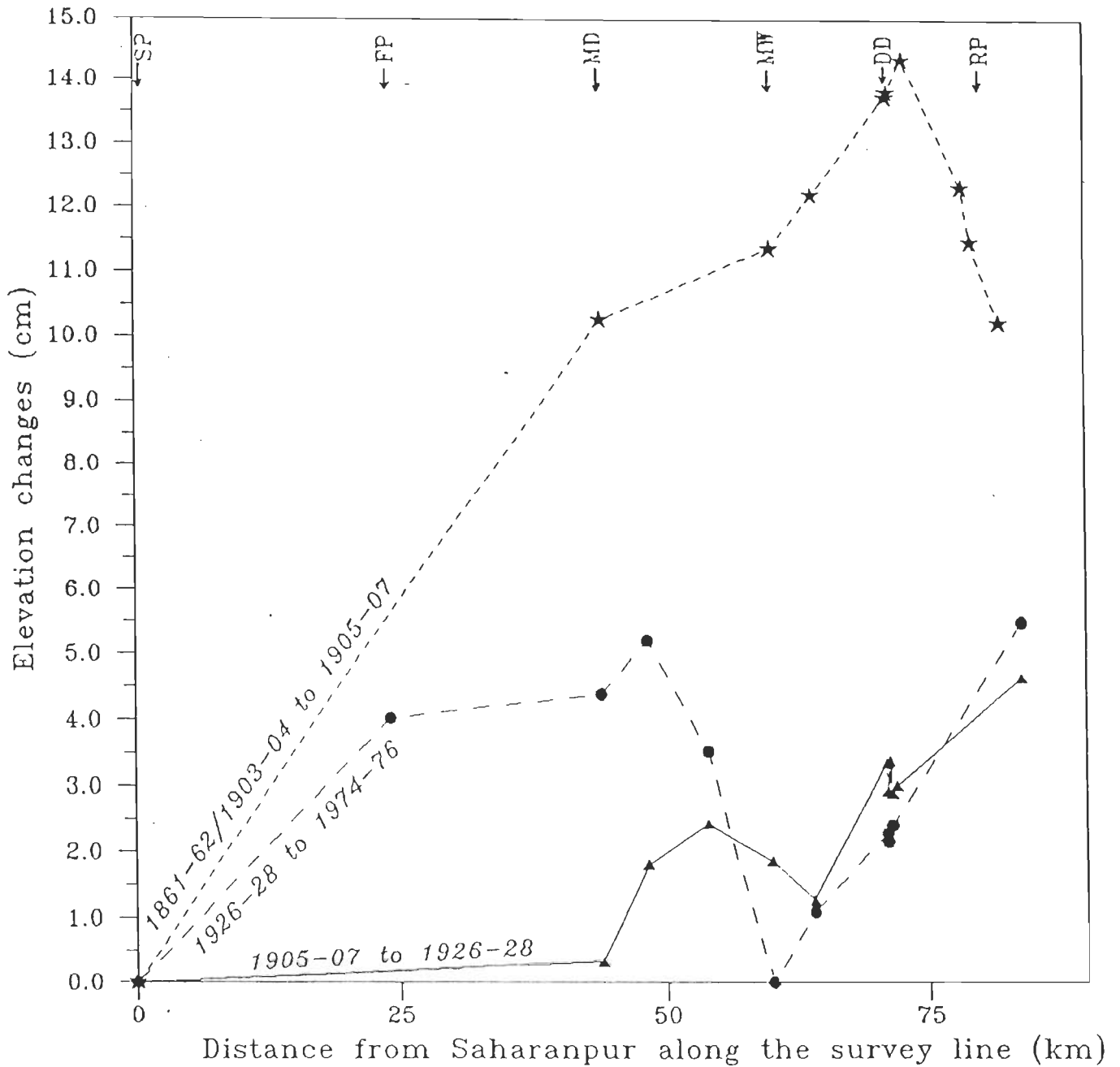


Fig.6.3 The elevation changes of the benchmarks along the levelling line in Fig.6.2 (Rajal et al., 1986) are plotted with distance from the Saharanpur benchmark. The elevation changes denoted by stars are due to coseismic uplift during the 1905 Kagra earthquake. The triangles and circles denote the interseismic uplift during the two periods indicated in the figure. These observations are used in this chapter. The abbreviations used are SP- Saharanpur, FP- Fatehpur, MD- Mohand, MW- Mohabawala, DD- Dehradun and RP- Rajpur.

additional benchmarks should be established near the existing one at Fatehpur and their heights should be monitored for a suitable period because, as speculated by Jackson et al. (1992), benchmarks established on the alluvium may be subject to instabilities. Thus we did not use the observed elevation change at this benchmark for the 47 year period. Secondly, for the section of levelling line between Mohabawala and Rajpur, the amount of elevation changes for 21 year and 47 year periods are similar in sign but dissimilar in magnitude (Fig.6.3). The region around Dehradun has witnessed explosive growth during the second half (1947 to 1974-76) of the 47 year period. Systematic ground subsidence due to withdrawal of ground water (Segall, 1985) may have partly negated the aseismic tectonic uplift occurring in the region and this could be a reason why the ground elevation changes between Mohabawala and Rajpur (Fig.6.3) during the 47 year period are not proportionately higher than those during the 21 year period. Thirdly, the gap of nearly five decades between two surveys is just too long for accurate geodetic monitoring of ground level changes. In short there are grave doubts about the ground elevation change data over nearly 75% of the levelling line between Saharanpur and Rajpur for the 47 year period between 1926-28 to 1974-75.

6.2.3 The elevation changes during 1905-07 and 1926-28 as the post-seismic changes

While the elevation changes observed during the 1905-07 and 1926-28 period can be regarded as post Kangra earthquake changes also, we interpret them on the assumption that they are interseismic changes in the Dehradun region. This is partly because of the following reasons (i) postseismic changes are also interseismic changes in a strict sense and (ii) the overall pattern of elevation change profile in the 21 year and 47 year periods is remarkably similar. The elevation changes of the 1926- 28 to 1974-75 period may be called interseismic changes. Therefore the elevation changes during the 1905-07 to 1926-28 period being broadly similar to those for the subsequent 47 year period may also be regarded as interseismic changes.

6.3 Method of analysis

We use the above two sets of ground elevation changes to estimate the slip on the subsurface faults. In view of the limited quantity and the poor quality of the data and the experience gained by the analysis in Chapter 4, we assumed a planar fault under the Outer and Lesser Himalaya. We divided this subsurface planar fault into several fault segments which are joined edge to edge along their strike. The width of each segment is 7.5 km. The slip is assumed to be constant in each segment but it varies from one segment to another. Thus the slip varies in dip direction of this planar fault. In these models the fault extend right upto the southwestern limit of the Outer Himalaya but it remains buried at a depth of 5 km. Thus, in short, we assume that these interseismic changes can be explained by variable slip on the same fault on which the rupture of 1905 Kangra earthquake occurred (see Section 4.6.1).

We apply the minimum norm inversion (see section 2.4.2) on the elevation changes during the periods between 1905-07 to 1926-28 and 1926-28 to 1974-75 to estimate the slip distribution on the subsurface fault.

6.4 Resulting model of slip variation

Fig.6.4a and Table 6.1 compare the observed elevation changes during the 1905-07 to 1926-28 period with the theoretically computed values. The computed elevation changes correspond to the inverted slip distribution shown in Fig.6.4b. The magnitude of the regularizing parameter in Eqn.2.10 is 1.0×10^{-3} which yielded the best results which is of the order of elements of matrix **A**.

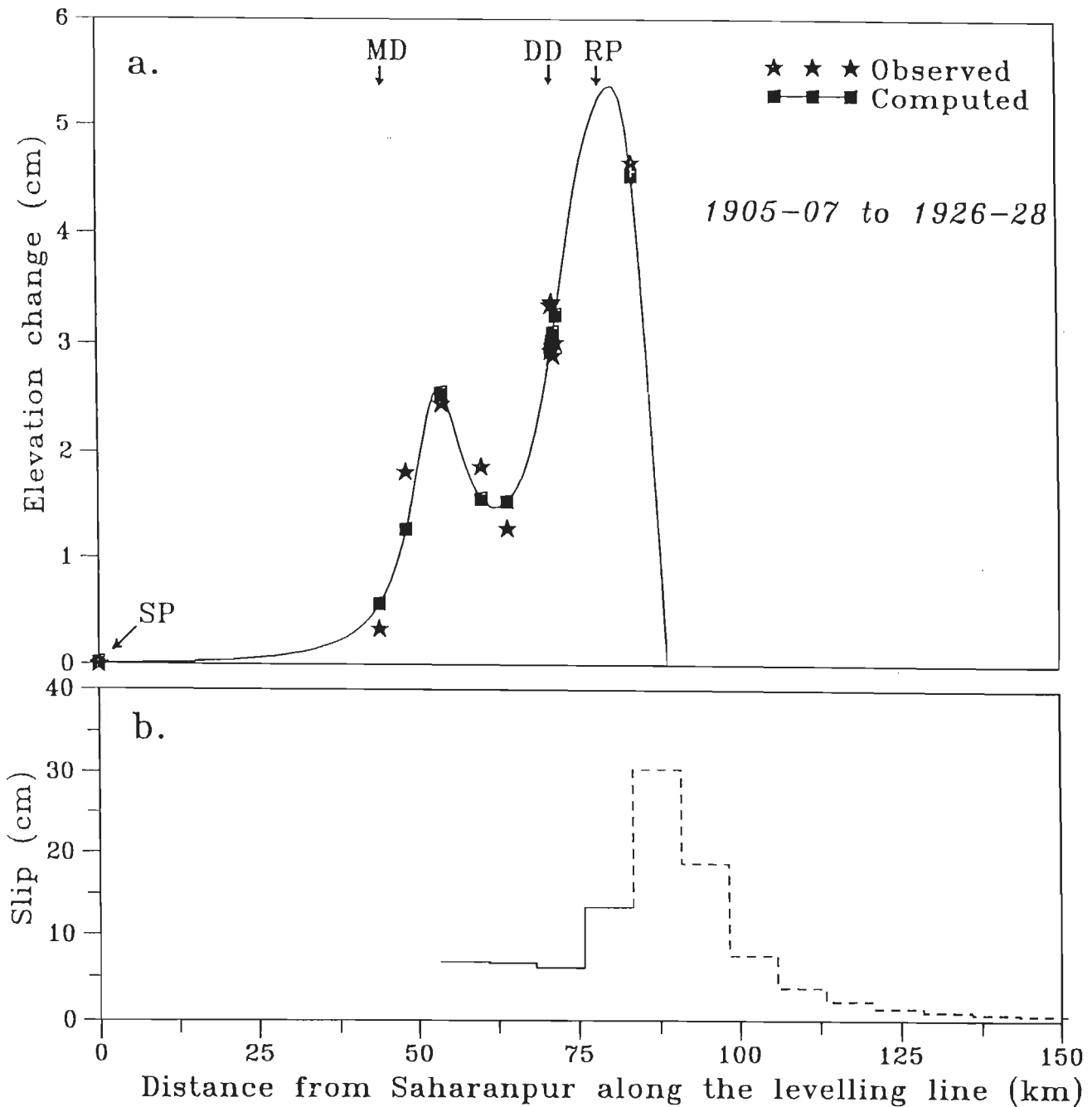


Fig.6.4 Comparison between observed and computed elevation changes, for the period 1905-07 to 1926-28, along the levelling line are shown in the upper part. Positions of benchmarks are also indicated. The estimated distribution of slip in the dip section of the planar fault is shown in lower part (b). The slip estimates shown by solid lines are well resolved by the data and those with the dashed lines are poorly resolved.

Table 6.1 Comparison of the observed and computed elevation changes for the 21 years period.

Description of the benchmark	Distance from Saharanpur (km)	Elevation changes (cm)	
		Observed	Computed
G.T.S.Saharanpur	0.00	0.00	0.01
Mohand	44.05	0.33	0.56
GTS on Iron BM bridge over Kheri Rao	48.32	1.81	1.27
GTS on Iron bridge	54.08	2.44	2.54
Mohabawala	60.17	1.86	1.56
Colonel Everest's upper mark Dehradun	64.20	1.28	1.53
GTS benchmark 1904 Survey Office	71.20	3.35	2.94
GTS iron plug, GB office, Dehradun	71.26	2.93	2.96
Colis Satelite station 1896	71.43	3.38	3.03
GTS near Haig SBM 1904 Observatory	71.64	2.89	3.10
GTS standard benchmark Dalanwala House	72.04	3.01	3.26
GTS on rock, 1.6 km from Rajpur	83.79	4.64	4.51

Similarly Fig.6.5 and Table 6.2 refer to the observed elevation change data during the period 1926-28 to 1974-75.

Table 6.2 Comparison of the observed and computed elevation changes for the 47 years period.

Description of the benchmark	Distance from Saharanpur (km)	Elevation changes (cm)	
		Observed	Computed
G.T.S.Saharanpur	0.00	0.00	0.02
Fatehpur	24.22	4.03	not used
Mohand	44.05	4.39	2.85
GTS on Iron BM bridge over Kheri Rao	48.32	5.21	5.95
GTS on Iron bridge	54.08	3.53	2.85
Mohabawala	60.17	0.00	0.64
Colonel Everest's upper mark Dehradun	64.20	1.10	0.63
GTS benchmark 1904 Survey Office	71.20	2.29	2.24
GTS iron plug, GB office, Dehradun	71.26	2.16	2.24
GTS near Haig SBM 1904 Observatory	71.64	2.41	2.31
GTS on rock, 1.6 km from Rajpur	83.79	5.49	5.29

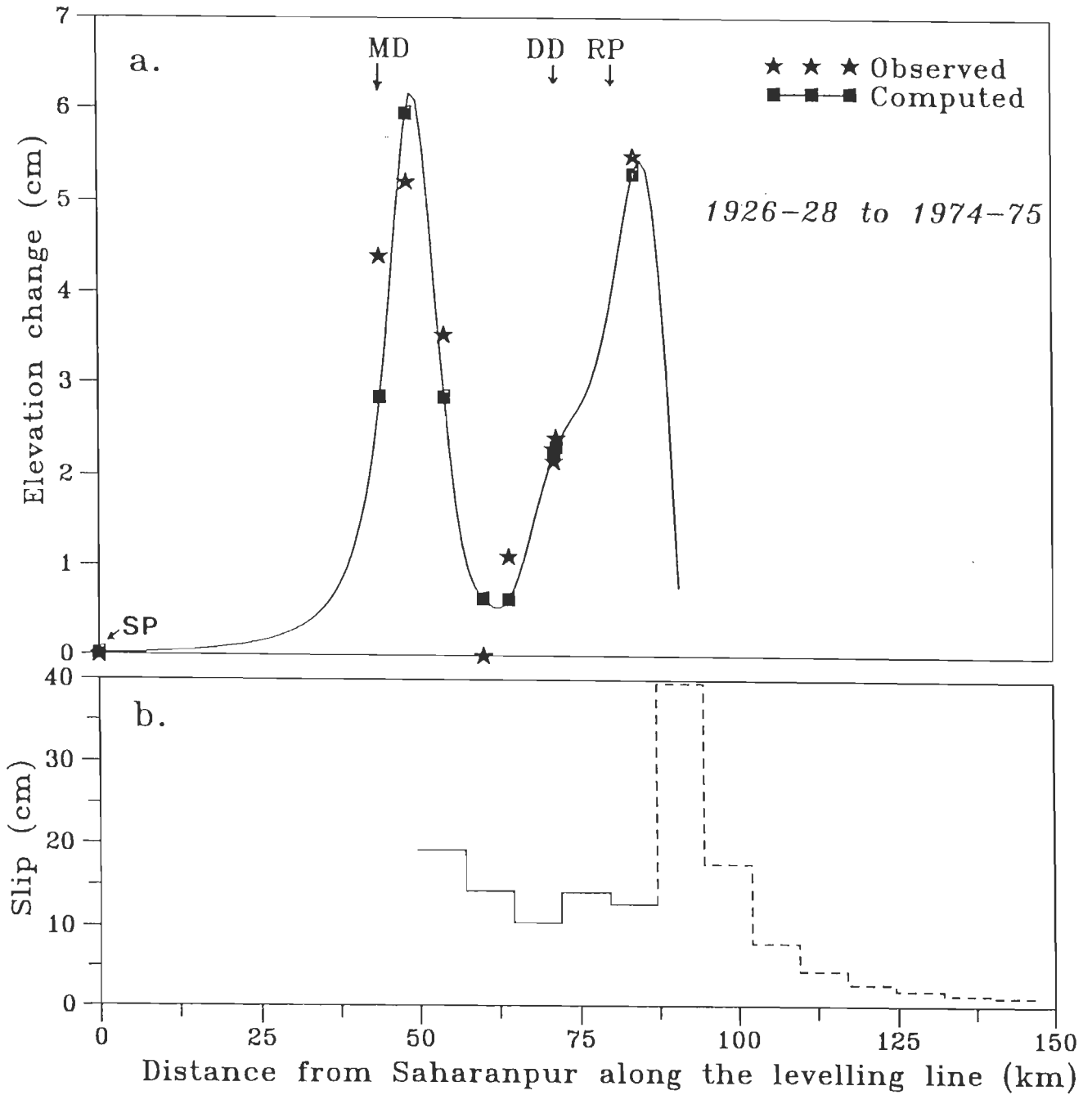


Fig.6.5 Same as Fig.6.4, but for the period 1926-28 to 1974-75.

6.4.1 Quality of inversion

6.4.1.1 1905-07 to 1926-28 data

The **R** and **S** matrices (Eqns.2.11 and 2.12) for the above inversion are given below.

$$\mathbf{R} = \begin{pmatrix} .99 & .00 & -.01 & .00 & .00 & .00 & .00 & .00 & .00 & .00 & .00 & .00 & .00 \\ .00 & .98 & .02 & -.02 & -.01 & .00 & .00 & .00 & .00 & .00 & .00 & .00 & .00 \\ -.01 & .02 & .94 & .04 & .00 & .00 & .01 & .01 & .01 & .00 & .00 & .00 & .00 \\ .00 & -.02 & .04 & .96 & .03 & -.06 & -.01 & .00 & .00 & .00 & .00 & .00 & .00 \\ .00 & -.01 & .00 & .23 & .45 & .42 & .16 & .08 & .04 & .03 & .02 & .01 & .01 \\ .00 & .00 & .00 & -.06 & .42 & .27 & .10 & .05 & .03 & .02 & .01 & .01 & .01 \\ .00 & .00 & .01 & -.01 & .16 & .10 & .04 & .02 & .01 & .01 & .00 & .00 & .00 \\ .00 & .00 & .01 & .00 & .08 & .05 & .02 & .01 & .01 & .00 & .00 & .00 & .00 \\ .00 & .00 & .01 & .00 & .04 & .03 & .01 & .01 & .00 & .00 & .00 & .00 & .00 \\ .00 & .00 & .00 & .00 & .03 & .02 & .01 & .00 & .00 & .00 & .00 & .00 & .00 \\ .00 & .00 & .00 & .00 & .02 & .01 & .00 & .00 & .00 & .00 & .00 & .00 & .00 \\ .00 & .00 & .00 & .00 & .01 & .01 & .00 & .00 & .00 & .00 & .00 & .00 & .00 \\ .00 & .00 & .00 & .00 & .01 & .01 & .00 & .00 & .00 & .00 & .00 & .00 & .00 \end{pmatrix}$$

$$\mathbf{S} = \begin{pmatrix} .00 & .00 & .00 & .00 & .00 & .00 & .00 & .00 & .00 & .00 & .00 & .00 & .00 \\ .00 & .03 & .08 & .15 & -.01 & .00 & .01 & .01 & .00 & .00 & -.01 & .00 & .00 \\ .00 & .08 & .21 & .39 & -.05 & .00 & .01 & .01 & .01 & .00 & -.02 & .00 & .00 \\ .00 & .15 & .39 & .75 & .03 & -.02 & .00 & .00 & .00 & .00 & -.01 & -.01 & .00 \\ .00 & -.01 & -.05 & .03 & .90 & .13 & -.10 & -.09 & -.04 & .02 & .14 & .00 & .00 \\ .00 & .00 & .00 & -.02 & .13 & .79 & .16 & .14 & .06 & -.04 & -.23 & .00 & .00 \\ .00 & .01 & .01 & .00 & -.10 & .16 & .22 & .21 & .19 & .17 & .13 & .00 & .00 \\ .00 & .01 & .01 & .00 & -.09 & .14 & .21 & .21 & .19 & .18 & .15 & .00 & .00 \\ .00 & .00 & .01 & .00 & -.04 & .06 & .19 & .19 & .20 & .19 & .20 & .00 & .00 \\ .00 & .00 & .00 & .00 & .02 & -.04 & .17 & .18 & .19 & .21 & .25 & .00 & .00 \\ .00 & -.01 & -.02 & -.01 & .14 & -.23 & .13 & .15 & .20 & .25 & .36 & .00 & .00 \\ .00 & .00 & .00 & -.01 & .00 & .00 & .00 & .00 & .00 & .00 & .00 & .00 & .98 \end{pmatrix}$$

Thus it is seen from the **R** matrix that the first four slip estimates are better resolved by the data which correspond to the slip values of 6-13.5 cm (Fig.6.4). The matrix **S** confirms that the elevation changes for all benchmarks except the Saharanpur and Mohand benchmarks have significant contributions to the solution.

6.4.1.2 1926-28 to 1974-75 data

The **R** and **S** matrices (Eqns.2.11 and 2.12) for this solution are given as follows.

$$\mathbf{R} = \begin{pmatrix} .99 & .00 & .00 & .00 & .00 & .00 & .00 & .00 & .00 & .00 & .00 & .00 & .00 \\ .00 & .99 & .00 & -.01 & .01 & -.01 & .00 & .00 & .00 & .00 & .00 & .00 & .00 \\ .00 & .00 & .99 & .01 & -.04 & .00 & .00 & .01 & .00 & .00 & .00 & .00 & .00 \\ .00 & -.01 & .01 & .85 & .33 & -.07 & -.02 & .00 & .00 & .01 & .00 & .00 & .00 \\ .00 & .01 & -.04 & .43 & .51 & .23 & .06 & .03 & .02 & .01 & .01 & .01 & .00 \\ .00 & -.01 & .00 & -.07 & .13 & .77 & .33 & .14 & .07 & .04 & .03 & .02 & .01 \\ .00 & .00 & .00 & -.02 & .06 & .33 & .14 & .06 & .03 & .02 & .01 & .01 & .01 \\ .00 & .00 & .01 & .00 & .03 & .14 & .06 & .03 & .01 & .01 & .01 & .00 & .00 \\ .00 & .00 & .00 & .00 & .02 & .07 & .03 & .01 & .01 & .00 & .00 & .00 & .00 \\ .00 & .00 & .00 & .01 & .01 & .04 & .02 & .01 & .00 & .00 & .00 & .00 & .00 \\ .00 & .00 & .00 & .00 & .01 & .03 & .01 & .01 & .00 & .00 & .00 & .00 & .00 \\ .00 & .00 & .00 & .00 & .01 & .02 & .01 & .00 & .00 & .00 & .00 & .00 & .00 \\ .00 & .00 & .00 & .00 & .00 & .01 & .01 & .00 & .00 & .00 & .00 & .00 & .00 \end{pmatrix}$$

$$\mathbf{S} = \begin{pmatrix} .00 & .00 & .00 & .00 & .00 & .00 & .00 & .00 & .00 & .00 \\ .00 & .17 & .37 & .04 & -.06 & .04 & .00 & .00 & .00 & .00 \\ .00 & .37 & .77 & .09 & -.12 & .06 & .00 & .00 & -.01 & -.01 \\ .00 & .04 & .09 & .69 & .38 & -.22 & .01 & .01 & .01 & -.01 \\ .00 & -.06 & -.12 & .38 & .49 & .28 & -.02 & -.02 & -.01 & .00 \\ .00 & .04 & .06 & -.22 & .28 & .82 & .02 & .02 & -.02 & -.01 \\ .00 & .00 & .00 & .01 & -.02 & .02 & .33 & .33 & .32 & -.01 \\ .00 & .00 & .00 & .01 & -.02 & .02 & .33 & .33 & .32 & -.01 \\ .00 & .00 & -.01 & .01 & -.01 & -.02 & .32 & .32 & .36 & .01 \\ .00 & .00 & -.01 & -.01 & .00 & -.01 & -.01 & -.01 & .01 & .98 \end{pmatrix}$$

From the **R** matrix, it is clear that the first five slip estimates are better resolved by the data. The corresponding slip estimates are 10-19 cm (Fig.6.5). The **S** matrix in this case also confirms that the elevation change data from Saharanpur and Mohand benchmarks are contributing least to the solution.

6.5 Interpretation of the estimated annual slip rate

Thus the above observed elevation changes in the 21 and 47 years periods can be explained by slip rates of about 3-7 and 2-4 mm/year respectively (Figs. 6.4 and 6.5). However, in view of the errors due to instability in 47 year data, as discussed in section 6.2.2, we use the slip

estimate for 21 years period data in our further calculations. Thus we adopt a value of 5 ± 2 mm/year for the slip rate in the Dehradun region.

6.5.1 Major similarities in uplift rate data of Dehradun and central Nepal regions

The Nepalese and Indian levelling lines are separated by a distance of about 1000 km. Still, inspite of the sparseness of Indian data, the relative highs and lows of the projected uplift rate profiles are remarkably similar across the Outer Himalaya in both the cases (Fig.6.6). Also, the magnitudes of uplift rates are quite comparable in both profiles.

This allows us to perform an analysis similar to that carried out by us on the Nepalese data for slip partitioning (see Section 5.4). Also conclusions drawn in that analysis can directly be applied to this analysis. The two relevant equations (comparable to Eqns.5.1 and 5.2) may be written in this case as follows.

$$U_a + U_c = 18 \pm 7 \text{ mm/year} \quad \dots(6.1)$$

$$U_a - U_c = 5 \pm 2 \text{ mm/year} \quad \dots(6.2)$$

Thus U_a and U_c should have a value of the order of 12 ± 5 and 7 ± 5 mm/year.

The immediate deduction from the similarities in the Nepalese and Dehradun data and the above analysis of the latter data is that recoverable elastic strain should be accumulating for a great earthquake in the Dehradun region also, the partitioned rate of slip on the detachment for strain accumulation being about 7 ± 5 mm/year.

The return periods of great earthquakes in the region cannot be estimated from the available data and analyses because of the following reasons. Firstly, all the observed elevation change data have been obtained along a single and very short profile. Secondly, the number of benchmarks established along the line is relatively small. Thirdly, the random errors in the observations are relatively large. Finally, reliable estimates of ground elevation changes arising from erosion in the region are not available (e.g. Burbank, 1992).

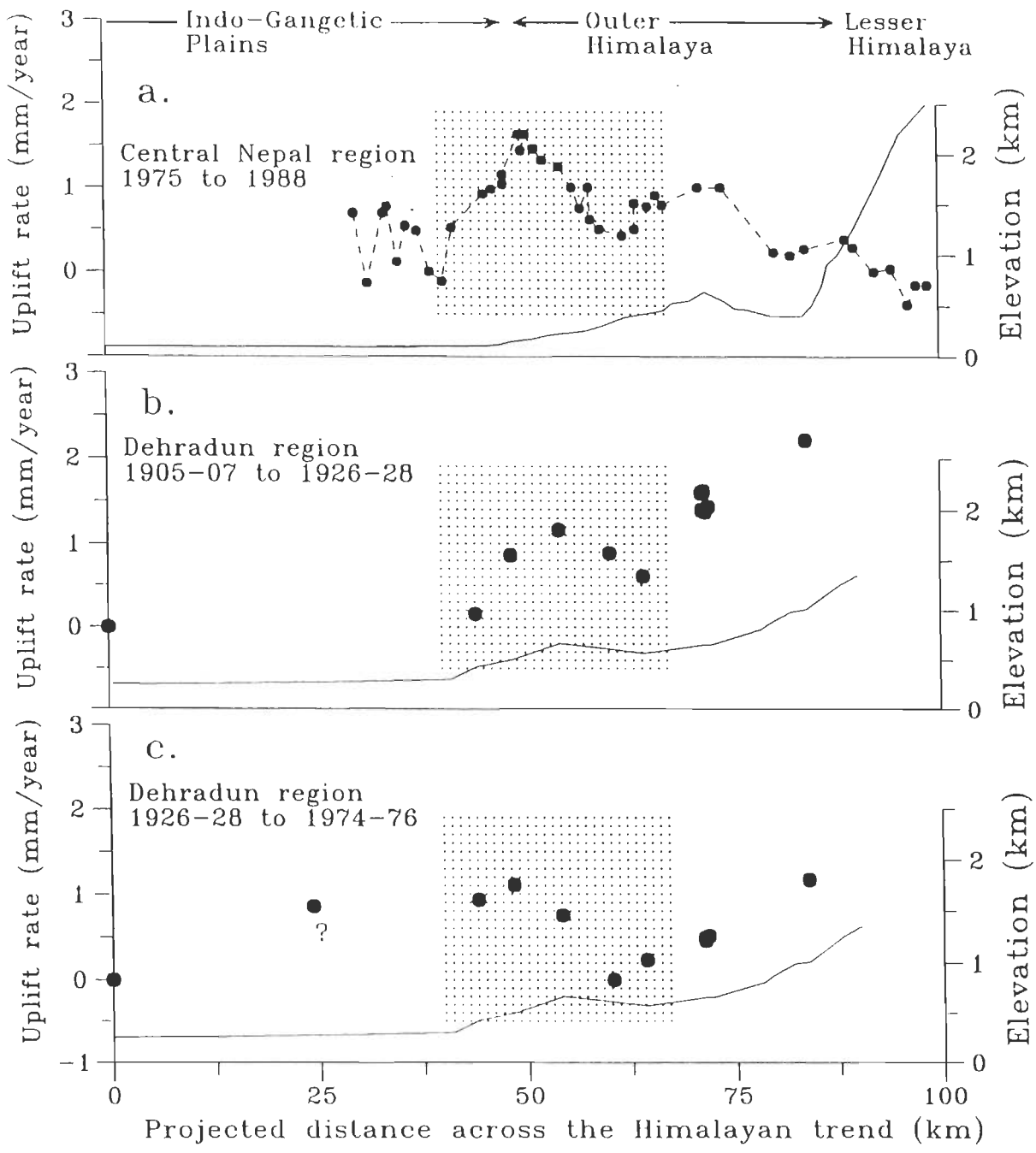


Fig.6.6 Comparison of uplift rates along Nepalese and Indian levelling lines. The periods between the levelling observations on which these rates are based are indicated. The shaded portions highlight data from the Outer Himalaya. The Topography along the levelling line is also shown.

6.6 Discussion

6.6.1 Sensitivity of the slip estimates

As discussed earlier (Section 6.2.1) the magnitude of random errors in the observations is relatively large. In Figs.6.7a and 6.8a the error bars corresponding to the observed elevation change at each benchmarks are shown. Thus we obtain the maximum and minimum possible estimates of elevation changes by adding and subtracting the respective random errors. Corresponding to these estimates we invert for the slip distribution on the same subsurface fault. The Figs.6.7b and 6.8b demonstrate that the errors in the first four slip estimates, which are better resolved by the observations, are of the order of about ± 10 cm. Thus, it is seen from these analyses that the slip estimates are very sensitive to the random errors in the observational data.

6.6.2 Possible influence of microseismicity on the elevation changes

The possibility that the ground elevation changes being analyzed here could be the result of coseismic elevation changes during a series of micro-, small and moderate earthquakes may be ruled out. This is because, as remarked in Chapter I, such earthquakes occur in the Garhwal region in the vicinity of the MCT (Ni and Barazangi, 1984 and Khattri et al., 1989) in a well defined belt. During the period between great earthquakes the Outer Himalaya of the Dehradun region are essentially aseismic.

6.6.3 Current tectonic status of MFT

A straight forward conclusion that can be drawn from the pattern of elevation change profile is that the Outer Himalaya are rising currently relative to the Indo-Gangetic plains. But does it imply that slip occurs on the MFT in the interseismic period?

In our models of Figs.6.4 and 6.5, we assumed that the slip occurs on the detachment in response to the continuing convergence of Indian-Eurasian plates. The main feature of the

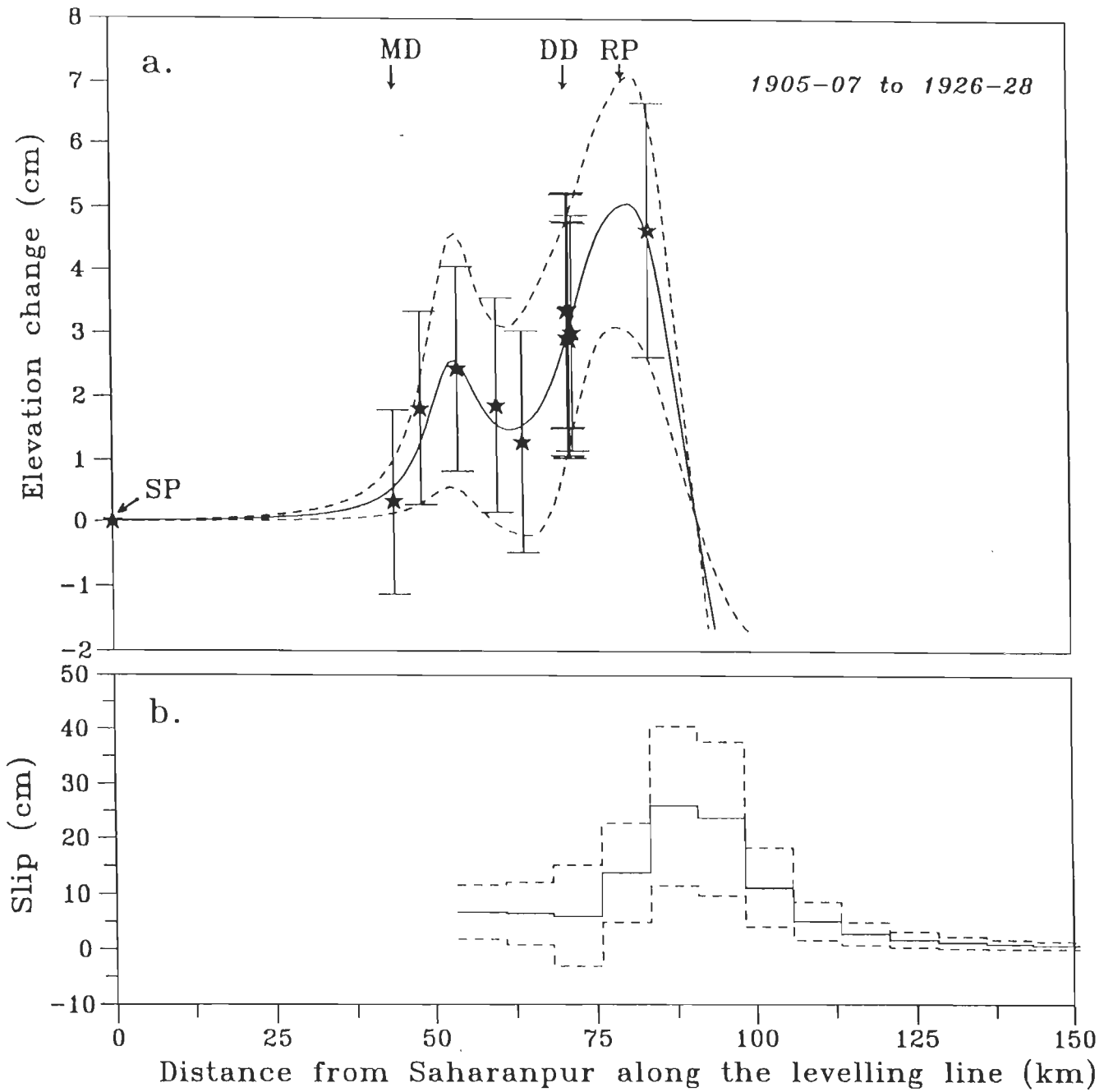


Fig.6.7 The influence of errors in the observations of the period 1905-07 to 1926-28 on the slip estimates is shown here. In the upper part of the figure the vertical bars denote the magnitude of random errors in the observations. The slip estimates in lower part of the figure, shown with the solid lines, correspond to the solid line curve of elevation changes in the upper part. The upper and lower slip estimates, denoted by the dashed lines in the lower part of the figure correspond to the dashed upper and lower curves of the elevation changes in the upper part.

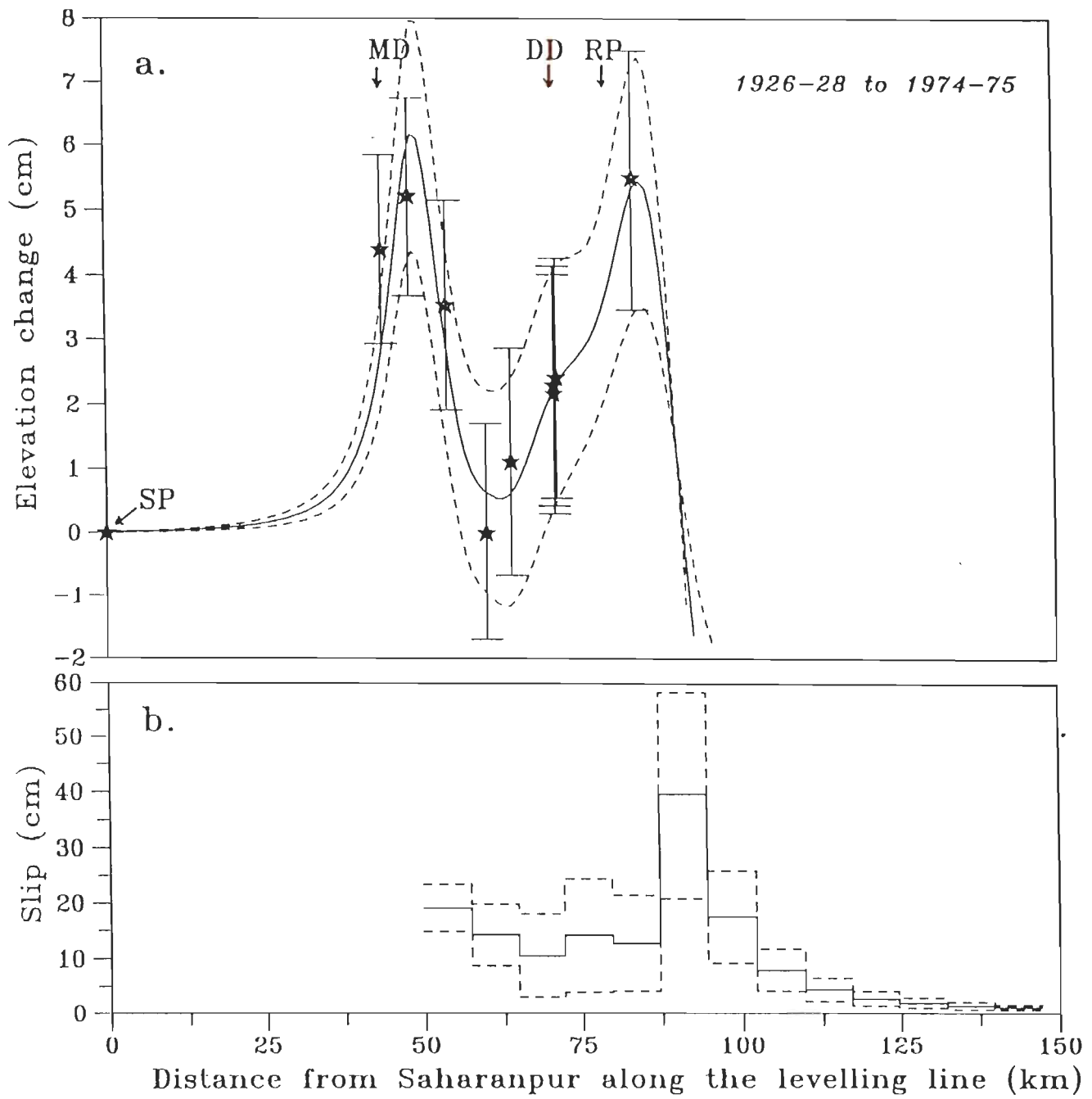


Fig.6.8 The same as Fig.6.7 but for the period 1926-28 to 1974- 75.

models, tried by us was that the detachment extends upto the southwestern limit of the Outer Himalaya. But in all the models tried here, it is required that the fault should remain buried. Thus, within the nonuniqueness of the interpretation and limited quantity and poor quality of data we conclude that although the surface trace of the geologically mapped MFT may not be involved in the interseismic deformation of the rocks, but the slip on its buried sections may not be ruled out.

6.6.4 Possibility of a locked zone on the detachment under the Dehradun region

Comparison of co- and post-Kangra earthquake elevation changes along the Saharanpur - Dehradun - Mussoorie line (Fig.6.3) shows the following important features. There was uplift throughout the Dehradun region during the Kangra earthquake. But over both the 21 and 47 year periods the Mohabawala benchmark, near the northern edge of the Siwalik ranges and southern limit of the Dehradun valley, shows markedly lower uplift than do the benchmarks to the north and south. As a result, whereas in our earlier analysis of Chapter IV, the coseismic slip on the detachment decreases systematically southward, in the model of Fig.6.5b a region of low slip intervenes between regions of higher slips to the north and south. Although the data are limited the observation raises the possibility that, in so far as interseismic slip is concerned, a locked zone may exist on the detachment in the geographic vicinity of Mohabawala (see e.g. Harris and Segall, 1987).

6.7 Summary

Within the nonuniqueness of the interpretation, the observed ground elevation changes in the Dehradun region over the 68 year period following the Kangra earthquake can be explained by a model of slips on the detachment. The present analysis supports the hypothesis that the elevation changes in the Dehradun region occur partly due to aseismic slip on the detachment

during periods between great earthquakes and partly due to coseismic slips during such earthquakes. The interseismic slip leads partly to accumulation of earthquake generating strains.

The analysis shows that strains accumulated due to a partitioned slip rate of about 7 ± 5 mm/year on the detachment in the Dehradun region atleast in the 68 year period following the Kangra earthquake. These stored strains will be released partially or fully in the future great earthquake(s) of the region.

CHAPTER VII

A simulation of stresses for nucleation of great and moderate earthquakes on the Himalayan detachment

7.1 Introduction

The continuous convergence of the Indian and Eurasian plates along the Himalayan convergent plate margin leads to the stress accumulation in the upper crust of the Himalayan region. The internal deformation of the rocks, differential uplift and the occurrence of the earthquakes are manifestations of the stress accumulation at this boundary. Thus the determination of the stress field is a matter of considerable importance as it would provide valuable information on the dynamics and driving mechanisms of plate tectonics in the region as well as on the relative importance of various plate driving forces. Information about the stress field should also facilitate the modelling of earthquake source processes occurring in the Himalaya and enhance the reliability of seismic risk estimates for the mountainous regions and the contiguous plains to the south.

We attempt in this chapter to estimate the stress field in the upper crust of the Himalaya that is conducive to nucleation of great earthquakes on the detachment under the Outer and Lesser Himalaya and also of the small to moderate magnitude earthquakes of the Himalayan seismic belt. The main, though somewhat restricted, aim of the exercise is to evaluate the role of Himalayan and Tibetan topography in the occurrence of these earthquakes as well as to estimate the stress field arising from a combination of all the plate tectonics related forces acting on the Himalayan lithosphere. We find that the stress field induced by the Himalayan and Tibetan topography and the buoyancy forces due to isostasy promote thrust faulting in the Himalaya. To adequately explain the occurrence of great Himalayan earthquakes on the detachment, although plate tectonic related stresses and pore pressures were considered yet a

satisfactory solution to the problem could not be found.

7.2 Review of the literature about the stress field in the Himalaya

A number of plate-tectonics based studies of stresses and deformations in the Himalayan and Tibetan regions have been reported in the recent literature. In this section we review briefly these studies.

Tapponier and Molnar (1976) argued that the pattern of faulting in Asia, specifically China, Tibet, Afghanistan and northern margin of the Indian subcontinent, as revealed by Landsat images, resembles the slip line field for plane strain indentation of a plastic medium by a rigid die. They regarded the Indian subcontinent as a horizontal die and the Eurasian plate as the deforming plastic medium. Further, using an estimate of the indentation pressure needed to maintain the high elevation of Tibet, they calculated estimates of the average horizontally oriented maximum principal stress in a 100 km thick lithosphere and its yield stress to be of the order of 50 MPa and 16 MPa respectively.

Using a two-dimensional elastic model, Burchfiel and Royden (1985) broadly explained the occurrence of normal faulting in the Higher Himalaya and southern Tibet in terms of a gravitational collapse of elevated topography of these regions.

Bird (1978) used the finite element method to explain the metamorphism, plutonism and crustal overthrusting that has occurred in the Himalaya during the Tertiary period. He estimated an upper limit of 20-30 MPa for the average shear stress on the intracontinental thrust faults that formed the Himalaya.

England and McKenzie (1982), England and Houseman (1985; 1986; 1988; 1989) and Villote et al. (1982; 1984; 1986) simulated the gross distribution of crustal deformation in and around Tibetan plateau and the mechanics of uplift of the plateau using the finite element modelling technique. Recently, Houseman and England (1993) investigated the partitioning of north-south convergence between crustal thickening and eastward expulsion of Tibet using the

thin viscous sheet model. They concluded that the collision partitioned between crustal thickening and eastward displacement in the ratio of at least 3:1 and more probably 4:1 (Houseman and England, 1993).

Cloetingh and Wortel (1986) modelled the state of stress in the Indo-Australian plate. Their numerical calculations included the estimation of various types of forces acting on the Indian plate. However, they did not consider the state of tectonic stress under the Himalaya specifically.

The World Stress Map (WSM) project of the International Lithosphere Program (ILP) has involved compilation of a global data base of contemporary in-situ crustal stress measurements using a variety of geophysical, geological and borehole techniques. The preliminary results of the WSM project were reported by Zoback et al. (1989) who recognized important features of the intraplate stress field. Final results of the WSM project were reported in a special issue of *Journal of Geophysical Research* in 1992. Zoback (1992) wrote a lead article which also contained a review of the other articles in the issue. In her results, Zoback (1992) reported confirmation and extension of the areal and internal consistency of the world wide stress measurements, as follows. Firstly, the vast majority of intraplate stress observations are compressional. Secondly, in several regions the stress field has uniform orientation over large areas. Thirdly, there is a strong correlation between direction of maximum horizontal stress and absolute plate motion. Finally, in most regions, the principal stresses lie in approximately horizontal and vertical planes.

Gowd et al. (1992) presented a map of maximum horizontal compressive stress (S_{Hmax}) orientations for the Indian subcontinent (Fig. 7.1). They identified that in the Himalayan region, which is a part of their mid-continental stress province, the S_{Hmax} is compressive in nature, it has NNE-ENE direction and is largely determined by tectonic collision processes.

References to the analyses of Molnar and England (1990) and England and Molnar (1993) may be made regarding the magnitude of the shear stress prevailing on major intracrustal thrust

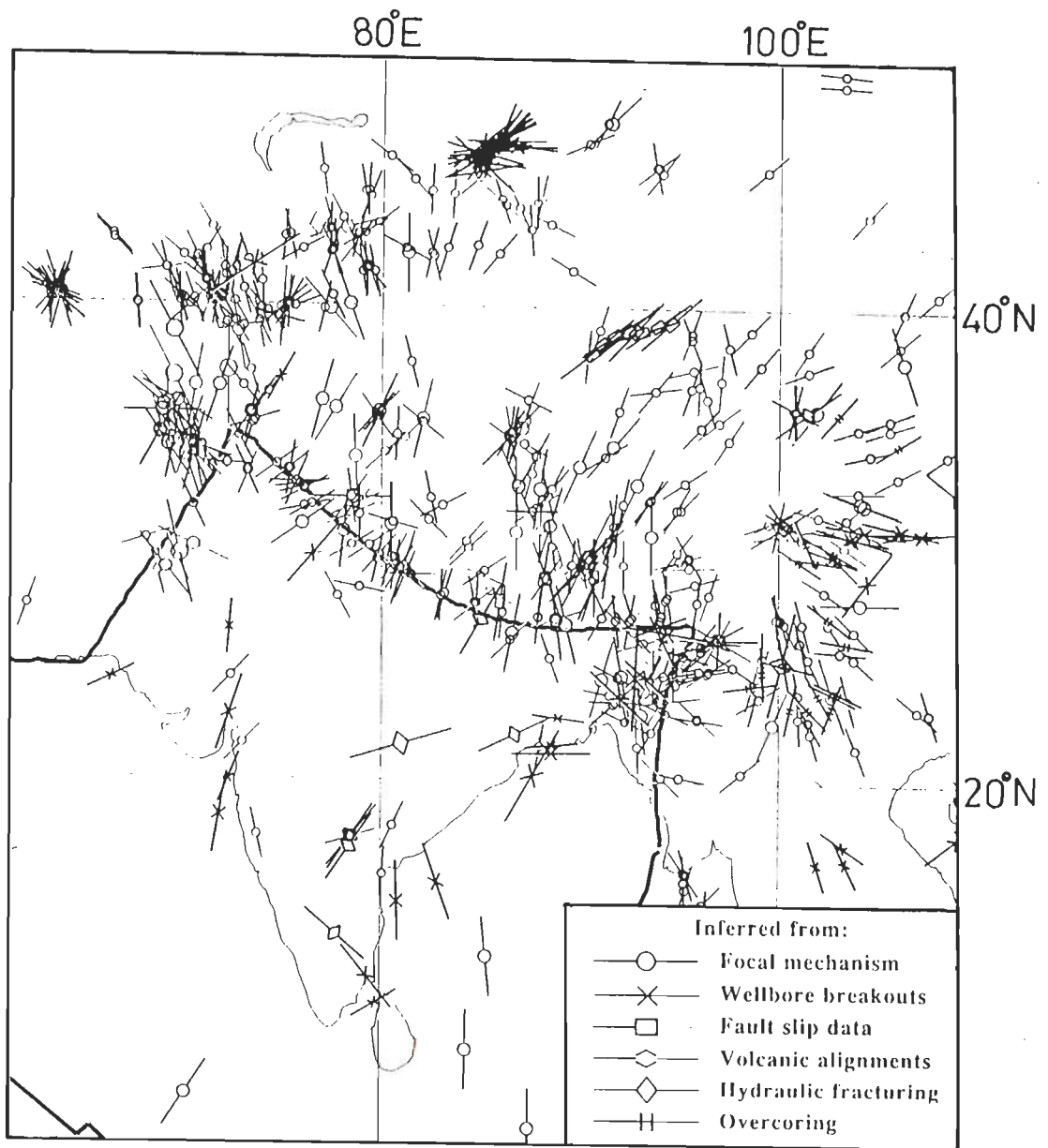


Fig.7.1 A map showing maximum horizontal stress orientation (Zoback, 1992)

faults in the Himalaya. Their calculations of temperatures appropriate for the Himalaya suggest that a shear stress of 100 MPa on the MCT is probably required to account for the Tertiary granites of the region. Further, they proposed that if the cut-off in seismicity at a depth of about 18 km in the Himalaya is due to temperatures exceeding 350° to 450°C, then the deviatoric stress should be close to 100 MPa. England and Molnar (1993) interpreted the inverted metamorphism in the Himalaya and the magnitudes of apparent inverted temperature gradients to confirm the earlier (Molnar and England's, 1990) estimates of shear stress (i.e., about 100 MPa) along the MCT.

7.3 Present simulation of stress field in the Himalaya

In view of the observations that (i) three great Himalayan earthquakes of past 100 years, namely, the 1905 Kangra, 1934 Bihar-Nepal and 1950 Assam, occurred by thrusting on a detachment dipping gently under the Outer and Lesser Himalaya (Seeber and Armbruster, 1981; Chander, 1988 and 1989; and Molnar, 1990; also see Chapter III of the thesis as to why the 1897 earthquake is excluded from this list), (ii) the depth distribution of the small and moderate earthquakes is consistent with the depth of detachment (Ni and Barazangi, 1984) and (iii) the analyses of Zoback et al. (1989), Gowd et al., (1992) and Zoback (1992), regarding the stress field in the Himalaya, we assume that the geodynamic processes are more or less uniform along the strike of the Himalaya. Thus we compute the stress field under the Himalaya considering two-dimensional plane strain theory. We consider in the first instance the effects of two sets of forces, namely, the forces due to topographic load of the Himalaya and Tibet and the buoyancy forces acting at the crust-mantle boundary due to the phenomenon of isostasy. Subsequently, we seek estimates of other stresses of plate tectonic origin and pore pressures to promote slip on the detachment. Although the present work had commenced earlier, we got encouragement from Zoback (1992) where she mentioned similar work of Sonder in 1990 for estimating a regional stress field from estimates of a uniaxial stress field of localized origin.

7.3.1 Notation

As noted above only two dimensional stress analyses are discussed in this and the following sections. The x axis is horizontal and positive pointing northward perpendicular to the local strike of the Himalaya, and y axis is positive pointing down into the crust. The origin of the coordinate system is at sea level at a point in the Indo-Gangetic plains. The precise location is shown in the relevant figures.

We follow the engineering notation and use σ for normal stresses and τ for shear stresses. Subscripts 1 and 3 on σ are used to denote maximum and minimum principal stresses respectively. Subscripts TB written together indicate stresses due to the combined effects of topography and buoyancy forces. Subscript E on stress symbols indicate overburden stresses as obtained in an elastic half space. Finally, subscript P is affixed to stress symbols to denote stress of plate tectonic origin. Thus we have the following notations used in various sections and subsections to follow.

- $\sigma_x, \sigma_y, \tau_{xy}$: normal and shear stresses along the x and y axes. General symbols.
- σ_1, σ_3 : maximum and minimum principal stresses. General symbols
- θ : the angle between σ_1 direction and the x axis, positive when the direction of σ_1 rises in the direction of positive x axis.
- L : vertical line load per unit length oriented along the y-axis.
- θ_1, θ_2 : angles used in Fig.7.3 and section 7.3.2.
- r_1, r_2 : distances as shown in Fig.7.3.
- $\Delta\sigma, \Delta\tau$: increments of normal and shear stresses on the detachment.
- μ : coefficient of friction.
- ϕ : angle of friction.
- $\sigma_{x,TB}, \sigma_{y,TB}, \tau_{xy,TB}$: normal and shear stresses due to the comined effect of topography and the buoyancy forces.

- $\sigma_{1,TB}, \sigma_{3,TB}$: maximum and minimum principal stresses due to combined effect of topography and buoyancy forces.
- $\sigma_{x,E}, \sigma_{y,E}$: normal stresses due to overburden assuming an elastic medium.
- $\sigma_{1,TBE}, \sigma_{2,TBE}$: maximum and minimum principal stresses due to combined effect of topography, buoyancy and overburden forces.
- $\sigma_{1,P}, \sigma_{3,P}$: maximum and minimum principal stresses of plate tectonic origin.
- $\sigma_{x,R}, \sigma_{y,R}, \tau_{xy,R}$: resultant normal and shear stresses along the axes arising from the combined effect of topography, buoyancy, overburden and plate tectonic causes.
- $\sigma_{1,R}, \sigma_{3,R}$: maximum and minimum principal stresses due to the combined effect of topography, buoyancy, overburden and plate tectonic causes.
- p : pore pressure.
- f : ratio of pore pressure to the lithostatic overburden.

7.3.2 Model

7.3.2.1 Topographic load

We approximate the topography of the Himalaya and Tibet as a combination of (i) linearly increasing load simulating topography of the Outer and Lesser Himalaya, (ii) a sequence of stepwise varying loads simulating topography of the Higher and Tethys Himalaya grossly, and (iii) a constant load simulating the Tibetan plateau (Fig.7.2). We assume that Boussinesq's (Jaeger and Cook, 1969) expressions for stresses due to a line load on the surface of an elastic half space may be used as Green's function kernels to compute the stresses generated by a general topography through integration. The following integrated expressions for the two types of loads, as given by Jaeger and Cook (1969, p.274-276), were used in the computation.

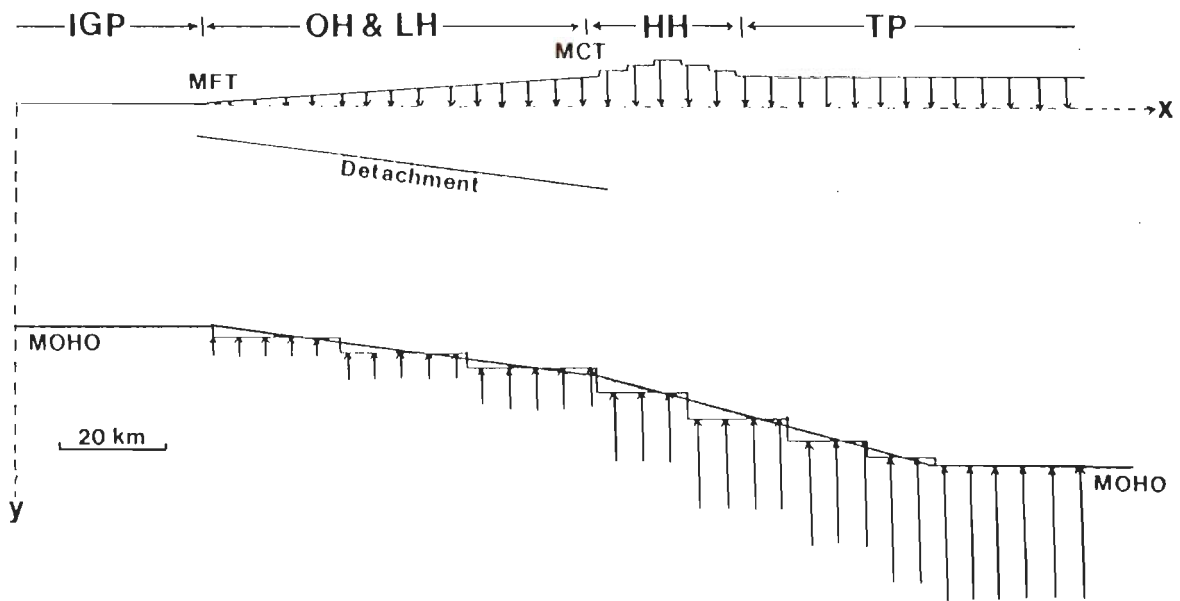


Fig.7.2 The approximation of the Himalayan and Tibetan topography as the sum of linearly increasing load and a sequence of stepwise varying loads is shown. Similarly the approximation of isostasy related buoyancy forces as a series of steps of increasing depth is also displayed. The depth of the Moho is adopted from the Lyon-Caen and Molnar's (1983 and 1985) gravity analysis. IGP- Indo-Gangetic Plains, OH, LH, HH and TP are the Outer, Lesser and Higher Himalaya and Tibetan Plateau. Approximate locations of Main Frontal Thrust (MFT) and Main Central Thrust (MCT) are also shown.

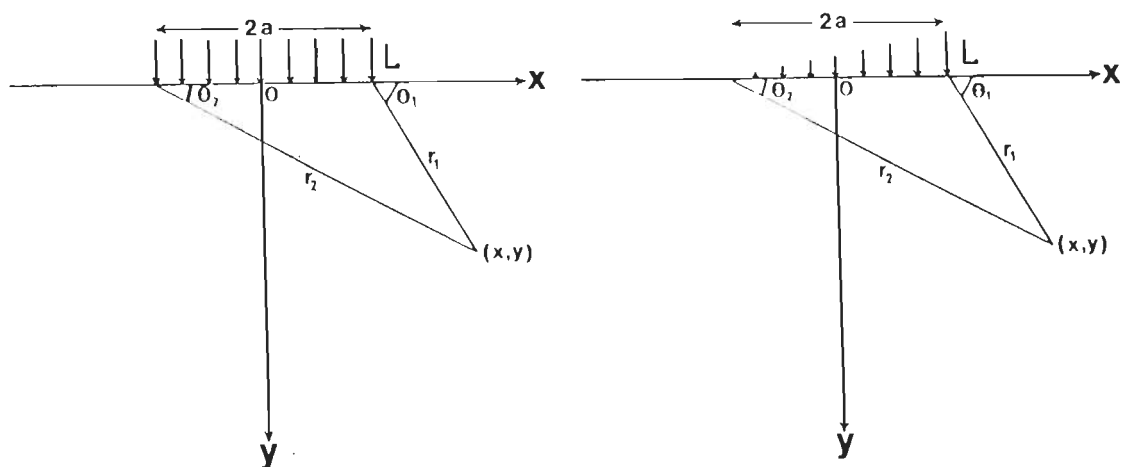


Fig.7.3 Coordinate system and the notations used in the chapter. The uniform (a) and linearly increasing loads (b) are also shown in the figure (after Jaeger and Cook, 1964).

(i) Stresses due to a uniform normal load L per unit length over a strip of width $2a$ (Fig.7.3a)

$$\sigma_x = (L/\pi)[\theta_1 - \theta_2 + \sin(\theta_1 - \theta_2)\cos(\theta_1 + \theta_2)] \quad \dots(7.1)$$

$$\sigma_y = (L/\pi)[\theta_1 - \theta_2 - \sin(\theta_1 - \theta_2)\cos(\theta_1 + \theta_2)] \quad \dots(7.2)$$

$$\tau_{xy} = (L/\pi)[\sin(\theta_1 - \theta_2)\sin(\theta_1 + \theta_2)] \quad \dots(7.3)$$

(ii) Stresses due to a normal load increasing linearly from zero to L per unit length over a strip of width $2a$ (Fig.7.3b)

$$\sigma_x = (L/2\pi)[\{1 + (x/a)\}(\theta_1 - \theta_2) + \sin(2\theta_1) - (y/a)\ln(r_2^2/r_1^2)] \quad \dots(7.4)$$

$$\sigma_y = (L/2\pi)[\{1 + (x/a)\}(\theta_1 - \theta_2) - \sin(2\theta_1)] \quad \dots(7.5)$$

$$\tau_{xy} = (L/2\pi)[1 - (y/a)(\theta_1 - \theta_2) - \cos(2\theta_1)] \quad \dots(7.6)$$

The density of the topographic load is assumed to be 2800 kg/m^3 .

7.3.2.2 Simulation of buoyancy forces

For estimation of buoyancy force we adopted the crustal model of Lyon-Caen and Molnar (1985). They inferred the depth of crust-mantle boundary under the Himalaya from an analysis of gravity data. We assume that the buoyancy force in response to the isostatic compensation of the Himalayan and Tibetan topography acts vertically upward at the crust-mantle boundary. The magnitude of this force is assumed to be related to the thickness of the crust that is in excess of 40 km under the Himalaya and Tibet. For our calculations, we approximate the form of crust-mantle boundary given by Lyon-Caen and Molnar (1985) as a series of steps of increasing depth as we proceed across Himalaya towards Tibet (Fig.7.2). After assuming that the elastic half space extends upwards from corresponding depths of 40 to 70 km, we estimate, using Eqns.7.1-6, the stresses in the crust due to these upward buoyancy loads. The magnitudes of the buoyancy loads were estimated by assuming a density contrast of 400 kg/m^3 between the crustal and mantle materials.

7.3.3 Results

7.3.3.1 First look at combined stresses due to topography and buoyancy

We used the following equations to compute from estimates of $\sigma_{x,TB}$, $\sigma_{y,TB}$ and $\tau_{xy,TB}$ the magnitudes and directions of $\sigma_{1,TB}$ and $\sigma_{3,TB}$.

$$\sigma_{1,TB} = (\sigma_{x,TB} + \sigma_{y,TB})/2 + \{[(\sigma_{x,TB} - \sigma_{y,TB})^2/4 + \tau_{xy,TB}^2]^{1/2}\} \quad \dots(7.7)$$

$$\sigma_{2,TB} = (\sigma_{x,TB} + \sigma_{y,TB})/2 - \{[(\sigma_{x,TB} - \sigma_{y,TB})^2/4 + \tau_{xy,TB}^2]^{1/2}\} \quad \dots(7.8)$$

$$\Theta = \frac{1}{2} \tan^{-1}(2\tau_{xy,TB}/\sigma_{x,TB} - \sigma_{y,TB}) \quad \dots(7.9)$$

Fig.7.4 is a display of the directions and magnitudes of principal stresses at various points of the crust upto a depth of 40 km below the sea level. The orientations of principal stresses are generally such as to destabilize low angle thrust faults dipping northerly under the Outer and Lesser Himalaya. But it is important to consider the magnitudes of these stresses to see further whether stabilization or destabilization of preexisting thrust faults of this nature is promoted. To be specific in the discussion, we assess the stability of the detachment assumed to dip at 5° under the Himalaya. Moreover we focus attention on two specific points in the

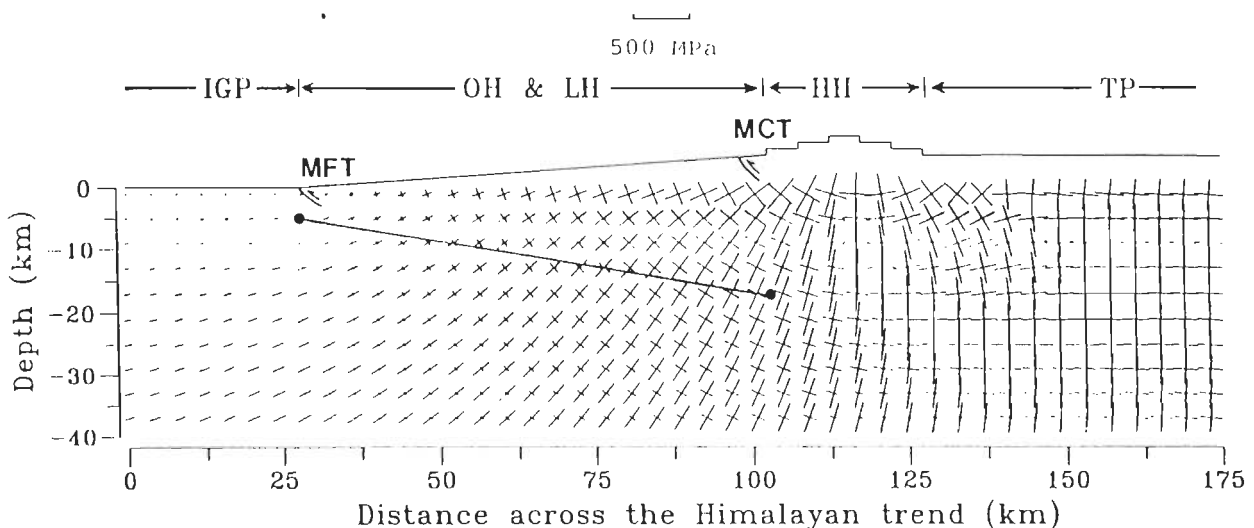


Fig.7.4 The directions and magnitudes of principal stresses due to the topographic load and isostasy related buoyancy forces are shown. The approximate location of the detachment under Outer and Lesser Himalaya is also shown with a thick solid line. The two points, on which the further calculations are performed, on the detachment under the MFT and MCT are indicated by solid circles.

detachment as seen in a vertical cross-section normal to the local strike of the Himalaya. One of these points is under the Main Central Thrust (MCT) and the other under the Main Frontal Thrust (MFT). In a great Himalayan earthquake, nucleation should take place at the former point and rupture should propagate up dip along the detachment towards the latter point. Table 7.1 is a display of the magnitudes and directions of above estimated principal stresses at these two points. The quantity $\Delta\tau - \mu\Delta\sigma$ (see for example Bell and Nur, 1978), induced on the detachment due to these principal stresses. using a μ of 0.65 (Zoback, 1992) is also listed. This quantity is positive for the point under MFT and negative for that under MCT. This indicates that the stresses due to topography and buoyancy forces promote destabilization of detachment under the MFT and stabilization under the MCT.

Table 7.1

Location of the point on the detachment	$\sigma_{1,TB}$ (MPa)	$\sigma_{3,TB}$ (MPa)	Θ (degree)	$\Delta\tau - \mu\Delta\sigma$ (MPa)
Under the MFT	24.5	2.2	14.2	+6.0
Under the MCT	166.5	95.1	66.9	-127.1

7.3.3.2 Consideration of additional stress from other sources: dry rock calculations

Speculation about the stresses necessary to nucleate great and moderate earthquakes under the MCT cannot be complete unless stresses due to overburden and plate tectonic causes as well as due to pore pressures are not taken into account. As regards the stresses due to overburden, assuming that the half space is a Poisson solid (Jaeger and Cook, 1969), we adopt the elastic half space model in which the vertical normal stress is the weight per unit area of the overburden and the horizontal normal stress is one third of the vertical normal stress. Our calculations for these combined stresses due to overburden and topographic and buoyancy

effects show that the maximum principal stress now is nearly perpendicular to the detachment and has a tendency to produce normal faulting on the detachment (Table 7.2). In addition, the magnitudes of induced shear and normal stresses on the detachment plane, in this case, are such that slip will not occur unless the friction coefficient is near zero.

Table 7.2

Location of the point on the detachment	$\sigma_{1,TBE}$ (MPa)	$\sigma_{3,TBE}$ (MPa)	Θ (degree)	$\Delta\tau - \mu\Delta\sigma$ (MPa)
Under the MFT	141.2	68.5	85.8	-1.14
Under the MCT	623.8	259.7	85.2	-25.96

We then considered the possibility of plate tectonics related stresses which when superimposed along with the above stresses would promote frictional failure. Here we did not consider a specific cause for these plate tectonic stresses. However, we assumed that the plate tectonics related maximum and minimum principal stresses at each point would be horizontal and vertical in the plane normal to the local strike of the Himalaya. We assumed further that, when these stresses are combined with the overburden, topographic and buoyancy induced stresses, the resultant stress tensor at the point of interest would be such that the resultant maximum principal stress could be oriented relative to the detachment, along a direction most favourable for fault reactivation. The phrase most favourable is used here in the sense of rock mechanics and implies an angle of $45^\circ - \phi/2$ between the maximum principal stress and the fault being reactivated.

Then we have two constraints available:

$$(i) \sigma_{1,R} = \sigma_{3,R} \tan^2(45^\circ + \phi/2); \quad \dots(7.10)$$

and (ii) $\sigma_{1,R}$ should make an angle of $45^\circ - \phi/2$ with the detachment so as to promote thrust type slip on this surface.

These conditions are sufficient to estimate $\sigma_{1,P}$ and $\sigma_{3,P}$. As per the assumptions stated already, $\sigma_{1,P}$ and $\sigma_{3,P}$ are horizontal and vertical respectively. Thus we have the following relations regarding stresses.

$$\tau_{xy,R} = \tau_{xy,TB} \quad \dots(7.11)$$

$$\sigma_{x,R} = \sigma_{1,P} + \sigma_{x,E} + \sigma_{x,TB} \quad \dots(7.12)$$

$$\sigma_{y,R} = \sigma_{3,P} + \sigma_{y,E} + \sigma_{y,TB} \quad \dots(7.13)$$

According to a relation given by Jaeger and Cook (1969), since $\sigma_{1,R}$ is to be oriented most favourably for reactivation of the detachment,

$$\begin{aligned} \tan 2(45^\circ - \phi/2 - 5^\circ) &= \frac{2 \tau_{xy,R}}{\sigma_{x,R} - \sigma_{y,R}} \\ &= \frac{2 \tau_{xy,TB}}{(\sigma_{1,P} - \sigma_{3,P}) + (\sigma_{x,TB} - \sigma_{y,TB})} \end{aligned} \quad \dots(7.14)$$

where 5° is the assumed dip of the detachment.

We can thus determine the magnitudes of $\sigma_{1,P}$ and $\sigma_{3,P}$. In the current calculations for the dry rocks, these quantities turn out (Table 7.3) to be large and tensile (Fig. 7.5). These estimates are unacceptable within the framework of plate tectonics. Various attempts to resolve the dilemma are taken up sequentially in the discussion.

Table 7.3

Location of the point on the detachment	ϕ (degree)	$\sigma_{1,P}$ (MPa)	$\sigma_{3,P}$ (MPa)
Under the MCT	33.0	-178.8	-581.3

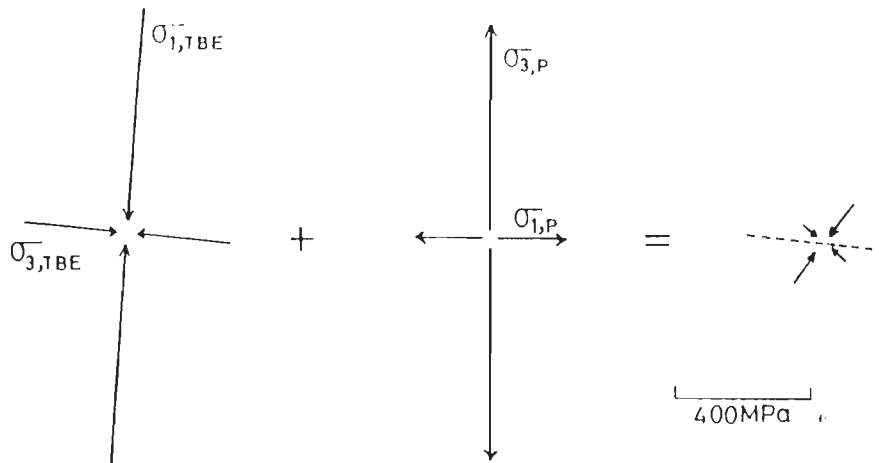


Fig.7.5 Stress rotation using the dry rock conditions. The angle of friction is chosen to be 33° . The maximum and minimum principal stresses of plate tectonic origin are tensile. The dashed line denotes the detachment.

7.4 Discussion

The preceding calculations lead us to conclude that the whole question of nucleation of great and moderate Himalayan earthquakes on the detachment under the MCT has to be addressed again considering various other possibilities.

7.4.1 Applicability of rock mechanics considerations for modelling earthquake nucleation

It has been known in seismology for quite some time that rock mechanics considerations impose very stringent conditions on models for earthquake occurrence due to fault reactivation. Scholz (1992) provides a recent review of the problem of earthquake nucleation and rupture growth in pre-existing faults. In the absence of adequate other seismological inputs, based on analyses of seismograms of Himalayan earthquakes, we are forced here to proceed further on the assumptions that traditional rock mechanics does provide a first model of fault reactivation of earthquakes.

7.4.2 Pore pressure versus low friction coefficient

If the available estimates of stresses indicate that fault reactivation is not possible in the dry state assuming nominal values of frictional coefficient on the fault, then two traditional solutions have been considered in rock mechanics, namely, the fault has low frictional coefficient and/or suitably high pore pressures exist in the region of interest on the fault.

7.4.2.1 Friction coefficient

The very concept of the detachment under the Himalaya is as yet hypothetical. The preceding paragraphs and chapters indicate that the concept is undoubtedly fertile within the framework of plate tectonics. Although different views about the depth and location of this geotectonic surface under the Himalaya have been mentioned in earlier parts of this thesis, one thing is clear that the possibility of obtaining specimens from and near the detachment is a remote dream and efforts to estimate the magnitudes of frictional coefficient along the detachment can be no more than hypothetical speculations. We find that in the dry rock conditions, considered in Section 7.3.2.2, the friction coefficient required, so that at least $\sigma_{1,p}$ is compressive, would have to be in the range of 0 to 0.05 or the angle of friction has to be less than 3° . Calculations based on the preceding formulae using a value of 3° for angle of friction lead to the result that $\sigma_{1,p}$ should be compressive with a magnitude of 250 MPa and $\sigma_{3,p}$ should be tensile having a magnitude of about 122 MPa (Table 7.4). Again it is difficult to conceive that vertical tensile stress of this magnitude would be obtained from plate tectonics causes under dry rock conditions. However, for a friction angle of 2.4° , both $\sigma_{1,p}$ and $\sigma_{3,p}$ are compressive (Table 7.4 and Fig.7.6).

Table 7.4

Location of the point on the detachment	ϕ (degree)	$\sigma_{1,P}$ (MPa)	$\sigma_{3,P}$ (MPa)
Under the MCT	3.0	249.9	-122.4
Under the MCT	2.4	374.4	2.7

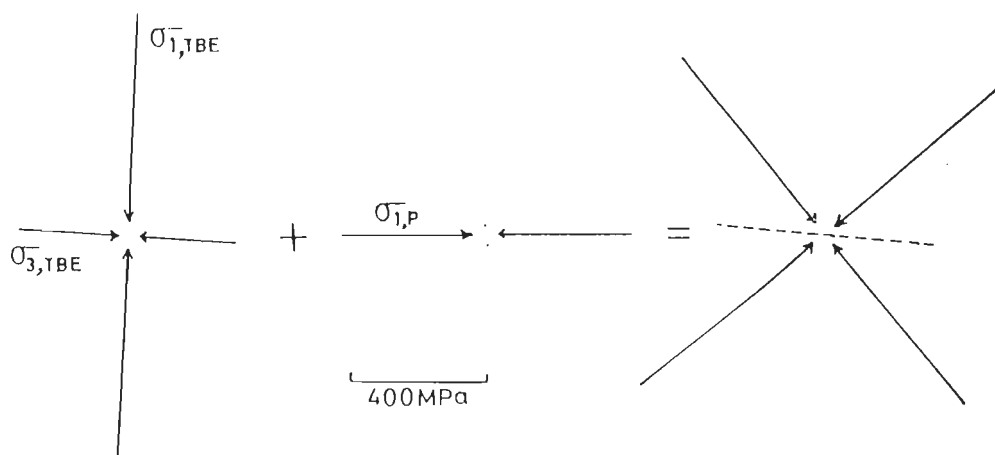


Fig.7.6 Same as Fig.7.5 but for less angle of friction (2.4°). The principal stresses of plate tectonic origin are compressive.

7.4.2.2 Considerations of pore pressure

As far as we can determine from our library resources, there is only one estimate of possible pore pressure under the Himalaya. This was provided by Davis et al. (1983) who considered a critically tapered wedge of Himalayan rocks in limit equilibrium for failure throughout in accordance with Coulomb- Mohr failure criterion. The required pore pressure turned out to be 0.76 lithostatic.

Eqns. 7.11-7.13 may be rewritten for the case of pore pressure as follows.

$$\tau_{xy,R} = \tau_{xy,TB} \quad \dots(7.15)$$

$$\sigma'_{x,R} = \sigma_{1,P} + \sigma_{x,E} + \sigma_{x,TB} - p \quad \dots(7.16)$$

$$\sigma'_{y,R} = \sigma_{3,P} + \sigma_{y,E} + \sigma_{y,TB} - p \quad \dots(7.17)$$

The primes indicate that we are considering effective normal resultant stresses in the presence of pore pressures.

It transpires that we have three unknowns ($\sigma_{1,p}$, $\sigma_{3,p}$ and p) but only two independent constraints, (see Eqn. 7.14) even when a value of ϕ is assumed. Thus a range of solution could be visualized. In the first instance we adopted the value of pore pressure according to the estimate of Davis et al., (1983). We assumed further that $\sigma_{3,p}$ equals the pore pressure exactly. Under these assumptions a solution exist only for friction angles less than 5.5° . For this value of friction angle, $\sigma_{1,p}$ has to be about 375 MPa, compressive and horizontal (Table 7.5). If the friction coefficient has to be 0.65 ($\phi=33^\circ$), then pore pressure has to be supralithostatic to the extent of $1.24xpgh$, where p is the density, g is acceleration to the gravity and h is depth of overburden. In this case $\sigma_{1,p}$ has to be 410 MPa, compressive and horizontal (Table 7.5 and Fig.7.7).

Table 7.5

Location of the point on the detachment	f	ϕ (degree)	$\sigma_{1,p}$ (MPa)
Under the MCT	0.76	5.5	374.7
Under the MCT	1.24	33.0	410.6

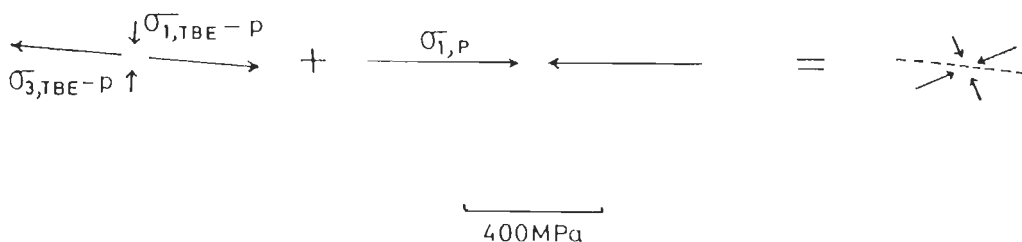


Fig.7.7 Stress rotation, considering the effect of pore pressure. Angle of friction is 33° and the pore pressure is sublithostatic ($f=1.24$). The detachment is shown with a dashed line.

The possibility of earthquakes occurring under compressive thrust fault type stresses acting on high angle reverse fault under supralithostatic pore pressures has been mooted by Sibson (1989). He even suggested ways in which such high pore pressures may exist in rocks. Whether those possibilities apply to the detachment under the Himalaya is a debatable question.

We are reluctant to accept such high values of pore pressures in the present state of information about the geodynamics of the Himalaya. Thus for a compromise, sub-, but near lithostatic, pore pressure of $0.95 \times p_{gh}$, we find that a low friction coefficient of about 0.15 has to be postulated.

7.4.2.3 Principal stresses of plate tectonic origin oriented obliquely

$\sigma_{1,p}$ is assumed horizontal along x axis in the calculations reported so far. It thus makes an angle of only 5° with the detachment. As a result not only the induced normal stress on the detachment is small, but the induced shear stress to promote failure on the detachment is also small. A well known result of Mohr circle theory (Jaeger and Cook, 1969) suggests that we should try to increase the angle between $\sigma_{1,p}$ and the detachment to some extent. A series of calculations were carried out to test this idea. It was observed that with all other parameters as in the calculations reported in section 7.4.2.2, the permissible friction angle increases as the angle between $\sigma_{1,p}$ and the detachment increases. For a pore pressure of 0.76 lithostatic, failure on the detachment can occur if $\sigma_{1,p}$ has a magnitude of 711 MPa and makes an angle of 18° with the detachment, even if the friction coefficient has the nominal value of 0.65 (Table 7.6).

Such a value of plate tectonic related stress is relatively high and it is difficult to conceive how $\sigma_{1,p}$ direction would have a rising trend under the Himalaya.

Table 7.6

Location of the point on the detachment	f	ϕ (degree)	$\sigma_{1,p}$ (MPa)
Under the MCT	0.76	33.0	710.8

7.4.3 Nature of detachment

Here it appears pertinent to recall that Scholz (1992) defines a detachment as a near horizontal ductile fault in a crystalline basement. In that case "...Anderson's theory does not apply because ductile shearing will occur on planes of maximum shear rather than at the Coulomb orientation..." (Scholz, 1992, p.103). In this case Scholz (1992) makes another pertinent observation that "...if the flow is fully plastic then Hubbert and Rubey's concept does not apply either because the strength is then independent of pressure..." (Scholz, 1992). We have not considered plastic failure on the detachment.

7.4.4 Triggering of earthquakes on the detachment by rupture initiation on high angle reverse faults normal to it

As mentioned in the review in Chapter I, a well controlled fault plane solution of a moderate Himalayan earthquake has one nodal plane dipping gently under the Himalaya and the other nodal plane dipping steeply southward, the strike of both the planes being subparallel to the local trend of the mountains (e.g. Molnar, 1990). The motion is reverse thrust on either nodal plane. Since Fitch's (1970) analysis, it has been customary to take the former nodal plane as a fault plane. Although the fault plane solution is available only for the 1950 Assam earthquake among the four great Indian earthquakes of last 100 years, Molnar (1990) has argued that this earthquake also occurred by thrusting motion along a low angle fault (see Chapter IV). Modelling of causative fault based on levelling data of the Kangra earthquake also

suggest thrusting of a low angle fault. The faults corresponding to the other nodal plane of this earthquake would also have been very steeply dipping reverse faults.

We have considered the possibility that the slip on this high angle reverse fault perpendicular to the detachment triggers ruptures of great and moderate earthquakes on the detachment. However, our analyses of the reactivation of such faults (Table 7.7) along the lines discussed earlier in the chapter for failure on the detachment, do not provide a significantly more favourable situation for initiation of rupture. The mildly more favourable situation in this case revolves around marginally lower estimates of plate tectonic stresses.

Table 7.7

Location of the point on the detachment	f	ϕ (degree)	$\sigma_{1,P}$ (MPa)
Under the MCT	0.76	5.5	356.4
Under the MCT	1.24	33.0	383.4

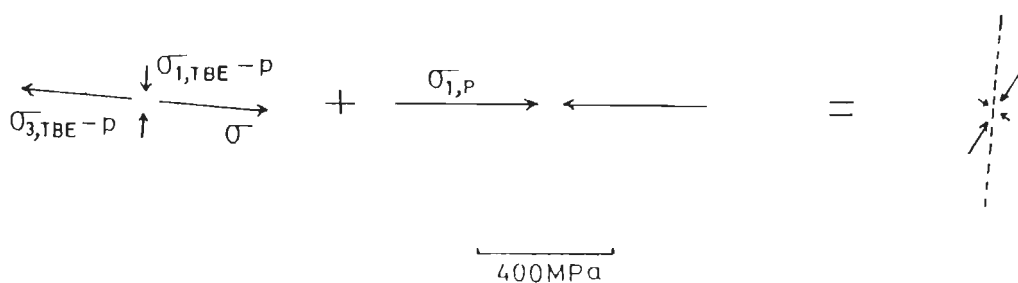


Fig.7.8 Same as Fig.7.7, but for a high angle reverse fault which is perpendicular to the detachment. Note the slightly less magnitude of maximum principal stress of plate tectonic origin as compared with that of Fig.7.7.

7.4.5 Triggering of moderate and great Himalayan earthquakes during episodes of uplift of the Higher Himalaya relative to the Lesser Himalaya

Recently Chander (1994) has suggested that many locally recorded small and micro-earthquakes of the Garhwal Himalaya occur in a crustal fault zone which facilitates the uplift of the Higher Himalaya relative to the Lesser Himalaya in response to plate convergence related underthrusting of the Indian shield beneath the Himalayan rocks. He estimated the dips of faults in the fault zone to be approximately 60° northerly subnormal to the local trend of the Himalaya. Chander (1994) visualized that faults of this fault zone coexist with the detachment and other detachment parallel thrust faults in the Himalayan upper crust. If the uplift of the Higher Himalaya relative to the Lesser Himalaya occurs partly continuously and partly in spurts episodically, then it is conceivable that, episodic uplift along steeply dipping reverse faults could lead to chattering or grating action on rock blocks bounded by low angle detachment parallel thrust faults. When these blocks are in the upswing during chattering there would be a significant reduction in the amount of friction along the detachment and its parallel faults. This may trigger moderate and great earthquakes of the Himalaya.

This idea is not yet amenable to quantification but suggests an interesting way to reduce friction along the detachment and to cause nucleation of great and moderate earthquakes.

7.5 Summary

In short the analyses of this chapter have shown that although the directions of shear stresses induced on the detachment by the topographic and isostasy related buoyancy forces are favourable for thrust faulting, yet the magnitudes of normal and shear stresses are such that Coulomb-Mohr type frictional failure is not easy to visualize for nominal values of frictional coefficient and pore pressure. Hence the processes attending the nucleation of great and moderate Himalayan earthquakes along the detachment bear further scrutiny both within and

outside the ambit of traditional rock mechanics. The dilemma exposed by these analyses for the Himalaya is similar, in many respects, to the dilemma about the occurrence of earthquakes and aseismic slip along the San-Andreas fault.

CHAPTER VIII

Retrodiction of the 1991 Uttarkashi earthquake

8.1 General

Research in earthquake prediction during the past few decades has been marked not by revolutionary breakthroughs but by slow and erratic progress inspite of substantial advances in our understanding of earthquake source processes and other related phenomena. One of the problems in understanding the source processes and predicting earthquakes is that everything relates to everything else. Although the divisions are artificial but, on the basis of physical arguments, distinction may be made in long-term, intermediate term and short term predictions. In the long term, phenomena based on elastic rebound theory may be involved, whereas in the short term, failure related phenomena may occur. However, for intermediate term prediction we are guided basically by recognition of patterns in earthquake occurrences. In all these cases, however, empiricism reigns supreme (Agnew and Ellsworth, 1991).

8.1.1 Long term prediction

The idea that earthquakes occur due to release of accumulated elastic strain formed the basis of first modern earthquake prediction by G.K.Gilbert in 1883. However, the first evidence of the elastic rebound of the earth's crust during an earthquake came from the study of the 1906 rupture in the San Andreas fault (Reid, 1910). Reid laid the foundation for quantitative analysis of the earthquake cycle and its application to earthquake prediction. This model of elastic rebound theory leads us to expect that the next earthquake on a specific fault will occur when the stress released in the last earthquake is recovered. Since tectonic stresses accumulate slowly, the prospect of another earthquake in the same locality is low for decades following a major earthquake. This led to the idea of seismic gap along major plate boundaries. According to this

hypothesis any part of the boundary that has not ruptured recently is more likely to have an earthquake in the next few decades than other parts that have experienced large earthquakes (Fedotov, 1965; Mogi, 1969; Kelleher, 1972; Kelleher et al., 1973 and McCann et al., 1979).

Currently however, opinion appears to be divided about the seismic gap concept. According to some (e.g., Nishenko, 1989) the seismic gap hypothesis has recently been used in long term earthquake prediction and has provided several successful long term forecasts of earthquakes. However, Kagan and Jackson (1991) statistically tested the hypothesis and concluded that the hypothesis of increased earthquake potential after a long period can be rejected with a large confidence.

8.1.2 Short term prediction

Prediction of an earthquake a few months, few days or a few hours in advance corresponds best to the popular notion of earthquake prediction. But it has not been achieved as yet except in a few rare cases. The most well known of these cases is the prediction of the Haicheng, China, earthquake. It was observed during the 1966-1973 period, following the 1966 Xingtai earthquake, that the seismic activity in northern China had increased considerably. Analyses of historical and recent seismic activity, observable crustal deformation, geomagnetic changes, etc., suggested that the area may be due for a large damaging earthquake in the future. Thus a long term prediction was issued. Finally the continuous increases in seismic activity, levelling anomalies as well as anomalies in well water levels, animal behaviour, radon emission and swarms of earthquakes led to the issuing of a short term prediction nine hours before the actual occurrence of the earthquake (Raleigh et al., 1977).

However, things have not worked out in the Parkfield region of San Andreas fault, where, on the basis of previous major earthquakes, a long term prediction gave 95% chance of occurrence of a major earthquake by Jan.1, 1993. In an attempt to predict earthquakes in Parkfield region on short term basis, various types of data are being collected which include

the continuous monitoring of seismicity, controlled source measurement of seismic travel times, amplitudes and anisotropy, ultra low frequency radio waves, radon emissions, crustal displacements measured geodetically using GPS, borehole strainmeters, creepmeters, etc. This is stated to be the most expensive earthquake prediction programme (Kerr, 1993). But, the anticipated earthquake has not yet occurred in the Parkfield region.

8.1.3 Intermediate term prediction

Intermediate term prediction covers efforts on time scales between the loading cycle of the fault and the development of the instability. Agnew and Ellsworth (1991) emphasized on three major types of intermediate term phenomena. Firstly, they considered crustal deformation because it has a direct link with the cycle of strain accumulation and release. We have covered this aspect in Chapters III to VI. Secondly, they considered seismicity because of its nearly universal availability. Finally they have considered seismic wave phenomena. In this chapter we shall be concentrating on the seismicity patterns.

We identify in the present study a seismicity pattern which preceded several strong earthquakes of the northwestern Himalayan region including the recent earthquake of 1991 near Uttarkashi in Garhwal Himalaya. The pattern may be treated as a precursor. Other related geodynamic implications of the study are also discussed.

8.2 Review of studies related to the prediction of earthquakes in the Himalaya and adjoining regions

Seismicity patterns have been studied in majority of the studies relating to earthquake prediction in the Himalaya and nearby regions. We briefly review them in this section.

Seeber and Armbruster (1981) studied the great earthquakes of the Himalaya and adjoining regions. They plotted the lengths of estimated rupture zones for major and great earthquakes, that had occurred on the detachment after 1800, on a space time diagram. Thus they identified

seismic gaps (discussed earlier in Chapter I) which are the likely locales of future great earthquakes. Khattri (1987) adopted a somewhat similar method in which he plotted the reported earthquakes since 1800 to construct a space time variation diagram of seismicity. He thus estimated a quiescence period of about 19 year duration before the occurrence of great earthquakes of the Himalaya. Further Khattri (1987) suggested that such quiescence is in progress in the central and Assam seismic gaps.

Gupta and Singh (1986) performed an analyses of seismic activity in the northeast Indian region and concluded that moderate to great earthquakes in this region are preceded first by earthquake swarms and immediately afterwards by quiescent periods. Further, on the basis of an earthquake swarm and quiescence period they identified a site of possible future earthquake of magnitude, $M=8\pm\frac{1}{2}$. Although an earthquake ($M_s=7.3$ and $m_b=6.8$) occurred on Aug.8, 1988 and Gupta and Singh (1989) claimed that this was the earthquake predicted by them earlier but this prediction and suggested precursors were not accepted by the panel of IASPEI Sub-commission on earthquake prediction (1990) due to many reasons. Important among them were the lack of definition and quantification of swarms, lack of quantitative analysis, lack of tests for randomness, identification of area etc. Moreover, the event of Aug.8, 1988 had a magnitude less than that predicted by Gupta and Singh (1986).

Keilis-Borok et al. (1980) attempted to identify seismicity patterns precursory to great earthquakes over most of the Himalayan and Tibetan regions. They used two seismicity patterns, (i) sigma, a function based on the earthquake energies taken over a sliding time window and (ii) swarms, comprising spatial clustering of earthquakes during time intervals when the seismicity is above average. They identified peaks in sigma in 1948-49, prior to the great 1950 Assam earthquake, and in 1976. Peaks in swarms occurred three times, in 1932-33, prior to great 1934 Bihar-Nepal earthquake, in 1946 and in 1978. Further they predicted that an event of magnitude 8 should occur within six years or an event of 8.5 within fourteen years.

Keilis-Borok and his team also applied pattern recognition techniques on the earthquake data. This led to the development of two algorithms, namely, the CN and M8 (Allen et al, 1986; Gabrilov et al, 1986; Keilis-Borok and Kossobokov, 1988; 1990; Keilis-Borok et al., 1988; Keilis-Borok, 1990 and Keilis-Borok and Rotwain 1990). The CN algorithm was first used for the California-Nevada region and hence its acronym name. The M8 algorithm was originally developed to predict earthquakes of magnitude more than 8 and hence its name. The algorithms have been applied by various investigators for examining data from different seismic belts of the world.

Bhatia et al. (1989) applied the M8 algorithm in the Himalayan region to identify, in retrospect, the 'Times of Increased Probabilities' (TIPs) for the occurrence of earthquakes of magnitude greater than 7.0, during the 1970-1987 period. In the region considered by them only one earthquake of magnitude 7.1 occurred on 29 May, 1976 in the north-east region and they identified a TIP that preceded this earthquake.

Bhatia et al. (1990) used CN algorithm also for the Himalayan region to identify the TIPs for the occurrence of earthquakes of magnitude greater than or equal to 6.4.

Gahalaut et al. (1992 a and b) independently applied CN and M8 algorithms to Himalayan seismicity data for the period between January 1964 and August 1991 for a threshold magnitude of 6.4.

In both the studies of Gahalaut et al. (1992 a) and of Bhatia et al. (1990), all the functions of CN algorithm, namely, level of seismic activity, quiescence, temporal variation of seismicity, spatial concentration, clustering of earthquakes and long-range interaction of earthquakes were considered. But no current alarm was diagnosed for the NW Himalaya, where a strong earthquake ($m_b=6.8$ and $M_s=7.1$) occurred near Uttarkashi in Garhwal Himalaya on Oct.19, 1991.

8.3 Present study

8.3.1 Motivation of the study

The absence of current alarm in the studies of Bhatia et al. (1990) and Gahalaut et al. (1992) for the Uttarkashi earthquake, forms the motivation of this study. The reason for lack of alarm is attributed to the fact that, of the above mentioned functions used in CN algorithm, only the function K (temporal variation of seismicity) yielded a high anomalous value (i.e. K showed activation) and rest of the functions yielded low values (or no activation). So the combination of all functions of the CN algorithm could not raise the alarm, because the activation of function K was averaged out by other functions.

For the investigation reported in this chapter, we have modified the regionalization scheme. Only the temporal variation of seismicity, function K, is investigated in a region because this was the only function of the CN algorithm which was activated for the 1991 Uttarkashi earthquake in earlier studies.

8.3.2 Data

To carry out our analysis, we have used the earthquake data since 1964, as this is the time period in which the catalogue appears to be complete for events of magnitude (m_b) 4 and above. The analysis actually starts after 1970 because for the definition of function K (discussed in the next section) it takes six years to accumulate the required number of quantiles. The USGS-NEIC (1991) catalogue till Dec.1990 and the PDE (1992) bulletins till Aug.1991 are used for the purpose (Fig.8.1). To avoid activation of functions due to the aftershocks following the strong shocks ($M \geq 6.4$), their aftershocks were removed using the time and space window given by Keilis-Borok et al. (1980) before the statistical analysis was carried out. All earthquakes with aftershocks removed are called mainshocks in the following.

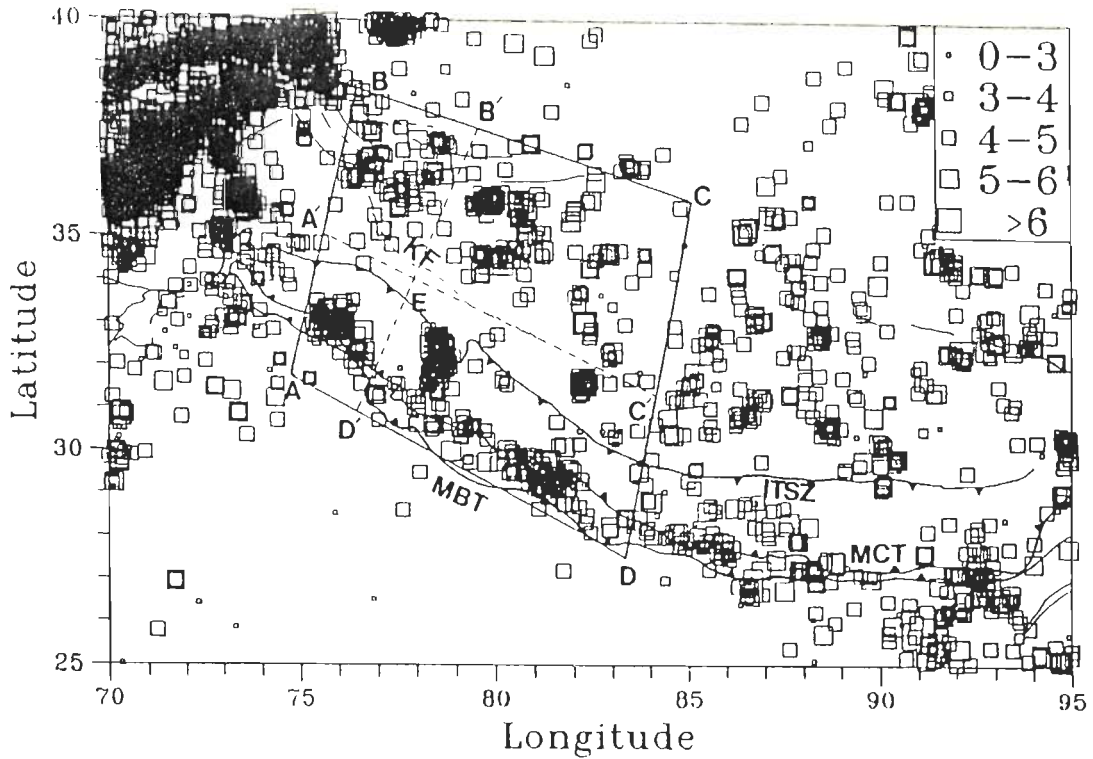


Fig.8.1 The earthquakes for the period 1970 to Aug.1991, reported by USGS-NEIC and PDE. Tectonic features adapted from Gansser, (1964). MBT- Main Boundary Thrust, MCT- Main Central Thrust, ITSZ- Indus Tsangpo Suture Zone and KF- Karakoram fault. The block ABCDE is also displayed.

8.4 Temporal variation of seismicity

The function K , the temporal variation of seismicity, is defined as follows (Keilis-Borok and Rotwain, 1990). Let t_i and M_i be the time and magnitude of the i th mainshock with the sequence number $t_{i+1} > t_i$. Like other integral traits of 'earthquakes flow' of CN algorithm, the function K is defined on a sliding time window $t-s < t_i < t$. Here s is the width of time window for this purpose. The level of seismic activity $N(t | \underline{M}, s)$ is first defined as the number of mainshocks with magnitude $M \geq \underline{M}$.

The difference between the number of mainshocks for two successive time intervals $(t-s, t)$ and $(t-2s, t-s)$ is called the temporal variation of seismicity and is defined as follows.

$$K(t | \underline{M}, s) = N(t | \underline{M}, s) - N(t-s | \underline{M}, s) \quad \dots(8.1)$$

Following Keilis-Borok and Rotwain (1990), the value of s is taken to be two years.

8.5 Results

8.5.1 Regionalisation

For the identification of a precursory trend, if any, and its spatial as well as temporal extent before the 1991 Uttarkashi earthquake, the earthquake epicentres are plotted for two successive periods from Jan., 1989 to Jan., 1990 and Jan., 1990 to Aug., 1991 in Fig.8.2a and b. The comparison of these two figures suggests that a precursory seismic sequence (preparation zone) for the earthquake of 1991 is present (shown in Fig.8.2b). As seen from the epicentral maps in Figs.8.1 and 2b, longitude 83°E roughly divides the belt into at least two blocks. There are few events in the eastern block in which the Bihar Nepal earthquake of 1988 occurred. However, numerous events are lined up parallel to the Himalayan seismic belt in the western block ABCD. Further west of the ABCD block, the earthquakes cluster again along the Hindukush-Pamir and Pakistan Himalaya (Fig.8.1). This forms the basis of the western limit of this block. From these figures of the preparation zones (Fig.8.2b) and the spatial distribution of earthquakes (Fig.8.1), the tectonic block ABCD (in Fig.8.1) is identified in which the strong mainshocks of 1975, 1980, 1982, 1986 and finally 1991 (Table 8.1) occurred (Fig.8.2b). The first four are the events which provide the pattern and have been to that extent retrodicted also. The earthquake of 1986 ($M_s=6.1$) is included in the table of these strong mainshocks because the number of aftershocks of this earthquake was as large as in the case of most other strong mainshocks listed in the Table 8.1. However, the earthquake of April, 28, 1975 ($M_s=6.3$, epicentre at 35.81°N and 79.91°E), is not included in Table 8.1 as the magnitude of this event is less than 6.4 and it had only four aftershocks. Even if it is included in the table of strong mainshocks, it does not make any difference in the interpretation as it is close to the event of Jan.19, 1975 in time. Except this event and those listed in Table 8.1 there were no earthquakes since 1970 with $M_s \geq 6.1$ that had six or more aftershocks.

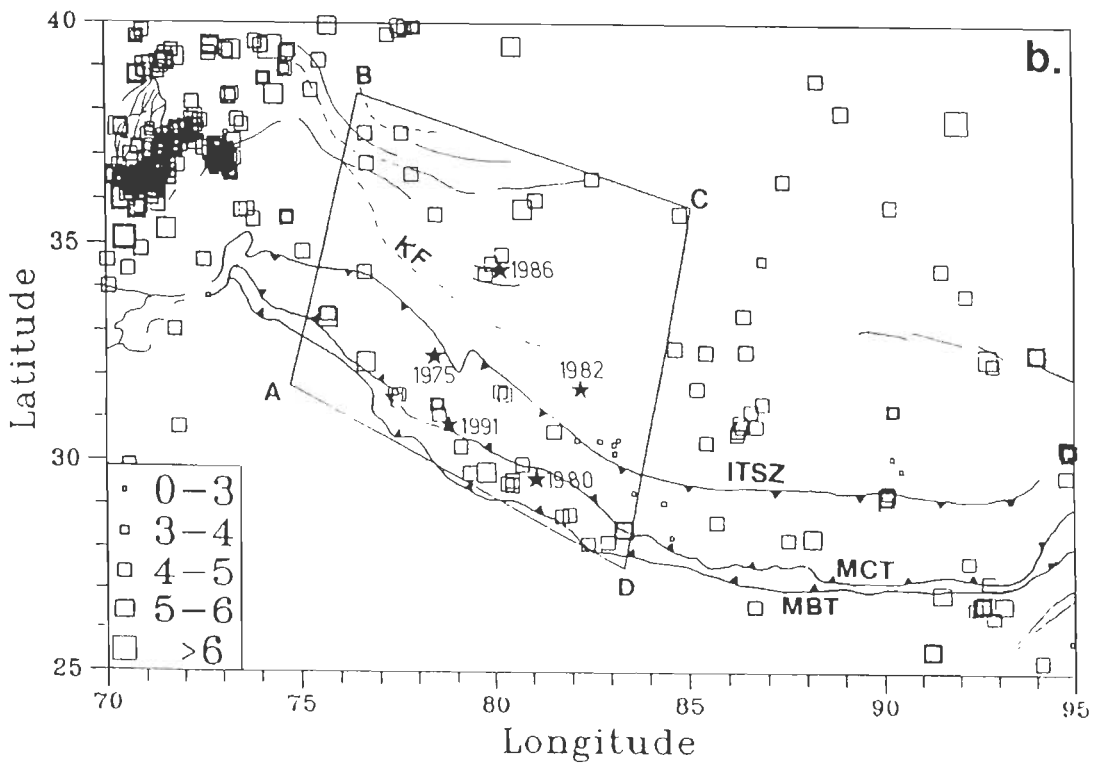
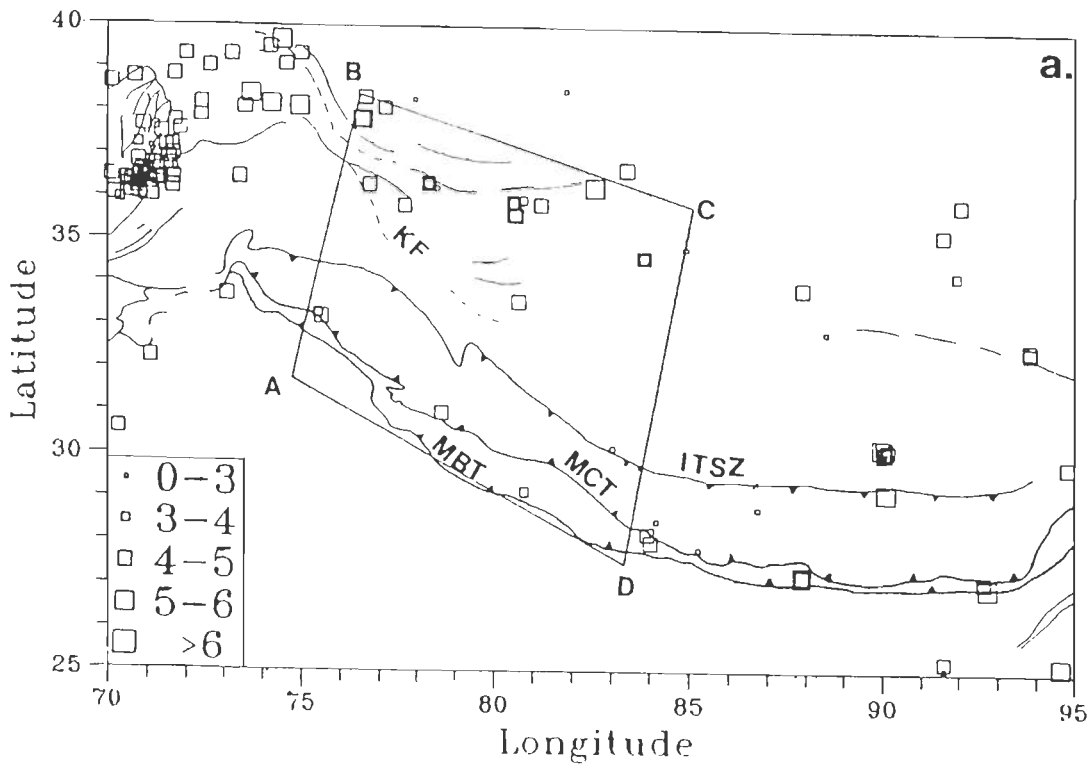


Fig.8.2 (a) The earthquakes in the period Jan.1989-Jan.90 are shown. (b) The earthquakes in the period Jan.1990-Aug.91 are shown. The strong earthquakes (Table 8.1) occurring in the block ABCD, are shown by stars.

Table 8.1 List of strong main shocks in block ABCD since 1970. The aftershocks of first four strong shocks are identified in this study using USGS earthquake catalogue. But aftershocks of the last event, i.e., the Uttarkashi earthquake, were recorded by local networks.

year	month	day	hour	minute	lat.	long.	depth	m_b	m_s	m_p	after shocks
1975	1	19	8	2	32.45	78.43	33	6.2	6.8	6.8	15
1980	7	29	14	58	29.59	81.09	18	6.1	6.5	6.6	6
1982	1	23	17	37	31.69	82.24	33	6.0	6.5	6.2	12
1986	7	6	19	24	34.42	80.16	9	5.8	6.1	-	7
1991	10	19	21	23	30.85	78.80	15	6.8	7.1	-	60

8.5.2 Behaviour of K function in the selected region

Fig.8.3.a shows the variation of function K with time for the events in the block ABCD of Fig.8.1. It is clear from the figure that the times of crests ($K \geq 2$) almost coincide with the times of occurrence of strong mainshocks. The graph tends to a high value during 1990-91 and the Uttarkashi earthquake actually occurred in October 1991. The level of seismicity increases in each case before the occurrence, of the retrodicted earthquake. We call this as a pattern and consider the period of increasing seismicity as period of high seismic risk. In other words, it is seen that when K equals or exceeds 2, the possibility of earthquake occurrence increases. TIPs (Time of Increased Probability of earthquake) are shown for the periods when $K \geq 2$ in the upper part of Fig.8.3a.

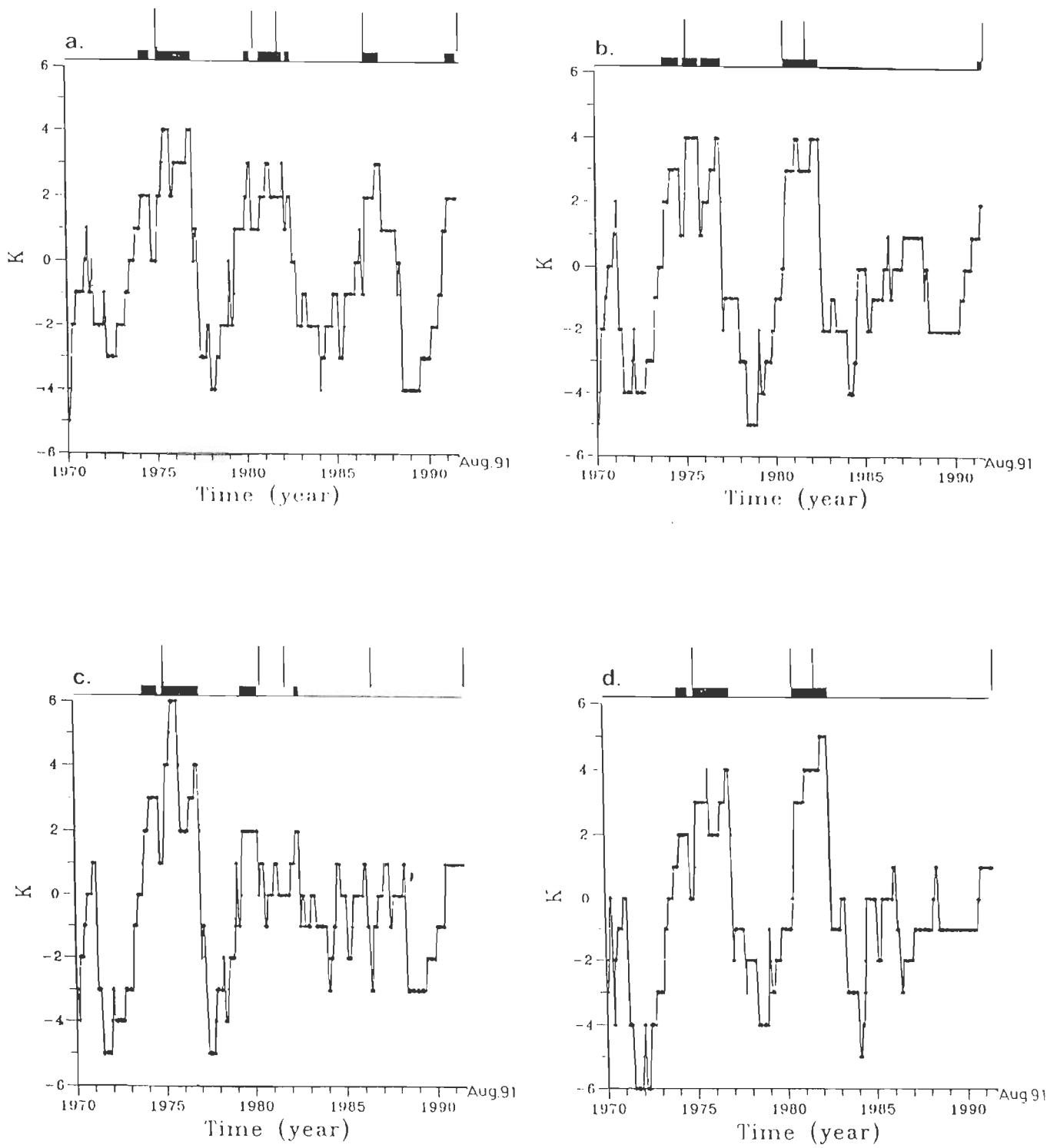


Fig.8.3 The graphs of function K versus time in different blocks identified in Fig.1. **a** in block ABCD **b** in block AA'C'D **c** in block D'B'CD and **d** in block D'EC'D. The arrows mark the times of strong mainshocks. The TIPs for $K \geq 2$ are also shown in the upper part of each figure.

8.6 Discussion

8.6.1 Further tests

The study was repeated for the blocks of smaller sizes within the block ABCD taking the clustering of earthquakes into consideration. The smaller blocks are also shown in Fig.8.1. The variation of K versus time in these blocks is shown in Fig.8.3b, c and d respectively.

In block ABCD the function K behaves in a regular, smooth (Fig.8.3a) and quasi-periodic manner (period 5-7 years). It is observed that there is a definite correspondence between crests ($K \geq 2$) of the graph and occurrence of strong main shocks. There is no failure or false alarm. This excludes the false TIPs just after the occurrence of the retrodicted strong earthquakes as they may be due to aftershocks which are not completely removed.

In block AA'C'D, where only the southern seismic belt of Fig.8.1 is considered, the K function is still capable of retrodicting all the strong mainshocks occurring within the block (Fig.8.3b). However, in the period 1986-1987, the K function approached the value of 2 but no strong earthquake occurred in the region in this period. This may indicate that the level of seismicity of the southern belt is somehow influenced by the strong earthquake about to occur in the northern belt. In other words the seismicity in the southern and northern belts might be interrelated. Because of this reason the block ABCD is preferred over block AA'C'D, since the former seems to represent a self-consistent seismic region. Moreover, it is in the larger block that the function K behaves in a regular manner and predicts all the events.

Fig.8.3c and d, refer to the blocks D'B'CD and D'EC'D respectively. The variation of K with time seems to be random and not as regular as it is for block ABCD, except in the early part of the 1970-91 period. It appears from the Figs. 8.3c and d that these blocks do not encompass complete seismicity sequences. Moreover, there are cases of failure in retrodiction in these blocks. So we suggest that the blocks D'B'CD and D'EC'D are not suitable for retrodicting the strong earthquakes considered in this study.

8.6.2 Behaviour of function K

It may be inferred from Table 8.1 that the recurrence period of the strong earthquakes in block ABCD is 5-7 years (with 1982 event being an exception) and that the period of K is the same as in Fig.8.3a. But the emphasis here is not on the periodicity of the precursor K, but on the fact that before the occurrence of a strong earthquake the level of seismicity is increased in the identified block. It is this behaviour of the function K which acts as a precursor with no false alarm or failures to retrodict in this block.

The observed behaviour of the K function in block ABCD suggests that although the focal mechanisms and local stresses in the frontal zone and in Tibet-China region may be different, yet the driving forces responsible for plate convergence, crustal uplift and deformation, and earthquake occurrence in the Himalaya and Tibet are the same. Such behaviour may prevail in other blocks in the Himalaya and adjoining regions too. Efforts should be made to verify this expectation.

8.6.3 A clarification

The retrodiction of the Uttarkashi earthquake is based upon the distribution of earthquakes in space in the long term, i.e., in the period from 1970 to Aug. 1991 (Fig.8.1) and variation of seismicity in space and time in the short term, i.e., in the period from Jan., 1989 to Aug., 1991 (Fig.8.2.a and b). The proposed precursor defines the spatio-temporal variation of seismicity, which is quasi-periodic in a specified geographic block and therefore appears to be more systematic than a random trend. In this scheme of predicting the events, i.e., the strong mainshocks, successes and failures are clearly defined. But even then, we accept that the precursor identified here must be tested further against the hypothesis of random occurrence of retrodicted earthquakes. This is because, in our case, the events occurred in just 21 years (1970-1991) in a small region. Thus they are not sufficiently numerous for the statistical testing in the manner of Kagan and Jackson, 1991.

If this precursor is considered a representative of the variation of the earthquake flow, it may be used in future for prediction using an updated catalogue in such Himalayan-Tibetan blocks.

8.7 Summary

Based on the short term (two years) spatial extent of the preparation zone of 1991 earthquake and the long term (between 1970 and 1991) spatial distribution of the earthquakes, a seismotectonic block is identified in the NW Himalaya between longitudes 75° and 83° E and latitudes 30° and 38° N. The result of a statistical analysis of the seismicity in this block, using the temporal variation of the seismicity (function K of Keilis-Borok and Rotwain, 1990), shows that all the earthquakes after 1970, including the 1991 Uttarkashi earthquake, were preceded by a definite pattern related to a short term increase of seismicity. This pattern may be treated as a diagnostic. It should be tested further, and if still found successful, it may be used in real time future earthquake prediction in this block. Also, it appears from the analysis that the seismicity in the Himalaya and southern Tibet region is somehow interrelated.

CHAPTER IX

General discussion

9.1 General

New research results have been presented in each of the chapters III to VIII. A discussion section has been included in each of these chapters and has involved comments specific to the preceding sections of that chapter. However, to round off this thesis there is need to generalise and assess the cumulative contributions of these chapters towards evolving a balanced view about seismicity and geodynamics of the Himalaya in the light of geodetic and other geophysical data presented.

Although it may appear that some of the results and calculations about Himalayan earthquakes are already well known, they have been derived here by analyses of geodetic and other data that had not been considered in detail by earlier investigators. Thus for example, we feel that the conclusions about the 1897 Assam earthquake are based on innovative reinterpretation of observations which were freely available for more than nine decades. Also our effort has been consistently to draw as far as possible quantitative conclusions even for qualitative data.

9.2 Applicability of plate tectonics to the Himalaya

As has been recognized a few times earlier in the thesis, geophysical inverse problems have multiple solutions. With limited observations it is not possible to select one of those solutions unequivocally over the remaining solutions. The desire to obtain firm and definite solutions has to be tampered. A realistic goal in this sense can be to assess whether the new observations are consistent with the models already conceived and tested. With accumulation of observations some models may turn out to be more versatile and others may have to be rejected because

they do not fit a segment of the observations. Our allusion here is to the Popperian method in which one tries consistently to falsify the hypothesis already proposed in light of newer observations.

Thus we cannot say that our work has put the question of applicability of the plate tectonics hypothesis to the Himalayan setting beyond all doubts. But we can say that this hypothesis is consistent with the observations examined and interpreted in this thesis. To that extent this hypothesis is reinforced through our work.

9.3 Association of great Himalayan earthquakes with the detachment

In our opinion a considerable advance in our understanding of the source processes of great Himalayan earthquakes was achieved by Seeber and Armbruster (1981) when they suggested that these earthquakes, with their large areas of perceptible damage, could occur only through extended ruptures in low angle thrust faults. Of course this view had been propounded earlier in connection with the 1897 Assam earthquake by Oldham (1899). Our analysis of macroseismic ground elevation changes observed and inferred for the 1897 earthquake and the geodetic observations of ground level changes due to the 1905 Kangra earthquake are consistent with the view that each of these earthquakes occurred by a large rupture in a low angle thrust fault type detachment surface. We agree with Seeber and Armbruster (1981) that the Kangra earthquake occurred on the detachment under the Outer and Lesser Himalaya of Himachal Pradesh and Garhwal (Fig.4.8). However, we are unable to agree with Seeber and Armbruster (1981) that the great 1897 Assam earthquake also occurred on the same tectonic surface. Inevitably we have been forced to postulate that the mid-crustal detachment under the western Shillong plateau in which this earthquake occurred, if continued northward would lie in the lower crust under the Outer and Lesser Himalaya of Bhutan and Arunachal Pradesh (Fig.3.1).

Also we have to note that our estimates of the extents of rupture zones of the 1897 and 1905 earthquakes are more modest than those envisaged by Seeber and Armbruster (1981). In fact they are in surprisingly good agreement with the estimates of Molnar (1990). However, for the 1897 earthquake we have differed with Molnar (1990) to the extent that, whereas he was vague on the possibility whether the northern limit of the 1897 rupture extended upto or under the Himalaya, we find from the observations about flooding of the Brahmaputra river that this rupture zone terminated in the northern direction under the Brahmaputra river.

9.4 About slip on the detachment under the Himalaya

The pre- and post-seismic levelling observations for the 1905 Kangra earthquake are consistent with the view that slips of 5 to 7 m atleast occurred coseismically in the ruptured section of the detachment. This should hold even for other great earthquakes with rupture zones in the Himalayan domain. Since the evidence of the past 100 years is that great earthquakes occur in different segment of the Himalaya episodically, we may conclude that coseismic slip in diferent strike-wise segments of the Himalaya is staggered in time. If the sequence in which different segments slip could be deciphered it should represent an important step towards prediction of earthquakes along the Himalayan seismic belt.

The interpretation of available geodetically measured level changes across the Himalaya in the interseismic period indicate that slip occurs on the detachment even when great earthquakes are not occurring. It is an expression of the fact that aseismic permanent deformations of Himalayan rocks and accumulation of recoverable earthquake generating strains are occurring simultaneously.

Although in chapter V of the thesis, a very simple model has been given for partitioning of the total annual plate convergence, accommodated at the Himalaya, into aseismic deformation and recoverable elastic strains, it is acknowledged that this could be a gross oversimplification. Considerably greater number of observations in different segments of the Himalaya are required

to resolve the question of this partitioning.

9.5 Stresses for the nucleation of great and moderate Himalayan earthquakes along the detachment

We were aware to some extent about the difficulty of applying rock mechanics considerations to the problem of stresses required for the occurrence of earthquakes generally. But the limitations of the approach could be brought home to us only through the analysis reported in Chapter VIII. The concept of first estimating the stresses due to the topographic and isostasy related buoyancy effects and then estimating in a general way the magnitude of the plate tectonics related stresses, that could lead to Coulomb-Mohr type failure on the detachment, appeared attractive at the outset. But the results of the analyses have made us somewhat wiser and humbler. The magnitude of these stresses predicted by the analyses appeared to be too large and tensile if dry rock conditions were assumed along with the nominal laboratory determined values of internal friction angle for rocks. Alternatively the friction angles have to be very small and pore pressures have to be high. The possibility of a plunging maximum principal stress of plate tectonic origin was considered also. It is then possible to consider nominal values of friction angles and sublithostatic pore pressures. However, the magnitude of maximum principal stress is still relatively high and it is difficult to conceive how the requisite plunge of upto about 20° toward the Indo-Gangetic plains could be imparted to the stresses under the predominantly horizontal compressive regime contemplated in plate tectonics of convergent plate margins. The problem holds much interest and bears further study.

9.6 A statistical search for a pattern in seismicity to predict moderate and great Himalayan earthquakes

In Chapter VIII, we have reported our attempts to examine why the CN algorithm of

Keilis-Borok and Rotwain (1990) failed to predict the Uttarkashi earthquake of 1991 in the Garhwal Himalaya. Through experimentation with different subsets of available information about Himalayan seismicity, we have been able to isolate the function which, among others that are considered in this algorithm for studying earthquake flow, is the most sensitive for predicting TTPs in the segment of the northwestern Himalaya that is of interest here. This function K displays a quasi-periodic trend which is statistically more significant than the assumption of a purely random process of earthquake occurrence in the region. The success in retrodicting the Uttarkashi earthquake using this trend of K function, encourages us to suggest that it should be tested further to see if it is capable of predicting future moderate and great earthquakes in this Himalayan segment. A significant byproduct of the exercise is the realization that too strong an adherence to the view that Himalayan seismicity is distinct from the seismicity of southern Tibet may hinder a proper understanding of the causes of great Himalayan earthquakes.

9.7 On the seismic hazards in the Himalaya

The preceding work sheds light on several aspects of seismic hazards in the Himalaya. We highlight them in the following subsections.

9.7.1 On the extent of seismic gap in the northeastern Himalaya

The concept of seismic gaps has been an important consideration for seismologists and earth scientists concerned with the problem of earthquake prediction. In recent years some criticisms and limitations of the seismic gap hypothesis have been put forward (e.g. Kagan and Jackson, 1991). Thus although the full utility of this concept is a matter of some debate, nevertheless in our opinion it is a useful consideration in assessing the overall seismic hazard potential of different segments of an active plate margin. It is in this light that we recall the discussion of Chapter III, where we have reviewed the recent views about the extent of seismic gap or gaps

in the northeastern Himalaya. Since we have put forward the view that the rupture zone of the 1897 Assam earthquake may have been entirely outside the Himalaya domain, we also hold the view that the seismic gap in the northeastern Himalaya may be much longer than thought hitherto. We realize, of course, the opposing argument that the location and strike-wise length of 1897 rupture zone still identify the part of the Himalayan convergent plate margin that has released strain within the last 100 years and to that extent the seismic hazard may have diminished. But adopting a conservative approach in which it is safer to overestimate seismic hazard we feel that the entire section of the Himalaya lying between the rupture zones of 1934 and 1950 earthquakes should be considered as a seismic gap (Fig.3.7).

Similarly, in Chapters IV and VI, we have simulated coseismic and interseismic elevation changes using a theory in which uniform slip is assumed on the ruptured section of the causative fault. But we realize, and have argued in Chapter IV, that slip on the ruptured section of the detachment in the 1905 episode may have been greater in the Kangra and Dharamshala region than in the Dehradun region. Consequently, at the present time the seismic hazard should be greater in the Dehradun region than in the Kangra-Dharamshala region. This again enlarges the region of relatively higher seismic hazard between rupture zones of 1905 and 1934 earthquake.

9.7.2 Implications for the Tehri dam

The hydroelectric potential of the Himalayan tributaries of the Ganges river is to be exploited by constructing several high dams. The most notable amongst these is the 260 m high earth and rock filled type Tehri dam on the Bhagirathi river (Fig.6.1). The project has become a subject of controversy on several grounds. But it is the seismic risk aspect which concerns us here. For most design purposes the geologically mapped surface traces of the MBT and the MCT have been taken into consideration. The distances involved are of the order of 30 to 40 km in map view. However, it is the detachment under the Outer and Lesser Himalaya that is

the main active thrust fault according to plate tectonics view. Our analyses in Chapter IV and VI are based on the assumption that the detachment has a depth of about 5 and 17 km under the MFT and MCT respectively. Thus in our view the detachment is the nearest active fault to the Tehri dam site and it lies at a depth of 13-17 km beneath the site. This is under the provision that an unmapped or currently buried thrust type splay from the detachment does not lie still closer and shallower to the dam site.

9.8 Evidence of preparation for great earthquakes in the Himalaya

The interpretation of interseismic levelling observations in central nepal and Dehradun regions leads to the conclusion that earthquake generating strains are currently accumulating in these two regions. Unfortunately, constraints of available data permit neither the estimation of return periods of great earthquakes in the Himalaya nor the determination of the current state of progress in the seismic cycles of these two regions.

9.9 Summary

Realisation of the limitations of the data has restrained us from venturing too far in proposing new models. Yet testing and reconciliation of existing models in light of mostly unused geodetic and other elevation change observations of the Himalayan convergent plate margin is progress in itself.

CHAPTER X

Conclusions

The following conclusions may be drawn reasonably from the analyses of elevation changes, stress simulation and a statistical study of earthquake data from the Himalayan region presented in the thesis.

1. The coseismic and interseismic geodetic observations from the Himalaya and the direct and indirect evidence for ground level changes during 1897 earthquake presented in this thesis are amenable to interpretation within the framework of the plate tectonics hypothesis.
2. The observations are consistent with the view that great earthquakes of the Himalayan convergent plate margin occur by extended ruptures in low angle thrust faults.
3. We estimate that the great Kangra earthquake of 1905 had a rupture of about $280 \times 80 \text{ km}^2$ in the detachment under the Himalaya. The great 1897 earthquake of the west Shillong plateau had a rupture of $170 \times 100 \text{ km}^2$ in a mid-crustal detachment under the Shillong plateau and Brahmaputra valley. We have argued that the latter detachment differs from the detachment under the Himalaya in which the great earthquakes of 1905, 1934 and 1950 are assumed to have occurred.
4. Our interpretations of ground level changes are on the assumption that in each case there was uniform slip in the affected segment of the causative fault. The estimated magnitude of slip is in the range of 5 to 7 m in the cases of 1897 and 1905 earthquakes. However, the possibility of nonuniform slip on the ruptured segments of the faults is clearly recognized in both cases. Small pockets in the

ruptured sections may have had slips several times these estimates.

5. Limited levelling observations in central Nepal and Dehradun regions establish that level changes occur in the Outer and Lesser Himalaya even during the interseismic periods between great earthquakes. We regard these as aseismic changes.
6. The interpretation of interseismic levelling observations is on the assumption that only slip on faults, mainly the detachment, accommodates plate convergence at the Himalaya. The possibility of crustal deformation as a result of ongoing folding in the Himalaya due to plate convergence is recognized but not considered for modelling.
7. The elastic rebound theory of earthquakes requires that ground level changes due to storage of earthquake generating strain should be opposite to those observed for coseismic slip. Since the interseismic ground elevation changes in the Outer Himalaya are similar in sign to the coseismic changes, we have to conclude that interseismic slip on the detachment leads to permanent deformations of Himalayan rocks as well as storage of earthquake generating strains. Although we estimate that the interseismic slip on the detachment is partitioned in the ratio of 2:1 for these purposes, we recognise that the estimate may vary with accumulation of more levelling data.
8. The recurrence periods of great earthquakes in different Himalayan segments cannot be estimated due to lack of suitable observations. But our analyses indicate strongly that preparations, in the form of accumulation of recoverable elastic strains, for great earthquakes are currently in progress in the central Nepal and Dehradun regions.
9. We conclude from our plane strain analyses that the directions of shear stresses induced by the Himalayan topography and buoyancy forces generally promote

thrust type slip on the detachment.

10. Our calculations of magnitudes of stresses suggest, within the framework of classical rock mechanics, that high pore fluid pressure and/or low frictional coefficients on the detachment are required for the nucleation of great and moderate earthquakes.
11. Function K of Keilis-Borok and Rotwain's (1990) CN algorithm has emerged as a sensitive parameter with a discernable spatio-temporal behaviour that appears to have potential for prognostication of earthquakes in the NW Himalaya between longitudes 75°E and 83°E . The occurrence of the Uttarkashi earthquake of Oct.19, 1991, could be retrodicted using data upto August 1991 on the basis of this function but not by the full CN algorithm.
12. The possibility has become stronger from this statistical analysis that seismicity of Himalaya and southern Tibet may be linked more closely than thought hitherto.
13. We conclude also from the foregoing analyses, in entirety, that earthquake hazards in the Himalaya are much more severe than has been recognized or is being acknowledged by most Indian opinion and policy makers so far. Thus, our analyses strongly suggest that the fraction of the length of the Himalaya that has been ruptured in the last 100 years is significantly less and the seismic gaps are larger than considered by recent investigators.
14. Also, for purposes of engineering seismology and earthquake engineering in connection with design of important structures and facilities in the Outer and Lesser Himalaya the detachment is the nearest active thrust fault in most, if not all, cases.
15. Although not intended at the outset, the thesis has turned out to be a scientific investigation in the the Popperian mode. The new geophysical data sets for the

Himalaya analysed here constituted tests of the reigning plate tectonics paradigm. That the tests have turned out to be affirmative does not take anything away from the desirability of acquiring more and diverse observations for further critical tests of the paradigm.

References

1. Agnew, D. C. and Ellsworth, W. L. (1991) Earthquake prediction and long-term hazard assessment. *Reviews of geophysics, supplement*. pp.877-889.
2. Allen, C., Keilis-Borok, V. I., Rotwain, I. M. and Hutton, K. (1986) A set of long-term seismological precursors: California and some other regions (in Russian) *Comput. Seismol.* Vol.19, pp.24-34.
3. Argand, E. (1924) La tectonique de L Asie, *Proc Int. Geol. Congr.* 13th, Vol.7, pp.171-372.
4. Armbruster, J., Seeber, L. and Jacob, K. H. (1978) The north western termination of the Himalayan mountain front active tectonics from microearthquakes. *J. Geophys. Res.* Vol.83, pp.269-281.
5. Armijo, R., Tapponnier, P. and Tonglin, H. (1989) Late Cenozoic right-lateral strike slip faulting in southern Tibet. *J. Geophys. Res.* Vol.94, pp.2787-2838.
6. Arur, M. G. and Hasija, N. L. (1986) Crustal movement studies across Ganga tear fault (in Siwaliks) at Haridwar in Uttar Pradesh, India. *Proceedings of International Symposium on Neotectonics in South Asia*, Survey of India, Dehradun. pp.330-344.
7. Arur, M. G. and Singh, A. N. (1986) Error Analysis of levelling data in the Shanan Extension project in Himachal Pradesh, India. *Proceedings of International Symposium on Neotectonics in South Asia*. Survey of India, Dehradun. pp.353-365.
8. Auden, J. B., (1972) Review of the tectonic map of India published by O.N.G.C. *J. Geol. Soc. India.* Vol.13, pp.101-107.
9. Avouac, J. P. and Tapponnier, P. (1993) Kinematic model of active deformation in central Asia. *Geophys. Res. Letters.* Vol.20, pp.895-898.



10. Baker, D. M., Lillie, R. J., Yeats, R. S., Johnson, G. D., Yousuf, M. and Zamin, A. S. H. (1988) Development of the Himalayan frontal thrust zone: Salt range, Pakistan. *Geology*. Vol.16, pp.3-7.
11. Baranowski, J., Armbruster, J., Seeber, L. and Molnar, P. (1984) Focal depths and fault plane solutions of earthquakes and active tectonics of the Himalaya. *J. Geophys. Res.* Vol.89, pp.6918-6928.
12. Barazangi, M. (1989) Continental collision zones: Seismotectonics and crustal structure in the *Encyclopedia of Solid Earth Geophysics*, edited by D. E. James, Van Nostrand Reinhold, New York. pp.58-75.
13. Barazangi, M. and Ni, J. (1982) Velocities and propagation characteristics of Pn and Sn beneath the Himalayan arc and Tibetan Plateau: possible evidence for underthrusting of the Indian continental lithosphere beneath Tibet, *Geology*, Vol.10, pp.179-185.
14. Beghoul, N. Barazangi, M. and Isacks (1993) Lithospheric structure of Tibet and western north America: Mechanisms of uplift and a comparative study. *J. Geophys. Res.* Vol.98, pp.1997-2016.
15. Bell, M. Z. and Nur, A. (1978) Strength changes due to reservoir induced pore pressure and stresses and application to Lake Oroville. *J. Geophys. Res.* Vol.83, pp.4469-4483.
16. Belousov, V. V., Belyaevsky, N. A., Borisov, A. A., Volvovsky, B. S., Bolkovsky, I. S., Resvov, D. P., Tal-Virsky, B. B., Kharmabeav, I. K., Kaila, K. L., Narain, H. Marussi, A. and Finetti, J. (1980) Structure of the lithosphere along deep seismic sounding profile Tien Shan- Pamirs- Karakorum- Himalayas. *Tectonophysics*. Vol.70, pp.193-221.
17. Ben-Menahem, A., Aboudi, E. and Schild, R. (1974) The source of the great Assam earthquake- an intraplate wedge motion. *Phys. Earth. Planet. Int.* Vol.9, pp.265-289.
18. Ben-Menaheam, A. and Gillon, A. (1970) Crustal deformation by earthquakes and explosions. *Bull. Seism. Soc. Am.* Vol.60, pp.193-215.

19. Benmanahem, A. and Singh, S. J. (1981) Seismic waves and sources. Springer-Verlag, New York. p.1108.
20. Ben Menahem, A., Singh, S. J. and Solomon F. (1969) Static deformation of spherical earth model by internal dislocations. Bull. Seism. Soc. Am. Vol.59, pp.813-853.
21. Ben Menahem, A., Singh, S. J. and Solomon F. (1970) Deformation of an homogeneous earth model by finite dislocations. Rev. Geophys. Space. Phys. Vol.8, pp.591-632.
22. Barrientos, S. E. (1988) Slip distribution of the 1985 central Chile earthquake. Tectonophysics. Vol.145, pp.225-241.
23. Barrientos, S. E. and Ward, S. N. (1990) The 1960 Chile earthquake: Inversion for slip distribution from surface deformation. Geophys. J. Int. Vol.103, pp.589-598.
24. Bhatia, S. C., Chalam, S. V., Gaur, V. K., Keilis-Borok, V. I. and Kosobokov, V. G. (1989) On intermediate-term prediction of strong earthquakes in the Himalayan arc region using pattern recognition algorithm M8. Proc. Indian Acad. Sci. Vol.98, pp.111-123.
25. Bhatia, S. C., Vorobieva, I. A. Gaur, V.K., Levshina, T.A., Subedi L. and Chalam, S. (1990) Diagnostics of times of increased probability of strong earthquakes in the Himalayan seismic belt by algorithm CN (in russian). Analysis of geophysical fields.- M. nauka. Computational Seismology. Vol.23.
26. Bird, P. (1978) Initiation of intracontinental subduction in the Himalaya. J. Geophys. Res. Vol.83, pp.4975-4987.
27. Bomford, G. (1978) Geodesy. Oxford, the Clarendon press, London. p.731.
28. Burbank, D. W. (1992) Causes of recent Himalayan uplift deduced from deposited patterns in the Ganges basin. Nature. Vol.357, pp.680-683.

29. Burchfiel, B. C. and Royden, L. H. (1985) North-south extension within the convergent Himalayan region. *Geology*. Vol.13, pp.679-682.
30. Chander, R. (1988) Interpretation of observed ground level changes due to the 1905 Kangra earthquake, Northwest Himalaya. *Tectonophysics*. Vol.149, pp.289-298.
31. Chander, R. (1989a) Southern limits of major earthquakes ruptures along the Himalaya between longitudes 75° and 90°E. *Tectonophysics*. Vol.170, pp.115-123.
32. Chander, R. (1989b) On applying the concept of rupture propagation to deduce the location of the 1905 Kangra earthquake epicentre. *J. Geol. Soc. India*. Vol.33, pp.150-158.
33. Chander, R. (1992) An assessment of Oldham's model for the cause of the 1897 Shillong plateau earthquake. *J. Him. Geol.* Vol.3, pp.119-120.
34. Chander, R. (1994) Earthquakes and elevation changes in the Himalaya. *Current Science*. Vol.67, pp.306-310.
35. Chandra, U. (1975) Seismicity, earthquake mechanisms and tectonics of Burma 20°N-28°N. *Geophys. J. Roy. Astro. Soc.* Vol.40, pp.1-15.
36. Chandra, U. (1978) Seismicity, earthquake mechanisms and tectonics along the Himalayan mountain range and vicinity. *Phys. Earth Planet. Inter.* Vol.16, pp.109-131.
37. Chandra, U. (1981) Focal mechanism solutions and their tectonic implications for the eastern Alpine-Himalayan region in Zagros, Hindu Kush Himalaya, *Geodynamic Evolution*. *Geodyn. Ser.* Vol.3, pp.243-271.
38. Chen, W. P. and Molnar, P. (1977) Seismic moments of major earthquakes and the average rate of slip in Central Asia. *J. Geophys. Res.* Vol.82, pp.2945-2969.

39. Chen, W. P. and Molnar, P. (1990) Source parameters of earthquakes and intra-plate deformation beneath the Shillong plateau and the northern Indo-Burman ranges. *J. Geophys. Res.* Vol.95, pp.12527-12552.
40. Chinnery, M. A. (1961) The deformation of ground around surface faults. *Bull. Seism. Soc. Am.* Vol.51, pp.355-372.
41. Chinnery, M. A. (1963) The stress changes that accompany strike slip faulting. *Bull. Seism. Soc. Am.* Vol.53, pp.921-932.
42. Chinnery, M. A. (1966) Secondary faulting, I, Theoretical aspects. *Can. J. Earth Sci.* Vol.3, pp.163.
43. Chinnery, M. A. and Jovanovich, D. B. (1972) Effect of earth layering on earthquake displacement fields. *Bull. Seism. Soc. Am.* Vol.62, pp.1629-1639.
44. Cloetingh, S. and Wortel, R. (1986) Stress in the Indo-Australian plate. *Tectonophysics.* Vol.132, pp.49-67.
45. Davis, P. M. (1983) Surface deformation associated with a dipping hydrofracture. *J. Geophys. Res.* Vol.88, pp.5826-5834.
46. Davis, D., Suppe, J. and Dahlen, F. A. (1983) Mechanics of fold-and-thrust and accretionary wedges. *J. Geophys. Res.* Vol.88, pp.1153-1172.
47. DeMets, C., Gordon, R. G., Argus, D. F. and Stein, S. (1990) Current plate motions. *Geophys. J. Inter.* Vol.101, pp.425-478.
48. Dewey, J. F. and Bird, J. M. (1970) Mountain belts and the new global tectonics. *J. Geophys. Res.* Vol.75, pp.2625-2647.
49. Dewey, J. F. and Burke, K. C. A. (1973) Tibetan, Variscan and Precambrian reactivation: Products of continental collision. *J. Geol.* Vol.81, pp.683-692.
50. Dragert, H., Hyndman, R. D., Rogers, G. C. and Wang, K. (1994) Current deformation and the width of the seismogenic zone of the northern cascadia subduction thrust. *J. Geophys. Res.* Vol.99, pp.653-668.

51. Dunn, J. A., Auden, J. B, Ghosh, A. M. N., Roy, S. C. and Wadia, D. N. (1939) The Bihar-Nepal earthquake of 1934. Mem. Geol. Surv. India. Vol.73.
52. Dziewonski, A. M., Ekstrom, G., Woodhouse, J. H. and Zwart. G. (1989) Centroid-moment tensor solutions for July-September 1988. Phys. Earth planet. Int. Vol.56, pp.165-180.
53. Ekström, G. A. (1987) A broad band method of earthquake analysis, Ph.D. Thesis, Harvard University, Harvard.
54. England, P. and Houseman, G. A. (1985) Role of lithospheric strength heterogeneities in the tectonics of Tibet and neighbouring regions. Nature. Vol.315, pp.297-301.
55. England, P. C. and Houseman, G. A. (1986) Finite strain calculations of continental deformation. 2. Comparison with the India-Asia collision zone. J. Geophys. Res. Vol.91, pp.3664-3676.
56. England, P. and Houseman G. (1988) The mechanics of the Tibetan Plateau. Philos. Trans. R. Soc. London Ser. A. Vol.326, pp.301-320.
57. England, P. and Houseman, G. (1989) Extension during continental convergence, with application to the Tibetan Plateau. J. Geophys. Res. Vol.94, pp.17561-17579.
58. England, P. C. and McKenzie, D. P. (1982) A thin viscous sheet model for continental deformation. Geophys. J. R. Astron. Soc. Vol.70. pp.295-321.
59. England, P. and Molnar, P. (1993) The interpretation of inverted metamorphic isograds using simple physical calculations. Tectonics. Vol.12, pp.145-157.
60. Evans, P. (1964) The tectonic framework of Assam. J. Geol. Soc. India. Vol.5, pp.80-96.
61. Fedotov, S. A. (1965) Regularities of the distribution of strong earthquakes in Kamchatka the Kuril Islands and northeast Japan Akad, Nauk, USSR Inst. Fiziki Zemli Trudy. Vol.36, pp.66-93.

62. Fitch, T. J. (1970) Earthquake mechanisms in the Himalayan, Burmese and Andaman regions and the continental tectonics in central Asia. *J. Geophys. Res.* Vol.75, pp.2699-2709.
63. Fitch, T. J. and Scholz, C. H. (1971) Mechanism of underthrusting in southwest Japan: A model for convergent plate Interactions. *J. Geophys. Res.* Vol.76, pp.7260-7292.
64. Fuchs, G. R. (1975) Contribution to the geology of the northwestern Himalaya, *Abh. Geol. B. A.* Vol.32, pp.1-59.
65. Gabrielov, A. M. and 15 others (1986) Algorithms of Long-Term earthquake prediction CERESIS, Lima, Peru, pp.1-66.
66. Gahalaut, V. K., Kuznetsov, I. V., Rotwain, I. M., Gabrielov, A. M. and Borok, V. I. K. (1992a) Application pattern recognition algorithm in the seismic belts of Indian convergent plate margin-CN algorithm. *Proc. Indian Acad. Sci.* Vol.101, pp.227-238.
67. Gahalaut, V. K., Kuznetsov, I. V., Kosobokov, V. G., Gabrielov, A. M. and Borok, V. I. K. (1992b) Application pattern recognition algorithm in the seismic belts of Indian convergent plate margin-M8 algorithm. *Proc. Indian Acad. Sci.* Vol.101, pp.239-254.
68. Gansser, A. (1964) *Geology of the Himalayas*. Intersci. publ. John Wiley, London. p.289
69. Gansser, A. (1977) The great suture zone between Himalaya and Tibet, a preliminary account *Colloq. Intern. C.N.R.S., 268 Ecologie et geologie del' Himalaya*, Paris, pp.181-191.
70. Gansser, A. (1980) The division between Himalaya and Karakorum. *Geol. Bull. Univ. Peshwar.* Vol.13, pp.9-22.
71. Gansser, A. (1993) Facts and theories on the Himalayas. *J. Geol. Soc. India.* Vol.41, pp.487-508.

72. Gaur, V. K., Chander, R., Sarkar, I., Khattri, K. N. and Sinval, H. (1985) Seismicity and the state of stress from investigations of local earthquakes in the Kumaon Himalaya. *Tectonophysics*. Vol.118, pp.243-251.
73. Gongjian, W., Xuchang, X. and Tingdong, L. (1990) The Yadong Golmud geoscience transect in the Qinghai-Tibet plateau. *Acta Geol. Sin.* Vol.3, pp.115-127.
74. Gowd, T. N., Srirama Rao, S. V. and Gaur, V. K. (1992) Tectonic stress field in the Indian Subcontinent. *J. Geophys. Res.* Vol.97, pp.11879-11888.
75. Grant, F. S. and West, G. F. (1965) *Interpretation theory in Applied Geophysics*. New York, McGraw Hill. p.583.
76. Gupta, H. K., and Singh, H. N. (1986) Seismicity of the northeast India region: Part II: earthquake swarms precursory to moderate magnitude to great earthquakes. *J. Geol. Soc. India*. Vol.28, pp.367-406.
77. Gupta, H. K. and Singh, H. N. (1989) Earthquake swarms precursory to moderate to great earthquakes in the northeast India region. *Tectonophysics*. Vol.167, pp.285-298.
78. HARRIS, R. and SEGALL, P. (1987) Detection of a locked zone at depth on the Parkfield, California segment of the San Andreas fault. *J. Geophys. Res.* Vol.92, pp.7945-7962.
79. Hirn, A. (1988) Features of the crust mantle structure of Himalayas-Tibet a comparison with seismic traverses of Alpine, Pyrenean and Variscan orogenic belts. *Phil. Trans. R. Soc. Lond. A*. Vol.326, pp.17-32.
80. Hirn, A. and Sapin, M. (1984) The Himalayan zone of crustal interaction suggestions from explosion seismology. *Ann. Geophysicae*. Vol.2 pp.123-30.
81. Hirn, A. and 11 others (1984) Crustal structure and variability of the Himalayan border with Tibet. *Nature*. Vol.307, pp.23-25.

82. Hirn, A., Jobert, G., Wittlinger, G., Zhongxin, Xu and Enyuan, G. (1984) Main features of the upper lithosphere in the unit between the high Himalayas and the Yarlung Zhangbo Jiang suture. *Ann. Geophysicae*. Vol.2, pp.113-117.
83. Houseman, G. and England P. (1993) Crustal thickening versus lateral expulsion in the Indian-Asian continental collision. *J. Geophys. Res.* Vol.98, pp.12233-12249.
84. Houseman, G. A., Mckenzie, D. P. and Molnar P. (1981) Convective instability of a thickened boundary layer and its relevance for the thermal evolution of continental convergent belts. *J. Geophys. Res.* Vol.86, pp.6115-6132.
85. IASPEI (1991) Sub-commission on earthquake prediction, M. Wyss (Chairman) pp. 1-93.
86. Ishii, H. and Takagi, A. (1967a) Theoretical study on the crustal movements Part I. The influence of surface topography (Two dimensional SH-torque source). *Sci. Rep. Tohoku Univ. Serv. 5, Geophys.* Vol.19, pp.77-94.
87. Ishii, H. and Takagi, A. (1967b) Theoretical study on the crustal movements. Part II. The influence of horizontal discontinuity *Sci. Rep. Tohoku. Univ. Serv. 5, Geophys.* Vol.19, pp.95-106.
88. Iwasaki, T. and R. Sato (1979) Strain field in a semi-infinite medium due to an inclined rectangular fault. *J. Phys. Earth.* Vol.27, pp.285-314.
89. Jackson, M., Barrientos, S., Bilham, R., Kyestha, D. and Shrestha, B. (1992) Uplift in the Nepal Himalaya revealed by spirit leveling. *Geophys. Res. Letters.* Vol.19, pp.1539-1542.
90. Jaeger, J.C. and Cook, N. (1969) *Fundamentals of rock mechanics*, Methuen, London, p.513.
91. Jordan, T. H., Lerner-Lam, A. L., and Creger, K. C. (1989) Seismic imaging of boundary layers and deep mantle convection, in *Mantle Convection, Plate Tectonics and Global Dynamics*, edited by W. R. Peltier, Gordon and Breach, New York. pp.97-201.

92. Jovanovich, D. B., Hussein, M. I. and Chinnery, M. A. (1974a) Elastic dislocations in layered half space. I. Basic theory and numerical methods. *Geophys. J. Rs. Astr. Soc.* Vol.39, pp.205-217.
93. Jovanovich, D. B. Hussein, M. I. and Chinnery, M. A. (1974b) Elastic dislocations in layered half space II. The point source. *Geophys. J. Astr. Soc.* Vol.39, pp.219-239.
94. Kagan, Y. Y. and Jackson, D. D. (1991) Seismic gap hypothesis: Ten years after. *J. Geophys. Res.* Vol.96, pp.21419-21431.
95. Kaila, K. L., Krishna, V. G., Choudhury, K. and Narain, H. (1978) Structure of the Kashmir Himalaya from deep seismic soundings. *J. Geol. Soc. India*, Vol.19, pp.1-20.
96. Karner, G. D. and Watts, A. B. (1983) Gravity anomalies and flexure of the lithosphere at mountain ranges. *J. Geophys. Res.* Vol.88, pp.10449-10477.
97. Kasahara, K. (1981) *Earthquake Mechanics*. University Press, Cambridge. p.248
98. Keilis-Borok, V. I., Knopoff, L. and Allen, C.R. (1980) Long term premonitory seismicity patterns in Tibet and the Himalayas. *J. Geophys. Res.* Vol.85, pp.813-820.
99. Keilis-Borok, V. I., Knopoff, L., Rotwain, I. M. and Allen, C. R. (1988) Intermediate-term prediction of times of occurrence of strong earthquakes in California and Nevada. *Nature*. Vol.335, pp.690-694.
100. Keilis-Borok, V. I. and Kossobokov, V. G. (1988) Premonitory activation of seismic flow: Algorithm M8 workshop. *Global geophysical informatics with applications to research in earthquake predictions and reduction of seismic risk*. Nov. 15- Dec. Vol.16, 1988, Trieste, Italy.
101. Keilis-Borok, V. I. and Kosobokov, V. G. (1990) Premonitory activation of earthquake flow: Algorithm M8. *Phys. Earth Planet. Inter.* Vol.61, pp.73-83.

102. Keilis-Borok, V. I. and Rotwain, I. M. (1990) Diagnosis of time of increased probability of strong earthquakes in different regions of the world : Algorithm CN. *Phys. Earth Planet. Inter.* Vol.61, pp.57-72.
103. Kelleher, J. A. (1972) Rupture zones of large south American earthquakes and some prediction. *J. Geophys. Res.* Vol.77, pp.2087-2103.
104. Kelleher, J. A., Sykes L. R. and Oliver, J. (1973) Possible criteria for predicting earthquake locations and their applications to major plate boundaries of the Pacific and Caribbean. *J. Geophys. Res.* Vol.78, pp.2547-2585.
105. Kerr, R. A. (1993) Parkfield quakes skip a beat. *Science.* Vol.259, pp.1120-1122.
106. Khattri, K. N. (1987) Great earthquakes, seismicity gaps and potential for earthquake disaster along the Himalaya plate boundary. *Tectonophysics.* Vol.138, pp.79-92.
107. Khattri, K. N., Chander, R., Gaur, V. K., Sarkar, I. and Kumar, S. (1989) New seismological results on the tectonics of the Garhwal Himalaya. *Pro. Indian Acad. Sciences.* Vol.98, pp.91-109.
108. Khattri, K. N., Gaur, V. K., Chander, R., Moharir, P. S., Singh, V. N., Sarkar, I., Mukhopadhyay, S., Kumar, S., Sriram, V., Khanal, K. N. and Chauhan, P. K. S. (1988) Seismological studies in Garhwal Himalaya and Northeastern region, India. Technical Report, Department of Earth Sciences, University of Roorkee, India. pp.132.
109. Khattri, K. N. and Tyagi, A. K. (1983a) Seismicity patterns in the Himalayan plate boundary and identification of the areas of high seismic potential. *Tectonophysics.* Vol.96, pp.281-297.
110. Khattri, K. N. and Tyagi, A. K. (1983b) The transverse tectonic features in the Himalaya. *Tectonophysics.* Vol.96. pp.19-29.
111. Khattri, K. N. and Wyss, M. (1978) Precursory variation of seismicity rate in the Assam area, India. *Geology.* Vol.6, pp.685-688.

112. Khattri, K. N., Wyss, M., Gaur, V. K., Saha, S. N. and Bansal, V. K. (1983) Local seismic activity in the region of Assam gap, North-East India. *Bull. Seismol. Soc. Am.* Vol.3, pp.459-469.
113. King, G. C. P., Stein, R. S. and Rundle, J. B. (1988) The growth of geological structures by repeated earthquakes; 1, Conceptual framework. *J. Geophys. Res.* Vol.93, pp.13307-13318.
114. Krishnaswamy, V. S., Jalote, S. P. and Shome, S. K. (1970) Recent crustal movements in NW Himalaya and the Gangetic foredeep and related patterns of seismicity. *Proceedings of IV Symposium on Earthquake Engineering, University of Roorkee. Sarita Prakashan, Meerut.* pp.419-439.
115. Le Dain, A. Y., Tapponier, P. and Molnar, P. (1984) Active faulting and tectonics of Burma and surrounding regions. *J. Geophys. Res.* Vol.89, pp.453-472.
116. Le Fort, P. L. (1975) Himalayas the collided range present knowledge of the continental arc. *American Journal of Science.* Vol.275A, pp.1-44.
117. Lepine, J. C., Hirn, A., Pandey, M. R. and Tater, J. M. (1984) Features of the P waves propagated in the crust of the Himalayas. *Ann. Geophysicae.* Vol.2, pp.119-121.
118. Lillie, R. J., Johnson, G. D., Yousuf, M., Zamin, A. S. H. and Yeats, R. S. (1987) Structural development within the Himalayan foreland fold-and-thrust belt in Northern Pakistan, In: Beaumont, C. and Tankard, A. J. (Eds.), *Sedimentary Basins and Basin-Forming Mechanisms.* Can. Soc. Petrol. Geol. Canada. Vol.12, pp.379-392.
119. Linde, A. T. and Silver, P. G. (1989) Elevation changes and the great 1960 Chilean earthquake: support for aseismic slip. *Geophys. Res. Letters.* Vol.16, pp.1305-1308.
120. Lin, J. and Stein, R. S. (1989) Coseismic folding, recurrence, and the 1987 source mechanism at Whittier Narrows, Los Angeles Basin, California. *J. Geophys. Res.* Vol.94, pp.9614-9632.

121. Love, A. E. H. (1944) A treatise on mathematical theory of elasticity. Cambridge Univ. Press, NY, U.S.A. p.643.
122. Lyon-Caen H. and Molnar, P. (1983) Constraints on the structure of the Himalaya from an analysis of gravity anomalies and a flexural model of lithosphere. *J. Geophys. Res.* Vol.88, pp.8171-8191.
123. Lyon-Caen, H. and Molnar, P. (1985) Gravity anomalies, flexure of the Indian plate and structure, support and evolution of the Himalaya and Ganga basin. *Tectonics.* Vol.4, pp.513-538.
124. Ma, X. Q. and Kusznir, N. J. (1993) Modelling of near-field subsurface displacements for generalized faults and fault arrays. *J. Str. Geol.* Vol.15, pp.1471-1484.
125. Mansinha, L. and Smylie, D. E. (1971) The displacement fields of inclined faults. *Bull. Seismol. Soc. Am.* Vol.61, pp.1433-1440.
126. Maruyama, T. (1964) Statical elastic dislocation in an infinite and semi-infinite medium. *Bull. Earthquake Res. Inst. Tokyo Univ.* Vol.42, pp.289-368.
127. Mathur, L.P. and Evans, P. (1964) Oil in India Spl.-Brochure, Int. Geol. Congr. 22nd Session New Delhi 64-79.
128. Matsuura, M. (1977) Inversion of geodetic data Part I Mathematical formulation. *J. Phys. Earth.* Vol.25, pp.69-90.
129. Matsuura, M. and Sato. R. (1975) Static deformation due to the fault spreading over several layers in multi-invered medium Part II strain and tilt. *J. Phys. Earth.* Vol.23, pp.1-29.
130. Matsuura, M. and Tanimoto, T. (1980) Quasi-Static deformation due to an inclined rectangular fault in a viscoelastic half-space. *J. Phys. Earth.* Vol.28, pp.103-118.

131. McCann, W. R., Nishenko, S. P., Sykes, L. R. and Krause, J. (1979) Seismic gaps and plate tectonics Seismic potential for major boundaries. *Pure Appl. Geophys.* Vol.117, pp.1082-1147.
132. McGinley, J. R. (1969) A comparison of observed permanent tilts and strains due to earthquakes with those calculated from displacement dislocation in elastic earth models Ph.D. Thesis, California Institute of Technology, Pasadena California.
133. McHugh, S. and Johnston, M. (1977) Surface shear stress strain and shear displacement for screw dislocation in a vertical slab with shear modulus contrast. *Geophys. J. R. Astr. Soc.* Vol.49, pp.715-722.
134. Menke, W. (1984) *Geophysical data analysis: Discrete inverse theory;* (Academic Press INC Orlando, Florida). p.260.
135. Menke, W. H. and Jacob, K. H. (1976) Seismicity patterns in Pakistan and northwestern India associated with continental collision. *Bull Seismol. Soc. Am.* Vol.66, pp.1695-1711.
136. Middlemiss, C. S. (1910) The Kangra earthquake of 4th April, 1905. *Mem. Geol. Surv. India.* Vol.37, pp.1-409.
137. Mogi, K. (1969) Some features of recent seismic activity in and near Japan (2) *Tokyo Univ. Earthquake Res. Instl. Bull.* Vol.47, pp.395-417.
138. Molnar, P. (1987a) Inversion of profiles of uplift rates for the geometry of dip-slip faults at depth with examples from the Alps and the Himalaya. *Ann. Geophysicae.* Vol.5, pp.663-670.
139. Molnar P. (1987b) The distribution of intensity associated with the great 1897. Assam earthquake and bounds on the extent of the rupture zone. *J. Geol. Soc. India.* Vol.30, pp.13-27.
140. Molnar, P. (1987c) The distribution of intensity associated with the 1905 Kangra earthquake and bounds on the extent of the rupture zone. *J. Geol. Soc. India.* Vol.29, pp.221-229.

141. Molnar, P. (1988) A review of geophysical constraints on the deep structure of the Tibetan Plateau, the Himalaya and the Karakorum and their tectonic implications. *Phil. Trans. Royal Soc. London.* Vol.326, pp.33-88.
142. Molnar, P. (1990) A review of the seismicity and the rates of active underthrusting and deformation at the Himalaya. *J. Himalayan Geol.* Vol.1, pp.131-154.
143. Molnar, P. (1992) A review of seismicity recent faulting and active deformation of the Tibetan Plateau. *J. Himalayan Geol.* Vol.3(1), pp.43-78.
144. Molnar, P., Burchfiel, B. C., Kuangyi, L. and Ziyun, Z. (1987) Geomorphic evidence for active faulting in the Altyn Tagh and northern Tibet and qualitative estimates of its contribution to the convergence of India and Eurasia. *Geology.* Vol.15, pp.249-253.
145. Molnar, P. and Chen, W. P. (1982) Seismicity and mountain building, In: Hsü, K. (ed.) *Mountain Building Processes.* Acad. Press, London. pp.41-55.
146. Molnar, P., Chen, W. P., Fitch, T. J., Tapponnier, P., Warsi, W. E. K. and Wu, F. T. (1977) Structure and tectonics of the Himalaya. A brief summary of relevant geophysical observations. In *Himalaya. Sciences de la Terre* (Paris, Centre National de la Recherche Scientifique). pp.269-294.
147. Molnar, P. & Deng Q. D. (1984) Faulting associated with large earthquakes and the average rate of deformation in Central and Eastern Asia. *J. Geophys. Res.* Vol.89, pp.6203-28.
148. Molnar P. and England P. (1990) Temperatures, heat flux, and frictional stress near major thrust faults. *J. Geophys. Res.* Vol.95, pp.4833-4856.
149. Molnar, P. and Lyon-Caen, H. (1989) Fault plane solutions of earthquakes and active tectonics of the northern and eastern parts of the Tibetan Plateau. *Geophys. J. Int.* Vol.99, pp.123-153.

150. Molnar P., Fitch, T. J. and Wu, F. T. (1973) Fault plane solutions of shallow earthquakes and contemporary tectonics of Asia. *Earth Planet. Sci. Letters*. Vol.16, pp.101-112.
151. Molnar, P. and Pandey, M. R. (1989) Rupture zones of Great Earthquakes in the Himalayan region. *Proc. Indian Acad. Sci.* Vol.98, pp.61-70.
152. Molnar, P. and Tapponnier, P. (1975) Cenozoic tectonics of Asia Effects of a continental collision. *Science*. Vol.189, pp.419-426.
153. Mukhopadhyay, S. (1990) Seismic velocity structure and seismotectonics of the Shillong massif, northeastern India. Ph.D Thesis, Department of Earth Sciences, University of Roorkee, India.
154. Nakata, T., Otsuki, K. and Khan, S. H. (1990) Active faults, stress field and plate motion along the Indo-Eurasian plate boundary. *Tectonophysics*. Vol.181, pp.83-95.
155. Nandi, D. R. and Dasgupta, S. (1986) Application of Remote Sensing in regional geological studies - A case study in the northeastern part of India. *Proc. Int. Seminar on Photogrammetry and Remote Sensing for Developing Countries*, N.Delhi. Vol.1, T.4-P/6.2-6.9.
156. Ni, J. and Barazangi, M. (1983) High frequency seismic wave propagation beneath the Indian Shield, Himalayan Arc., Tibetan Plateau and surrounding regions: high uppermost mantle velocities and efficient Sn propagation beneath Tibet. *Geophys. J. R. astr. Soc.* Vol.72, pp.665-689.
157. Ni, J. and Barazangi, M. (1984) Seismotectonics of the Himalayan Collision zone: Geometry of the underthrusting Indian plate beneath the Himalaya. *J. Geophys. Res.* Vol.89, pp.1147-1163.
158. Niewiadomski, J. and Rybicki, K. (1984) The stress field induced by antiplane shear cracks application to earthquake study. *Bull. Earthquake Res. Inst. Tokyo Univ.* Vol.59, pp.67-81.

159. Nishenko, S. P. (1989) Earthquakes: Hazards and predictions. In: The encyclopedia of solid earth geophysics edited by D.E. James. Van Nostrand Reinhold, New York. pp.260-268.
160. Okada, Y. (1985) Surface deformation due to shear and tensile faults in a half space. Bull. Seismol. Soc. Am. Vol.75, pp.1135-1154.
161. Oldham, R. D. (1899) Report on the great earthquake of 12 June 1897. Mem. Geol. Surv. India. Vol.29, pp.1-379.
162. Omura, M., Yokoyama, K. and Kubo, S. (1986) Geodetic Monitoring of Crustal Movements in the Himalayas-at the MCT and MBT, Central Nepal. Proc.Inter. Symp. Neotectonics in South Asia. Survey of India, Dehradun. pp.345-352.
163. PDE (1992) Preliminary Earthquake data report USGS, Jan.1991-Aug.1991
164. Peltzer, G. and Tapponnier, P. (1988) Formation and evolution of strike slip faults, rifts and basins during the India-Asia collision: An experimental approach. J. Geophys. Res. Vol.93, pp.15085 - 15117.
165. Pennock, E. S., Lillie, R. J., Zaman, A. S. H. and Yousaf, M. (1989) Structural interpretation of seismic reflection data from eastern salt range and Potwar Plateau, Pakistan. Am. Assoc. Pet. Geol. Bull. Vol.73, pp. 41-857.
166. Phillimore, R. H. (1945) Historical records of the survey of India, Survey of India, Dehradun (UP), India. Vol.1, pp.1-400.
167. Plafker, G. (1972) Alaskan earthquake of 1964 and Chilean earthquake of 1960: Implications for arc tectonics. J. Geophys. Res. Vol.77, pp.901-925.
168. Prescott, W. H. and Yu, S. B. (1986) Geodetic measurement of Horizontal deformation in the northern san francisco bay region, California. J. Geophys. Res. Vol.91, pp.7475-7484.
169. Press, F. (1965) Displacements, Strains and tilts at teleseismic distances. J. Geophys. Res. Vol.70, pp.2395-2412.

170. Powell, C. M. (1979) A speculative tectonic history of Pakistan and surroundings some constraints from the Indian Ocean. In Geodynamics of Pakistan (eds) A farah and K. DeJong (Quetta: Geol. Surv. of Pakistan). pp. 5-24.
171. Powell, C. M. and Conaghan, P. J. (1973) Plate tectonics and the Himalayas. Earth Planet. Sci. Letters. Vol.20, pp.1-12.
172. Powell, C. M. and Conaghan, P. J. (1975) Tectonic models of the Tibetan Plateau. Geology. Vol.3. pp.727-731.
173. Qureshy, M. N. and Warsi, W. E. K. (1980) A bouguer anomaly map of India and its relation to broad tectonic elements of the sub-continent. Geophys. J. R. Astron. Soc. Vol.61, pp.235-242.
174. Raiverman, V., Kunte, S. V. and Mukherjee, A. (1983) Basin geometry, Cenezoic sedimentation and hydrocarbon prospects in NW Himalaya and Indo-Gangetic plains. Pet. Asia J. Vol.6. pp.67-92.
175. Rajal, B. S., Viridi, N. S. and Hasija, N. L. (1986) Recent crustal uplift in the Dun valley. Proc. Int. Symp. on Neotectonics in South Asia. Survey of India, Dehradun. pp.146-159.
176. Raleigh, B., Bennett, G., Craig, H., Hanks, T., Molnar, P., Nur, A., Savage, J., Scholtz, C., Turner, R. and Wu, F. (1977) Prediction of the Haicheng earthquake EOS(AGU Trans). Vol.58, pp.236-272.
177. Ramchandra Rao, M. B. (1953) A compilation of papers on the Assam earthquake of August 15, 1950. Publ. NO.1, The Central Board of Geophysics, Govt. of India. pp.112.
178. Richter, C. F. (1958) Elementary Seismology. Freeman, San Francisco, California. pp.764.
179. Ried, H. F. (1910) The mechanics of the earthquake, the California earthquake of April 18, 1906, report of the State Investigation Commission, Carnegie Institution of Washington, Washington, D.C. Vol.2, pp.16-28.

180. Rochester, M. G. (1956) The application of dislocation theory of fracture of the Earth's crust. M.A. Thesis, Univ. of Toronto, Toronto, Canada.
181. Rybicki, K. (1971) The elastic residual field of a very long strike slip fault in the presence of a discontinuity. Bull. Seismol. Soc. Am. Vol.61, pp.79-92.
182. Rybicki, K. (1978) Static deformation of a laterally inhomogeneous half space by a two dimensional strike slip fault. J. Phys. Earth. Vol. 26, pp.351-366.
183. Rybicki, K. and K. Kasahara (1977) A strike slip fault in a laterally inhomogeneous medium. Tectonophysics. Vol.42, pp.127-138.
184. Sato, R. (1971) Crustal deformation due to dislocation in a multi layered medium. J. Phys. Earth. Vol.19, pp.31-46.
185. Sato, R. (1974) Static deformations in an obliquely layered medium Part I Strike slip fault. J. Phys. Earth. Vol.22, pp.455-462.
186. Sato, R. and Matsuura, M. (1973) Static deformations due to the fault spreading over several layers in a multilayered medium Part I displacement. J. Phys. Earth. Vol.21, pp.227-249.
187. Sato, R. and Matsuura, M. (1974) Strains and tilts on the surface of a semi infinite medium. J. Phys. Earth. Vol.22, pp.213-221.
188. Sato, R. and Yamashita, T. (1975) Static deformations in an obliquely layered medium Part II Dip-slip fault J. Phys. Earth. Vol 23, pp. 113-125.
189. Savage, J. C. (1983) A dislocation Model of Strain Accumulation and Release at a subduction zone. J. of Geophys. Res. Vol.88, pp.4984-4996.
190. Savage J. C. and Gu, G. (1985) A plate flexure approximation to postseismic and interseismic deformation. J. Geophys. Res. Vol.90, pp.
191. Savage, J. C. and Hastie, L. M. (1966) surface deformations associated with dip slip faulting. J. Geophys, Res. Vol.71, pp.4897-4904.

192. Savage, J. C. and Hastie, L. M. (1969) A dislocation model for the Fairview Peak, Nevada, earthquake. *Bull. Seism. Soc. Am.* Vol.59, pp.1937.
193. Schelling, D. (1992) The tectono stratigraphy and structure of the eastern Nepal Himalaya. *Tectonics*. Vol.11, pp.925-943.
194. Scholz, C. H. (1992) *The mechanics of earthquakes and faulting*. Cambridge Univ. Press, NY, U.S.A. p.439.
195. Scholz, C. H. and Kato, (1978) The behavior of a convergent plate boundary crustal deformation in the south Knato district, Japan. *J. Geophys. Res.* Vol.83, pp.783-797.
196. Seeber, L. and Armbruster, J. (1981) Great detachment earthquakes along the Himalayan arc and long-term forecasts, *Earthquake prediction. An international review*, Maurice Ewing series 4 (eds) D.W. Simpson and P.G. Richards (Washington DC. Am. Geophys. Union). pp.259-277.
197. Seeber, L. and Armbruster, J. G. (1984) Some elements of continental subduction along the Himalayan front. *Tectonophysics*. Vol.105, pp.263-278.
198. Seeber, L., Armbruster, J. and Farhatullah, S. (1980) Seismic activity at the Tarbela dam site and surrounding region. In: R. A. K. Tahirkheli, M. Q. Jan, and M. Majid (Editors). *Proceedings of the International Committee on Geodynamics, Group 6 Meeting*, Univ. Peshwar, Peshwar. pp.169-191.
199. Seeber, L., Armbruster, J. G. and Quitmeyer, R. C. (1981) Seismicity and continental subduction in the Himalayan arc. In: H. K. Gupta and F. Delany (Editors). *Zagros, Hindu Kush, Himalaya Geodynamic Evolution*. Am. Geophys. Union *Geodyn. Ser.* Vol.3, pp.215-242.
200. Segall, P. (1985) Stress and subsidence resulting from subsurface fluid withdrawal in the epicentral region of the 1983 Coalinga earthquake. *J. Geophys. Res.* Vol.90, pp.6801-6816.

201. Segall, P. and McTigue, D. F. (1984) Vertical displacements from a dip slip fault beneath surface topography, Abstract Chapman Conference on vertical crustal Motion. Measurement and Modeling AGU, Washington, D.C.
202. Shimazaki, K. (1974) Preseismic crustal deformation caused by an underthrusting oceanic plate, in eastern Hokkaido, Japan. *Phys. Earth Planet. Inter.* Vol.8, pp.148-157.
203. Sibson, R. H. (1989) High angle reverse faulting in northern new Brunswick, Canada, and its implications for fluid pressure levels. *J. Struct. Geol.* Vol.11, pp.873-877.
204. Singh, S. J. (1970) Static deformation of a multilayered half space by internal sources. *J. Geophys. Res.* Vol.75, pp.3257-3263.
205. Singh, S. J. and Garg, N.R. (1985) On two dimensional elastic dislocations in a multilayered half-space. *Phys. Earth Planet. Int.* Vol.40, pp.135-145.
206. Sinha-Roy, S. (1982) Himalaya main central thrust and its implications for Himalayan inverted metamorphism. *Tectonophysics.* Vol.84, pp.197-224.
207. Smylie, D. E. and Mansinha, L. (1971) The elasticity theory of dislocations in real earth models and changes in the rotation of the earth. *Geophys. J. R. Astr. Soc.* Vol.23, pp.329-354.
208. Stein, R. S. and Barrientos, S. E. (1985) High angle normal faulting in the intermountain seismic belt: Geodetic investigations of the 1983 Borah Peak, Idaho, earthquake. *J. Geophys. Res.* Vol.90, pp.11355-11366.
209. Stein, R. S. and Lisowski, M. (1983) The 1979 Homestead valley earthquake sequence, California : Control of aftershocks and post-seismic deformation. *J. Geophys. Res.* vol.88, pp.6477-6490.
210. Steketee, J. A. (1958) On Volterra's dislocations in a semi-infinite elastic medium. *Can. J. Phy.* Vol.36, pp.192.

211. Stocklin, J. (1980) Geology of Nepal and its regional frame. *J. Geol. Soc. London*. Vol.137, pp:1-34.
212. Takemoto, S. (1981) Effects of local inhomogeneities on tidal strain measurements. *Bull Disas. Prev. Res. Inst. Kyoto. Univ.* Vol.31, pp.211-237.
213. Tandon, A. N. (1955) Direction of faulting in the great Assam earthquake of August 15, 1950, *Indian J. Meteorol. Geophys.* Vol.6, pp.61-64.
214. Tapponnier, P. and Molnar, P. (1976) Slip-line field theory and large-scale continental tectonics. *Nature*. Vol.264, pp.319-324.
215. Tapponnier, P., Peltzer, G., LeDain, A. Y., Armijo, R. and Cobbold, P. (1982) Propagating extrusion tectonics in Asia: New insights from simple experiments with plasticine. *Geology*. Vol.10, pp.611-616.
216. Thatcher, W. (1979) Systematic inversion of geodetic data in central California. *J. Geophys. Res.* Vol.84, pp.2283-2295.
217. Thatcher, W. (1983) Nonlinear strain buildup and the earthquake cycle on the San Andreas fault. *J. Geophys. Res.* Vol.88, pp.5893-5902.
218. Thatcher, W. (1984) The earthquake deformation cycle in the Nankai trough, southwest Japan. *J. Geophys. Res.* Vol.89, pp.3087-3101.
219. USGS-NEIS (1991) World Hypocenters Data File, 1900- 1991, Denver.
220. Valdiya, K. S. (1976) Himalayan transverse faults and folds and their parallelism with subsurface structures of north Indian plains. *Tectonophysics*. Vol.23, pp.353-386.
221. Valdiya, K. S. (1980) The two intracrustal boundary thrusts of the Himalaya. *Tectonophysics*. Vol.66, pp.323-348.
222. Valdiya, K. S. (1981) Geology of Kumaun Lesser Himalaya. Wadia Institute of Himalayan Geology, Dehradun, India.

223. Valdiya, K. S. (1986) Neotectonic activities in the Himalaya belt. Proc. Int. Symp. on Neotectonics in South Asia, Survey of India, Dehradun. pp.241-267.
224. Verma, R. K. and Krishna Kumar, G. V. R. (1987) Seismicity and the nature of plate movement along the Himalayan arc, Northeast India and Arakan Yoma : A review. Tectonophysics Vol.134 pp.153-175.
225. Verma, R. K. and Mukopadhyay, M. (1977) An analysis of the gravity field in northeastern India. Tectonophysics. Vol.42, pp.283-317.
226. Verma, R. K. and Prasad, K. A. V. L. (1987) Analysis of gravity fields in the northwestern Himalayas and Kohistan region using deep seismic sounding data. Geophys. J.R. Astron, Soc. Vol.91, pp.869-889.
227. Verma, R. K., Mukhopadhyay, M. and Ahluwalia, M. S. (1976) Earthquake mechanisms and tectonics features of northern Burma. Tectonophysics. Vol.32, pp.387-399.
228. Vilotte, J. P., Daigneieres, M. and Madariaga, R. (1982) Numerical modeling of intraplate deformation: simple mechanical models of continental collision, J. Geophys. Res. Vol.87, pp.10709-10728.
229. Vilotte, J. P., Madariaga, R. Daignieres, M. and Zienkiewicz, O. (1984) Numerical study of continental collision influence of buoyancy forces and an initial stiff inclusion. Geophys. J. Int. Vol.84, pp.279-310.
230. Vilotte, J. P., Madariaga, R., Daignieres, M. and Zienkiewicz, O.C. (1986) Numerical study of continental collision: influence of buoyancy forces and a stiff inclusion Geophys. J. R. Astron Soc. Vol.84, pp.279-310.
231. Wadia, D. N. (1976) Geology of India. Macmillan Press, London. p.536.
232. Warsi, W. E. K., and Molnar, P. (1977) Gravity anomalies and plate tectonics in the Himalaya, colloques internationaux du CNRS, in Himalaya: Sciences de la Terre, pp.463-478.

233. Ward, S. N. and Barrientos, S. E. (1986) An inversion for slip distribution and fault shape from geodetic observation of the 1983, Borah Peak, Idaho, earthquake. *J. Geophys. Res.* Vol.91, pp.4909- 4919.
234. Ward, S. N. and Valensise, G. (1989) Fault parameters and slip distribution of the 1915, Avezzano, Italy earthquake derived from geodetic observations. *Bull. Seismol. Soc. Am.* Vol.79, pp.690-710.
235. Weldon, R. J. and Sieh, K. E. (1985) Holocene rate of slip and tentative recurrence interval for large earthquakes on the San Andreas fault, Cajon Pass, southern California. *Geol. Soc. Am. Bull.* Vol.96. pp.793-812.
236. Yamazaki, K. (1975) The strains and tilts at the free surface due to an inclined fault Differential formulae of the displacement fields given by Mansinha and Symlie Zisin. Vol.28, pp.215-217 (In Japanese).
237. Yeats, R. S. and Lillie, R. J. (1991) Contemporary tectonics of the Himalayan frontal fault system: folds, blind thrusts and the 1905 Kangra earthquake. *J. Struct. Geol.* Vol.13, pp.215-225.
238. Zhao, W. L. and Morgan, W. J. (1985) Uplift of Tibetan Plateau. *Tectonics.* Vol.4, pp.359-369.
239. Zhao, W. L. and Morgan, W. J. (1987) Injection of Indian crust into Tibetan lower crust: A two dimensional finite element model study. *Tectonics.* Vol.6, pp.489-504.
240. Zhao, W., Nelson, K. D. and Project INDEPTH team (1993) Deep seismic reflection evidence for continental underthrusting beneath southern Tibet. *Nature.* Vol.366, pp.557-559.
241. Zhao, W. L. and Yuen, D. A. (1987) Injection of Indian crust into Tibetan lower crust: A temperature-dependent viscous model. *Tectonics.* Vol.6, pp.505-514.
242. Zoback, M. L. (1992) First-and Second-order patterns of stress in the lithosphere: The world stress map project. *J. Geophys. Res.* Vol.97, pp.11703-11728.

243. Zoback, M. L. and 28 others (1989) Global patterns of tectonic stress. *Nature*. vol.341, pp.291-298.

Papers published on the basis of studies in the thesis

(i) Papers in refereed journals

1. Gahalaut, V.K. and Chander,R. (1992) : A rupture model for the great earthquake of 1897, Northeast India. **Tectonophysics**, V.204, pp.163-174.
2. Gahalaut, V.K. (1994) : Temporal variation of seismicity in a Himalayan tectonic block and 1991 Uttarkashi earthquake, India. **Physics of the Earth and Planetary Interiors**, V.85, pp.339-347.
3. Gahalaut, V.K. and Chander,R. (1992) : On the active tectonics of Dehra Dun region from observations of ground elevation changes. **Journal Geological Society of India**. V. 39, No.1, pp.61-68.
4. Gahalaut, V.K., Gupta, P.K., Chander, R. and Gaur, V.K. (1994): Minimum norm inversion of elevation change data for slips on the causative faults during the 1905 Kangra earthquake. **Proc. of the Indian Acedemy of Sciences, Earth and Planetary Sciences** (accepted, in press).
5. Chander, R. and Gahalaut, V.K. (1994): Preparations for great earthquakes seen in levelling observations along two lines across the Outer Himalaya. **Current Science** (accepted, in press).
6. Gahalaut V.K. and Chander R. (1994) : Geotectonic and seismic risk implications of ground level changes in the Dehradun region during the 1905-28 period. **Journal Geological Society of India** (accepted, in press).

(ii) Paper in Symposium

1. Gahalaut,V.K. and Chander,R.: Cross-sectional model for the 1905 Kangra earthquake. In Proceedings of the "Ninth Symposium on Earthquake Engg."(Dec.14-16, 1990) Deptt. of Earthquake Engg. U.O.R. Roorkee, India, Vol.1 (1) : 09-15.